MITOCHONDRIAL DYNAMICS IN THE REGULATION OF ADULT NEUROGENESIS

MOHAMED ARIFF IQBAL

Thesis submitted to the University of Ottawa

in partial Fulfillment of the requirements for the

Doctor of Philosophy in Cellular and Molecular Medicine

Department of Cellular and Molecular Medicine

Cellular and Molecular Medicine Program

Faculty of Medicine

University of Ottawa

2023

ACKNOWLEDGMENTS

At first, I would like to express my utmost gratitude to my supervisor Dr. Ruth Slack. With her effort, I was able to attain many opportunities to hone on my expertise, critical and analytical thinking to become an independent scientist. I honour Ruth's dedication and commitment to help me progress through the past seven years. Dear Ruth, thank you for believing in me and all the tremendous support you gave me throughout the PhD program. I could have not asked for any other supportive lab like Slack lab.

I would like to express my gratitude to the members of my Thesis Advisory Committee, Dr. Mary-Ellen Harper, Dr. Diane Lagace, Dr. Keir Menzies, and Dr. David Park. Their constant support shaped the project in its current form. Your support during the pandemic guided me through those difficult times.

This thesis would not have been possible without the support of my fantastic colleagues. I am a half person without their support. My sincere thankfulness is for Smitha Paul. I am indebted to her for not only contributing to complete this research but also to the moral support she has given when things were challenging. I appreciate the motivation and the positivity I received which kept me moving my project and grow as a professional. I cannot thank you enough for listening and guiding through all my personal and professional uphill challenges.

I would like to express my deep appreciation to Dr. Bensun Fong, who I could call him more of a family. I am proud to say he was the first colleague I met from Slack lab during CAN-ACN 2015. From the day I joined the lab, he has been that awesome colleague who takes those extra steps to make anyone feel included. Besides, supporting with research, he helped me navigate through this tough path as we shared the same "Fate decision" to pursue PhD. All the great times of the slack lab has Ben's name in it. I will always cherish the road trips to conferences, Curling games, the pumpkin carving, movie nights and you name it. Ben you are a rockstar!

I am paralyzed without the awesome colleague scientists who helped immensely throughout the time. Thank you, Bing, for your expert opinion and generous time in improving the data quality. Thank you, Iman, for your critiques and guidance, that helped me immensely in critical thinking improving data quality. I would like to thank my bench mate and collaborator Maria. We shared a good quality time in the beginning. I still remember fondly of the sample preps together and great scientific discussions we had. My immense Thanks to you Vanessa for all the hard work you did without the breaks and the ones that actually went into the manuscript.

Next, I would like to thank few of the past members of Slack lab who made the long PhD program memorable. In particular, I would like to thank Jason for making the initial phase of the PhD program a breeze. I would like to thank Dr. Mireille Khacho for the setting the stage for my PhD thesis. I would like to thank Richard for introducing me to the world of the Dungeons and Dragons. He made the Fridays a friYAY! I must mention the time with Jingwei and his crazy ideas for startups and genuine troubleshooting that worked in the lab. I would like to thank Ujval and Devon for the lunchtime chats and David Patten for the quality time. I would like to thank Eddy, Daniel, MMM for their quality time and discussion.

Last but not least, I would like to thank my family for their immense support and freedom through out my life. Without their tremendous support and sacrifice, I could not have ever been here doing the things I treasure. I give my heart and brain to my awesome wife, who was on board with this crazy amazing journey. She is the unsung hero in shaping this thesis and our married life. She made the work-life balance easy that we could discuss science wherever we are. Fahmida, I forever indebted to you for your support. Finally, I like to thank our cutest baby Faiz for bringing joy and cheer into our life.

I acknowledge the location of RGN campus on the traditional, unceded territories of the Algonquin nation. I appreciate the funding by Mito2i their financial support and CIHR for funding this research project through a grant to R.S.S.

ABSTRACT

Long-term maintenance of adult neural stem cells (NSCs) is an intricate process of activation, expansion, and differentiation while preserving the stem cell pool. Several regulatory mechanisms underlie the delicate balance in the choice between quiescence versus activation for lifelong NSC maintenance and continuous neurogenesis. Perturbations in this dynamic process result in disease manifestation. The quiescence/activation of NSC was shown to be regulated by the Rb/E2F axis through a molecular program mediated by REST (RE1 Silencing Transcription Factor). Loss of Rb family increased NSC activation at the expense of quiescence through activator E2F transcription factors. The activation and neurogenesis of NSCs were impaired by the loss of effector E2Fs, as well as loss of Opa1, the latter indicating that mitochondrial dynamics is important to maintain stem cell state. Single-cell transcriptome analysis from NSC lineages isolated from adult mouse hippocampus revealed that stem cell progenies are uniquely affected in Opa1-KO leading to impairments in NSC activation and differentiation. Unbiased transcriptional profiling suggested a mitochondrial dysfunction in Opa1-KO that results in activation of classic cellular stress response pathway genes (*Atf4*, Slc7a11 and *Chac1*). Thus, the regulatory gene network comprising quiescence (Rb) and activation (E2Fs) programs, and mitochondrial metabolism (Opa1) and their interplay ensures the maintenance of the molecular program of NSC, particularly revealing how it enables stem cells survive stress.

Table of Contents

LIST OF FIGURES AND TABLES

LIST OF ABBREVIATIONS

AIF	apoptosis inhibiting factor
ASCL1	(achaete-scute family bHLH transcription factor 1)
ATF4	Activating transcription factor 4
bZIP	basic leucine zipper
CHOP	C/EBP Homology Protein
CMT2A	Charcot–Marie–Tooth disease (CMT) type 2A
CPEO	chronic progressive external ophthalmoplegia
DG	dentate gyrus
Drp1	Dynamin-related protein 1
eIF2α	eukaryotic translation initiation factor 2
ER	endoplasmic reticulum
Fasn	Fatty Acid Synthase
GCN2	general control non-derepressible 2
HRI	heme-regulated eIF2α kinase
HSC	hematopoietic stem cell
ID4	(Inhibitor of differentiation/DNA binding)
IRES	internal ribosome entry site
ISR	Integrated stress response
LD	Lipid droplets
l-Opa1	long Opa1
LT-HSC	long-term HSC
MFN1&2	Mitofusin 1 and 2
MPC	mitochondrial pyruvate carrier
NAC	N-acetyl cysteine
NeuN	neuronal nuclei
Nfe2l2	Nuclear factor erythroid 2-related factor 2
NSCs	Neural stem cells
ORF1	open reading frame
OXPHOS	oxidative phosphorylation
OPA1	Optic atrophy 1

OB	olfactory bulb
DOT1L/KMT4	DOT1-like, histone H3 methyltransferase
PERK	PKR-like ER kinase
PGC1α	Peroxisome proliferator-activated receptor (PPAR) γ co-activator-1α
PKR	RNA-dependent protein kinase
qNSCs	quiescent NSCs
RGL	glia-like stem cells
REST	RE1-Silencing Transcription factor
RMS	rostral migratory stream
ROS	reactive oxygen species
SGZ	subgranular zone
SGZ	subgranular zone
s-Opa1	short Opa1
SVZ	subventricular zone
TAP	Transiently amplifying progenitors
UPR	unfolded protein response
V-SVZ	ventricular-subventricular zone

CHAPTER 1

GENERAL INTRODUCTION

1. Embryonic to adulthood maintenance of neural stem cells

Neural stem cells (NSCs) have the capacity to generate the entire nervous system (Ming and Song 2011). NSCs are multipotent cells that that can self-renew their own population, have the ability of fate commitment and differentiate into neurons, astrocytes and oligodendrocytes (Alvarez-Buylla and Temple 1998). During early cortical development, NSCs go through symmetrical cell division to self-renew and expand. Later, the NSCs asymmetrically divide to give rise to apical radial glia, which can directly convert to a neuron or indirectly to generate intermediate progenitors that also self-renew and contribute to expanding neuronal differentiation (Taverna, Gotz, and Huttner 2014). After the rapid expansion of embryonic brain, the stem cells go quiescent to maintain a subset of adult NSCs in multiple stem cell niche (Merkle et al. 2004). The adult CNS holds reservoirs of NSCs in the ventricular-subventricular zone (V-SVZ) and subgranular zone (SGZ) of the dentate gyrus (DG) in the hippocampus (Morshead, Craig, and van der Kooy 1998). These stem-like cells are concentrated in the V-SVZ lining the lateral ventricles and the SGZ of the DG in the hippocampus of adult brain (Morshead, Craig, and van der Kooy 1998; Garcia-Verdugo et al. 1998; Goncalves, Schafer, and Gage 2016; Kempermann, Song, and Gage 2015; Ming and Song 2011). NSCs are shown to be maintained largely in a quiescent stage by their microenvironment (niche) but can be activated to proliferate upon any appropriate stimuli or during injury (Arvidsson et al. 2002; van Praag, Kempermann, and Gage 1999). NSCs are further distinguished into subpopulations based on their protein markers. Developmental progression is marked by temporal changes in the subset of genes expression pattern (Andersen et al. 2014; Kempermann, Song, and Gage 2015). In the following section, I will review the importance, function and regulation of adult neural stem cells.

1.1 Adult neurogenic niches

In the adult brain, NSCs are found in niches and retain their neurogenic capacity, which is believed to support neuronal plasticity and regenerative capacity (Kempermann, Song, and Gage 2015; Bond, Ming, and Song 2015). In the murine brain, V-SVZ and SGZ are the two extensively studied stem cell niches. V-SVZ stem cells are enriched in the lateral ventricular walls that migrate and differentiate throughout the rostral migratory stream (RMS). SGZ also continually produce neurons in the granular cell layer and integrate into the hippocampal network, providing synaptic plasticity. Due to the microenvironment and distinct nature of these NSCs, V-SVZ and SGZ stem cells serves different purposes. While V-SVZ-born NSCs repopulate olfactory interneurons, it also can be stimulated during injury and NSCs can migrate to the injury site for endogenous repair. SGZ-born NSCs reside within the hippocampus that has primary role in learning-associated neuronal plasticity.

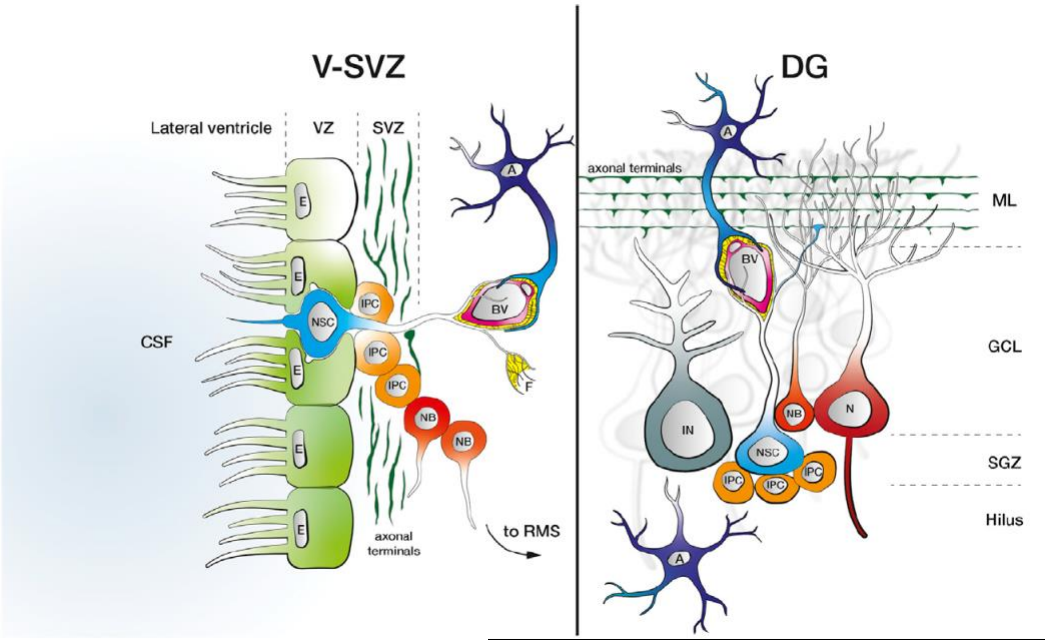

Adapted from (Urban, Blomfield, and Guillemot 2019)

Figure 1: Schematic representation of the niches of the ventricular-subventricular zone (V-SVZ) and dentate gyrus (DG) Adult neural stem cells in these two locations share many

characteristics but are also regulated by different signals arising from their distinct environments. For instance, V-SVZ NSCs are directly regulated by factors present in the cerebrospinal fluid, while DG NSCs receive feedback from the neurons they generate, which settle in the granule cell layer. A, astrocytes; BV, blood vessel; CSF, cerebrospinal fluid; E, endothelial cell; F, fractone; GCL, granule cell layer; IN, interneuron; IPC, intermediate progenitor cell; ML, molecular layer; N, neuron; NB, neuroblast; NSC, neural stem cell; RMS, rostral migratory stream; SGZ, subgranular zone; V-SVZ, subventricular zone; VZ, ventricular zone. Adapted from (Urban, Blomfield, and Guillemot 2019).

1.2 Subventricular zone stem/progenitor cell pool

The V-SVZ is considered the largest germinal region in the adult brain and the niche consists of three subpopulations: quiescent NSC pool (Type B), progenitors (Type C), and committed neuroblasts (Type A) (Garcia-Verdugo et al. 1998). Type B cells exist in quiescent or activated state, proliferative stem cells go through symmetrical division to expand the NSC pool while asymmetric division generate transiently amplifying progenitors (Type C cells).

Ventricular V-SVZ type B cells are derived from embryonic radial glia cell that is both self-renewing and multipotent in nature. V-SVZ NSCs are in contact with ependymal cells and adjacent ventricles vascular layer and inherently pose apical-basal polarity. Basal NSCs significantly contribute to olfactory neurogenesis and the apical NSCs, which contacts lateral ventricle through Notch signalling, and maintain NSC homeostasis in V-SVZ niche (Baur et al. 2022). The molecular signature of these cells consists of several identifying markers include GFAP, Nestin, BLBP, CD133, and GLAST. Oct4+GFAP- primitive cells are thought to have given rise to the GFAP+ NSCs in the niche (Cebrian-Silla et al. 2021). These definitive NSCs also pose dorsal and ventral differences due to regional identity. This dorsal-ventral identity is thought to have a distinct molecular signature of the neuronal lineage transition (Otsuki and Brand 2019).

Transiently amplifying progenitors (TAP), classically marked by *Ascl1*, *Tbr2*, and *Dlx2* are a rapidly expanding population that migrates along the RMS. Neuronal subtype specifications are

diversified in these clonal cells depending on their location. These neuronal commitments are regulated by transcription factors partly specified by the molecular gradients in the niche (Batista-Brito et al. 2008). Since type B cells are multipotent, GFAP+ NSCs generate astrocytic lineage and oligodendrocyte precursors. Mature astrocytes and oligodendrocytes are differentiated through these progenitors along the RMS periodically and upon stimuli (Menn et al. 2006).

Upon specification, the neuroblasts migrate along the RMS and distribute radially in the olfactory bulb (OB). Neuroblasts migrating through the RMS is a distinctive process and connect to each other to form a chain and navigate through the glial sheath along the stream, which is known as 'chain migration'. The interaction between cells is facilitated by β1 integrin and laminin to form the cell chain. Secreted factors are also shown to help guide the neuroblasts in the RMS (Belvindrah et al. 2007; Zhao et al. 2022). While migrating towards the OB, neuronal specification of differentiating neuroblasts also acquire diversification programming through several transcription factors dominating among subsets of interneurons (Mizrak et al. 2019). V-SVZ NSCs therefore play an important role in neural plasticity. Adult V-SVZ and OB neurogenesis is an important model to understand stem cell regulation, diversification, and neural plasticity.

1.3 Adult Hippocampal Neurogenesis

New neuronal integration in pre-existing circuits of hippocampal network is essential in cognitive functions such as consolidating novel experiences and learning (Toda et al. 2019). The source of adult-born new neurons in the SGZ are Type I cells, which are primarily quiescent radial glia-like stem cells (RGL) expressing the self-renewal gene, *Sox2*, and are marked by expression of Nestin and GFAP. Unlike V-SVZ stem cells, *Hopx*, an exclusive marker of resident NSCs in adult hippocampus can be traced back to hippocampus development during embryonic development (Berg et al. 2019). Type IIa transiently amplifying progenitor cells are distinctly

defined by *Tbr2* and *Ascl1*, in addition to continued *Sox2* expression (Arnold et al. 2008). Type IIb cells are distinct from Type IIa by a further commitment to neuronal lineage and become progenitors, expressing *Dcx* and *NeuroD1*. Thus, this reflects a transition from self-renewal ability towards neuronal determination (Suh et al. 2007). Type III migratory neuroblasts express *Prox1*, a marker for further neuronal commitment, continue to express *Dcx* and *NeuroD1*, and a complete lack of *Sox2* expression (Iwano et al. 2012). Type III neuroblasts lose their proliferative capacity by exiting the cell cycle and entering a terminally differentiated stage (Lavado and Oliver 2007). Adult-born neurons arise from NSCs that continually integrate into the hippocampus. According to rodent studies, it takes 4 to 6 weeks for RGL cells to become mature neurons and functionally integrate into the hippocampal network. Thus 4-6 weeks is considered the critical period for any manipulation of hippocampal neuronal plasticity in the context of learning and memory formation (Gu et al. 2012; Denny et al. 2012). In rodents, neurogenic niches are suggested to contribute to new memory formation and replenish interneurons in the olfactory bulb throughout their lifetime. DG neurogenesis in the adult hippocampus allows synaptic plasticity to improve learning and memory (Clelland et al. 2009; Shors et al. 2001). Maturation of newly formed neurons in the DG integrates into a three-synaptic network to form the DG-CA3-CA1-Entorhinal cortex circuit, which is essential for adult hippocampal-dependent spatial memory formation (Deng, Aimone, and Gage 2010). Physical activity-dependent enhanced neurogenesis is believed to improve cognitive function in aging conditions (van Praag et al. 2005). Results from subsequent studies which investigated pharmacological substances that alter NSC suggest a correlation of many antidepressants and mood stabilizers with increased hippocampal neurogenesis (Scharfman and Hen 2007). Thus, the importance of adult neurogenesis is becoming increasingly clear, yet regulation of neurogenesis remains to be explored.

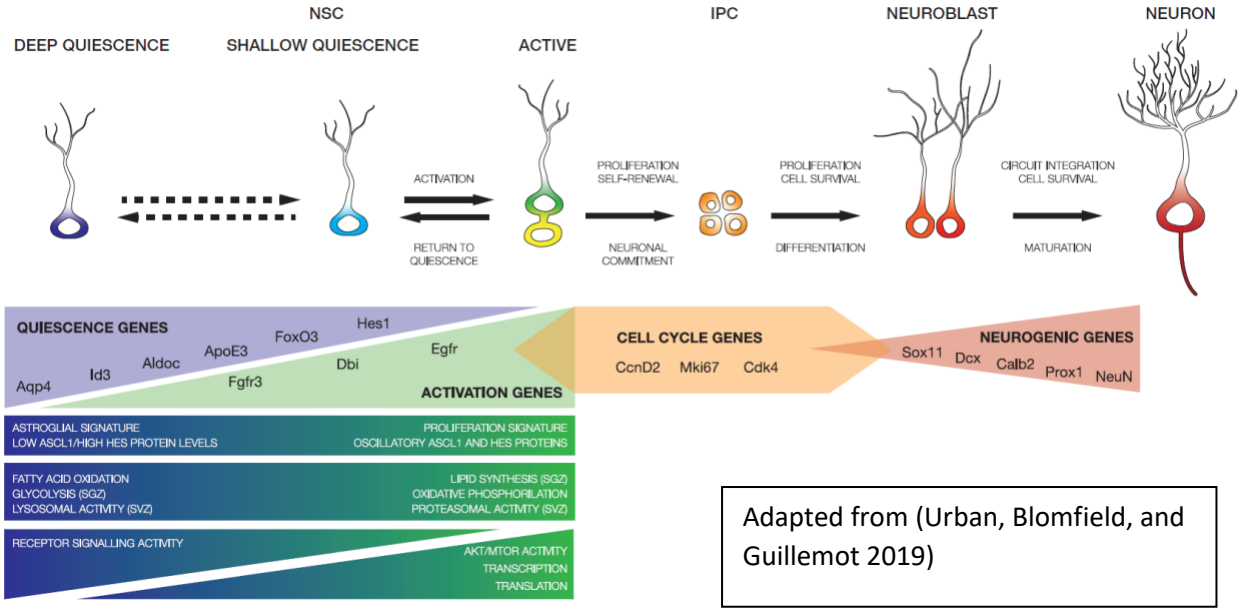

Figure 2: Regulation of adult NSC fate regulation Neural stem cells in the subgranular zone and ventricular-subventricular zone display extensive changes in gene expression and cellular physiology as they transit between deep quiescence, shallow quiescence, and active state and differentiate into intermediate precursor cells, neuroblasts, and neurons. Extracellular signals can regulate the transitions between quiescent and active states as well as later stages in the neurogenic lineage. Adapted from (Urban, Blomfield, and Guillemot 2019).

RGL cells shuttle between quiescence and activated states. While symmetric division expands RGL cells and self-renewal, asymmetric division maintains the RGL pool and leads to hippocampal neurogenesis. Long-term maintained RGL cells are activated to give rise to highly proliferative non-radial glial cells that expand to give rise to daughter neurons (Pilz et al. 2018). These RGL cells can be further characterized by their proliferation behavior that are marked by expression of *Gli1* and *Ascl1*. Live *in vivo* clonal analysis studies of RGL cells labeled with *Gli1* showed that their progeny gave rise to smaller clonal cells suggesting Gli1+ RGL are slow dividing and self-renewing population. *Ascl1*+ traced RGL cells are generally activated and potentiate neurogenesis (Bottes et al. 2021).

RGL cell-derived TAP cells are highly proliferative and marked by *Eomes* or *Tbr2* in the embryonic and adult neurogenic niche. This specification is due to *Tbr2*-mediated suppression of

the stem cell marker *Sox2* (Hodge et al. 2012). Rapidly dividing TAP cells expand several times and differentiate into neurons (Pilz et al. 2013). Knockout studies suggest that loss of *Tbr2* blocks the progression of TAP and increases the stem cell pool due to the lack of *Sox2* repression (Hodge et al. 2012). On the contrary, *Tbr2* over expression decreases *Sox2+* stem cells in pluripotent stem cells (Teo et al. 2011). These studies highlight the tight regulation of transcription factors in specification of cell types.

Newborn neurons are the population formed after rapid expansion of progenitors that exit the cell cycle. Transition from TAPs to neuroblast is marked by expression of *Dcx*, a microtubule associated protein (Koizumi et al. 2006); mutations in *Dcx* results in lissencephaly. The *Dcx+* cell also acquires a neuronal morphology by extending neurites. Majority of the newly formed neurons do not survive in the adult hippocampus unless the cell makes functional connections with the hippocampal pyramidal neurons. Once the newborn neurons exit cell cycle, there is a persistent expression of neuronal nuclei (*NeuN*), which- marks postmitotic neuronal specification (Brandt et al. 2003). Newly formed neurons display plasticity in structure and function. Maturation of neurons extensively occurs during dendritic remodelling and functional integration.

2. Neural stem cell regulation

During adult neurogenesis, various mechanisms impact quiescence, activation, proliferation, and commitment of NSCs. Maintenance and neurogenesis of NSCs are dynamic processes driven by an ever-growing list of stratified gene regulations. Cell-intrinsic mechanism and niche stimuli concurrently modulate the responsiveness of NSCs and influence neurogenesis. There has been a intense pursuit to identify the origin of NSCs in the adult niche soon after the identification of adult-born neurons. A subset of slowly dividing embryonic origin neural stem cells gives rise to

the adult born quiescent NSCs (qNSCs) that are maintained during the animal's lifespan (Furutachi et al. 2015). Symmetric cell division of qNSCs results in maintenance of NSC pool while asymmetric division gives rise to the expansion of progenitor population and eventual neuronal progeny. Previous studies posited that RGLs divide slowly to maintain cell identity and give rise to TAPs, which divide once or twice and exit the cell cycle to make newborn neurons. However, a recent model suggests that RGLs divide symmetrically two to three times and then stochastically produce neuronal progenitors and TAP cells. Unlike previously thought, TAP cells undergo multiple cell cycles to generate newborn neurons that have an immense role in long-term neurogenesis (Gotz 2018; Pilz et al. 2018). Although existing studies suggest how the NSC pool is maintained, novel mechanisms are being explored on how neurogenesis is regulated throughout life.

In the mammalian brain, the adult hippocampal DG harbors NSCs, which generate new neurons throughout adulthood. Canonical transcriptional machinery, growth factors, sonic hedgehog, Notch, Wnt signaling, proneural gene *Ascl1*, and metabolism are just a few of the many factors known to regulate the stem cell niche and function (Raposo et al. 2015; Andersen et al. 2014; Lange et al. 2016; Madhavan, Ourednik, and Ourednik 2006; Lugert et al. 2010). Niche plays a vital role in determining the cell fate by physical interaction with other cell types (Goncalves, Schafer, and Gage 2016).

Neural plasticity in the adult niche provides new neuronal circuit interactions that continues throughout life. It is interesting that neural plasticity is observed only in few exceptional regions of the brain. In rodents, olfactory neurogenesis-derived interneurons fine tunes novel olfactory sensations and enrichment in odour discrimination that is critical for rodent spatial navigation and learning (Lledo and Valley 2016). Adult hippocampal neurogenesis is crucial for forming new

episodic memories with implications in cognitive learning and emotion. Pattern separation is a process by which the DG transforms experiences into discrete, non-overlapping representations (Treves et al. 2008). Adult new-born neurons in the DG modulates pattern separation and thus provides strategies to treat anxiety disorder and age-related memory impairment (Sahay et al. 2011). Consolidation of reversal in spatial learning (in response to new location) is cued by novel exploration, thereby registering the spatiotemporal pattern (Vorhees and Williams 2006). Memory persistence is a process of reactivating the patterns of neural activity (Richards and Frankland 2017). Adult neurogenesis uniquely modulates the memory persistence by increasing neurogenesis during infancy or in adulthood by exercise, which promotes forgetfulness. Conversely, a suppression of neurogenesis following training leads to the memory persistence and retention (Akers et al. 2014). Thus, adult hippocampal neurogenesis provides the flexibility to promote natural forgetfulness and adaptive neural plasticity (Ryan and Frankland 2022).

Aging, neurodegenerative diseases, and oxidative stress exhibit impaired long-term maintenance, activation, and function of NSCs contributing to cognitive decline (Hamilton et al. 2015; Villeda et al. 2011). Conversely, physical exercise, dietary supplements, and neurotrauma induce NSC proliferation (van Praag, Kempermann, and Gage 1999; Zhang et al. 2016). Thus, understanding the physiological and pathological mechanisms that modify stem cell maintenance, proliferation, and neurogenesis is important for future therapies directed to improve cognitive function (Lugert et al. 2010). Recent studies have shown that changes in mitochondrial function have a major impact on the fate of embryonic and adult NSCs (Khacho et al. 2016; Khacho et al. 2017). Thus, targeting mitochondrial function in NSCs could provide clues to identify novel regulatory mechanisms.

2.1 Stem cell quiescence and activation

The choice between quiescence and activation is one of the prominent stem cell regulatory processes. NSCs in the adult hippocampus are largely quiescent (Type 1 RGL cells) and are activated when they receive signals to become Type 2 cells expressing activation markers and neurogenic factors that distinguish cell types (Codega et al. 2014). Stem cell quiescence and activation are polarizing cellular states that maintain stem cells in the adult niche. Novel transcriptomic analysis at single cell resolution revealed that NSC heterogeneity possibly stems from differences in the depth of quiescence (Artegiani et al. 2017; Basak et al. 2018; Hochgerner et al. 2018; Llorens-Bobadilla et al. 2015). Quiescence is an inactivated state where cells remain in postmitotic G0 phase of the cell cycle and is graded into several categories based on the responsiveness of stem cells to exit transient cell cycle arrest (Urban and Cheung 2021; Harris et al. 2021a). A general feature of quiescence is the global reduction in mRNA production, protein synthesis and metabolic activity (Cheung and Rando 2013). Loss of quiescence can lead to premature differentiation and exhaustion of the stem cell pool (Renault et al. 2009). On the other hand, processes such as aging and neurodegeneration enhance deep quiescence that results in failed stem cell activation. Entry mechanisms into quiescent state are regulated at the level of cell cycles through CDKs, cyclins, and cyclin inhibitors. Recent understanding in stem cell maintenance reveals that adult NSCs are specified at the embryonic stage during brain expansion. A subset of slowly dividing embryonic, p57-expressing NSCs maintain their quiescent stem cell state and populate adult niche (Furutachi et al. 2015). Preservation of NSCs maintains adult neurogenesis throughout life. More emerging evidence are emerging about the embryonic origin of adult NSCs. For instance, Hopx+ cells are the pioneering cells that initiate, develop, and reside the adult

hippocampus (Berg et al. 2019). Hopx+ cells in adult hippocampus are resident NSCs which are activated throughout life.

Exit from quiescence in NSCs removes cell cycle repression and is triggered by neuronal hyperactivity or injury, however chronic activation can deplete the qNSC pool (Sierra et al. 2015). Cellular organelles and their activity regulate other mechanisms. For example, dysfunctional lysosomes with large protein aggregates are present in qNSCs of aging hippocampus. Clearing these aggregates by enhancing lysosomal catabolism triggers stem cell activation and rejuvenation (Leeman et al. 2018). Thus, lysosomal activity is crucial in autophagy and maintenance of intracellular organelles including mitochondria. These mechanisms imply the application of therapeutic strategies for modulating aging related quiescence vs activation.

2.2 Transcriptional regulation of neurogenesis

The interplay between intrinsic/extrinsic signalling leads to classic genetic regulation by set of transcription factors that play a vital role in NSC signaling, activation, and neurogenesis. NSCs are known to be regulated by stage-specific transcription factors that are reviewed here (Goncalves, Schafer, and Gage 2016). The knowledge of transcriptional interactions altered by key regulators is ever increasing with recent findings using single cell RNAseq (Borrett et al. 2020; Harris et al. 2021a). Activation of several factors depending on the redox status of a cell regulates classic stem cell functions such as self-renewal. In this dissertation, regulators such as Ascl1, E2Fs, Rb, REST are highlighted, with an emphasis on NSC fate determination.

2.2.1 Rb-E2F interaction in the NSC fate decision

Rb is a tumor suppressor and a gatekeeper of the cell cycle S phase progression, which prevents cell cycle re-entry in postmitotic neurons and other differentiated cells. Dysregulation of the Rb pathway leads to unregulated cell proliferation. Rb and its family of proteins (pRb, p107 and p130)

regulate G1/S cell cycle transition through the active form of monophosphorylated Rb family whereas hyperphosphorylation inactivates Rb family through Cyclin E/Cdk2 complexes, which enables the cell to proceed through cell cycle.

The E2F family of transcription factors plays a critical role in cell cycle DNA synthesis and cell cycle regulation and are considered a prime target of Rb family tumor suppressor activity (Chellappan et al. 1991). Functionally E2Fs consist of activator E2Fs (E2F1/2/3a) and repressor E2Fs (E2F3b, E2F4-8). The activator E2Fs include DNA polymerase α and cyclins A/E (Lundberg and Weinberg 1998), whose induction targets late G1 to early S phase and is sufficient for cells to enter cell cycle from a quiescent state (Takahashi, Rayman, and Dynlacht 2000). The repressor E2F4 binds certain promoters and recruits p130 in G0 and early G1, resulting in transcriptional repression and decreased histone acetylation (Takahashi, Rayman, and Dynlacht 2000).

The requirement for pRb-E2F interaction in nervous system development through cell cycle progression affects NSC fate decision, entry and exit from quiescence and also in the regulation of neuronal migration by repressing Neogenin, an E2F3 target and a repressive guidance molecule. Loss of pRb-induced aberrant Neogenin expression and interaction with Netrin1 resulted in embryonic neuronal migration defect (Andrusiak et al. 2011). In the adult V-SVZ NSCs, Rb influences progenitor proliferation and long-term survival of newborn neurons while having no apparent effect on NSC self renewal in RMS.

2.2.2 ASCL1

Ascl1 (achaete-scute family bHLH transcription factor 1) is a key transcription factor in proneural transition and has been well studied in embryonic brain development. Ascl1 and its target genes play an essential role in cell cycle exit and activating proneural transcription factors to proceed with neurogenesis. In the embryonic cortex, Ascl1 inversely oscillates with Hes1 and

then stably express in GABAergic neuronal specification. Recent focus has shifted to Ascl1 function in residing NSCs and progenitors in embryonic and adult brains. Ascl1 targets in the embryonic cortex are regulators of canonical cell cycle genes such as E2f1 in progenitors (Castro et al. 2011; Andersen et al. 2014). The oscillation dynamic of Ascl1 and Hes1 regulates adult DG NSCs at the level of activation/quiescence. Hes1-mediated repression of Ascl1 prevents NSC activation thereby maintaining a quiescent NSC pool (Sueda et al. 2019). Knockout of Ascl1 in the adult hippocampus results in failed activation and the NSCs remain quiescent, suggesting that Ascl1 functions in priming and transcriptional control of mitogenic activity of the NSCs (Andersen et al. 2014).

Given the abundance-dependent effect of Ascl1 in NSC activation, this transcription factor is considerably regulated to limit its levels. For example, the E3 ubiquitin ligase Huwe1 (HECT, UBA, and WWE domain–containing 1) regulates Ascl1 post translationally by degrading Ascl1. in the embryonic and adult nervous systems. Loss of Huwe1 increases Ascl1 protein levels and disrupts the oscillation. Excessive Ascl1 increases NSC activation and proliferation while decreasing progenitor pool and neuroblasts in the adult hippocampus (Urban et al. 2016). This interaction has been studied in physiological conditions by time course analysis of NSC proliferation in the adult hippocampus in an age dependent manner. Juvenile mice harbor the highest number of activated Ascl1+ RGLs, which declines steeply in adulthood and this finding is supported by the age-dependent accumulation of Huwe1, which further deepens the quiescence state of adult cells (Harris et al. 2021a).

The abundantly present inhibitor of differentiation/DNA binding protein 4 (ID4) in qNSCs sequesters Ascl1 and inhibits its DNA binding and degrades Ascl1 through the proteosome pathway. By regulating Ascl1 levels, ID4 regulates NSC quiescence in the adult hippocampus and

this process has been demonstrated *in vitro* by the addition of BMP4 and FGF2, which regulates Ascl1 levels wherein BMP4 triggers ID4 levels that decreases the activation marker Ascl1 (Blomfield et al. 2019).

2.2.3 REST

RE1-Silencing Transcription factor (REST), one of the Gli-Kruppel family of transcriptional repressors, once characterized as a neuron restrictive silencer factor is a repressor of neural genes in non-neuronal cell types. REST-mediated gene repression was then elaborated to a wider cell type including postmitotic neurons, which is reviewed in (Martin and Grapin-Botton 2017). Due to the broader landscape of chromatin binding, REST targets are unique in stage-specific control of neuronal commitment. REST-mediated transcriptional repression affects genes encoding characteristic neuronal function such as neurite outgrowth, axonal guidance, ion channels, synaptic vesicle proteins, and neurotransmitter receptors. Several studies show the importance of REST function in NSC maintenance. In chicken embryonic neurogenesis, REST restricts Sox4 and Sox11 in undifferentiated neural cells independent of cell cycle exit (Bergsland et al. 2006). In type I cells, REST inhibits precocious neuronal differentiation (Gao et al. 2011). In mammalian adult hippocampal neurogenesis, REST maintains undifferentiated state of NSCs by restricting neuronal differentiation genes such as *Ascl1* and *NeuroD1* in a biphasic manner. REST is enriched in qNSCs and in subset of activated Ascl1+ and NeuroD1+ neuroblasts the REST levels go down. But then REST, upregulates in terminally differentiated granular neurons. Loss of REST in qNSCs result in NSC activation (by *Ascl1*) and progenitor proliferation. Targeted deletion of REST in progenitors decreases TAP proliferation and increased neurogenesis (Mukherjee et al. 2016).

Collectively, REST is a master regulator of NSC maintenance through two key steps. First, in early requirement at the qNSC stage to maintain the pool and second, during neuronal specification.

2.3 Metabolic regulation of NSCs

Cellular metabolism plays a central role in generation of energy for varying NSC functions (Chandel et al. 2016; Chakrabarty and Chandel 2021). NSCs have a unique metabolic signature that is distinct from their differentiated counterparts. As development progress and nutritional requirements change, there is a shift from glycolysis to oxidative phosphorylation (OXPHOS) (Homem, Repic, and Knoblich 2015; Zheng et al. 2016). Early embryonic NSCs are mostly dependent on glycolysis, while differentiated neurons rely more on OXPHOS (Shyh-Chang, Daley, and Cantley 2013; Zheng et al. 2016). Mitochondrial biomass increases with differentiation to cope with an increase in energy demand. Quiescent stem cells residing in the V-SVZ are like a primitive cell type and depend on glycolysis. NSCs that undergo active proliferation show distinct changes in *de novo* fatty acid oxidation (FAO), suggesting a concurrent metabolic shift in cells during lineage progression (Knobloch et al. 2013; Knobloch et al. 2017). Although glycolysis and FAO are believed to be the major energy sources for NSCs, OXPHOS also contributes to metabolism in proliferating NSCs (Adusumilli et al. 2021; Ahlqvist et al. 2012; Beckervordersandforth et al. 2017). Self-renewing NSCs in the adult brain express glycolytic and FAO enzymes, and any disruption results in abnormalities in the NSC niche (Hamilton et al. 2015). A basal level of mitochondrial metabolism is however considered important in NSCs function. Recently, the focus has shifted from energy production to the regulatory role of metabolism in stem cells (Shin et al. 2015; Chandel et al. 2016). The metabolic signatures and shifts described

above are now considered on par with the stage-specific regulation of neurogenesis. The scope of these metabolic signatures on NSCs will be discussed in the sections below.

2.3.1 Metabolic profiling of NSCs

The diversity within the NSC pool stems from their morphology, cellular markers, and transcriptional profiles. Similar mechanisms in metabolic preferences distinguish stem cells and their activity. Fatty acids are one of the primary sources of energy in adult NSCs. Proliferative activity in hippocampal NSCs is coupled with lipid metabolism, particularly *de novo* lipogenesis (Knobloch et al. 2013). The authors showed that lipogenesis is active in highly proliferating NSCs through Fatty Acid Synthase (Fasn) utilizing malonyl-CoA and thus generation of new complex fatty acids. Quiescent NSCs show high carnitine palmitoyltransferase (Cpt)1 activity and hallmarks of increased FAO. Quiescent NSCs restrict their proliferation by expressing Spot14 (Thrsp), a negative regulator of Fasn, which inhibits liponeogenesis and thus limiting levels of malonyl-CoA (Knobloch et al. 2013). The allosteric inhibition of Cpt1 by malonyl-CoA during fatty acid synthesis prevents a futile cycle. Concurrent decrease in Spot14 and elevation of malonyl-coA primes NSCs to actively proliferate (Knobloch et al. 2017). Collectively, presence of Spot14 is now recognized as a hallmark of qNSCs whereas Fasn marks activated NSCs.

In embryonic cortex development, Fasn requirement is important for brain development, suggesting its role in active proliferation. Fasn-knockout results in microcephaly due to failure in progenitor formation from radial glia (Gonzalez-Bohorquez et al. 2022). Molecular profiling through single cell analysis shows high glycolytic and lipid metabolism in adult V-SVZ qNSCs (Llorens-Bobadilla et al. 2015) as well as *de novo* synthesis, and high levels of FAO in qNSCs. It has been suggested that increase in the rate-limiting levels of Cpt1a and its mitochondrial shuttle of fatty acids are crucial for the qNSC state along with increase in Spot14 levels (Knobloch et al.

2017). As lipid metabolism is intricate in stem cell maintenance, certain neurodegenerative diseases such as Alzheimer's Disease shows certain abnormalities in lipid metabolism with lipid accumulation in the brain along with other dementia-related pathologies. Particularly, accumulation of lipid droplets (LD) in the V-SVZ is responsible for induced quiescence in NSC and negative regulation of NSC activation and proliferation (Hamilton et al. 2015).

2.3.2 Metabolic shift in NSCs

The NSC developmental process is coordinated by preferred transcriptional regulation, cell signalling and metabolism unique to every progressive stage. Metabolic pathways provide energy and the metabolites serve as precursors of several cellular functions. The cellular requirement and metabolic preferences of proliferating, non-proliferating and differentiating population of adult NSCs are unique. NSCs utilize metabolites from the TCA cycle and glycolysis to produce nucleotide biosynthesis for cell growth. Postmitotic neurons, due to their high energy demands and mature mitochondrial structure, utilize OXPHOS to maximize energy production (Zheng et al. 2016). Highly glycolytic mature astrocytes supply building blocks for neurotransmitter to surrounding neurons. Acquiring unique metabolic signature through differentiation is being studied extensively. Single cell analysis using "Waterfall" algorithm quantifies gene expression to reconstruct molecular transition that organizes these cells in transition. This pseudotime analysis characterizes cells in continuous transition based on transcriptome dynamics (Shin et al. 2015). NSCs retain astrocytic features and quiescence due to ensured dependency on glycolysis (Beckervordersandforth et al. 2017; Llorens-Bobadilla et al. 2015). A decrease in glycolytic genes and increase in OXPHOS occur in the neuronal differentiation program (Beckervordersandforth et al. 2017; Shin et al. 2015; Khacho et al. 2016). Accumulation of LDs and LD coat protein Perilipin2 (Plin2) abundance is unique in NSCs, which significantly decreases in differentiated

neurons *in vitro*. Furthermore, asymmetrical accumulation ensures quiescence in high LD-containing NSCs *in vitro* (Ramosaj et al. 2021).

3. Mitochondrial function in NSC regulation

Mitochondria have been in the spotlight given the amount of information on metabolic requirement in NSC regulation. A recent report suggests that forced disruption of mitochondrial metabolism in NSCs switches their metabolism to glycolysis resulting in oncogenic transformation via p53 inactivation (Bartesaghi et al. 2015). Another study found the loss of mitochondrial transcription factor TFAM in adult NSCs disrupts OXPHOS, thereby accelerating aging phenotype through impaired neurogenesis (Beckervordersandforth et al. 2017). These findings suggest a coupling of energy metabolism with NSC lineage progression.

Recent evidence suggests that metabolic changes are not a consequence but a contributing factor in stem cell fate decisions (Wei et al. 2018). Metabolic shifts are accompanied by increase in mitochondrial mass and integrity, which are essential in lineage progression (Wang et al. 2010). Mitochondria mature during hippocampal neurogenesis as the NSC progresses through neurons. Mitochondrial DNA mutations increase the vulnerability to oxidative stress. Such mitochondrial dysfunction hinders neuronal differentiation (Wang et al. 2011). Not only through metabolism, but mitochondria as an organelle, contributes to NSC function partly because of reactive oxygen species (ROS) generation in mitochondria. Thus, emerging evidence suggests an intrinsic role for mitochondrial dynamics/metabolism in shaping NSC fate decision.

3.1 Mitochondrial dynamics

Mitochondria are dynamic organelles that undergo structural changes such as fusion and fission, which are believed to alter its function. Mitochondrial structure undergoes modification

during the course of development and in various tissues (Chan 2006a). Mitochondrial fusion is essential in matrix content exchange between mitochondria. During fusion, a network of mitochondria forms an elongated structure. Fusion is a result of mitochondrial membrane GTPases including Optic atrophy 1 (OPA1) and Mitofusin 1 and 2 (MFN1&2) working together; which are expressed in the inner and outer mitochondrial membranes, respectively (Chen et al. 2003; Cipolat et al. 2004). Mitochondrial fission is initiated by the recruitment of Dynamin-related protein 1 (Drp1) from the cytosol to the mitochondrial outer membrane causing outer membrane constriction and organelle fission. Endoplasmic reticulum (ER) contact sites become the origin of the fission process that led to fragmentation (Friedman et al. 2011; James et al. 2003). Human OPA1 or MFN2 mutations result in disrupted mitochondrial fusion and are associated with hereditary neurodegenerative diseases such as Autosomal Dominant Optic atrophy (Alexander et al. 2000; Delettre et al. 2000) and Charcot-Marie-Tooth Disease (Zuchner et al. 2004). Opa1 in the inner mitochondrial membrane plays a critical role in mitochondrial membrane integrity. Opa1 deletion can result in mitochondrial DNA mutation as it affects cell growth (Chan 2006b). Opa1 exhibit short (s-Opa1) and long Opa1 (l-Opa1) due to proteolytic processing by OMA1 or YME1L (Anand et al. 2014). Both forms retain GTPase activity while s-Opa1 loses fusion capacity. Reports suggest an essential role of s-Opa1 in mitochondrial function and cristae structure maintenance (Varanita et al. 2015).

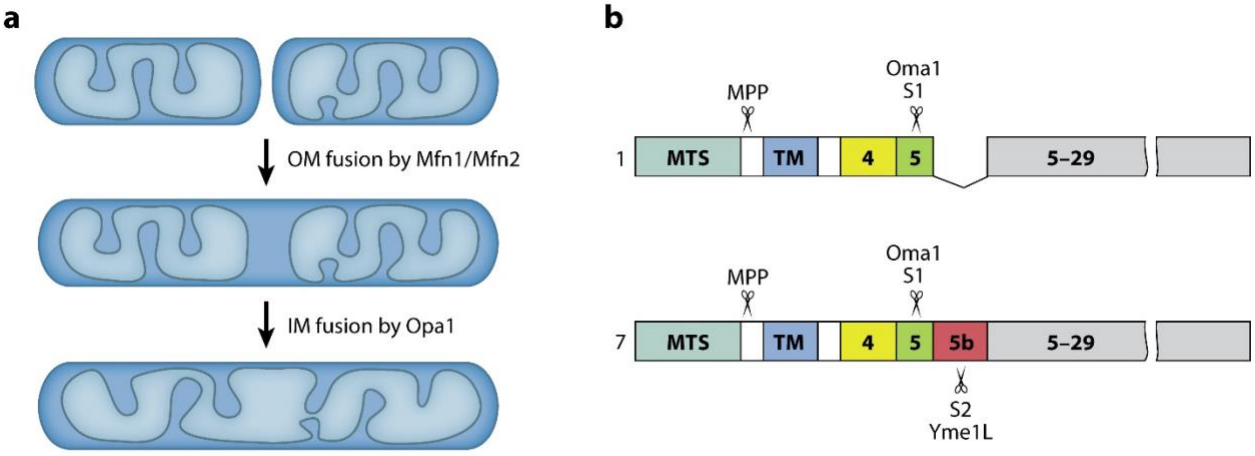

Chan DC. 2020.
Annu. Rev. Pathol. Mech. Dis. 15:235–59

Figure 3: The fusion machinery (a) Mitofusins mediate outer membrane (OM) fusion; Optic Atrophy 1 (Opa1) mediates inner membrane (IM) fusion. (b) Schematic of two of the eight RNA splice forms of Opa1. Isoform 1 generates a precursor whose N-terminal mitochondrial targeting sequence (MTS) is cleaved upon import to yield long Opa1. This long form can be further processed by Oma1 at the S1 site to yield short Opa1. For isoform 7, the long form can be processed by either Oma1 at the S1 site or Yme1L at the S2 site. Abbreviations: MPP, matrix processing protease; TM, transmembrane. Adapted from (Chan 2020).

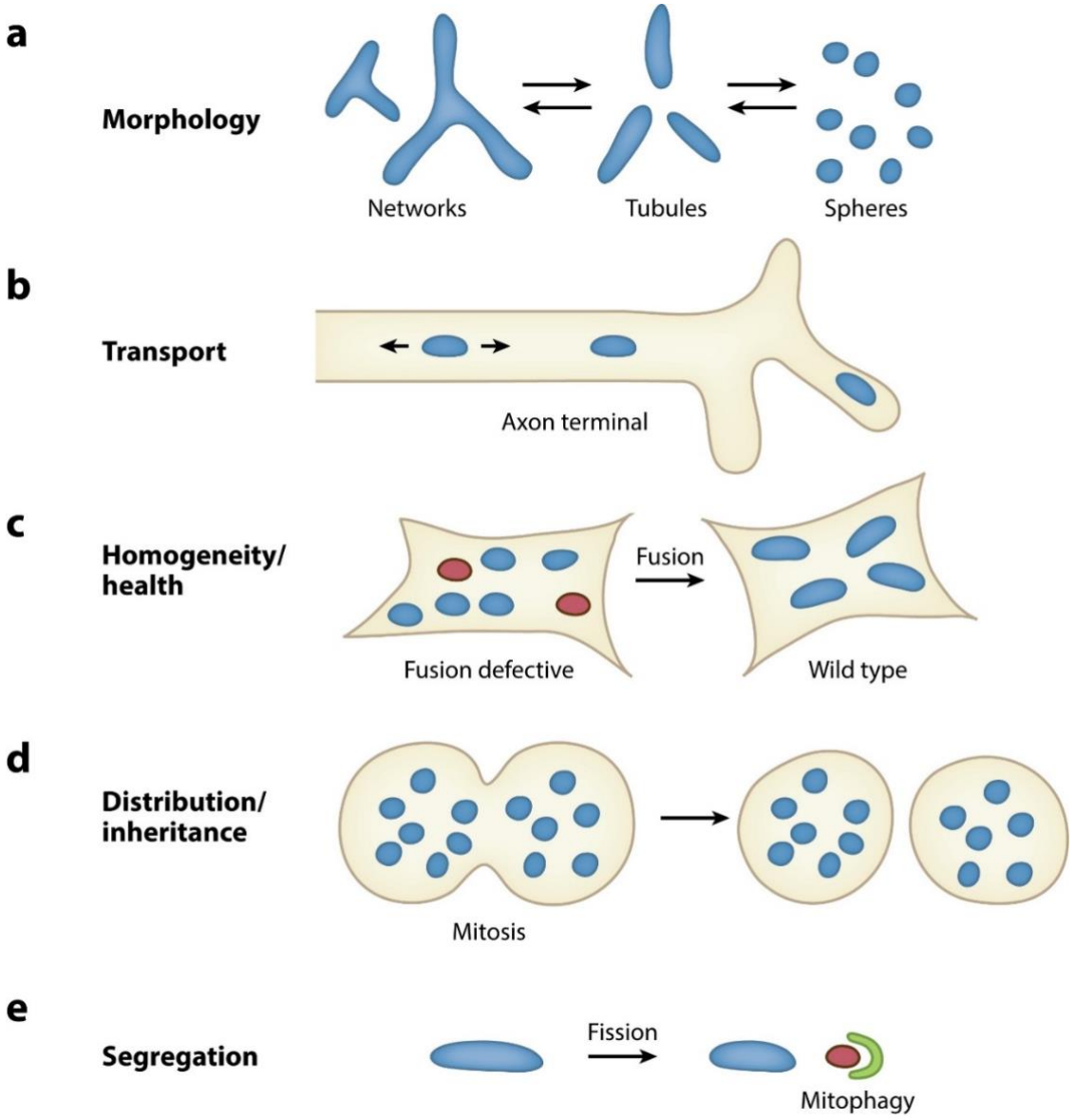

Figure 4: The benefits of mitochondrial dynamics Schematic shows how mitochondrial fusion and fission affect mitochondrial function. Red indicates a damaged or dysfunctional mitochondrion. (a) The balance between fusion and fission controls mitochondrial shape, number, and size. (b) Mitochondrial fission results in smaller mitochondria that are more efficiently transported in axons. (c) Mitochondrial fusion promotes maintenance of a homogeneous mitochondrial population that can tolerate higher levels of mitochondrial DNA mutations. (d) Mitochondrial fission during mitosis facilitates equitable inheritance by daughter cells. (e) Mitochondrial fission generates small mitochondrial fragments that can be engulfed by autophagosomes during mitophagy. Adapted from (Chan 2020).

While in the steady state, mitochondrial dynamics is a coordinated cycle of fission and fusion, increase in either fusion or fission occurs in certain contexts. For instance, increased mitochondrial fusion occurs during neuronal differentiation and energy starvation. This stress-induced mitochondrial tubulation is important for efficient energy production and mixing the mitochondrial metabolites and DNA content. Fission is a selective process depending on cellular contexts such as cell division and selective mitophagy. During cell division, the midzone division yields two equal sized mitochondria that occur in the proximity of the ER. A peripheral division occurs when a portion of mitochondria that separates due to lower membrane potential or high levels of ROS in the proximity of lysosome for effective mitophagy (Kleele et al. 2021). Thus, fusion and fission have their own roles to maintain mitochondrial dynamics that are important for mitochondrial health with respect to metabolism, apoptosis, autophagy, and calcium homeostasis. How mitochondrial dynamics regulates biogenesis during neuronal fate determination is currently being explored.

Data from our laboratory and others suggest that the neuronal lineage progression of uncommitted NSCs to mature neurons is fueled by metabolic shifts in mitochondria. In the developing mouse brain, uncommitted $Sox2^{+}$ stem cells are predominantly glycolytic and possess elongated mitochondria, whereas committed, proliferating $Tbr2^{+}$ neural progenitor cells possess fragmented mitochondria, showing a clear cell-type specific difference in mitochondrial dynamics (Khacho et al. 2016). Mitochondrial structural maturity is correlated with metabolic activity of the cells. Uncommitted NSCs that pose fragmented mitochondria are predominantly glycolytic, whereas neurons that harbor mature networks of mitochondria are more reliant on OXPHOS machinery. Although NSCs are glycolysis dependent, mitochondria play a crucial function in their cellular state, metabolism, nuclear gene regulation, signaling cascade and stress response (Khacho

et al. 2016; Khacho et al. 2017; Beckervordersandforth et al. 2017; Zhang et al. 2016). Electron microscopic ultrastructural analysis of mitochondrial volume in adult SGZ showed a similar, but slightly, unique mitochondrial structural diversity compared to the embryonic layers. In adult hippocampal NSCs, mitochondrial structural morphology is different in cellular compartment. Near the cell body and primary process of RGL cells, mitochondria assume a globular and tubular shape with more volume when compared to mitochondria in the fine processes of RGL cells. The intermediate progenitors maintain slightly elongated and voluminous mitochondria compared to NSCs. Similar to embryonic cortex whereas mature neurons maintain much longer and mature mitochondria in DG (Beckervordersandforth et al. 2017). These data highlight the involvement of mitochondrial shape and implied metabolism, which partly regulates stem cell transition.

As the mitochondrial dynamics is an intricate process, its disruption would impact stem cell function. *Opa1* and *Mfn1/2* are crucial genes that control mitochondrial fusion and their deletion in NSCs result in fragmented mitochondria, impaired NSC self-renewal and premature commitment to differentiation, thus depleting the NSC pool. Deletion of *Mfn1/2* in adult NSCs depletes stem cell pool, impairs neurogenesis, resulting in cognitive defects. In addition, deletion of pro-fusion proteins elevates mitochondrial and cytosolic ROS levels. This results in an abrupt metabolic shift in uncommitted Type I cells causing a premature commitment to differentiation to more committed Type II cells. Addition of N-acetyl cysteine (NAC), a ROS scavenger, rescued mitochondrial fragmentation as well as stem cell self-renewal (Khacho et al. 2016; Ahlqvist et al. 2012).

A recent study postulates that the length of mitochondria and its distribution in postmitotic cells can determine cell fate decision. It has been suggested that cells that acquire fragmented mitochondria upon mitotic division eventually takes neuronal fate whereas cells that acquire fused

mitochondria retains stem cell fate (Iwata, Casimir, and Vanderhaeghen 2020). Chemical-mediated disruption of mitochondrial fission inhibits postmitotic cells from neuronal differentiation. These studies show the crucial role of mitochondrial proteins in stem cell identity and function.

3.2 Mitochondrial metabolic specification in stem cells

Due to its diverse function, mitochondria are a central hub for relaying and regulating cellular signalling. Glycolysis is evolutionarily conserved in stem cells due to its low energy demand (Agathocleous et al. 2012; Homem et al. 2014). Glycolysis-derived pyruvate enters mitochondria through mitochondrial pyruvate carrier (MPC) to feed the TCA cycle and OXPHOS. Though NSCs have immature mitochondrial ultrastructure and decreased mitochondrial DNA copies (Sun and St John 2016), they express abundant MPC, which is important in maintaining quiescence, as shown in *in vitro* and *in vivo* studies. Genetic knockout or pharmacological inhibition of MPC in qNSCs elevates aspartate levels and NSC activation. MPC-deficient NSCs can differentiate to neurons with increase in aspartate levels and reduced TCA intermediates suggesting a metabolic shift. MPC depletion increases hippocampal neurogenesis by activating dormant cells that normally are not activated in aged mice, providing a proof of concept that metabolite levels alters NSC quiescence/activation state (Petrelli et al. 2023). One of the primary nuclear regulations of mitochondrial function is Peroxisome proliferator-activated receptor (PPAR) γ co-activator-1α (PGC1α) and its downstream effector TFAM. PGC1α is a key player in modulating metabolism. Fasting, cold shock and exercise induces PGC1α in several tissues including the brain and improves cognitive function (Wrann et al. 2013). PGC1α increase gluconeogenesis and FAO upon cold shock. PGC1α increases mitochondrial biogenesis and nuclear expressed mitochondrial ETC complex subunits (Wu et al. 1999), which is involved in embryonic hippocampal neuronal spine

formation, density, and synapse formation (Cheng et al. 2012). Loss of TFAM in adult hippocampal NSCs reduces stem cell proliferation and causes defects in neurogenesis suggesting the importance of PGC1α-TFAM pathway in maintaining ETC function in NSCs (Beckervordersandforth et al. 2017). Mitochondrial complex I-derived NAD/NADH plays a crucial role in redox balance and Sirtuin function. Decrease in complex I function reduces NAD+ pool. Also Nampt is a rate-limiting enzyme recycles nicotinamide to NAD+. Depletion of NAD+ through loss of Nampt in NSCs results in decline in number and function. NAD+ pool has been shown to decline during aging process (Stein and Imai 2014). Thus, boosting NAD+ through nicotinamide riboside (NR) improves V-SVZ stem cell proliferation in young animals and rescues defects in aging NSCs (Zhang et al. 2016). Therefore, mitochondrial function, metabolites and consequent transcriptional regulation play a compelling role in NSC function.

3.3 ROS regulation in NSCs

ROS is a collective term for metabolic byproducts of incomplete reduction of molecular oxygen and ROS is generated in the plasma membrane through NADPH oxidase (NOX) family of enzymes that has role in inflammation regulation. ROS is maintained in a dynamic homeostasis by antioxidant systems that are unique to cell types. ROS is currently considered as relay stations of physiological signals. Mitochondrial ROS generation is coupled with OXPHOS complexes I and III. Any disruption in electron flow through mitochondrial complexes results in free radical formation (Murphy 2009). There are mitochondrial and cytoplasmic antioxidants that scavenge ROS and maintain homeostasis. Such dynamic ROS maintenance provides physiological functions through cell signaling (Sena and Chandel 2012). Increased ROS within the physiological range positively influences NSC proliferation. Actively proliferating NSCs contain increased levels of ROS, and experimental manipulation of their ROS levels severely affect normal NSC proliferation

in vitro and *in vivo* (Le Belle et al. 2011). In a recent study, acknowledging several aspects of stem cell heterogeneity, adult NSCs were subdivided based on ROS levels (Adusumilli et al. 2021). In the adult DG, NSCs possess varying gradients of ROS levels. Cells with high ROS are generally quiescent and have reduced cell cycle activity and possess the hallmark qNSC phenotype (Berg et al. 2019; Shin et al. 2015). Physical activity induces a surge in cellular ROS levels, which prime the cells to proceed with activation and proliferation. Further, Nox2, a potential source of cellular ROS mediates the spike in ROS and stem cell activation (Adusumilli et al. 2021). These studies suggest a physiological role for cellular ROS in regulation of NSC function.

On the other hand, pathological increase in ROS contributes to elevated oxidative damage by protein oxidation and mitochondrial DNA mutation. Thus, excess ROS beyond the capacity of ROS defense decreases self-renewal in NSCs, which can be rescued by antioxidants such as NAC (Ahlqvist et al. 2012). Excessive suppression of ROS through high levels of antioxidants diminishes cell signaling and result in decreased proliferation (Hamalainen et al. 2015). These studies suggest, with high confidence, a prominent role for ROS in NSC proliferation and differentiation (Khacho and Slack 2017b). This may also imply the potential application of antioxidants for diseases that are associated with abnormal changes in NSC proliferation (Hamalainen et al. 2015). Mitochondria are one of the major sources of cellular ROS and certain ROS can leak through the membrane affecting overall cell health. Mitochondrial structural dynamics are also known to affect ROS generation that can influence self-renewal and differentiation in NSCs (Khacho et al. 2016). Recent findings from our laboratory suggest that embryonic $Sox2^+$ NSCs contain elongated mitochondria and have lower ROS levels compared to $Sox2^-$ progenitors with fragmented mitochondria and higher ROS levels. Moreover, low ROS in $Sox2^+$ NSCs that express reduced Nrf2 levels enhances Notch signaling, thus maintaining NSCs

self-renewal. $Sox2^-$ progenitors exhibit elevated ROS that activates Nrf2 signaling, resulting in reduced self-renewal and increased differentiation (Khacho et al. 2016). Another study also suggests a novel function of mitochondrial apoptosis inhibiting factor (AIF) in embryonic and adult neurogenesis (Khacho et al. 2017). Deletion of AIF in embryonic and adult NSCs result in impaired self-renewal, proliferation, and aberrant neurogenesis (Khacho et al. 2017).

3.4 Mitochondrial failure in brain diseases

Mitochondrial diseases are primarily manifested in development and brain malfunctions suggesting an important role in tissue energetics. Inherited mitochondrial DNA mutations lead to human disease by loss of mitochondrial function in multiple tissues including the brain (Wallace, Fan, and Procaccio 2010). Mutations in mitochondrial dynamics proteins can cause human diseases affecting the nervous system. As discussed earlier, mutations in MFN2 results in Charcot–Marie–Tooth disease (CMT) type 2A (CMT2A), a neuropathy impacting sensory and motor functions (Zuchner et al. 2004). Optic atrophy impacts optic nerve with additional symptoms including hearing loss, myopathy, and peripheral neuropathy. Parkinsonism symptoms were observed in patients with Opa1 mutation, resulting in chronic progressive external ophthalmoplegia (CPEO) (Carelli et al. 2015). An induced pluripotent stem cell (iPSC) model of Opa1 mutation phenocopies PD symptoms including oxidative stress and lysosomal impairment in patient-derived dopaminergic neurons. Inhibition of necroptosis in such iPSC cell lines rescued neuronal differentiation, protects dopaminergic neuronal cell death and attenuates oxidative stress (Iannielli et al. 2018).

4. Integrated stress response

Integrated stress response (ISR) is a conserved multistep signaling pathway by which multiple physiological stress converge to execute eukaryotic cellular adaptation. Cell-extrinsic stressors such as viral infection, nutrient deprivation (amino acid or glucose), and change in oxygen levels can activate ISR. Cell-intrinsic stressors such as unfolded protein response (UPR) in the ER, and a recent additional mitochondrial dysfunction (discussed later in this section) can also trigger ISR. ISR is executed by four major kinases; double-stranded RNA-dependent protein kinase (PKR), PKR-like ER kinase (PERK), heme-regulated eIF2α kinase (HRI), general control non-derepressible 2 (GCN2). ISR kinases phosphorylate the alpha subunit of eukaryotic translation initiation factor 2 (eIF2α) on serine 51. Phosphorylation of eIF2α decreases its activity and subsequent reduction in global translation. This attenuates 5'Cap-dependent translation, but certain stress response mRNAs have internal ribosome entry site (IRES) that are translated. Activating transcription factor 4 (ATF4) is one of the key regulators of stress response that has alternatively spliced transcriptional variant that uses upstream open reading frame (ORF1) for translation reinitiation. Translation control plays a crucial role in long-term memory formation. *De novo* protein synthesis is shown to be involved in memory formation (Sharma et al. 2020; Costa-Mattioli et al. 2005; Costa-Mattioli and Walter 2020). Neurodegenerative diseases show distinct features of protein aggregation, misfolding, oxidative stress and mitochondrial dysfunction. Thus, ISR could play a central role in disease manifestation and therapeutic context (Costa-Mattioli and Walter 2020). ISR has been shown to be involved in several of neurodegenerative diseases such as Alzheimer's disease (Chang et al. 2002), Parkinson's disease (Hoozemans et al. 2007), amyotrophic lateral sclerosis (Atkin et al. 2008) and traumatic brain injury (Chou et al. 2017). Different cell types exhibit unique metabolic demands. Under stress, they exhibit distinguished

adaptive mechanisms through metabolic rewiring, such as amino acid transport, amino acid biosynthesis, tRNA charging. The timing and duration of the stress response is a critical process by which the survival of the cell is decided. A chronic or severe ISR activation could lead to maladaptation (Chou et al. 2017) while induction of ISR can be beneficial in improving cell fitness and metabolic adaptation to stress (Costa-Mattioli and Walter 2020; Torrence et al. 2021).

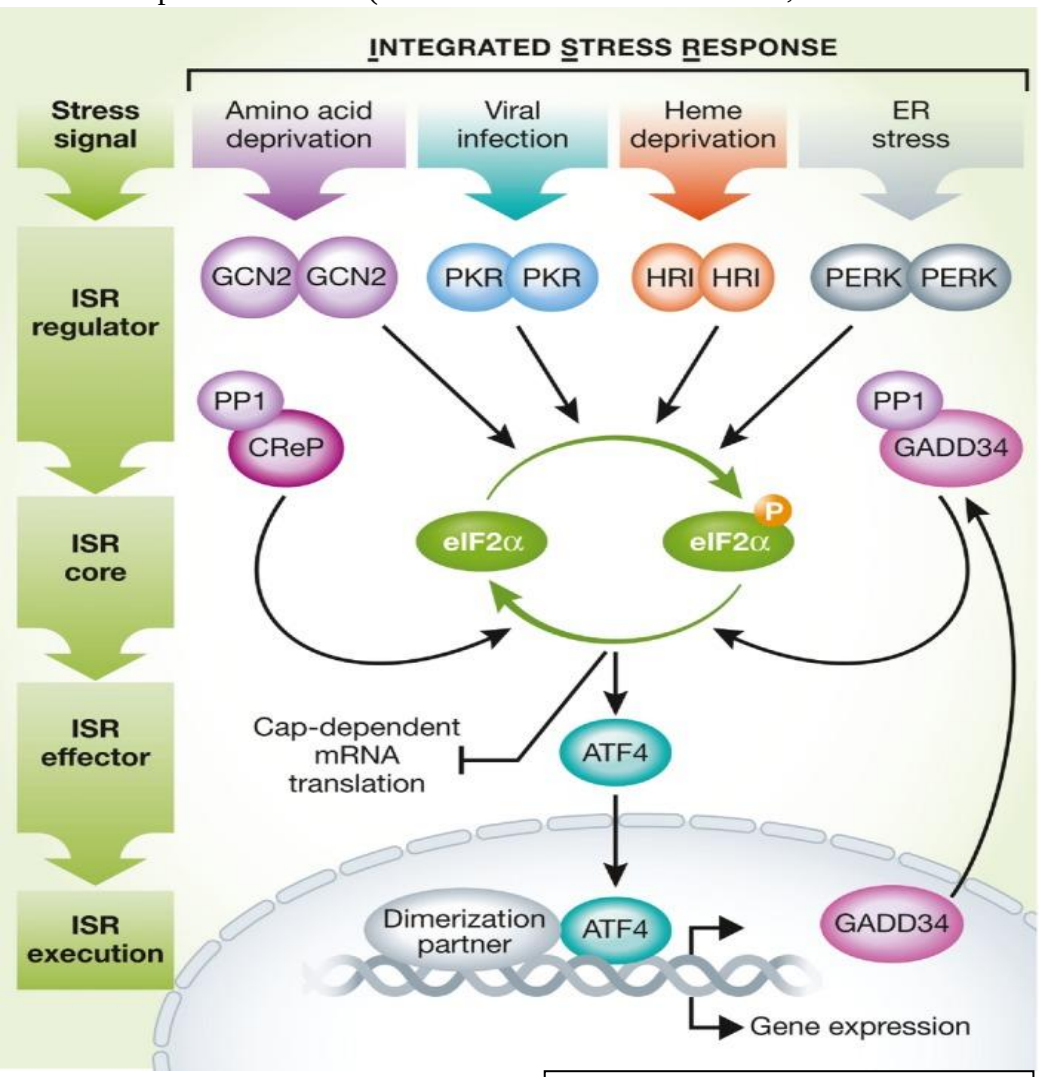

Adapted from (Pakos-Zebrucka et al.

Figure 5: The regulators of ISR pathway ER stress, viral infection, and other cellular stress signals activate PERK, PKR, HRI, and GCN2 kinases that converge on phosphorylation of eIF2α, the core of ISR. This leads to global attenuation of Cap-dependent translation while concomitantly initiates the preferential translation of ISR-specific mRNAs, such as ATF4. ATF4 is the main effector of the ISR. It forms homo- and heterodimers that bind to DNA targets to control the expression of genes involved in cellular adaptation. Arrows denote activation or induction, while blunt lines indicate inhibition. Adapted from (Pakos-Zebrucka et al. 2016).

ATF4 is a basic leucine zipper (bZIP) transcription factor that enables adaptation to cell stress. ATF4 is emerging as a master regulator of metabolism, and its activation induces genes related to metabolic regulation, nutrient reuptake, oxidative stress response and other related transcription factors. ATF4 heterodimerizes with other bZIP transcription factors such as CCAAT Enhancer Binding Protein Alpha (Cebpa) (Mann et al. 2013), C/EBP Homology Protein (CHOP) (Han et al. 2013), or Nuclear factor erythroid 2-related factor (2Nfe2l2) (He et al. 2001). ATF4 exerts stress response and its amelioration; persistent stress signaling through ATF4 is linked to cell death and is implicated in neuronal diseases (Demmings et al. 2021; Aime et al. 2015). Under basal conditions, ATF4 expression is low in basal condition; upon stimuli, ATF4 levels rapidly increase, suggesting a transcriptional and translational regulation of precise ATF4 levels and dynamic transition in response.

4.1 Mitochondrial dysfunction and induction of ATF4

Among the classic ISR, ATF4 has recently been shown as a critical regulator of mitochondrial dysfunction. A multi-omics study suggests that mitochondrial dysfunction through stressors affecting protein translation, OXPHOS stability, membrane potential and respiration effectively induce ATF4, which mediates mitonuclear communication (Quiros et al. 2017). ATF4 is a responsive target to mitochondrial dysfunction as described (Fessler et al. 2020; Guo et al. 2020). These studies mechanistically provide evidence of how mitochondrial stress activates ISR kinase. Mitochondrial dysfunction leads to proteolytic activity of OMA1 on DELE1. Cleaved DELE1 moves from the mitochondrial inner membrane to the cytosol and activates HRI (Fessler et al. 2020; Guo et al. 2020). Additionally, a direct correlation of loss in mitochondrial dynamics, fitness and ISR activation is provided by OMA1-Dele1-ATF4 signaling in the adult mouse heart, where

loss of ATF4 function under stress aggravated cardiomyopathy through ferroptosis (Ahola et al. 2022).

4.2 Role of ATF4 in stem cell regulation

Considering the diverse function of ATF4, it is important to understand its involvement in stem cell function. Studies from human cord blood hematopoietic stem cell (HSC) revealed that ISR is active in long-term HSC (LT-HSC) maintenance and ATF4 is shown to be important for HSC survival under basal and nutrient deprivation conditions (van Galen et al. 2018). Primitive HSCs share similar ATF4 signature with malignant tumor leukemia suggesting the importance of ATF4 in HSC maintenance and how tumor cells take advantage of ATF4 function to thrive under varying stress conditions. In a recent mouse study, the authors utilized a loss-of-function approach to understand the role of ATF4 in HSC maintenance. ATF4-knockout resulted in an increase in LT-HSC pool and reduced its colony-forming ability and myeloid differentiation capacity that phenocopies aging. The mechanism by which ATF4 regulate HSCs is shown to be through HIF1α (Sun et al. 2021).

ATF4 regulation of embryonic neurogenesis is important in brain development and cell proliferation. ATF4-knockout embryonic brain is relatively smaller compared to that of its wildtype counterpart (Frank et al. 2010). ATF4 is enriched in proliferative progenitors in the embryonic cortex where it is expressed until embryonic day 11, after which it declines during the neurogenesis stage, suggesting a role for ATF4 in NSC proliferation, highlighting a timely regulation of ATF4 levels in the neurogenesis program. Oscillation of ATF4 levels and its degradation occurs during the cell cycle S phase. ATF4 protein stability is directed by its phosphorylation sites. During S phase, ATF4 is phosphorylated and degraded by the F-box protein β-TrCP-mediated ubiquitin proteosome system and its degradation is required for cell cycle

progression; phosphorylation-resistant mutant ATF4 results in accumulation of cells at G1/G0 stage (Frank et al. 2010). In a recent *in vitro* study, loss of lysine methyltransferase, DOT1-like, histone H3 methyltransferase (DOT1L/KMT4) resulted in ISR activation that impacted NSC proliferation and survival. Loss of DOT1L/KMT4 altered histone modifications, including H3K4me3, H3K14ac, and H3K79me2, resulting in increased transcriptional activity of ISR genes. Prolonged inhibition of DOT1L/KMT4 resulted in persistent ISR and cell death (Roidl et al. 2016). Since disruption of transcriptional regulation and mitochondrial dynamics affect NSC function and neurogenesis, our laboratory was interested in understanding how the Rb family and Opa1 regulate adult neurogenesis. The goal of this study was to understand the molecular mechanisms and a common interplay of the Rb family and Opa1 in distinct models of neurogenesis.

Statement of Objectives

The primary objective of this thesis is to determine the regulation of adult neurogenesis by RB/E2F axis and mitochondrial fusion protein Opa1. The main body of this thesis consists of two manuscripts, with one published and one in submission.

In Chapter 2, published as (Fong et al. 2022), the hypothesis that Rb/E2F axis is a master regulator of adult NSCs, and functions as a key mechanism instructing the choice of quiescent and activated states through cellular and transcriptomic changes was tested. This expanded the scope of RB/E2F axis more than cell cycle regulation and broadened the scope to further encompass adult neurogenesis in both the V-SVZ and SGZ.

In Chapter 3, the hypothesis that the mitochondrial dynamics protein Opa1 is an essential regulator of adult neurogenesis, and functions as a metabolic regulator controlling general neurogenesis process was tested. This established the requirement for mitochondrial dynamics and fusion protein Opa1 in regulating adult neurogenesis and identified how stem cell fate is regulated through metabolic changes and stress response. At the time of thesis submission, this manuscript is submitted for publication as Iqbal et al., 2023.

Chapter 2

Cell Reports

Published: November 1, 2022

Article

The Rb/E2F axis is a key regulator of the molecular signatures instructing the quiescent and activated adult neural stem cell state

Bensun C. Fong 1, Imane Chakroun 1, **Mohamed Ariff Iqbal** 1, Smitha Paul 1, Joseph Bastasic 1, Daniel O'Neil 1, Edward Yakubovich 1, Anthony T. Bejjani 6, Nastaran Ahmadi 1, Anthony Carter 1, Alysen Clark 1, Gustavo Leone 2, David S. Park 3 4 5, Noël Ghanem 6, Renaud Vandenbosch 7 8, Ruth S. Slack 1 9

1 University of Ottawa Brain and Mind Research Institute, Department of Cellular and Molecular Medicine, University of Ottawa, Ottawa, ON K1H 8M5, Canada

2 MCW Cancer Centre, Medical College of Wisconsin, Milwaukee, WI, USA

3 Department of Clinical Neurosciences, University of Calgary, Calgary, AB T2N 4N1, Canada

4 Department of Cell Biology, University of Calgary, Calgary, AB T2N 4N1, Canada

5 Department of Anatomy, University of Calgary Calgary AB T2N 4N1 Canada

6 Department of Biology, American University of Beirut, PO Box 11-0236, Riad El Solh, Beirut 1107 2020, Lebanon

7 Laboratory of Developmental Neurobiology, GIGA Stem Cells & GIGA Neurosciences, University of Liège, Liège, Belgium

8 Division of Histology, Department of Biomedical and Preclinical Sciences, University of Liège, Liège, Belgium

Received 7 January 2022, Revised 11 August 2022, Accepted 7 October 2022, Available online 1 November 2022, Version of Record 1 November 2022.

MAI performed several experiments, including animal experiments, FACS sorting, neurosphere culture, Lentiviral vectors preparation and manuscript editing.

ABSTRACT

The long-term maintenance of the adult neurogenic niche is dependent on the proper regulation of entry and exit from quiescence. The NSC quiescence to activation transition is a complex process requiring precise cell cycle control, co-ordinated with transcriptional and morphological changes. How NSC fate transitions co-ordinate with the cell cycle machinery remains poorly understood. Here we show that the Rb/E2F axis functions by linking the cell cycle machinery to pivotal regulators of NSC fate. Deletion of Rb family proteins results in activation of NSCs, inducing a transcriptomic transition towards activation. Deletion of their target activator E2Fs1/3 results in intractable quiescence and the cessation of neurogenesis. We show that the Rb/E2F axis mediates these fate transitions through the regulation of factors essential to NSC function, including REST and ASCL1. Thus, the Rb/E2F axis is an important regulator of NSC fate, coordinating cell cycle control with NSC activation and quiescence fate transitions.

INTRODUCTION

Compelling evidence reveals that neurogenesis, which occurs in the adult mammalian brain, plays an important role in memory and cognition, and has therapeutic potential for endogenous repair (Gonçalves et al., 2016). The generation of neurons throughout life depends on the long-term maintenance of a population of quiescent neural stem cells (NSCs), which reside in defined niches. Critical to this process is the ability to maintain and effectively regulate NSC entry and exit from quiescence. The dynamic transition from quiescence to activation is a complex process requiring not only precise cell cycle control, but also a co-ordinated phenotypic transition involving transcriptional and morphological changes (Urbán et al., 2019). Single-cell transcriptomic studies have shown that NSCs progressing between states of quiescence and activation possess distinct gene expression profiles, essential for NSCs to maintain both a quiescent state and competence to respond to niche environmental cues. Quiescent NSCs are enriched in cell signaling, communication and adhesion genes, while activated NSCs express a repertoire of genes necessary for activation, including ribosomal and RNA synthesis as well as DNA replication and repair (Basak et al., 2018; Codega et al., 2014). Presently, it remains elusive how such a complex repertoire of factors interact and function in a co-ordinated manner with the core cell cycle machinery to mediate these critical NSC fate transitions.

The Retinoblastoma gene Rb was the first tumor suppressor gene to be cloned (Friend et al., 1986; Lee et al., 1987) and has been intensively studied in the field of oncogenesis. While Rb family proteins have been shown to interact with multiple cellular factors, the best known binding partners are the E2F family of transcription factors through which the Rb family regulates G1-S transition. Three Rb family proteins share overlapping functions: pRb, p107 and p130, and interact with E2Fs to regulate proliferation, self-renewal and the onset of differentiation. We and others have shown that the Rb family and their regulatory targets control the expression of pluripotency factors such as Sox2 (Julian et al., 2013; Kareta et al., 2015). Studies have identified an essential role for the Rb family in regulating haematopoetic stem cell homeostasis by repressing tissue-specific E2F targets (Kim et al., 2017; Viatour et al., 2008).

Here we show that the Rb/E2F pathway is a key regulator of NSC fate, by co-ordinating the transcriptional program that controls quiescence and activation. We show that the Rb/E2F axis functions as an on-off switch for NSC quiescence and activation, by linking the cell cycle machinery to pivotal regulators of NSC fate. Compound deletion of Rb family proteins results in activation and expansion of NSCs, and induces a transcriptomic transition towards NSC activation followed by niche depletion in the subgranular zone (SGZ) of the dentate gyrus (DG). By contrast, deletion of activator E2Fs, E2F1 and E2F3, results in the failure of NSCs to undergo activation, and the acquisition of a transcriptome associated with intractable NSC quiescence. The Rb/E2F axis mediates these fate transitions by regulating factors essential to NSC function, including REST and ASCL1. This places the Rb/E2F axis as an important regulator of NSC fate, coordinating cell cycle control with NSC activation and quiescence fate transitions.

RESULTS

Our previous results revealed that Rb is required to regulate proliferation and survival of committed neuroblasts in the adult brain (Naser et al., 2016; Vandenbosch et al., 2016), however, Rb itself was dispensable in regulating the function of the adult NSC population. Given that cell cycle regulation is a crucial requirement to control NSC quiescence and long-term maintenance, we asked whether there was redundancy in Rb family protein function, and whether these pocket proteins played a critical role in the regulation of the NSC population. To test this, we used tamoxifen (Tam)-inducible NestinCreER^{T2};EYFP mice to conditionally delete Rb and p130 in adult NSCs, together with a germline deletion of p107 (Rb-TKO). Mice triple-heterozygous for Rb family (Rb-THC), which exhibited a phenotype similar to wild type animals (Fig.S1A), were used as littermate controls.

In the subgranular zone (SGZ), Rb family loss results in a dramatic 6.3-fold expansion of the total YFP+ recombined cell population, 4 weeks post-Tam (wpi) (Fig.1A). This population, 75% labelled with proliferation marker Ki67, is comprised of over 80% Sox2-expressing cells, suggesting that Rb family proteins are essential to maintain NSC quiescence in the dentate gyrus. This increase in YFP+ cell proliferation could be rescued with the replacement of a single allele of Rb (Fig.S1B-C). To define the phenotype of YFP+ cells generated in Rb-TKO mice, we co-stained for YFP and Prox1, a marker for commitment to a granule cell neuron fate, and NeuN, a marker for mature neurons. Rb-TKO cells exhibited a 2.5-fold impairment in the induction of Prox1 (Fig.1B), and absence of terminal neuronal differentiation (NeuN) (Fig.1C). Rb-TKO cells underwent cell death, evident by an 3.2-fold increase in percentage of active Caspase-3 (AC3) staining (Fig.1D, actual numbers in SFig.1D). By 8 weeks post-Tam, the entire adult NSC niche was depleted, exhibiting a 5.7-fold depletion of the Sox2+ population (Fig.1E). Co-labelling with YFP and S100B, a marker for astrocytes, revealed a significant 1.8-fold increase in S100B labelling in YFP+ recombined cells, consistent with the disposable stem cell model, whereby NSC terminal differentiation to an astrocytic lineage contributes to SGZ niche depletion (Encinas et al., 2011). These results demonstrate that Rb family proteins are essential for the control of SGZ NSC quiescence and long-term niche maintenance.

As the subventricular zone (SVZ) represents another adult NSC niche with distinct properties from the SGZ, we asked if the Rb family requirement was similar between niches. In the SVZ, there was a 3.4-fold and 2.5-fold increase in proliferation in recombined (YFP+) cells at 4 and 8 weeks (resp), resulting in an expansion of the YFP+ population at 4 weeks post-Tam in Rb-TKO. This includes a 1.9 fold increase in Dcx+ cells (Fig.1F), and a 2.7-fold expansion of recombined %Nestin/GFAP radial glia-like cells at 4wpi (Fig.1G). While there was an expansion of the Dcx+ cells, the proliferation rate of this population was similar to controls (Fig.S2A), suggesting that this expansion is not due to Rb action on neuroblast cell cycling, but in their production. The YFP+ cell numbers began to decline 8 wpi, with a concomitant 39-fold increase in cell death (Fig.1G, S1D). Consistent with an impairment in differentiation, the Rb-TKO SVZ generated periventricular heterotopias (Fig.S2B), characterized by an accumulation of Dcx+ cells which developed as a mass in the lateral ventricle, a structure observed in human disease (Ferland et al., 2009), while cultured NSCs continuously proliferate throughout induced

differentiation (Fig.S2C). In summary, our results show that Rb family proteins play a critical role in the control of cell division, survival and differentiation in the SVZ neurogenic niche, however, niche depletion was not evident by 8 weeks as seen in the SGZ.

To interrogate the mechanisms by which Rb family proteins control NSC fate, we FACS-isolated the recombined YFP+ cells directly from the SVZ of adult Rb-THC and Rb-TKO mice, to define transcriptomic profiles 10 days post-Tam. We used bulk RNA-Seq to ensure the necessary sequencing depth for differential expression analyses. Proportionally, the YFP+ fraction of Rb-TKO cells was 3-fold greater than Rb-THC (Fig.2A, Quadrant Q2), in line with SVZ characterization (Fig.1F). Efficient knock-down of Rb family proteins was confirmed(Fig.2B, Fig.S3A-C). Transcriptomic analysis identified 4817 significantly differentially expressed genes (DEGs) with DESeq2-adjusted p-value <0.05 (Fig.2C). The DEGs were broken down into signature themes including cell cycle, genes associated with NSC quiescence, activation, differentiation and signaling (Fig.2D). Loss of pRb/p107/p130 resulted in upregulation of genes associated with cell cycle activation (Cyclins A2, E2, Cdks1/2, Thymidine kinase, Cdc6) and downregulation of genes associated with quiescence including Aqp4, Id3, Pdgfrb, Aldoc, Fgfr3 and Dbi (Delgado et al., 2021; Urbán et al., 2019). By contrast, genes and signaling pathways associated with NSC activation were significantly induced, including Ezh2, Suz12, Pcna, together with upregulation of activated NSC markers including Nestin, Pax6, and Shh, Wnt, and Jak2 pathways (Kim 2017). Thus, Rb family proteins are not only required for cell cycle control, but also for the control of genes required to regulate the phenotypic signature of quiescent NSCs.

As Rb family proteins function by regulating transcription through several factors, we next pursued the E2F family, their best known regulatory targets. RNA-seq reveals that activator E2Fs1/2/3, repressor E2Fs5/6, and atypical E2Fs7/8 were significantly upregulated in the absence of the Rb family (Fig.2E,F). Given that expression of activator E2Fs is significantly induced in the NSCs of Rb-TKO animals, and that E2F1 and E2F3 are highly expressed in this population (Callaghan et al., 1999), we asked if Rb family proteins mediate their function through activator E2Fs1/3. We generated Tam-inducible NestinCreER^{T2};EYFP mice to delete E2F3, together with germline deletion of E2F1 (E2F1/3-DKO); with mice double-heterozygous (E2F1/3-HET) as littermate controls. Recombined YFP+ cells were FACS-isolated directly from the SVZ of adult E2F1/3-HET and E2F1/3-DKO mice 10 days post-Tam. We identified 4514 significant DEGs with DESeq2-adjusted p-value < 0.05 (Fig.3A). Efficient knock-down of activator E2Fs1/3 was confirmed (Fig.3B, Fig.S3D-F). E2F1/3-DKO mice exhibited the opposite phenotype found in Rb-TKO mice, as NSCs failed to undergo activation, showing a cessation of adult neurogenesis (Fig.3C). Cell cycle genes were significantly downregulated; quiescence genes (Aqp4, Id3, Pdgfrb, Apoe, Fgfr3, Dbi) were highly induced and validated (Fig.3D), while genes associated with NSC activation were downregulated. To confirm this deep quiescence phenotype, we examined the SGZ NSC niche of E2F1/3-DKO and E2F1/3 HET controls, 4 and 8 weeks post-Tam (Fig.3E, SFig.3G). There was a striking impairment in NSC activation and cessation of neurogenesis, with a 15.2-fold decrease in Ki67+ cells and11.8-fold decrease in Dcx+ neuroblasts at 4 weeks, which continued to decline at 8 weeks (Fig.3F). Loss of E2F1/3 resulted in a major reduction in Sox2+ cell

proliferation in the SVZ and SGZ (Fig.S3G,H). These data reveal a critical requirement for activator E2Fs, E2F1 and E2F3, to execute NSC activation.

We find that Rb-TKO and E2F1/3-DKO populations exhibit opposing regulation of gene transcripts associated with quiescence and activation signatures (Fig.4A, S4A-B), the co-ordinated function of which is critical to maintain the NSC niche. We compared each of our transcriptomic profiles against two published datasets, first against a single-cell RNASeq dataset, with distinct clusters spanning all stages of adult SVZ neurogenesis (Basak et al., 2018). Rb-TKO populations exhibited a striking upregulation of genes specific to activated NSC and progenitor cells, accompanied by simultaneous downregulation of quiescence-specific genes (Fig.4B). By contrast, loss of activator E2Fs1/3 resulted in upregulation of genes specific to quiescent NSCs, and downregulation of genes associated with NSC activation (Fig.4D). The transcriptomes were then compared against datasets characterizing activated and quiescent NSC populations (Codega et al., 2014). In our Rb-TKO signature, 611 significant and majority-downregulated DEGs overlap with the quiescent NSC signature, while 478 significantly and majority-upreglated DEGs overlap with the activated NSC signature (Fig.4C). In the E2F1/3-DKO signature, 512 significant and vastly-upregulated DEGs overlap with the quiescent NSC signature, while 553 significant and downregulated DEGs overlap with the activated NSC signature (Fig.4E). In summary, alignment with published datasets suggest important roles for Rb family proteins and activator E2Fs1/3 in the regulation of the molecular signatures associated with NSC quiescence and activation.

To uncover the mechanisms underlying Rb-E2F-mediated regulation of NSC fate, we searched for master transcriptional regulators and key pathways controlled by the Rb/E2F axis (Fig. 5A). We used iRegulon to establish the enrichment of transcription factor motifs surrounding the transcriptional start sites of significantly downregulated genes. We found consistent evidence in both Rb-TKO and E2F1/3-DKO supporting a role for the Rb/E2F axis as an upstream regulator of REST, the RE1-Silencing Transcription factor, a transcriptional repressor (Chong et al., 1995; Schoenherr and Anderson, 1995) known to control neuron-specific gene promoters (Mu et al., 2012). Studies have demonstrated a requirement for REST in maintaining adult NSC quiescence in the SVZ and SGZ (Gao et al., 2011; Mukherjee et al., 2016; Soldati et al., 2015). The Rb-TKO dataset revealed REST-regulated RE1 motifs on 738 gene targets (31% of input), as well as motifs corresponding to known REST target Sox11 (Bergsland et al., 2006) on 151 gene targets (6% of input). Similarly, the E2F1/3-DKO dataset revealed RE1 and Sox11 motifs on 76 and 603 gene targets (representing 3% and 28% of input), respectively. We used Network Analyst to construct a molecular network, and compare significant DEG targets against the ENCODE transcription factor-gene interactions database. For both datasets, REST cofactors SIN3A and CoREST (Rcor1) were significantly interconnected with the DEGs. This is supported by the significant upregulation of REST in either dataset, accompanied by the significant downregulation of REST targets Sox4 and Sox11 (Fig.5B). The dysregulation of REST, REST cofactors and downstream regulatory targets together suggest that the Rb/E2F axis may regulate REST function.

To determine whether REST is regulated by the Rb/E2F axis, we first asked whether endogenous REST protein was altered in the absence of Rb family proteins. FACS-isolated SVZ NSCs from Rb-THC and Rb-TKO mice, 10 days post-Tam, were cultured and early differentiation was evaluated over a time course of 3 days. In Rb-THC NSCs, Western blots revealed that REST expression decreases within 1 day of differentiation, consistent with previous findings (Ballas et al., 2005; McGann et al., 2020). By contrast, REST remains highly-expressed in Rb-TKO NSCs induced to differentiation (Fig.6A). To ask if the Rb family proteins and activator E2Fs may regulate REST expression, we first searched for E2F consensus sites at REST regulatory regions and identified 5 motifs within REST introns/exons (Fig.6B). Using Chromatin Immunoprecipitation (ChIP), we found significant binding by p107, p130, E2F3 and E2F4 at motifs in close proximity: 1 (bs1), 2 and 3 (bs2/3) (Fig.6C). Significant E2F1 binding was found at bs2/3 (Fig.6D). The identified binding at REST was significant compared to both IgG and negative locus control Cacng1 (Fig.6C,D). p107, p130, E2F3 and E2F binding was further confirmed with p107-deficient and Rb-TKO NSCs (Fig.6C,D, S5A,B). Binding at Ccna2 (Fig.S5C) was used as positive target of Rb family proteins and E2Fs (Julian et al., 2016; Litovchick et al., 2007). These results identify binding of Rb/E2F proteins within REST regulatory regions, and suggest a requirement for Rb family proteins in regulation of REST in NSCs.

To ask if dysregulation of REST contributes to the Rb-TKO NSC phenotype, we examined the expression of neuronal differentiation markers by Western blot (Fig.6E). In Rb-TKO NSCs, expression of neuroblast markers Dcx and βIII-tubulin was impaired, while the pro-activation factor ASCL1 was elevated (Fig.6E,F). To ask if a dominant negative REST (dnREST) could rescue the phenotype of Rb-TKO NSCs, cells were transduced with lentivectors expressing either dnREST-V5-mCherry (Chong et al., 1995) or mCherry control. While dnREST-V5 was not able to rescue expression of differentiation markers in Rb-TKO NSCs, it resulted in a significant increase in ASCL1 expession (Fig.6E,F). These results suggest a requirement for the Rb/E2F pathway in repressing REST activity to enable expression of REST target genes, including ASCL1.

Recent studies have defined a dynamic role for ASCL1 in the regulation of activation and quiescence, as ASCL1 is localized to activated NSCs in both the SVZ and SGZ, becoming induced upon activation (Andersen et al., 2014), and eliminated upon re-entry into quiescence through HUWE1-mediated degradation (Urbán et al., 2016). Using immunohistochemistry in the SGZ, we observed strong upregulation of ASCL1 in response to Rb-TKO (Fig.7A), reflecting a 2.1-fold increase in the proportion of recombined cells expressing ASCL1. Performing ChIP against a E2F site at the ASCL1 promoter that we previously reported in embryonic NSCs (Julian et al., 2016), revealed E2F3, E2F4, p107 and p130 binding in wild-type adult NSCs differentiated for 0 or 1 days (Fig.7B), with Ccna2 promoter used as a positive control (Fig.S5C). These results reveal consistently elevated ASCL1 expression in absence of Rb Family proteins, suggesting that the Rb/E2F axis plays an important role in the regulation of ASCL1.

Given the increase in ASCL1 expression in response to dnREST-V5 (Fig.6E,F), we next asked if Rb/E2F regulation of ASCL1 may be influenced by REST. Although previous studies revealed regulation via a RE-1 site 49kb downstream of the ASCL1 (Ballas et al.,

2005; Jørgensen et al., 2009), we uncovered REST binding at a distinct peak, 94kb upstream of ASCL1 (Fig.S6A-C); with REST being the closest regulated gene to this peak (Fig.S6D,E). ChIP in wild-type adult NSCs differentiated for up to 3 days confirms significant binding of REST at the 94 kb peak alone, increasing with differentiation time; with Snap25 used as a positive REST target (Fig.7C). Together, these results show that the Rb/E2F axis plays an important role in the regulation of REST and ASCL1, with additional functional interaction on ASCL1 by REST.

As REST and its regulatory network play a critical role in the control of adult NSC quiescence and onset of differentiation, we examined the functional consequence of REST dysregulation by performing rescue experiments in the SGZ niche. Two weeks post-Tam, we performed dual stereotaxic injections of lentivectors into both hemispheres, respectively carrying dnREST-V5-mCherry or mCherry control, targeting the dentate gyrus of Rb-THC and Rb-TKO mice. We first asked if dnREST could rescue the expression of the REST target gene, ASCL1, by measuring the proportion of ASCL1+YFP+ expression in mCherry-transduced cells at 4 and 14 dpi (Fig.7D, S7A,B). At 4 days post injection, there was a 2.8-fold increase in the proportion of ASCL1+YFP+-expressing cells in Rb-TKO in response to dnREST-V5, suggesting that dnREST results in an early increase in ASCL1 expression in NSCs. This increase in ASCL1+YFP+ expression was also maintained at 14 days post injection in Rb-TKO mice, suggesting that dnREST increases the expression of ASCL1 in NSCs of Rb-TKO animals.

To ask whether dysregulated REST contributes to the exhaustion of adult NSCs in Rb-TKO animals, we tested whether dnREST could rescue NSC depletion at 14 dpi (Fig.7E). While transduction of Rb-THC controls with either mCherry or dnREST-V5 had no effect on NSC maintenance after 14 days (Fig S7B), dnREST resulted in a partial rescue of mCherry+YFP+ expressing cells in Rb-TKO. While double labelled cells were readily detected at 4 days in Rb-TKO animals (Fig S7A), by 14 days there was a 14.6-fold depletion of LV-mCherry-transduced cells. Transduction of NSCs with dnREST-V5 resulted in a reduction in the number of apoptotic cells (AC3+ cells) consistent with a partial rescue (only a 3.8-fold depletion) of Rb-TKO double labelled cells at 14 days (Fig. 7E, S7C,D). Thus, dnREST can partially rescue NSC depletion in Rb-TKO NSCs, showing that the Rb/E2F axis is required for proper regulation of REST, which is important for the long-term maintenance of the adult NSC population.

In conclusion, the Rb/E2F axis regulates NSC function through the coordination of cell cycle control with the transcriptional networks instructing phenotypes of adult NSC quiescence and activation, an important function for the long term maintenance of NSC and neurogenesis throughout life.

DISCUSSION

The results of these studies support a number of conclusions: First, we show that Rb family proteins are required for the long-term maintenance of the adult neural stem cell pool, by playing an essential role in regulating NSC quiescence and activation, preventing niche depletion in the SGZ. Second, we show that activator E2Fs1/3 are critical Rb family

regulatory targets that are essential for NSC activation as, in their absence, adult NSCs fail to become activated and neurogenesis cannot proceed. Third, we show that the Rb/E2F axis is not only important for cell cycle control, but also for the induction of genes associated with the activation and quiescence molecular signature. Fourth, Rb/E2F controls entry and exit from quiescence through regulation of key transcription factors, including REST and ASCL1. Taken together, the Rb/E2F axis serves as an important regulator, which coordinates cell cycle control with the molecular signature associated with the activation/quiescence phenotype, a function that is essential in the long-term maintenance of adult NSCs and neurogenesis.

Rb family proteins are essential for adult NSC maintenance

Earlier studies by our group and others have shown that Rb is dispensable for adult NSC function in the SVZ and SGZ (Jaafar et al., 2016; Vandenbosch et al., 2016), while p107 is required for balancing self-renewal versus differentiation mediated through Hes1 (Vanderluit et al., 2004, 2007). Here, we show that loss of all Rb family proteins results in a loss of quiescence and activation of the adult NSC pool, playing a crucial role in regulating the function of adult NSCs. While studies in other systems have established ectopic proliferation following Rb family deletion (Jiang et al., 2010; Sage, 2000; Viatour et al., 2008, 2011), functional compensation between Rb family proteins (Ajioka et al., 2007; Burkhart et al., 2010; Sage et al., 2003) and the promotion of reprogramming following Rb inactivation (Kareta et al., 2015), the impact on the adult NSC population is dramatic, as Rb family proteins regulate not only cell cycle control but the molecular signature associated with NSC quiescence and activation. Thus, the global changes identified in Rb-TKO signify an important role for Rb family proteins as broad transcriptional regulators of NSC fate.

Our data suggest that the NSC activation in the Rb-TKO is a cell-autonomous phenomenon that results from the absence of pRb/p107/p130 pocket proteins. First, we have previously shown that inducible knock-outs of Rb only is not compatible with neuronal survival in the embryo or the adult hippocampus (Vandenbosch et al, 2016); however; we did not observe any activation (ie more proliferation) of Sox2 NSCs following neuronal cell death. Secondly, in SFig.1C we show that expansion of the NSC pool occurs very early after TKO induction (10 dpi), also suggesting that NSC activation is a direct consequence of Rb/p107/p130 loss. It should be noted, however, that previous evidence suggests that loss of Tbr2+ intermediate progenitors (Hodge et al., 2012) or loss of neuroblast and neurons after hypoxic-ischemic injury or traumatic brain injury may also contribute to adult NSC activation (Miles and Kernie, 2008; Wang et al., 2016). Given that significant progenitor and neuroblast loss occurs in the Rb-TKO, we cannot rule out that a proportion of the NSC activation found in these animals is, at least in part, indirect due to the loss of progenitors and neuroblasts, contributing to the widespread NSC activation.

Activator E2Fs E2F1 and E2F3 are essential for NSC activation

Rb family proteins are known to associate with at least 110 regulatory targets that modulate transcription (Morris and Dyson, 2001), with the best-characterized being E2F family transcription factors: activators E2F1-3a and repressors E2F3b-6. Here we show that E2F1 and E2F3 are critical for NSC function, as absence of both of these factors

results in a complete cessation of NSC activation and neurogenesis. Previous studies have demonstrated a moderate decrease in adult NSC proliferation (Cooper-Kuhn et al., 2002), while we have shown that loss of E2F3 or individual isoforms, E2F3a or E2F3b, result in imbalances in self-renewal/commitment decisions (Julian et al., 2013; McClellan et al., 2007). None of the phenotypes previously reported with individual E2Fs have resulted in the dramatic phenotypes generated by the loss of E2Fs1/3, where adult NSCs are unable to exit quiescence. Interestingly, earlier studies revealed that retinal progenitors and activated Müller glia could proliferate in the absence of all activator E2Fs1/2/3, unlike that seen in the adult neurogenic niches described here (Chen et al., 2009). Thus, our results demonstrate that activator E2Fs 1/3 are essential for adult NSC activation and for the generation of the molecular signature required for NSC activation and neurogenesis.

The Rb/E2F axis regulates phenotypes of adult NSC quiescence and activation

These results highlight a function for the Rb/E2F axis, revealing a critical requirement not only for cell cycle control but for the acquisition of the cell and transcriptomic phenotypes associated with quiescence and activation. Recent studies have demonstrated that quiescence is an active, dynamic process, wherein NSCs progressing between states of quiescence and activation possess distinct gene expression profiles, which allow quiescent NSCs to respond to environmental cues ultimately culminating in NSC activation (Basak et al., 2018; Codega et al., 2014) Alignment of our transcriptomic profiles with published population-specific signatures reveals a striking alignment, in which loss of Rb family proteins aligns with an activated state, and loss of E2Fs1/3 aligns with the molecular signature of the quiescent state. The depth of cell quiescence and reduced sensitivity to growth signals reflected in these signatures has yet to be evaluated; previous studies have suggested that quiescence depth may be associated with increased threshold required to activate a Rb/E2F switch (Kwon et al., 2017). Taken together, we show that the Rb/E2F axis not only controls the cell cycle in NSCs, but also plays an important role to generate the molecular signature of quiescent and activated cells.

The Rb/E2F axis regulates NSC fate via REST

Our transcriptomic profiles suggest an Rb/E2F-dependent mechanism regulating the molecular signatures of NSC quiescence and activation. Following loss of Rb family proteins or activator E2Fs, we observe dysregulation of the REST gene regulatory network, with elevated REST and downregulation of numerous proneural targets containing RE-1 sites, including Dcx, L1cam and SoxC proteins Sox4/Sox11 (Bergsland et al., 2006; Lepagnol-Bestel et al., 2009; Mu et al., 2012). REST has been recently shown to maintain both NSC quiescence as well as progenitor proliferation and number, to prevent precocious differentiation (Mukherjee et al., 2016). Given that Rb-TKO and E2F1/3-DKO generate opposing phenotypes in the regulation of NSC quiescence and activation, the common induction of REST and its targets may appear contradictory. While activator E2Fs can function as transcriptional activators in proliferating cells, they have also been shown to serve as transcriptional repressors to silence E2F target genes in differentiating cells, such that activating E2Fs serve as a tether to recruit Rb family proteins to target genes (Chong et al., 2009). In the context of the adult neurogenic niche,

our data suggest that activator E2Fs1/3 are essential for Rb family-mediated repression of REST. Analysis of both transcriptomic and ChIP data demonstrate binding by p107/p130 and E2F3/E2F4 at the REST regulatory regions, consistent with a model whereby E2Fs1/3 recruit Rb family proteins to repress REST in adult NSCs. The increased magnitude of REST target gene repression in response to E2F1/3 deficiency is consistent with activator E2Fs mediating Rb family protein function to regulate REST. In response to E2F1/3-DKO, the lack of REST cofactor (CoREST and Sin3A) upregulation suggests that activator E2Fs are required to recruit REST cofactors. This may link activator E2Fs with a reported requirement for CoREST in modulating REST target expression despite REST dissociation (Ballas et al., 2005). Based on this model, we show that Rb-family proteins and activator E2Fs1/3 together are required for REST regulation.

The Rb/E2F axis and REST are required for ASCL1 regulation

In response to loss of Rb family proteins, we observe that the transcriptional shift towards activation is accompanied by an increased number of ASCL1-expressing activated NSCs. Together with ChIP data demonstrating direct ASCL1 binding by p107/p130 and E2F3/E2F4, our data suggest a role for the Rb/E2F axis in repressing ASCL1 expression to maintain NSC quiescence. While ASCL1 regulation occurs at multiple levels, most notably at the level of protein degradation mediated by E3 ubiquitin ligase Huwei1 (Urbán et al., 2016), we also demonstrate that dnREST transduction results in increased ASCL1 expression, consistent with ASCL1 being a regulatory target for REST (Gao et al., 2011). Distinct from a previously described site (Ballas et al., 2005; Jørgensen et al., 2009), in the context of adult NSCs, we have identified REST binding at a distinct peak 94kb upstream of ASCL1. REST regulation of ASCL1 is also supported by our findings in vivo, as dnREST transduction results in an increased percentage of ASCL1-expressing cells in the adult SGZ. Interestingly, dnREST partially rescued the depletion of adult NSCs following loss of Rb family proteins, as dnREST resulted in a significant increase in Ascl1-expressing cells after 14 days. This suggests that the Rb/E2F regulatory axis is required for proper REST regulation, which is important for the maintenance of the NSC niche in the adult SGZ.

Limitations of the study: Here, we describe an important role for the Rb-E2F axis in regulating adult NSC function in the two adult neurogenic niches, however, it is important to note that the SVZ and SGZ function in different ways. We used the Nestin promoter to drive Cre, however, contrary to SGZ where Nestin is expressed in both activated NSCs (aNSCs) and quiescent (qNSCs), in the SVZ Nestin expression is restricted to aNSCs and ependymal cells (Codega et al., 2014). Thus, in SVZ, we can assert the function of Rb-E2F on aNSCs themselves, and not on the switch between qNSCs and aNSCs. A portion of the aNSCs, both in SVZ and SGZ, return to quiescence after activation to maintain the NSC pool, reviewed in (Obernier and Alvarez-Buylla, 2019; Urbán et al., 2019). Thus, in the RbTKO SVZ, our data reveal a critical requirement for RB Proteins to enable the re-entry of adult aNSCs into quiescence. Furthermore, our E2F1/3 DKO data, also using the same Nestin-CreERT2, support a role for the Rb/E2F pathway in the regulation of NSC activation/quiescence, as we observe an impairment of NSC activation in vivo both in the SGZ and SVZ, along with a transcriptional signature towards quiescence in aNSCs from SVZ. Thus, targeting aNSCs, a cycling population that is

expressing high levels of activator E2Fs, drives aNSCs to re-enter a qNSC-like state. Finally, based on the phenotypic data obtained in the SGZ of Rb TKO and E2F1/3 DKO, we postulate that the mechanisms highlighted in our study may be extrapolated to the qNSC—>aNSC switch. Further transcriptomic studies using Cre-drivers that specifically target the quiescent NSC population (eg. GLAST-CreERT2) along with single cell RNA-seq will be required to definitively confirm this hypothesis.

The studies examining niche exhaustion also reveal differences between the SGZ and the SVZ. While the SGZ niche exhibits exhaustion by 8 weeks, there is no exhaustion in the SVZ at 8 weeks. We have assessed the phenotype inside the SVZ, particularly proliferation of aNSCs and neuroblasts, as well as cell death. Our data reveal that in TKO, there is significant proliferation of neuroblasts inside the SVZ at 4w and 8w; however, there is a gradual decline at 8w vs 4w post-Tam. We also find an increase in cell death that persists at 8w albeit at a lower level, resulting in a reduction in cell numbers in the SVZ. While these results clearly underline a reduction in the size of the NSC/progenitor pool in the SVZ and suggest that niche exhaustion may indeed occur, future experiments (including birthdating studies) should examine the phenotype after longer time points and evaluate whether niche exhaustion also occurs in the SVZ.

While the loss of pocket proteins or their E2F1/3 targets result in dramatic gene expression changes identified by RNA-seq, it is also important to note that manipulation of the Rb-E2F axis results in a change in the cellular composition of the neurogenic niche. Thus, a significant proportion of the DEG identified could be due to indirect effects rather than direct changes in Rb-E2F target gene regulation. Identification of direct Rb-E2F target genes among the differentially expressed genes and regulatory pathways will require further validation and manipulation in future studies.

In conclusion, we describe an important function for Rb family proteins and their target activator E2Fs1/3, in the regulation of NSC activation and quiescence. We demonstrate how transcriptional signatures of quiescence and activation among adult NSCs are co-ordinated with cell cycle control, and show that the Rb/E2F axis serves as a key regulator of the molecular program instructing adult NSC exit from and re-entry into quiescence, essential for niche maintenance and ultimately adult neurogenesis.

Accession Numbers

Data have been deposited in GEO under accession number GEO: GSE190766.

Acknowledgments

This work was supported by core facilities at uOttawa, The Ottawa Hospital, and The Hospital for Sick Children, Toronto. This work was funded by CIHR grants to RSS, Belgian National Funds for Scientifc Research (FRS-FNRS, Belgium), the Fondation Léon Fredericq (ULiège, Belgium) and the Fonds spéciaux (ULiège, Belgium) to RV, University Research Board (URB), the Mamdouha El-Sayed Bobst Deanship Fund (FAS) at American University of Beirut (AUB), and, the Lebanese National Council for Scientific Research (CNRS-L) to NG, and an Ontario Graduate Scholarship to BCF.

Author contributions

Conceptualization, Methods, B.C.F., I.C., S.P., Al.C., N.G., R.V., R.S.S.; Investigation, B.C.F., I.C., M.A.I., S.P., J.B., D.O., E.Y., A.T.B., N.A., An.C., Al.C., N.G., R.V.; Resources, G.L., D.S.P., R.S.S.; Writing B.C.F., I.C., RSS, Review: all authors

Declaration of interests

The authors declare no competing interests.

Figure Legends

Figure 1: Rb family are essential to regulate adult NSC activation and quiescence.
IHC and quantification of cells in the DG (**A-E**) and SVZ (**F-G**) in genotypes shown.
A. Total YFP+ recombined cells per DG, %Sox2+, %Ki67+ cycling cells of YFP+ recombined cells. **B.** %Prox1+ committed cells of YFP+ recombined cells. **C.** %NeuN+ neurons of YFP+ recombined cells. **D.** %AC3+ apoptotic cells of YFP+ recombined cells. **E.** Total YFP+ recombined cells per DG; total Sox2+/YFP+ cells per DG; %S100B+ astrocytes of YFP+ recombined cells. **F.** Total YFP+ recombined cells per SVZ, %Sox2, DCX, Ki67, AC3 of YFP+ recombined cells in the SVZ. **G.** %Nestin+/GFAP+ cells of YFP+Nestin+ recombined cells. Scale bars, 100μm. Statistics: Error bars, mean ± SD. Unpaired 2-tailed Student's t-test, *p<0.05, **p<0.01, ***p<0.001, ****p<0.0001. N=3 biological replicates.

Figure 2: Transcriptomic analysis of Rb Family function in Neurogenic Niche
A. Representative 488FL-Log Height vs SSC-Log Height FACS plots demonstrating gating strategy. YFP+ enriched population is defined in Q2. **B.** qPCR analysis of Rb, p107 and p130 mRNA, normalized to GAPDH. **C.** MA-plot for the shrunken $\log_2$ fold changes. Significantly differentially expressed genes (p<0.05) are indicated in red.
D. Relative expression of significantly differentially expressed genes, grouped by curated functional category. **E.** Relative expression of E2F family transcription factors. **F.** qPCR of E2F7 and E2F8, normalized to GAPDH. Statistics: Error bars, mean ± SD. qPCR analysis (B,F) unpaired 2-tailed Student's t-test; relative expression plots (D,E) DESeq2-adj p-val. *p<0.05, **p<0.01, ***p<0.001, ****p<0.0001. N=3 biological replicates.

Figure 3: Activator E2Fs 1 and 3 are essential for adult NSC activation and neurogenesis.
A. MA-plot for the shrunken log2 fold changes. Significantly differentially expressed genes (p<0.05) in red. **B.** qPCR of E2F1 and E2F3 mRNA, GAPDH-normalized to 1 following $2^{-\Delta\Delta Ct}$ method. **C.** Relative expression of significantly differentially expressed genes, grouped by curated functional category. **D.** qPCR of quiescence-associated genes Tgfbr3, Bmp6, S100β, and differentiation-associated genes Dcx and Dlx1. Values were GAPDH-normalized to 1 following $2^{-\Delta\Delta Ct}$ method. **E.** IHC of YFP+ recombined cells and DCX+ neuroblasts (red) in DG. Scale bar, 100μm. **F.** IHC and quantification of total YFP+ recombined cells, total Ki67+ cycling cells, and total Dcx+ neuroblasts in the DG at 4 and 8 wpi. Statistics: Error bars, mean ± SD. IHC and qPCR analysis (B,D,F) unpaired 2-tailed Student's t-test; relative expression plot (C) DESeq2-adj p-val, *p<0.05, **p<0.01, ***p<0.001, ****p<0.0001. N=3 biological replicates (A-D); N=5 biological replicates (E-F).

Figure 4: Rb/E2F pathway transcriptomic regulation of NSC activation and quiescence
A. Relative expression of significantly differentially expressed qNSC-associated and aNSC-associated genes, across both datasets. **B.** Genes differentially expressed in response to Rb-TKO, including direction and significance, overlapped with Basak et al., 2018 signature. **C.** Significantly differentially expressed genes in response to Rb-TKO,

overlapped with qNSC and aNSC signatures from Codega et al., 2011, and proportional directionality of overlap. **D.** Genes differentially expressed in response to E2F1/3-DKO, including direction and significance, overlapped with Basak et al., 2018 signature. **E.** Significantly differentially expressed genes in E2F1/3-DKO, overlapped with qNSC and aNSC signatures from Codega et al., 2011, and proportional directionality of overlap. Statistics: Relative expression plot, DESeq2-adj p-val. Genes with DESeq2-adj p<0.05 used as input for respective signatures in (B,D) and (C,E). *p<0.05, **p<0.01, ***p<0.001, ****p<0.0001. N=3 biological replicates.

Figure 5: The Rb/E2F pathway regulates NSC fate via REST
A. Medial: Curated significant GO:BP gene sets using genes downregulated (in response to knockout) as input. iRegulon transcription factor enrichment results, using significantly downregulated genes as input. REST and Sox11 are highlighted in each. Lateral: Network Analyst TF-Protein enrichment results, using all significant genes as input. REST cofactors SIN3A and CoREST are highlighted in each. **B.** Lateral: Summary of significant differential gene expression affecting the REST/SoxC pathway. Medial: qPCR of REST and SoxC, Sox4 and Sox11 normalized to GAPDH. Statistics: Error bars, mean ± SD. qPCR analysis (B) 2-tailed Student's t-test; summary table, DESeq2-adj p-val. Genes with DESeq2-adj p<0.05 considered significant for analysis using iRegulon and Network Analyst in (A). *p<0.05, **p<0.01, ***p<0.001, ****p<0.0001. N=3 biological replicates.

Figure 6: Rb family proteins regulate REST expression in adult NSC.
A. Western blot (WB) on total protein from NSCs differentiated for 0, 1, or 3 days, β-actin is loading control. **B.** Schematic of REST gene indicating presence of 5 E2F motifs. **C.** ChIP on NSC chromatin from wild-type +/+ and p107-null -/- mice. Error bars, mean ± SEM. **D.** ChIP from p107-null -/- NSCs and Rb-TKO NSCs. Error bars, mean ± SEM. **E.** WB from NSCs infected with LV- mCherry or dnREST-V5 at P2, and differentiated at P3 for 0, 1, or 3 days. eNS is from embryonic neurospheres to test LV expression vectors. **F.** Quantification of WB in (E) using Image J. Statistics: WB analysis (F) paired 2-tailed Student's t-test. *p<0.05, **p<0.01, ***p<0.001, N=3-6. ChIP analysis, unpaired 2-tailed Student's t-test. *p<0.05 vs IgG and Cacng1, ***p<0.05 in wt vs p107 null (C) or p107 null vs Rb-TKO mice (D). N=3-7 biological replicates, cell culture = 3 technical replicates.

Figure 7. The Rb-E2F pathway regulates NSC activation and quiescence through REST and ASCL1.
A.IHC staining of ASCL1+ and YFP+ recombined cells in the DG. Scale bar, 50μm. Quantification of %YFP+ASCL1+ of YFP+ recombined cells. **B.** Schematic of ASCL1 gene indicating E2F3/4 peak at promoter (Julian et al, 2016). ChIP on NSC chromatin from wild-type +/+ mice, differentiated for 0, 1, or 3 days, targeting this peak. **C.** ChIP on NSC chromatin from wild-type +/+ mice, differentiated for 0, 1, or 3 days, targeting the specified peak. **D.** IHC staining and quantification of ASCL1+/YFP+ recombined cells of total mCherry+ cells at indicated time points. **E.** IHC staining and quantification of %YFP+ of total mCherry+, 14 days after injection; and %AC3+ apoptotic cells of total mCherry+/YFP+ recombined cells. Scale bar, 100μm. Statistics: Error bars, mean ± STD. Unpaired 2-tailed Student's t-test. ChIP analysis (B,C) *p<0.05 vs IgG. N=3 biological

replicates, 3 technical replicates. IHC (A,D,E), *p<0.05, **p<0.01, ***p<0.001, ****p<0.0001. N=3 biological replicates.

Figures

Figure 1

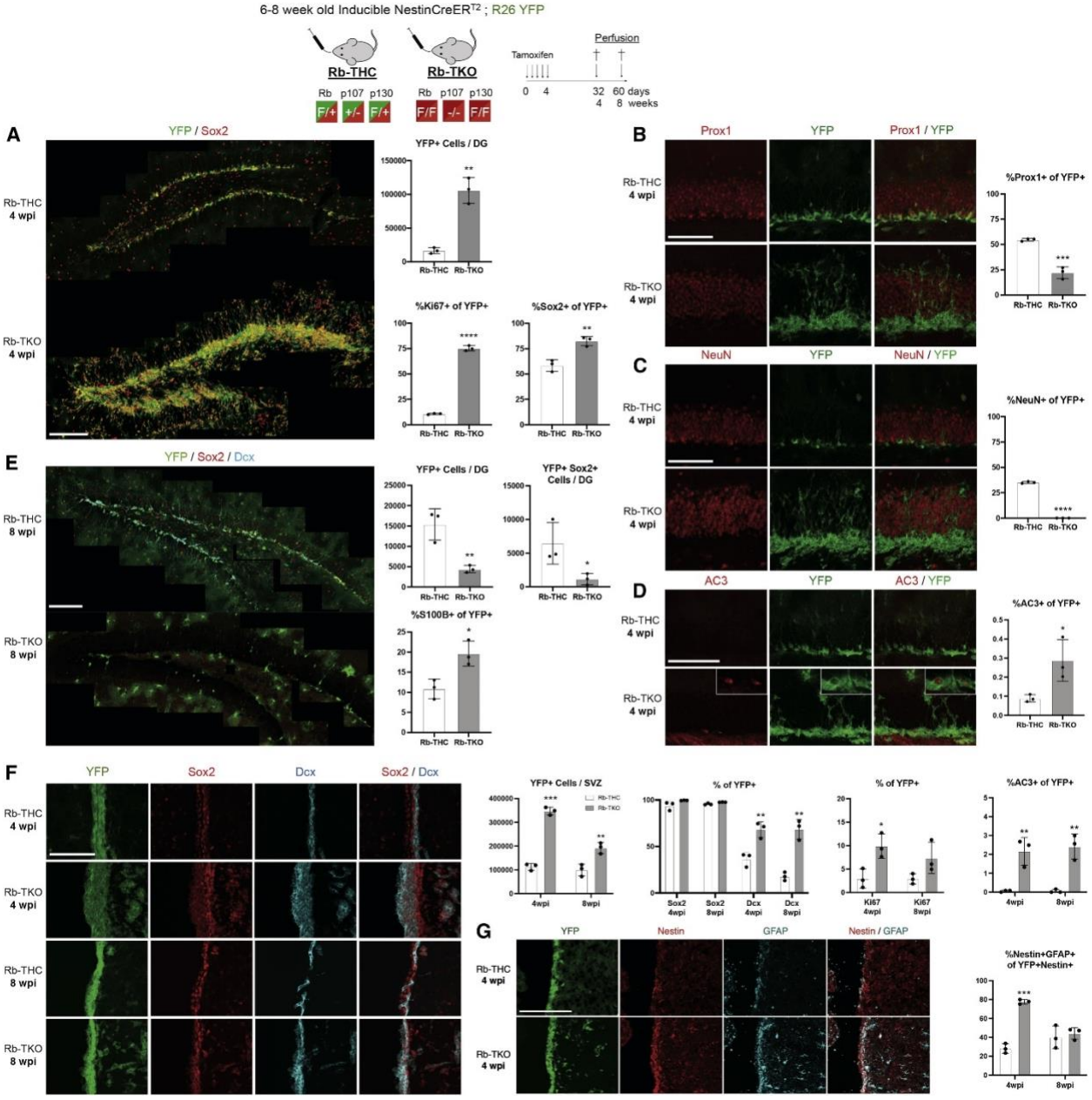

Figure 2

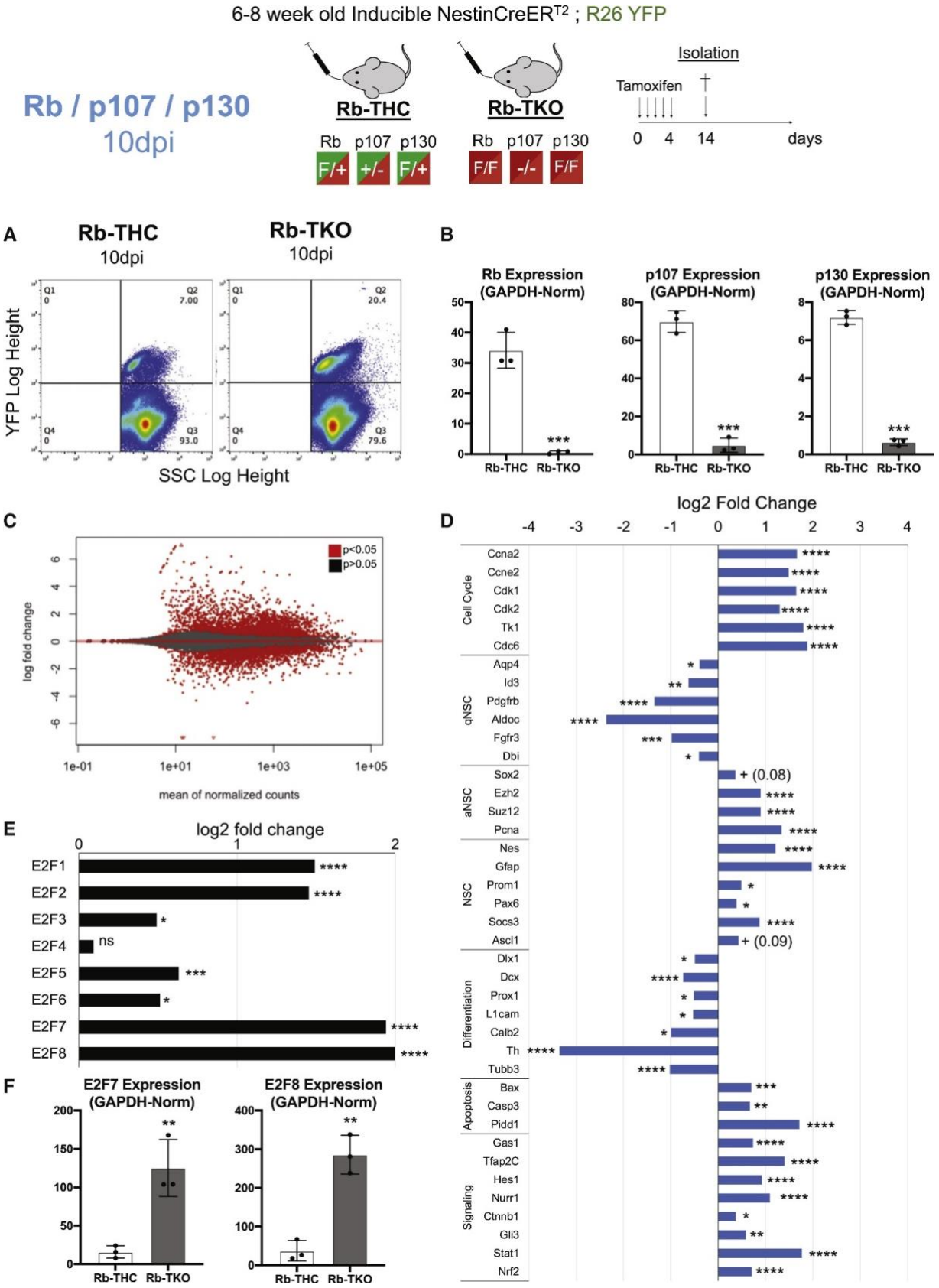
6-8 week old Inducible NestinCreER^{T2} ; R26 YFP
Rb / p107 / p130
10dpi
Rb-THC
Rb-TKO
Rb p107 p130
F/+ +/- F/+
Rb p107 p130
F/F -/- F/F
Isolation
Tamoxifen
0 4 14 days
A
Rb-THC
10dpi
Rb-TKO
10dpi
YFP Log Height
SSC Log Height
Q2 7.00
Q3 93.0
Q2 20.4
Q3 79.6
B
Rb Expression (GAPDH-Norm)
p107 Expression (GAPDH-Norm)
p130 Expression (GAPDH-Norm)
Rb-THC Rb-TKO
C
p<0.05
p>0.05
log fold change
mean of normalized counts
D
log2 Fold Change
Cell Cycle
Ccna2
Ccne2
Cdk1
Cdk2
Tk1
Cdc6
qNSC
Aqp4
Id3
Pdgfrb
Aldoc
Fgfr3
Dbi
aNSC
Sox2
Ezh2
Suz12
Pcna
NSC
Nes
Gfap
Prom1
Pax6
Socs3
Ascl1
Differentiation
Dlx1
Dcx
Prox1
L1cam
Calb2
Th
Tubb3
Apoptosis
Bax
Casp3
Pidd1
Signaling
Gas1
Tfap2C
Hes1
Nurr1
Ctnnb1
Gli3
Stat1
Nrf2
+ (0.08)
+ (0.09)
E
log2 fold change
E2F1
E2F2
E2F3
E2F4
E2F5
E2F6
E2F7
E2F8
ns
F
E2F7 Expression (GAPDH-Norm)
E2F8 Expression (GAPDH-Norm)
Rb-THC Rb-TKO

Figure 3

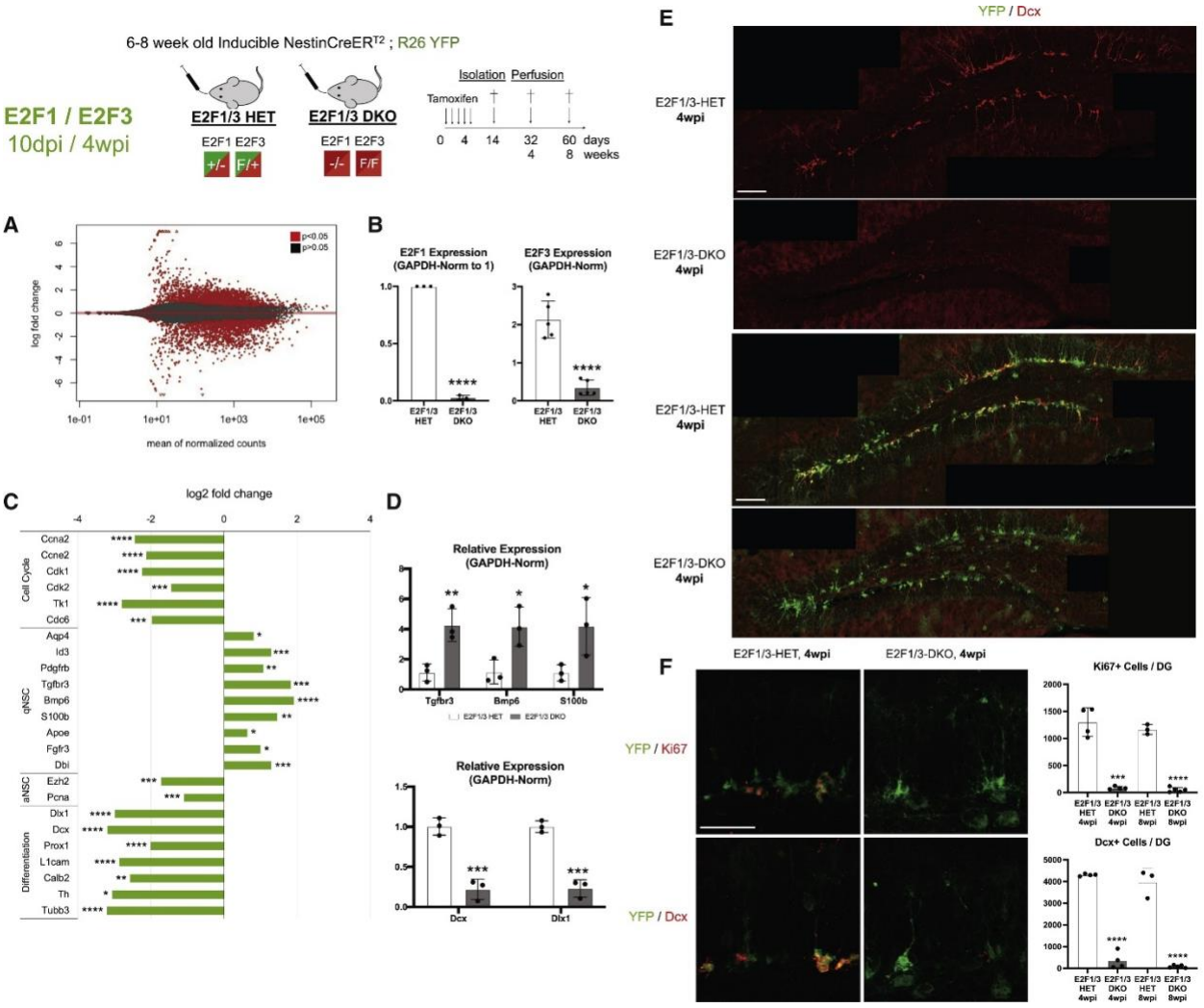
6-8 week old Inducible NestinCreER^{T2} ; R26 YFP
E2F1 / E2F3
10dpi / 4wpi
E2F1/3 HET
E2F1 E2F3
+/- F/+
E2F1/3 DKO
E2F1 E2F3
-/- F/F
Isolation Perfusion
Tamoxifen
0 4 14 32 60 days
4 8 weeks
A
log fold change
mean of normalized counts
B
E2F1 Expression (GAPDH-Norm to 1)
E2F3 Expression (GAPDH-Norm)
C
log2 fold change
Cell Cycle
qNSC
aNSC
Differentiation
Ccna2
Ccne2
Cdk1
Cdk2
Tk1
Cdc6
Aqp4
Id3
Pdgfrb
Tgfbr3
Bmp6
S100b
Apoe
Fgfr3
Dbi
Ezh2
Pcna
Dlx1
Dcx
Prox1
L1cam
Calb2
Th
Tubb3
D
Relative Expression (GAPDH-Norm)
Tgfbr3
Bmp6
S100b
Dcx
Dlx1
E
YFP / Dcx
E2F1/3-HET 4wpi
E2F1/3-DKO 4wpi
E2F1/3-HET 4wpi
E2F1/3-DKO 4wpi
F
E2F1/3-HET, 4wpi
E2F1/3-DKO, 4wpi
YFP / Ki67
YFP / Dcx
Ki67+ Cells / DG
Dcx+ Cells / DG

Figure 4

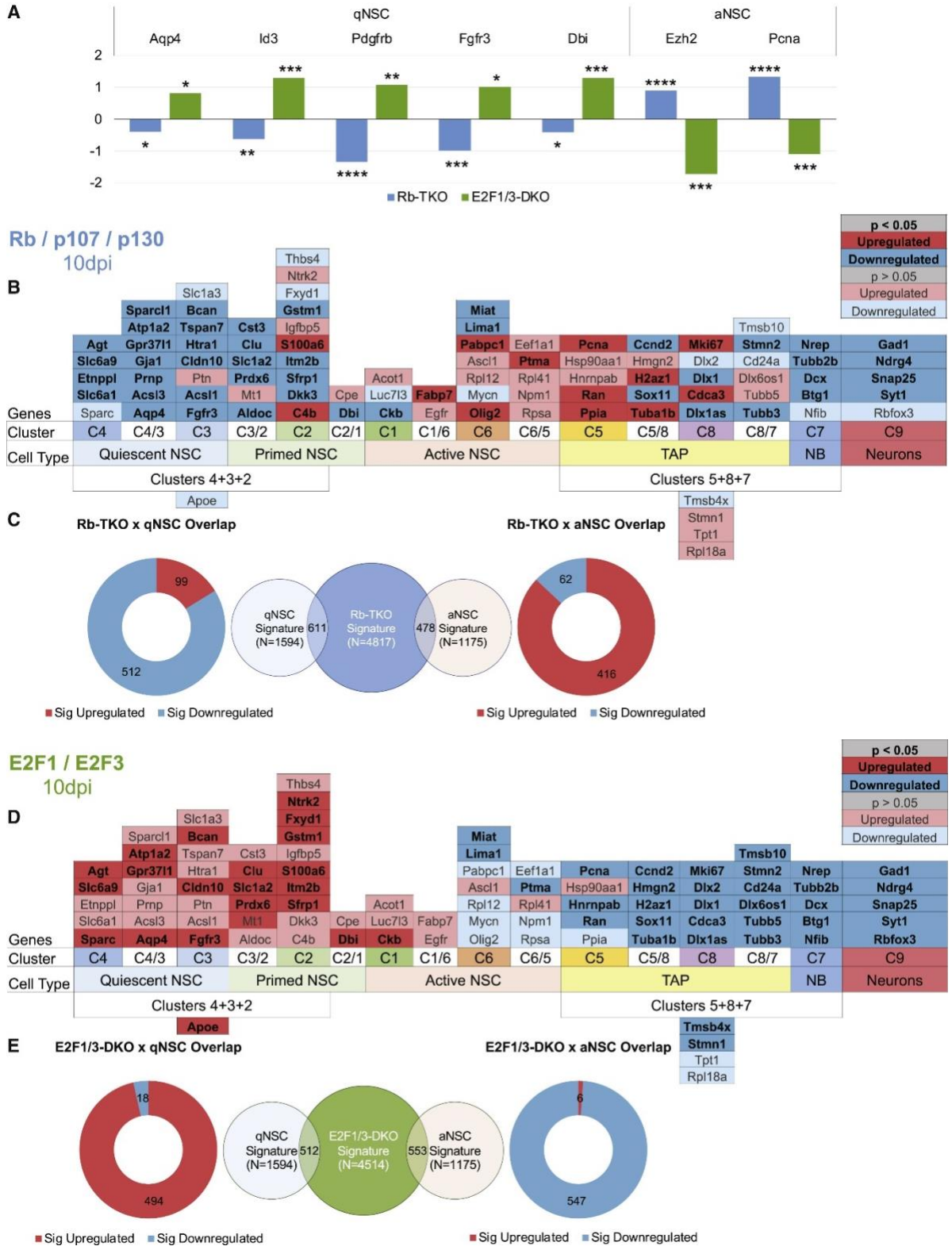
A
qNSC
aNSC
Aqp4
Id3
Pdgfrb
Fgfr3
Dbi
Ezh2
Pcna
Rb-TKO
E2F1/3-DKO
Rb / p107 / p130
10dpi
B
p < 0.05
Upregulated
Downregulated
p > 0.05
Upregulated
Downregulated
Genes
Cluster
Cell Type
Quiescent NSC
Primed NSC
Active NSC
TAP
NB
Neurons
Clusters 4+3+2
Clusters 5+8+7
C
Rb-TKO x qNSC Overlap
Rb-TKO x aNSC Overlap
qNSC Signature (N=1594)
Rb-TKO Signature (N=4817)
aNSC Signature (N=1175)
611
478
99
512
62
416
Sig Upregulated
Sig Downregulated
E2F1 / E2F3
10dpi
D
E
E2F1/3-DKO x qNSC Overlap
E2F1/3-DKO x aNSC Overlap
E2F1/3-DKO Signature (N=4514)
512
553
18
494
6
547

Figure 5

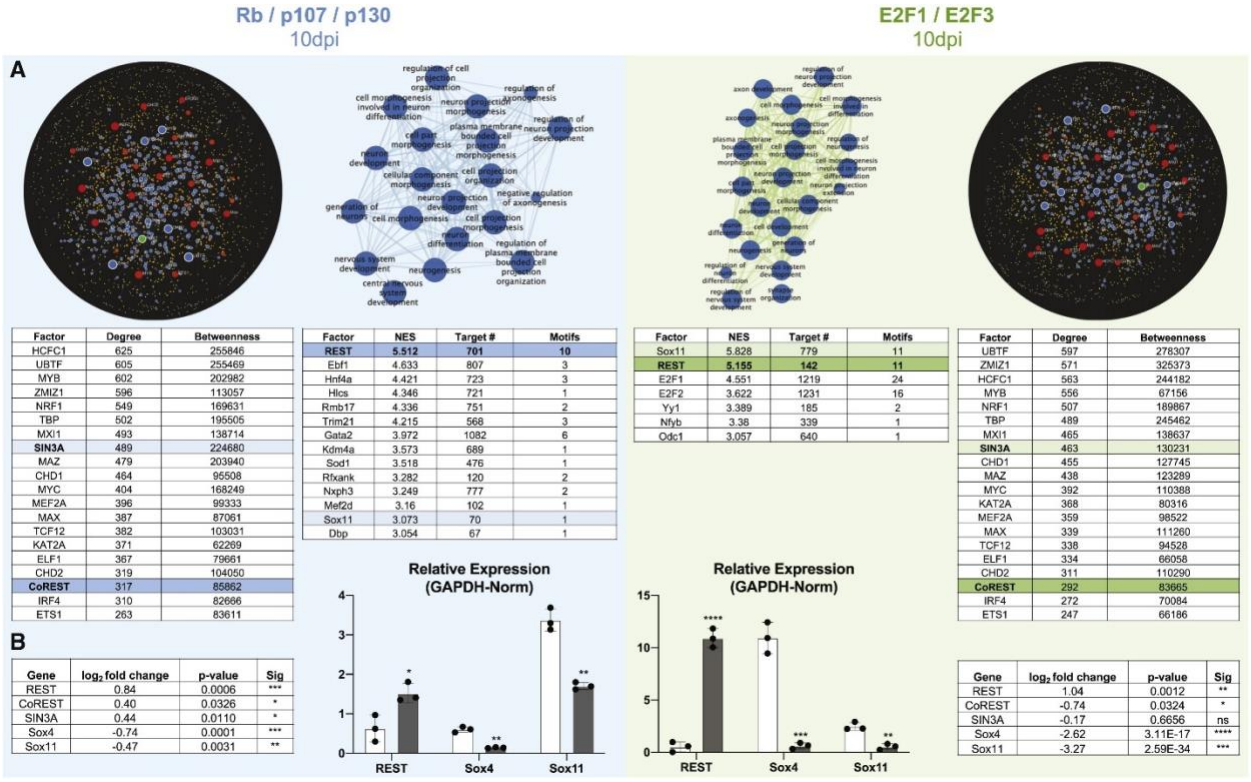

Factor	Degree	Betweenness
HCFC1	625	255846
UBTF	605	255469
MYB	602	202982
ZMIZ1	596	113057
NRF1	549	169631
TBP	502	195505
MXI1	493	138714
SIN3A	489	224680
MAZ	479	203940
CHD1	464	95508
MYC	404	168249
MEF2A	396	99333
MAX	387	87061
TCF12	382	103031
KAT2A	371	62269
ELF1	367	79661
CHD2	319	104050
CoREST	317	85862
IRF4	310	82666
ETS1	263	83611

Factor	NES	Target #	Motifs
REST	**5.512**	**701**	**10**
Ebf1	4.633	807	3
Hnf4a	4.421	723	3
Hlcs	4.346	721	1
Rmb17	4.336	751	2
Trim21	4.215	568	3
Gata2	3.972	1082	6
Kdm4a	3.573	689	1
Sod1	3.518	476	1
Rfxank	3.282	120	2
Nxph3	3.249	777	2
Mef2d	3.16	102	1
Sox11	3.073	70	1
Dbp	3.054	67	1

Factor	NES	Target #	Motifs
Sox11	5.828	779	11
REST	**5.155**	**142**	**11**
E2F1	4.551	1219	24
E2F2	3.622	1231	16
Yy1	3.389	185	2
Nfyb	3.38	339	1
Odc1	3.057	640	1

Factor	Degree	Betweenness
UBTF	597	278307
ZMIZ1	571	325373
HCFC1	563	244182
MYB	556	67156
NRF1	507	189867
TBP	489	245462
MXI1	465	138637
SIN3A	463	130231
CHD1	455	127745
MAZ	438	123289
MYC	392	110388
KAT2A	368	80316
MEF2A	359	98522
MAX	339	111260
TCF12	338	94528
ELF1	334	66058
CHD2	311	110290
CoREST	292	83665
IRF4	272	70084
ETS1	247	66186

Gene	log_2 fold change	p-value	Sig
REST	0.84	0.0006	***
CoREST	0.40	0.0326	*
SIN3A	0.44	0.0110	*
Sox4	-0.74	0.0001	***
Sox11	-0.47	0.0031	**

Gene	log_2 fold change	p-value	Sig
REST	1.04	0.0012	**
CoREST	-0.74	0.0324	*
SIN3A	-0.17	0.6656	ns
Sox4	-2.62	3.11E-17	****
Sox11	-3.27	2.59E-34	***

Figure 6

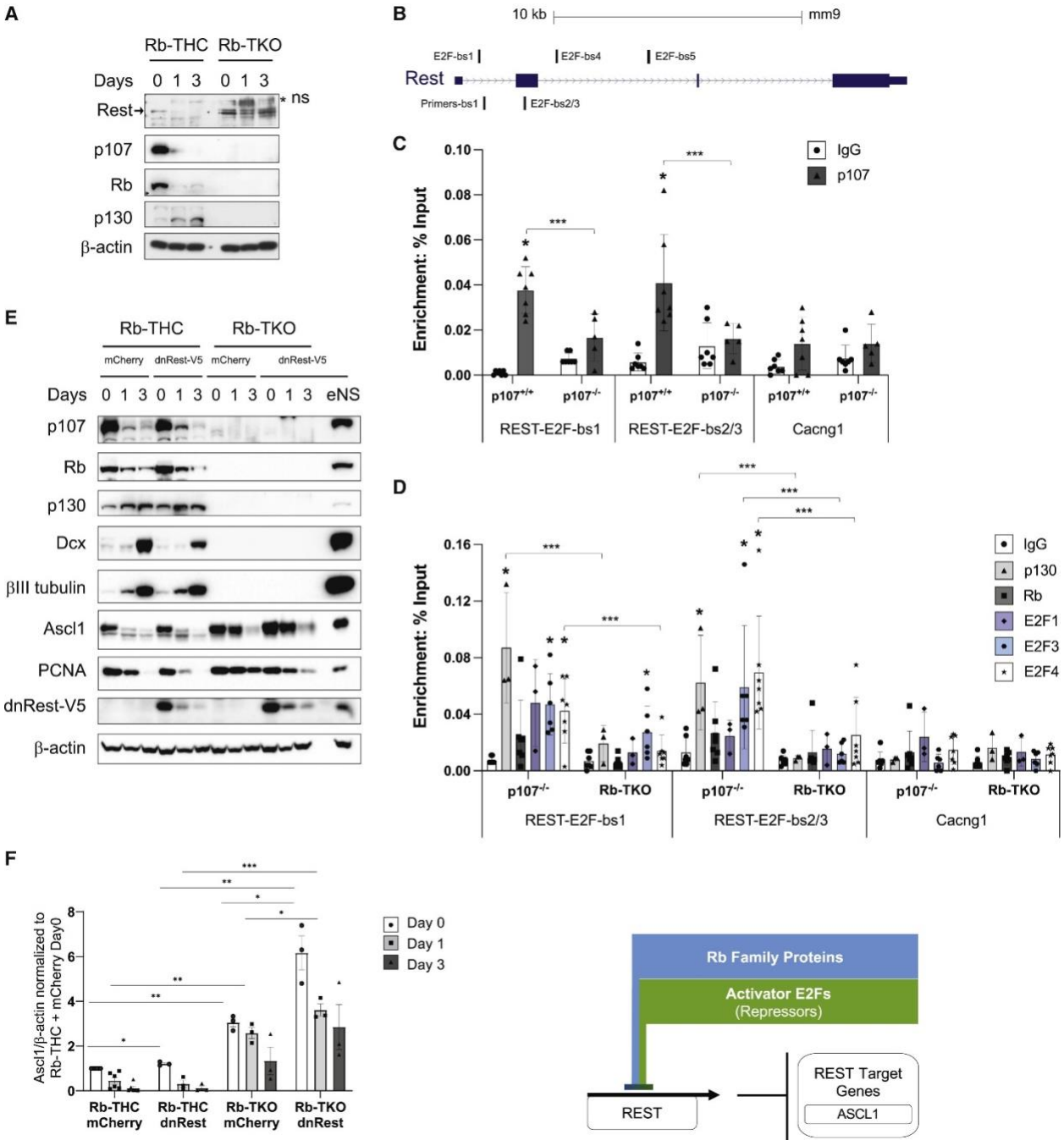
A
Rb-THC
Rb-TKO
Days 0 1 3 0 1 3
Rest→
* ns
p107
Rb
p130
β-actin
B
10 kb
mm9
E2F-bs1
E2F-bs4
E2F-bs5
Rest
Primers-bs1
E2F-bs2/3
C
IgG
p107
Enrichment: % Input
0.10
0.08
0.06
0.04
0.02
0.00
***
*
p107+/+
p107-/-
REST-E2F-bs1
REST-E2F-bs2/3
Cacng1
D
IgG
p130
Rb
E2F1
E2F3
E2F4
Enrichment: % Input
0.16
0.12
0.08
0.04
0.00
p107-/-
Rb-TKO
REST-E2F-bs1
REST-E2F-bs2/3
Cacng1
E
Rb-THC
Rb-TKO
mCherry
dnRest-V5
Days 0 1 3 0 1 3 0 1 3 0 1 3 eNS
p107
Rb
p130
Dcx
βIII tubulin
Ascl1
PCNA
dnRest-V5
β-actin
F
Ascl1/β-actin normalized to Rb-THC + mCherry Day0
Rb-THC mCherry
Rb-THC dnRest
Rb-TKO mCherry
Rb-TKO dnRest
Day 0
Day 1
Day 3
Rb Family Proteins
Activator E2Fs
(Repressors)
REST
REST Target Genes
ASCL1

Figure 7

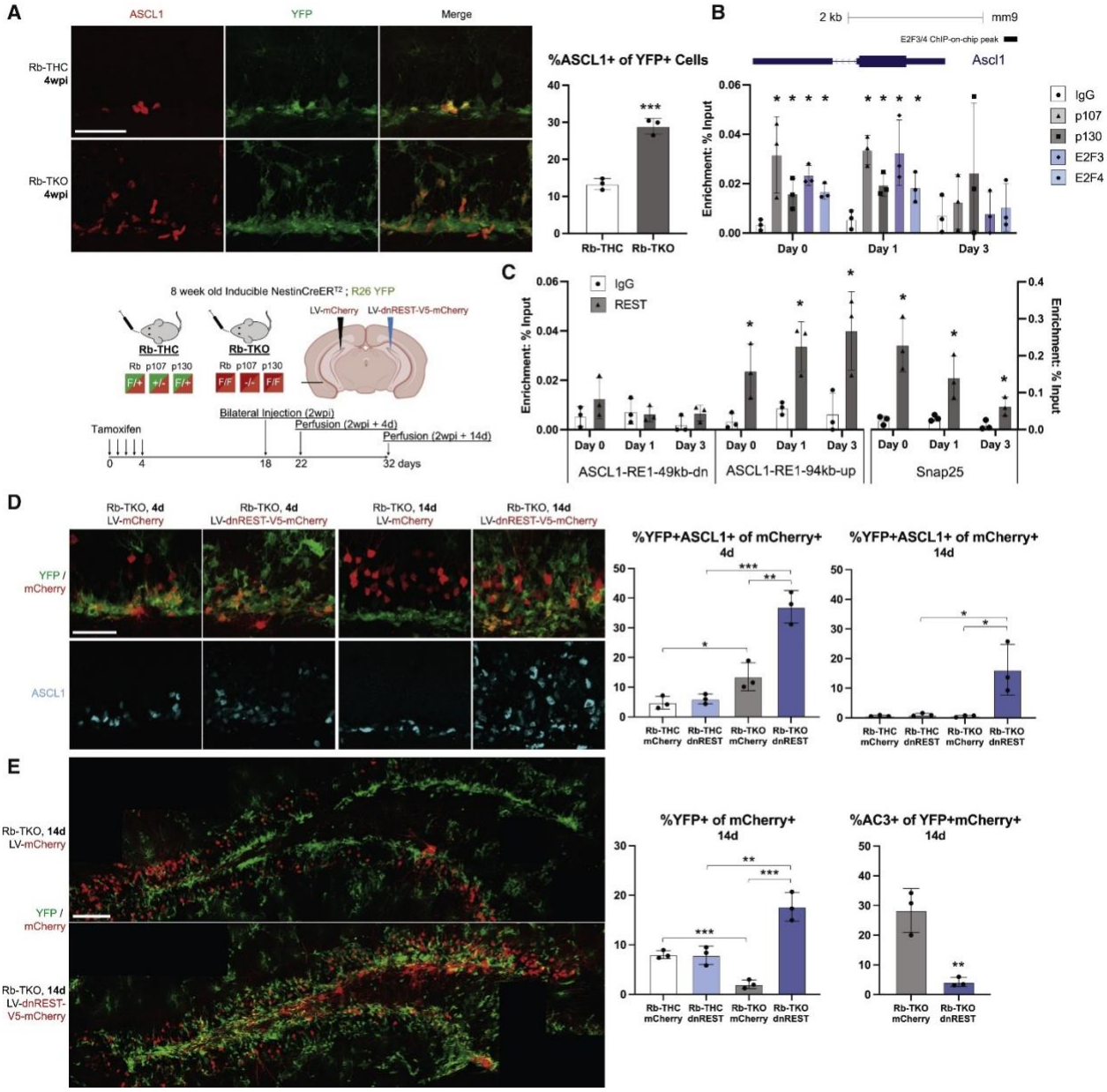
A
ASCL1
YFP
Merge
Rb-THC 4wpi
Rb-TKO 4wpi
%ASCL1+ of YFP+ Cells
Rb-THC
Rb-TKO
B
2 kb
mm9
E2F3/4 ChIP-on-chip peak
Ascl1
Enrichment: % Input
Day 0
Day 1
Day 3
IgG
p107
p130
E2F3
E2F4
8 week old Inducible NestinCreER^{T2} ; R26 YFP
Rb-THC
Rb-TKO
Rb p107 p130
F/+ +/- F/+
F/F -/- F/F
LV-mCherry
LV-dnREST-V5-mCherry
Tamoxifen
Bilateral Injection (2wpi)
Perfusion (2wpi + 4d)
Perfusion (2wpi + 14d)
0 4 18 22 32 days
C
IgG
REST
Enrichment: % Input
Enrichment: % Input
ASCL1-RE1-49kb-dn
ASCL1-RE1-94kb-up
Snap25
D
Rb-TKO, 4d LV-mCherry
Rb-TKO, 4d LV-dnREST-V5-mCherry
Rb-TKO, 14d LV-mCherry
Rb-TKO, 14d LV-dnREST-V5-mCherry
YFP / mCherry
ASCL1
%YFP+ASCL1+ of mCherry+ 4d
%YFP+ASCL1+ of mCherry+ 14d
Rb-THC mCherry
Rb-THC dnREST
Rb-TKO mCherry
Rb-TKO dnREST
E
Rb-TKO, 14d LV-mCherry
YFP / mCherry
Rb-TKO, 14d LV-dnREST-V5-mCherry
%YFP+ of mCherry+ 14d
%AC3+ of YFP+mCherry+ 14d

STAR Methods

- **KEY RESOURCES TABLE**
- **RESOURCE AVAILABILITY**
  - Lead Contact
  - Materials Availability
  - Data and Code Availability
- **EXPERIMENTAL MODEL AND SUBJECT DETAILS**
  - Animals
  - Cell Lines
- **METHOD DETAILS**
  - Perfusion, Freezing and Sectioning
  - Immunohistochemistry and Imaging
  - FACS and RNA isolation
  - qRT-PCR
  - RNASeq
  - Bioinformatic Analysis
  - Network Analysis
  - Lentiviral vectors
  - Stereotaxic Injections
  - Western Blot
  - ChIP
  - ChIP-seq analysis
- **QUANTIFICATION AND STATISTICAL ANALYSIS**

KEY RESOURCES TABLE

REAGENT or RESOURCE	SOURCE	IDENTIFIER
Antibodies		
E2F1 (Rabbit; ChIP)	Santa Cruz	CAT#sc-193
E2F3 (Rabbit; ChIP)	Abcam	CAT#ab-50917
E2F4 (Rabbit; ChIP)	Santa Cruz	CAT#sc-1082
E2F4 (Rabbit; ChIP)	NovusBio	CAT#NBP1-21374
IgG (Rabbit; ChIP)	Sigma-Aldrich	CAT#I8140
p130 (Rabbit; ChIP)	Santa Cruz	CAT#sc-317
REST (Rabbit; ChIP)	Millipore	CAT#07-579
p107 (Rabbit; WB, ChIP)	Santa Cruz	CAT#sc-318
p130 (Mouse; WB, ChIP)	BD Biosciences	CAT#610262
Rb (Rabbit; WB, ChIP)	Santa Cruz	CAT#sc-50
Rb (Rabbit; WB)	Abcam	CAT#ab181616
β-actin-HRP (Mouse; WB)	Santa Cruz	CAT#sc-47778
βIII tubulin (Rabbit; WB)	Covance	CAT#PRB 435P
Dcx (Rabbit; WB)	Cell Signaling	CAT#4604
Mash1 (Mouse; WB)	BD Biosciences	CAT#556604
Rest (Rabbit; WB)	Abcam	CAT#ab-21635
PCNA (Mouse; WB)	Santa Cruz	Cat#sc-056
V5-tag (Rabbit; WB)	Bethyl	CAT#A190-120A
β tubulin (Mouse; WB)	DSHB	CAT#E7
GFP (Chicken; IHC)	Abcam	CAT#ab13970
GFP (Rabbit; IHC)	EnCor	CAT#RPCA-GFP
Nestin (Goat; IHC)	R&D Systems	CAT#AF2736
Nestin (Chicken; IHC)	Abcam	CAT#ab134017
GFAP (Mouse; IHC)	Millipore	CAT#MAB3402
GFAP (Goat; IHC)	Santa Cruz	CAT#sc-6170
Sox2 (Goat; IHC)	Santa Cruz	CAT#sc-17320
Sox2 (Goat; IHC)	Neuromics	CAT#GT15098
ASCL1 (Rabbit; IHC)	Abcam	CAT#ab211327
Ki67 (Rabbit; IHC)	Cell Marque	CAT#275R
Tbr2 (Rat; IHC)	Invitrogen	CAT#14-4875-82
Dcx (Goat; IHC)	Santa Cruz	CAT#SC-8066
Dcx (Guinea Pig; IHC)	Millipore	CAT#AB2253
Dcx (Rabbit; IHC)	Cell Signaling	CAT#4604S
Prox1 (Rabbit; IHC)	Millipore	CAT#AB5475
NeuN (Rabbit; IHC)	Millipore	CAT#MAB377
mCherry (Rat; IHC)	ThermoFisher	CAT#M11217
Active Caspase 3 (Rabbit; IHC)	Cell Signaling	CAT#9664S
S100-β (Rabbit; IHC)	Dako	CAT#Z0311

Chemicals, Peptides, and Recombinant Proteins		
Tamoxifen	Millipore Sigma	CAT#T5648
EdU	BaseClick	CAT#BCK647-IV-IM-M
Paraformaldehyde	E COM	CAT#Px0055-3
Tissue-Tek OCT Compound	VWR	CAT#25608-930
DAPI	Millipore Sigma	CAT#D9542
Epredia™ Immu-Mount™	Fisher	CAT#9990412
Percoll	Millipore Sigma	CAT#GE17-0891-02
DMEM/F12	Gibco	CAT#11330-032
B27 without Vitamin A	Gibco	CAT#12587010
EGF	Millipore Sigma	CAT#E-1257
bFGF	Millipore Sigma	CAT#F-0291
heparin	Millipore Sigma	CAT#H-3149
Penicillin/Streptomycin	Gibco	CAT#1570-063
Matrigel	VWR	CAT#CACB356230
B27 with Vitamin A	Gibco	CAT#17504044
N2	Gibco	CAT#17502048
HI-FBS	Wisent	CAT#080-150
Clarity Enhanced chemiluminescence Western Blotting Substrate	Bio-Rad	CAT#1705061
Papain	Cedarlane	CAT#LS003126
DNase I	Roche	CAT#11284932001
RNaseZAP	ThermoFisher	CAT#AM9780
Critical Commercial Assays		
Arcturus® PicoPure® RNA Isolation Kit	ThermoFisher	CAT#KIT0204
Rotor-Gene SYBR® Green PCR Kit	Qiagen	CAT#204074
SMART-Seq® v4 Ultra® Low Input RNA Kit for Sequencing	Takara	CAT#634890
Nextera XT DNA Library Preparation Kit	Illumina	CAT#FC-131-1024
Deposited Data		
Gene signatures of cell clusters in the adult mouse V-SVZ	Basak et al., 2018	GSE65970
Gene signatures of Quiescent and Activated NSC populations in the adult mouse V-SVZ	Codega et al., 2014	GSE54653

ChIP-seq data on REST in rat cells (QNP and TAP)	Mukherjee et al., 2016	SRP060618
ChIP-seq data on Rest in human cells	ENCODE	SRP008797
ChIP-seq data on Rest in human cells	ENCODE	SRP012412
RNA-seq data on Rb-THC, Rb-TKO, E2F1/3-HET and E2F1/3-DKO in mouse neural stem cells	This paper	GSE190766
Experimental Models: Cell Lines		
Micro-dissected and FACS-isolated SVZ YFP+ NSCs	N/A	N/A
Micro-dissected SVZ NSCs	N/A	N/A
293T HEK Cells	ATCC	CRL3216
Experimental Models: Organisms/Strains		
Mouse: Rb-TKO (Rb conditional mutant; p107 -/- ; p130 conditional mutant) on 129Sv/J X C57/BL6 background	Dr. Julien Sage	Viatour et al., 2008
Mouse: E2F1/3-DKO (E2F1 -/- ; E2F3 conditional mutant) on FVB/N X 129Sv/J X C57/BL6 background	Dr. Gustavo Leone	E2F1: Field et al., 1996; E2F3: Wu et al., 2001
Mouse: Nestin-CreER^{T2}; R26-stop-enhanced yellow fluorescent protein (YFP)	Dr. Suzanne Baker	Cicero et al., 2009
Oligonucleotides		
Genotyping Primers, see Supplementary Table 2	N/A	N/A
qRT-PCR Primers, see Supplementary Table 3	N/A	N/A
ChIP Primers, see Supplementary Table 4	N/A	N/A
Recombinant DNA		
pLVX-EF1a-IRES-mCherry	Clontech	631987
Software and Algorithms		
Fiji	Schindelin et al., 2012	https://fiji.sc
FastQC	Andrews et al., 2012	https://www.bioinformatics.babraham.ac.uk/projects/fastqc/
HiSat2	Kim et al., 2019	http://daehwankimlab.github.io/hisat2/
IGV	Robinson et al., 2011	https://software.broadinstitute.org/software/igv/

featureCounts	Liao et al., 2014	http://subread.sourceforge.net
R 3.5.3	Team, 2021	https://www.r-project.org
DESeq2	Love et al., 2014	https://bioconductor.org/packages/release/bioc/html/DESeq2.html
IHW	Ignatiadis et al., 2016	https://bioconductor.org/packages/release/bioc/html/IHW.html
biomaRt	Durinck et al., 2009	https://bioconductor.org/packages/release/bioc/html/biomaRt.html
g:Profiler	Raudvere et al., 2019; Reimand et al., 2007	https://biit.cs.ut.ee/gprofiler/gost
Cytoscape 3.8.2	Shannon et al., 2003	https://cytoscape.org
Enrichment Map	Merico et al., 2010	https://www.baderlab.org/Software/EnrichmentMap
iRegulon	Janky et al., 2014	http://iregulon.aertslab.org
NetworkAnalyst	Zhou et al., 2019	https://www.networkanalyst.ca
ImageJ	Schneider et al., 2012	https://imagej.net/software/imagej/
Prism 9.4.0	GraphPad	https://www.graphpad.com/scientific-software/prism/

RESOURCE AVAILABILITY

Lead Contact

Further information and requests for resources and reagents should be directed to and will be fulfilled by the lead Contact, Ruth Slack (rslack@uottawa.ca)

Materials Availability

This study did not generate new unique reagents.

Data and Code Availability

- Data have been deposited in GEO under accession number GEO: GSE190766.
- The published article includes all datasets generated or analyzed during this study and no new code was produced.
- Any additional information required to reanalyze the data reported in this paper is available from the lead contact upon request.

EXPERIMENTAL MODEL AND SUBJECT DETAILS

Animals

All experiments were approved by the Animal Care Ethics Committee of the University of Ottawa and adhered to the Guidelines of the Canadian Council on Animal Care.

Rb-TKO (Rb conditional mutant; p107 -/-; p130 conditional mutant) mice were provided by Dr. Julien Sage (Viatour et al., 2008), and crossed with Nestin-CreER^{T2} (Cicero et al., 2009); R26-stop-enhanced yellow fluorescent protein (YFP) (Srinivas et al., 2001) mice. All Rb-TKO mice were maintained on a mixed 129Sv/J X C57/BL6 background; Rb-THC mice were generated by crossing Rb-TKO mice with wild-type 129Sv/J X C57/BL6 mice from Charles River to generate a triple-heterozygous control.

E2F1/3-DKO (E2F1 -/- (Field et al., 1996); E2F3 conditional mutant (Wu et al., 2001)) mice were provided by Dr. Gustavo Leone, and crossed with Nestin-CreER^{T2};R26EYFP mice described above. All E2F1/3-DKO mice were maintained on a mixed FVB/N X 129Sv/J X C57/BL6 background; E2F1/3-HET mice were generated by crossing E2F1/3-DKO mice with wild-type FVB/N X 129Sv/J X C57/BL6 mice from Charles River to generate a double-heterozygous control.

Animals were genotyped according to standard protocols with previously published primers, listed in Supplementary Table 2. All Nestin-CreER^{T2} animals used were heterozygotes for Cre expression. In all experiments, both females and males were used; all animals were 6-10 weeks old upon initial intervention.

For Cre induction in adult NestinCreERT2 animals, mice were administered tamoxifen (TAM) at 200 mg/kg/d for 5d (gavage; dissolved in 10% EtOH/90% corn oil), with initial

weight used for dose calculation; weight after final injection was monitored, and semi-weekly wellness checks were performed until euthanization. Animals in Figure S1B-C were administered TAM at 150 mg/kg/d for 5d (intraperitoneal; dissolved in 10% EtOH/90% sunflower oil), following same calculation/monitoring/wellness protocol. To analyze cell proliferation, NestinCreERT2 mice were given a single injection of EdU (50mg/kg, i.p) 2 hours before euthanization and perfusion.

Primary Cell Cultures

YFP+ cells and NSCs were isolated from SVZ tissue obtained from mice 10 days post-tamoxifen injection as previously described (Iqbal et al., 2022). Briefly, brains were micro-dissected in cold ACSF, tissue was digested in a Papain suspension (Cedarlane) and resuspended in FBS (Wisent) and DNase I (Roche), before using a 22% (v/v) PBS-buffered Percoll solution (Millipore Sigma) to achieve cells suitable for suspension. Cells were then either FACS-isolated to provide a YFP+ fraction for bulk RNA-Seq or cell culture or, to compensate for the absence of FACS, rinsed in DMEM:F12 (Gibco) to remove excess Percoll from the cell surface.

Cells were plated at a concentration of 10 cells/μL in stem cell media as previously described (Reynolds and Weiss, 1992). Briefly, DMEM/F12 (Gibco) is supplemented with B27 without Vitamin A (Gibco), EGF (Sigma), bFGF (Sigma), heparin (Sigma) and Penicillin/Streptomycin (Gibco) to encourage neurosphere growth. Neurospheres were passaged after 6-7 days, up to three times, plated at a concentration of 4 cells/μL. For differentiation, plates were coated with 10% Matrigel (VWR) in serum-free media. Cells were plated as neurospheres and grown in differentiation media; DMEM/F12 supplemented with B27 with Vitamin A (Gibco), N2 (Gibco), 2% HI-FBS (Wisent) and Penicillin/Streptomycin. Cells were differentiated for 0, 1 and 3 days, with a media change on Day 2.

Cell Lines

HEK-293T cells (ATCC) were maintained in Biolite cell culture treated dishes (Thermo Scientific) with DMEM (Gibco) supplemented with 1% penicillin-streptomycin and 10% FBS (Gibco) in an incubator (37°C, 5% CO2). Cell line was obtained from a high-quality source (ATCC) and cross-referenced against the ICLAC Register of Misidentified Cell Lines.

METHOD DETAILS

Perfusion, Freezing and Sectioning

Tissue perfusion and fixation was performed as previously described (McClellan et al., 2007). Briefly, 4% Paraformaldehyde was prepared fresh within 2 hours of perfusion. Animals were perfused transcardially, employing chilled 0.9% saline in advance of PFA. Brains were immersed in PFA overnight, followed by wash in 1X PBS

and storage in 20% sucrose the following morning. Once the brains had sunken in the sucrose, they were suitable for freezing. Brains were removed from sucrose, lightly patted dry on Kimwipe, and the cerebellum removed with a razor blade to establish a flat coronal edge.

Freezing occurred in isopentane pre-chilled to between -30 and -40 ºC, and maintained at temperature with dry ice. PFA-fixed brains were immersed in isopentane for duration following two criteria: minimum 60 seconds and ceasing of bubbles from brain. Frozen brains were wrapped in aluminum foil and stored at -80 until sectioning.

For sectioning, brains were mounted on a cryostat at -24ºC, using VWR Tissue-Tek OCT compound. Brains were sectioned maintaining temperature between -18 and -20ºC, in 30 µm sections, skipping the OB but comprising the SVZ and hippocampal formation. Free-floating sections were collected in 1X PBS with 0.1% NaCN, into 9 wells following a 1:9 serial section pattern, separating SVZ and SGZ tissue. Brains were stored long-term in 24-well plates, under film to protect against drying out, at 4ºC.

Immunohistochemistry and Imaging

IHC was performed as previously described (Vandenbosch et al., 2016). Briefly, free-floating sections were triple-washed 3x/5min in 1X PBS before incubation at 4°C with primary antibodies for between overnight to 48 hours. After a second triple-wash, sections were incubated with dye-coupled secondary Donkey antibodies (Jackson) and DAPI (Sigma) for between 2 hours to overnight. Primary antibodies listed in Supplementary Table 1, as well as secondary antibodies, were diluted in 1x PBS containing 0.1% Triton, 0.1% Tween-20. Following a final triple-wash, sections were mounted and dried at room temperature; slides were cover-slipped with Epredia™ Immu-Mount™ (Fisher) and dried at 4°C overnight.

Sections for quantifications of colocalized cells were imaged using Zeiss LSM510, and later Zeiss LSM800 confocal microscopes, employing a 40x objective. Z-stacks spanned 10 µm of post-processing section width, with 2.0 µm spacing between Z-positions. Sections quantifying single labelling were quantified on an Olympus BX-51 microscope. Images were analyzed using Fiji (Schindelin et al., 2012).

FACS and RNA isolation

FACS was performed on isolated SVZ NSCs, suspended in DMEM/F12 (without phenol red; Invitrogen) at the University of Ottawa Flow Cytometry Core as well as OHRI StemCore Laboratories, isolating the YFP+ cell population using a cutoff of 488-FL-Log-Height ≥ 10^2.

For RNA-Seq input, cell pellets containing minimum 200,000 YFP+ cells were frozen, and RNA isolated using the Arcturus® PicoPure® RNA Isolation Kit (ThermoFisher). Cell pellets were divided into four: I was sent for fragment analysis at OHRI StemCore

Facility; II was used for qPCR validation of knockout or differential gene expression; III was sent for sequencing; IV was reserved as a backup.

qRT-PCR

Samples for RNA quantification were prepared using the Rotor-Gene SYBR® Green PCR Kit (Qiagen) and quantified on a Qiagen Rotor-Gene Q Real-Time PCR Machine. RNA concentrations for each primer set were normalized using standard curves prepared from wild-type adult NSCs as standard. Primers used are listed in Supplementary Table 3, and RNA quantifications are expressed relative to GAPDH (normalized to 1).

RNASeq

RNA input for NGS was only considered sufficient if three criteria were met: 1) concentration ≥7 ng/μL, for submission of minimum 35ng of RNA, 2) 260/280 ≥ 2 and RQN ≥ 8.0.

RNASeq was performed at TCAG at the Hospital for Sick Children, following internal QC. Samples were run in sets of 6, reflecting 3 biological replicates. cDNA conversion used the SMART-Seq® v4 Ultra® Low Input RNA Kit for Sequencing (Clontech, now Takara), while Library Preparation used the Nextera XT DNA Library Preparation Kit (Illumina). Sequencing was performed on an Illumina HiSeq 2500, using a multiplexed PE126bp high output flow cell.

Bioinformatic Analysis

Raw reads as FastQ files were first validated as downloads using md5sum and subjected to FastQC (Andrews et al., 2012) to ensure run quality and suitability for the standard protocol of analysis without trimming or phred scores. For alignment, FastQ files were aligned to Hisat2 GRCm38 index using HiSat2 (Kim et al., 2019) to generate BAM files. Aligned reads were visualized in IGV (Robinson et al., 2011). For read assignment, BAM files were converted to feature counts using featureCounts, part of the subread package (Liao et al., 2014), as well as the Ensembl GRCm38.101 GTF file, build dated August 2020.

Differential expression analysis of feature counts was established in R 3.5.3 (Team, 2021) using DESeq2 (Love et al., 2014), and employed Independent Hypothesis Weighting using the IHW package (Ignatiadis et al., 2016). For the Rb-TKO dataset, batch correction was employed to account for batch effects distinguishing samples RB_THC_1 and RB_TKO_1, stemming from sample preparation; effects are visible in Supp.Fig S3C. Ensembl Stable IDs were converted to MGI symbols using biomaRt (Durinck et al., 2009).

Network Analysis

Pathway and network enrichment analysis generally followed a published protocol (Reimand et al., 2019). Enrichment analysis with Gene Ontology: Biological Process was performed using g:GOSt and g:Convert as part of the g:Profiler toolset (Raudvere et al., 2019; Reimand et al., 2007), and visualized in Cytoscape 3.8.2 (Shannon et al., 2003) using Enrichment Map (Merico et al., 2010).

Gene regulatory network analysis was performed using iRegulon (Janky et al., 2014), analyzing a putative regulatory region spanning 20kb centred around the TSS, using a motif rankings database from 10 species; significant genes ($p<0.05$) were used as input. ENCODE TF-gene interactions were assessed using NetworkAnalyst (Zhou et al., 2019); all genes were used as input.

Lentiviral vectors

A pLVX-EF1a-IRES-mCherry lentiviral expression vector construct was commercially obtained (Clontech 631987) and used as control. A truncated, dominant-negative REST (Bergsland et al., 2006; Chen et al., 1998) was generated, and cloned to include a V5 tag. This construct was subcloned into the expression vector to generate a pLVX-EF1a-dnREST-V5-IRES-mCherry.

Lentiviruses were produced in 293T cells using PEI and ultracentrifugation, following established protocols (TANG et al., 2015), and was resuspended in PBS into small aliquots. Live titre confirmed achieving a minimum concentration of 1.2E+09 TU/mL.

For use *in vitro*, passaged cells at P2 were infected with lentiviral particles at a multiplicity of infection (MOI) of 30, before neurosphere differentiation after 5-7 days.

Stereotaxic Injections

Bilateral injections of lentivirus were performed at the uOttawa Surgery Core by Dr. Anthony Carter. In order to target the SGZ, lentiviruses were bilaterally injected into the dentate gyrus following published co-ordinates (Xi et al., 2016): -1.7mm anterior/posterior, ±1.2 mediolateral, -2.4mm dorsoventral from Bregma; injection volume was 1.0 µL, at a rate of 0.2 µL/min.

Western Blot

Cell pellets of cultured adult NSCs were solubilized in a lysis buffer containing 20 mM Tris pH 6.8, 6M urea and 0.1% SDS (Liu et al., 2010). 20 ug of proteins were separated on 10% SDS-PAGE. After transfer and blocking, membranes were incubated with primary antibodies overnight at 4° C, washed 3 times with TTTBS buffer (Tris-buffered saline, TBS with 0.05% TritonX-100 and 0.05% Tween 20), incubated with HRP-tagged secondary antibody for 1 hour, and washed at room temperature. Alternatively, β-actin blot was incubated for 1 hour at room temperature. Finally, signal was developed using Clarity Enhanced chemiluminescence Western Blotting Substrate

(BioRad). Antibodies used in Western Blot are listed in Supplementary Table 1. Western blot bands were quantified using Image J.

ChIP

ChIP assays followed by quantitative real-time PCR (qPCR) were performed as previously described (Julian et al., 2016; Liu et al., 2010). Briefly, neurosphere cultures were prepared from wild-type, Rb-THC or Rb-TKO mice at 8-10 weeks of age as described above, proliferating neurospheres were triturated, cross-linked with formaldehyde, lysed, sonicated, and centrifuged at 14,000 × g to remove cellular debris. 10 µg of 30 min cross-linked chromatin and 0.8 µg of antibodies were used in ChIP assays. Antibodies are listed in Supplementary Table 1, and qPCR primers are listed in Supplementary Table 4.

ChIP-seq analysis

ChIP-seq data on REST in rat cells (QNP and TAP) were performed by (Mukherjee et al., 2016) and obtained from NCBI as Short Reads Archive under accession number SRP060618. ChIP-seq data on Rest in different human cells were performed by ENCODE and obtained from NCBI under accession numbers SRP008797 (ECC-1, GM12878, H1-hESC, H1-neurons, HCT-116, HeLa-S3, HepG2, HL-60, k562, MCF-7, PANC-1, PFSK-1, SK-N-SH) and SRP012412 (A549, GM23338, H1-hESC, HEK293 eGFP-REST, K562, K562 eGFP-REST). Sequencing read data were analyzed following ENCODE pipeline. Conditions with more than one technical or biological replicates were combined into single FastQ files. Human data were aligned to the GRCh38 (hg38) version of the human genome, while rat data were aligned to the Rnor_6.0 (rn6) version of the rat genome.

QUANTIFICATION AND STATISTICAL ANALYSIS

For cell quantification in the adult SGZ, every ninth section throughout the DG was quantified and counts were summed and multiplied by 9 to generate an estimate of the total number of cells in the DG. For cell quantification in the adult SVZ, given the larger structure, every eighteenth section throughout the SVZ was quantified and counts were summed and multiplied by 18 to generate an estimate of the total number of cells in the SVZ.

Statistical details of all experiments can be found in the figure legends. All statistical comparisons in this study were performed using an unpaired two-tailed Student's t-test, with the exception of Figure 6F, which employs a paired two-tailed Student's t-test. Differences were considered significant with a p value of < 0.05 (*), **$p< 0.01$, ***$p < 0.001$, ****$p<0.0001$. Unless otherwise stated, all data is presented as the arithmetic mean, plus or minus the standard deviation of the mean (mean ± SD). For each experiment, a minimum of 3 animals per genotype were used, with N referring

to biological replicates. Prism 9.4.0 (Graphpad) was used to perform statistical analysis.

Bibliography

Ajioka, I., Martins, R.A.P., Bayazitov, I.T., Donovan, S., Johnson, D.A., Frase, S., Cicero, S.A., Boyd, K., Zakharenko, S.S., and Dyer, M.A. (2007). Differentiated horizontal interneurons clonally expand to form metastatic retinoblastoma in mice. Cell *131*, 378–390. https://doi.org/10.1016/j.cell.2007.09.036.

Andersen, J., Urban, N., Achimastou, A., Ito, A., Simic, M., Ullom, K., Martynoga, B., Lebel, M., Göritz, C., Frisén, J., et al. (2014). A transcriptional mechanism integrating inputs from extracellular signals to activate hippocampal stem cells. Neuron *83*, 1085–1097. https://doi.org/10.1016/j.neuron.2014.08.004.

Andrews, S., Krueger, F., Segonds-Pichon, A., Biggins, L., Krueger, C., and Wingett, S. (2012). FastQC.

Ballas, N., Grunseich, C., Lu, D.D., Speh, J.C., and Mandel, G. (2005). REST and Its Corepressors Mediate Plasticity of Neuronal Gene Chromatin throughout Neurogenesis. Cell *121*, 645–657. https://doi.org/10.1016/j.cell.2005.03.013.

Basak, O., Krieger, T.G., Muraro, M.J., Wiebrands, K., Stange, D.E., Frias-Aldeguer, J., Rivron, N.C., Wetering, M. van de, Es, J.H. van, Oudenaarden, A. van, et al. (2018). Troy+ brain stem cells cycle through quiescence and regulate their number by sensing niche occupancy. Proc National Acad Sci *115*, E610–E619. https://doi.org/10.1073/pnas.1715911114.

Bergsland, M., Werme, M., Malewicz, M., Perlmann, T., and Muhr, J. (2006). The establishment of neuronal properties is controlled by Sox4 and Sox11. Genes Dev *20*, 3475–3486. https://doi.org/10.1101/gad.403406.

Burkhart, D.L., Ngai, L.K., Roake, C.M., Viatour, P., Thangavel, C., Ho, V.M., Knudsen, E.S., and Sage, J. (2010). Regulation of RB Transcription In Vivo by RB Family Members. Molecular and Cellular Biology *30*, 1729–1745. https://doi.org/10.1128/mcb.00952-09.

Callaghan, D.A., Dong, L., Callaghan, S.M., Hou, Y.X., Dagnino, L., and Slack, R.S. (1999). Neural precursor cells differentiating in the absence of Rb exhibit delayed terminal mitosis and deregulated E2F 1 and 3 activity. Dev Biol *207*, 257–270. https://doi.org/10.1006/dbio.1998.9162.

Chen, D., Pacal, M., Wenzel, P., Knoepfler, P.S., Leone, G., and Bremner, R. (2009). Division and apoptosis of E2f-deficient retinal progenitors. Nature *462*, 925–929. https://doi.org/10.1038/nature08544.

Chen, Z.-F., Paquette, A.J., and Anderson, D.J. (1998). NRSF/REST is required in vivo for repression of multiple neuronal target genes during embryogenesis. Nat Genet *20*, 136–142. https://doi.org/10.1038/2431.

Chong, J.A., Tapia-Ramirez, J., Kim, S., Toledo-Aral, J.J., Zheng, Y., Boutros, M.C., Altshuller, Y.M., Frohman, M.A., Kraner, S.D., and Mandel, G. (1995). REST: A mammalian silencer protein that restricts sodium channel gene expression to neurons. Cell *80*, 949–957. https://doi.org/10.1016/0092-8674(95)90298-8.

Chong, J.-L., Wenzel, P.L., Sáenz-Robles, M.T., Nair, V., Ferrey, A., Hagan, J.P., Gomez, Y.M., Sharma, N., Chen, H.-Z., Ouseph, M., et al. (2009). E2f1-3 switch from activators in progenitor cells to repressors in differentiating cells. Nature *462*, 930–934. https://doi.org/10.1038/nature08677.

Cicero, S.A., Johnson, D., Reyntjens, S., Frase, S., Connell, S., Chow, L.M.L., Baker, S.J., Sorrentino, B.P., and Dyer, M.A. (2009). Cells previously identified as retinal stem cells are pigmented ciliary epithelial cells. Proceedings of the National Academy of Sciences *106*, 6685–6690. https://doi.org/10.1073/pnas.0901596106.

Codega, P., Silva-Vargas, V., Paul, A., Maldonado-Soto, A.R., Deleo, A.M., Pastrana, E., and Doetsch, F. (2014). Prospective identification and purification of quiescent adult neural stem cells from their in vivo niche. Neuron *82*, 545–559. https://doi.org/10.1016/j.neuron.2014.02.039.

Cooper-Kuhn, C.M., Vroemen, M., Brown, J., Ye, H., Thompson, M.A., Winkler, J., and Kuhn, H.G. (2002). Impaired Adult Neurogenesis in Mice Lacking the Transcription Factor E2F1. Mol Cell Neurosci *21*, 312–323. https://doi.org/10.1006/mcne.2002.1176.

Davis, C.A., Hitz, B.C., Sloan, C.A., Chan, E.T., Davidson, J.M., Gabdank, I., Hilton, J.A., Jain, K., Baymuradov, U.K., Narayanan, A.K., et al. (2018). The Encyclopedia of DNA elements (ENCODE): data portal update. Nucleic Acids Res *46*, D794–D801. https://doi.org/10.1093/nar/gkx1081.

Delgado, A.C., Maldonado-Soto, A.R., Silva-Vargas, V., Mizrak, D., Känel, T. von, Tan, K.R., Paul, A., Madar, A., Cuervo, H., Kitajewski, J., et al. (2021). Release of stem cells from quiescence reveals gliogenic domains in the adult mouse brain. Science *372*, 1205–1209. https://doi.org/10.1126/science.abg8467.

Dunham, I., Kundaje, A., Aldred, S.F., Collins, P.J., Davis, C.A., Doyle, F., Epstein, C.B., Frietze, S., Harrow, J., Kaul, R., et al. (2012). An Integrated Encyclopedia of DNA Elements in the Human Genome. Nature *489*, 57–74. https://doi.org/10.1038/nature11247.

Durinck, S., Spellman, P.T., Birney, E., and Huber, W. (2009). Mapping identifiers for the integration of genomic datasets with the R/Bioconductor package biomaRt. Nat Protoc *4*, 1184–1191. https://doi.org/10.1038/nprot.2009.97.

Edgar, R., Domrachev, M., and Lash, A.E. (2002). Gene Expression Omnibus: NCBI gene expression and hybridization array data repository. Nucleic Acids Res *30*, 207–210. https://doi.org/10.1093/nar/30.1.207.

Encinas, J.M., Michurina, T.V., Peunova, N., Park, J.-H., Tordo, J., Peterson, D.A., Fishell, G., Koulakov, A., and Enikolopov, G. (2011). Division-Coupled Astrocytic Differentiation and Age-Related Depletion of Neural Stem Cells in the Adult Hippocampus. Cell Stem Cell *8*, 566–579. https://doi.org/10.1016/j.stem.2011.03.010.

Ferland, R.J., Batiz, L.F., Neal, J., Lian, G., Bundock, E., Lu, J., Hsiao, Y.-C., Diamond, R., Mei, D., Banham, A.H., et al. (2009). Disruption of neural progenitors along the ventricular and subventricular zones in periventricular heterotopia. Hum Mol Genet *18*, 497–516. https://doi.org/10.1093/hmg/ddn377.

Field, S.J., Tsai, F.-Y., Kuo, F., Zubiaga, A.M., Kaelin, W.G., Livingston, D.M., Orkin, S.H., and Greenberg, M.E. (1996). E2F-1 Functions in Mice to Promote Apoptosis and Suppress Proliferation. Cell *85*, 549–561. https://doi.org/10.1016/s0092-8674(00)81255-6.

Friend, S.H., Bernards, R., Rogelj, S., Weinberg, R.A., Rapaport, J.M., Albert, D.M., and Dryja, T.P. (1986). A human DNA segment with properties of the gene that predisposes to retinoblastoma and osteosarcoma. Nature *323*, 643–646. https://doi.org/10.1038/323643a0.

Gao, Z., Ure, K., Ding, P., Nashaat, M., Yuan, L., Ma, J., Hammer, R.E., and Hsieh, J. (2011). The Master Negative Regulator REST/NRSF Controls Adult Neurogenesis by Restraining the Neurogenic Program in Quiescent Stem Cells. The Journal of Neuroscience *31*, 9772–9786. https://doi.org/10.1523/jneurosci.1604-11.2011.

Gonçalves, J.T., Schafer, S.T., and Gage, F.H. (2016). Adult Neurogenesis in the Hippocampus: From Stem Cells to Behavior. Cell *167*, 897–914. https://doi.org/10.1016/j.cell.2016.10.021.

Hodge, R.D., Nelson, B.R., Kahoud, R.J., Yang, R., Mussar, K.E., Reiner, S.L., and Hevner, R.F. (2012). Tbr2 Is Essential for Hippocampal Lineage Progression from Neural Stem Cells to Intermediate Progenitors and Neurons. J Neurosci *32*, 6275–6287. https://doi.org/10.1523/jneurosci.0532-12.2012.

Ignatiadis, N., Klaus, B., Zaugg, J.B., and Huber, W. (2016). Data-driven hypothesis weighting increases detection power in genome-scale multiple testing. Nature Methods *13*, 577–580. https://doi.org/10.1038/nmeth.3885.

Iqbal, M.A., Fong, B.C., and Slack, R.S. (2022). Direct FACS Isolation of Neural Stem/Progenitor Lineages from the Adult Brain. Methods Mol Biology Clifton N J *2515*, 117–127. https://doi.org/10.1007/978-1-0716-2409-8_8.

Jaafar, C., Omais, S., Lafi, S.A., Jamal, N.E., Noubani, M., Skaf, L., and Ghanem, N. (2016). Role of Rb during Neurogenesis and Axonal Guidance in the Developing Olfactory System. Frontiers in Molecular Neuroscience *9*, 171–15. https://doi.org/10.3389/fnmol.2016.00081.

Janky, R., Verfaillie, A., Imrichová, H., Sande, B.V. de, Standaert, L., Christiaens, V., Hulselmans, G., Herten, K., Sanchez, M.N., Potier, D., et al. (2014). iRegulon: From a Gene List to a Gene Regulatory Network Using Large Motif and Track Collections. PLoS Computational Biology *10*, e1003731-19. https://doi.org/10.1371/journal.pcbi.1003731.

Jiang, Z., Deng, T., Jones, R., Li, H., Herschkowitz, J.I., Liu, J.C., Weigman, V.J., Tsao, M.-S., Lane, T.F., Perou, C.M., et al. (2010). Rb deletion in mouse mammary progenitors induces luminal-B or basal-like/EMT tumor subtypes depending on p53 status. J Clin Invest *120*, 3296–3309. https://doi.org/10.1172/jci41490.

Jørgensen, H.F., Terry, A., Beretta, C., Pereira, C.F., Leleu, M., Chen, Z.-F., Kelly, C., Merkenschlager, M., and Fisher, A.G. (2009). REST selectively represses a subset of RE1-containing neuronal genes in mouse embryonic stem cells. Development *136*, 715–721. https://doi.org/10.1242/dev.028548.

Julian, L.M., Vandenbosch, R., Pakenham, C.A., Andrusiak, M.G., Nguyen, A.P., McClellan, K.A., Svoboda, D.S., Lagace, D.C., Park, D.S., Leone, G., et al. (2013). Opposing regulation of Sox2 by cell-cycle effectors E2f3a and E2f3b in neural stem cells. Cell Stem Cell *12*, 440–452. https://doi.org/10.1016/j.stem.2013.02.001.

Julian, L.M., Liu, Y., Pakenham, C.A., Dugal-Tessier, D., Ruzhynsky, V., Bae, S., Tsai, S.-Y., Leone, G., Slack, R.S., and Blais, A. (2016). Tissue-specific targeting of cell fate regulatory genes by E2f factors. Cell Death and Differentiation *23*, 565–575. https://doi.org/10.1038/cdd.2015.36.

Kareta, M.S., Gorges, L.L., Hafeez, S., Benayoun, B.A., Marro, S., Zmoos, A.-F., Cecchini, M.J., Spacek, D., Batista, L.F.Z., O'Brien, M., et al. (2015). Inhibition of pluripotency networks by the Rb tumor suppressor restricts reprogramming and tumorigenesis. Cell Stem Cell *16*, 39–50. https://doi.org/10.1016/j.stem.2014.10.019.

Kim, D., Paggi, J.M., Park, C., Bennett, C., and Salzberg, S.L. (2019). Graph-based genome alignment and genotyping with HISAT2 and HISAT-genotype. Nat Biotechnol *37*, 907–915. https://doi.org/10.1038/s41587-019-0201-4.

Kim, E., Cheng, Y., Bolton-Gillespie, E., Cai, X., Ma, C., Tarangelo, A., Le, L., Jambhekar, M., Raman, P., Hayer, K.E., et al. (2017). Rb family proteins enforce the homeostasis of quiescent hematopoietic stem cells by repressing Socs3 expression. The Journal of Experimental Medicine *214*, 1901–1912. https://doi.org/10.1084/jem.20160719.

Kwon, J.S., Everetts, N.J., Wang, X., Wang, W., Croce, K.D., Xing, J., and Yao, G. (2017). Controlling Depth of Cellular Quiescence by an Rb-E2F Network Switch. Cell Reports *20*, 3223–3235. https://doi.org/10.1016/j.celrep.2017.09.007.

Lee, W.-H., Shew, J.-Y., Hong, F.D., Sery, T.W., Donoso, L.A., Young, L.-J., Bookstein, R., and Lee, E.Y.H.P. (1987). The retinoblastoma susceptibility gene encodes a nuclear phosphoprotein associated with DNA binding activity. Nature *329*, 642–645. https://doi.org/10.1038/329642a0.

Lepagnol-Bestel, A.-M., Zvara, A., Maussion, G., Quignon, F., Ngimbous, B., Ramoz, N., Imbeaud, S., Loe-Mie, Y., Benihoud, K., Agier, N., et al. (2009). DYRK1A interacts with the REST/NRSF-SWI/SNF chromatin remodelling complex to deregulate gene clusters involved in the neuronal phenotypic traits of Down syndrome. Hum Mol Genet *18*, 1405–1414. https://doi.org/10.1093/hmg/ddp047.

Liao, Y., Smyth, G.K., and Shi, W. (2014). featureCounts: an efficient general purpose program for assigning sequence reads to genomic features. Bioinformatics *30*, 923–930. https://doi.org/10.1093/bioinformatics/btt656.

Litovchick, L., Sadasivam, S., Florens, L., Zhu, X., Swanson, S.K., Velmurugan, S., Chen, R., Washburn, M.P., Liu, X.S., and DeCaprio, J.A. (2007). Evolutionarily Conserved Multisubunit RBL2/p130 and E2F4 Protein Complex Represses Human Cell Cycle-Dependent Genes in Quiescence. Mol Cell *26*, 539–551. https://doi.org/10.1016/j.molcel.2007.04.015.

Liu, Y., Chu, A., Chakroun, I., Islam, U., and Blais, A. (2010). Cooperation between myogenic regulatory factors and SIX family transcription factors is important for myoblast differentiation. Nucleic Acids Res *38*, 6857–6871. https://doi.org/10.1093/nar/gkq585.

Love, M.I., Huber, W., and Anders, S. (2014). Moderated estimation of fold change and dispersion for RNA-seq data with DESeq2. Genome Biology *15*, 31–48. https://doi.org/10.1186/s13059-014-0550-8.

McClellan, K.A., Ruzhynsky, V.A., Douda, D.N., Vanderluit, J.L., Ferguson, K.L., Chen, D., Bremner, R., Park, D.S., Leone, G., and Slack, R.S. (2007). Unique Requirement for Rb/E2F3 in Neuronal Migration: Evidence for Cell Cycle-Independent Functions. Molecular and Cellular Biology *27*, 4825–4843. https://doi.org/10.1128/mcb.02100-06.

McGann, J.C., Spinner, M., Garg, S.K., Mullendorf, K., Woltjer, R.L., and Mandel, G. (2020). Genome-wide assessment of REST binding profiles reveals distinctions between human and mouse hippocampus. Biorxiv 2020.07.07.192229. https://doi.org/10.1101/2020.07.07.192229.

Merico, D., Isserlin, R., Stueker, O., Emili, A., and Bader, G.D. (2010). Enrichment Map: A Network-Based Method for Gene-Set Enrichment Visualization and Interpretation. Plos One *5*, e13984. https://doi.org/10.1371/journal.pone.0013984.

Miles, D.K., and Kernie, S.G. (2008). Hypoxic-ischemic brain injury activates early hippocampal stem/progenitor cells to replace vulnerable neuroblasts. Hippocampus *18*, 793–806. https://doi.org/10.1002/hipo.20439.

Morris, E.J., and Dyson, N.J. (2001). Retinoblastoma protein partners. Adv Cancer Res *82*, 1–54. https://doi.org/10.1016/s0065-230x(01)82001-7.

Mu, L., Berti, L., Masserdotti, G., Covic, M., Michaelidis, T.M., Doberauer, K., Merz, K., Rehfeld, F., Haslinger, A., Wegner, M., et al. (2012). SoxC Transcription Factors Are Required

for Neuronal Differentiation in Adult Hippocampal Neurogenesis. J Neurosci *32*, 3067–3080. https://doi.org/10.1523/jneurosci.4679-11.2012.

Mukherjee, S., Brulet, R., Zhang, L., and Hsieh, J. (2016). REST regulation of gene networks in adult neural stem cells. Nature Communications *7*, 1–14. https://doi.org/10.1038/ncomms13360.

Naser, R., Vandenbosch, R., Omais, S., Hayek, D., Jaafar, C., Lafi, S.A., Saliba, A., Baghdadi, M., Skaf, L., and Ghanem, N. (2016). Role of the Retinoblastoma protein, Rb, during adult neurogenesis in the olfactory bulb. Scientific Reports *6*, 20230. https://doi.org/10.1038/srep20230.

Obernier, K., and Alvarez-Buylla, A. (2019). Neural stem cells: origin, heterogeneity and regulation in the adult mammalian brain. Development *146*, dev156059. https://doi.org/10.1242/dev.156059.

Raudvere, U., Kolberg, L., Kuzmin, I., Arak, T., Adler, P., Peterson, H., and Vilo, J. (2019). g:Profiler: a web server for functional enrichment analysis and conversions of gene lists (2019 update). Nucleic Acids Res *47*, W191–W198. https://doi.org/10.1093/nar/gkz369.

Reimand, J., Kull, M., Peterson, H., Hansen, J., and Vilo, J. (2007). g:Profiler—a web-based toolset for functional profiling of gene lists from large-scale experiments. Nucleic Acids Res *35*, W193–W200. https://doi.org/10.1093/nar/gkm226.

Reimand, J., Isserlin, R., Voisin, V., Kucera, M., Tannus-Lopes, C., Rostamianfar, A., Wadi, L., Meyer, M., Wong, J., Xu, C., et al. (2019). Pathway enrichment analysis and visualization of omics data using g:Profiler, GSEA, Cytoscape and EnrichmentMap. Nat Protoc *14*, 482–517. https://doi.org/10.1038/s41596-018-0103-9.

Reynolds, B., and Weiss, S. (1992). Generation of neurons and astrocytes from isolated cells of the adult mammalian central nervous system. Science (New York, N.Y.) *255*, 1707–1710. https://doi.org/10.1126/science.1553558.

Robinson, J.T., Thorvaldsdóttir, H., Winckler, W., Guttman, M., Lander, E.S., Getz, G., and Mesirov, J.P. (2011). Integrative Genomics Viewer. Nat Biotechnol *29*, 24–26. https://doi.org/10.1038/nbt.1754.

Sage, J. (2000). Targeted disruption of the three Rb-related genes leads to loss of G1 control and immortalization. Genes Dev *14*, 3037–3050. https://doi.org/10.1101/gad.843200.

Sage, J., Miller, A.L., Pérez-Mancera, P.A., Wysocki, J.M., and Jacks, T. (2003). Acute mutation of retinoblastoma gene function is sufficient for cell cycle re-entry. Nature *424*, 223–228. https://doi.org/10.1038/nature01764.

Schindelin, J., Arganda-Carreras, I., Frise, E., Kaynig, V., Longair, M., Pietzsch, T., Preibisch, S., Rueden, C., Saalfeld, S., Schmid, B., et al. (2012). Fiji: an open-source platform for biological-image analysis. Nat Methods *9*, 676–682. https://doi.org/10.1038/nmeth.2019.

Schneider, C.A., Rasband, W.S., and Eliceiri, K.W. (2012). NIH Image to ImageJ: 25 years of image analysis. Nat Methods *9*, 671–675. https://doi.org/10.1038/nmeth.2089.

Schoenherr, C.J., and Anderson, D.J. (1995). The Neuron-Restrictive Silencer Factor (NRSF): A Coordinate Repressor of Multiple Neuron-Specific Genes. Science *267*, 1360–1363. https://doi.org/10.1126/science.7871435.

Shannon, P., Markiel, A., Ozier, O., Baliga, N.S., Wang, J.T., Ramage, D., Amin, N., Schwikowski, B., and Ideker, T. (2003). Cytoscape: A Software Environment for Integrated Models of Biomolecular Interaction Networks. Genome Res *13*, 2498–2504. https://doi.org/10.1101/gr.1239303.

Soldati, C., Caramanica, P., Burney, M.J., Toselli, C., Bithell, A., Augusti-Tocco, G., Stanton, L.W., Biagioni, S., Buckley, N.J., and Cacci, E. (2015). RE1 silencing transcription factor/neuron-restrictive silencing factor regulates expansion of adult mouse subventricular zone-derived neural stem/progenitor cells in vitro. J Neurosci Res *93*, 1203–1214. https://doi.org/10.1002/jnr.23572.

Srinivas, S., Watanabe, T., Lin, C.-S., William, C.M., Tanabe, Y., Jessell, T.M., and Costantini, F. (2001). Cre reporter strains produced by targeted insertion of EYFP and ECFP into the ROSA26 locus. BMC Developmental Biology *1*, 4. https://doi.org/10.1186/1471-213x-1-4.

TANG, Y., GARSON, K., LI, L., and VANDERHYDEN, B.C. (2015). Optimization of lentiviral vector production using polyethylenimine-mediated transfection. Oncol Lett *9*, 55–62. https://doi.org/10.3892/ol.2014.2684.

Team, R.C. (2021). R: A Language and Environment for Statistical Computing.

Urbán, N., Berg, D.L.C. van den, Forget, A., Andersen, J., Demmers, J.A.A., Hunt, C., Ayrault, O., and Guillemot, F. (2016). Return to quiescence of mouse neural stem cells by degradation of a proactivation protein. Science *353*, 292–295. https://doi.org/10.1126/science.aaf4802.

Urbán, N., Blomfield, I.M., and Guillemot, F. (2019). Quiescence of Adult Mammalian Neural Stem Cells: A Highly Regulated Rest. Neuron *104*, 834–848. https://doi.org/10.1016/j.neuron.2019.09.026.

Vandenbosch, R., Clark, A., Fong, B.C., Omais, S., Jaafar, C., Dugal-Tessier, D., Dhaliwal, J., Lagace, D.C., Park, D.S., Ghanem, N., et al. (2016). RB regulates the production and the survival of newborn neurons in the embryonic and adult dentate gyrus. Hippocampus *26*, 1379–1392. https://doi.org/10.1002/hipo.22613.

Vanderluit, J.L., Ferguson, K.L., Nikoletopoulou, V., Parker, M., Ruzhynsky, V., Alexson, T., McNamara, S.M., Park, D.S., Rudnicki, M., and Slack, R.S. (2004). p107 regulates neural precursor cells in the mammalian brain. J Cell Biol *166*, 853–863. https://doi.org/10.1083/jcb.200403156.

Vanderluit, J.L., Wylie, C.A., McClellan, K.A., Ghanem, N., Fortin, A., Callaghan, S., MacLaurin, J.G., Park, D.S., and Slack, R.S. (2007). The Retinoblastoma family member p107 regulates the rate of progenitor commitment to a neuronal fate. J Cell Biol *178*, 129–139. https://doi.org/10.1083/jcb.200703176.

Viatour, P., Somervaille, T.C., Venkatasubrahmanyam, S., Kogan, S., McLaughlin, M.E., Weissman, I.L., Butte, A.J., Passegué, E., and Sage, J. (2008). Hematopoietic stem cell quiescence is maintained by compound contributions of the retinoblastoma gene family. Cell Stem Cell *3*, 416–428. https://doi.org/10.1016/j.stem.2008.07.009.

Viatour, P., Ehmer, U., Saddic, L.A., Dorrell, C., Andersen, J.B., Lin, C., Zmoos, A.-F., Mazur, P.K., Schaffer, B.E., Ostermeier, A., et al. (2011). Notch signaling inhibits hepatocellular carcinoma following inactivation of the RB pathway. J Exp Medicine *208*, 1963–1976. https://doi.org/10.1084/jem.20110198.

Wang, X., Seekaew, P., Gao, X., and Chen, J. (2016). Traumatic Brain Injury Stimulates Neural Stem Cell Proliferation via Mammalian Target of Rapamycin Signaling Pathway Activation. ENeuro *3*, 1–14. https://doi.org/10.1523/eneuro.0162-16.2016.

Wu, L., Timmers, C., Maiti, B., Saavedra, H.I., Sang, L., Chong, G.T., Nuckolls, F., Giangrande, P., Wright, F.A., Field, S.J., et al. (2001). The E2F1–3 transcription factors are essential for cellular proliferation. Nature *414*, 457–462. https://doi.org/10.1038/35106593.

Xi, Y., Dhaliwal, J.S., Ceizar, M., Vaculik, M., Kumar, K.L., and Lagace, D.C. (2016). Knockout of Atg5 delays the maturation and reduces the survival of adult-generated neurons in the hippocampus. Cell Death Dis *7*, e2127. https://doi.org/10.1038/cddis.2015.406.

Zhou, G., Soufan, O., Ewald, J., Hancock, R.E.W., Basu, N., and Xia, J. (2019). NetworkAnalyst 3.0: a visual analytics platform for comprehensive gene expression profiling and meta-analysis. Nucleic Acids Res *47*, gkz240-. https://doi.org/10.1093/nar/gkz240.

Chapter 3
Manuscript

The Integrated Stress Response promotes neural stem cell survival under conditions of mitochondrial dysfunction.

Mohamed Ariff Iqbal [1], Vanessa Jabre [1], Bensun C. Fong [1], Maria Bilen [1], Imane Chakroun [1], Yubing Liu [1], Smitha Paul [1], Jingwei Chen [1], Michel Kanaan [2], Mary-Ellen Harper [2], Mireille Khacho [2] and Ruth S. Slack [1]

1 University of Ottawa Brain and Mind Research Institute, Department of Cellular and Molecular Medicine, University of Ottawa, Ottawa, ON K1H 8M5, Canada

2 Department of Biochemistry, Microbiology and Immunology, Ottawa Institute of Systems Biology (OISB), Faculty of Medicine, University of Ottawa, Ottawa, ON K1H 8M5, Canada

The experiments were performed by MAI. Chromatin immunoprecipitation were performed in collaboration with IC. Immunohistochemical staining and quantification of the 2 & 8-week timepoint were performed in collaboration with VJ & MB. Immunohistochemical staining and quantification of the EdU retention was performed in collaboration with SP. Bioinformatic analysis was performed in collaboration with BCF and YL. Lentiviral cloning was done in collaboration with JC.

MEH provided Sut mice. GSH HPLC was performed in collaboration with M. Kanaan & MEH

Experiments were conceptualized by MAI, M.Khacho & RSS. The manuscript was written by MAI. Review and editing were done by MAI, M. Khacho and RSS. All authors contributed to critical review of the manuscript.

ABSTRACT

Impaired mitochondrial function is a hallmark of aging that is augmented in neurodegenerative diseases. We have shown that disrupted mitochondrial dynamics alters the fate of neural stem cells leading to impairments in learning and memory. Presently, little is known regarding the mechanisms by which adult neural stem and progenitor cells survive and adapt to mitochondrial dysfunction. Using Opa1-inducible knockouts as a model of aging and neurodegeneration, we identify a decline in neurogenesis due to impaired stem cell activation and progenitor proliferation, which can be rescued under conditions of reduced oxidative stress. Through sc-RNA-seq, we identify ATF4 pathway as a critical mechanism underlying cellular adaptation to stress. Knock-down of ATF4 in Opa1 deficient NSCs accelerates cell death, while increased expression enhances proliferation and survival. While ATF4 has multiple targets, using Slc7a11 knock-outs, we show that ATF4-mediated glutathione production, through Slc7a11, plays a critical role in maintaining NSC survival and function under stress conditions.

INTRODUCTION

Defective mitochondrial function has been attributed to accelerated aging and neurodegeneration. Mitochondrial disorders manifest through cumulative dysfunction or neonatal inheritance resulting in neurodegenerative and neurodevelopmental diseases. Mutations in the mitochondrial dynamics proteins Drp1, Mfn1/2 and Opa1, have been shown to contribute to psychomotor, cognitive, and neurodegenerative disorders (Longo et al. 2020; Kijima et al. 2005; Zuchner et al. 2004; Alexander et al. 2000; Delettre et al. 2000). We have recently shown that impaired mitochondrial dynamics alters the fate of neural stem cells leading to impairments in learning and memory (Khacho et al. 2016; Khacho et al. 2017; Khacho, Harris, and Slack 2019; Khacho and Slack 2017a). Thus, neural stem cells and their progeny are highly affected by mitochondrial dysfunction in the developing and adult brain.

Continuous neurogenesis through adult neural stem and progenitor cells (NSC) play an important role in learning and memory (Deng, Aimone, and Gage 2010; Luna et al. 2019; Denoth-Lippuner and Jessberger 2021; Kee et al. 2007). Impairment of this process has been associated with neurodegenerative diseases in humans suggesting that a decline in adult-born neurons contributes to the associated memory deficits (Moreno-Jimenez et al. 2019; Terreros-Roncal et al. 2021). In iPSC models and murine neurogenesis, there is a clear distinction in metabolism of undifferentiated NSCs and differentiated neurons. Quiescent NSCs and iPSC-derived uncommitted NSCs are distinctly glycolytic, however upon differentiation cues metabolic regulators such as PGC1a and TFAM trigger mitochondrial biogenesis and metabolic shifts (Zheng et al. 2016; Inak et al. 2021; Beckervordersandforth et al. 2017). Furthermore, studies from our lab and others have shown that the maintenance of mitochondrial dynamics is essential for ongoing neurogenesis (Iwata, Casimir, and Vanderhaeghen 2020; Khacho et al. 2016). Specifically, mitochondrial shape is dynamically regulated in a stage specific manner during NSCs lineage progression in development and in adult niche (Khacho et al. 2016; Beckervordersandforth et al. 2017; Iwata, Casimir, and Vanderhaeghen 2020). Importantly, changes in mitochondrial dynamics have a direct influence on mitochondrial metabolism and signalling which then influence cell fate decisions (Inak et al. 2021; Beckervordersandforth et al. 2017; Khacho et al. 2016; Iwata, Casimir, and Vanderhaeghen 2020). Thus, mitochondria play a crucial function in their dynamic cellular state which impacts metabolism and the downstream signaling cascades which impact gene regulation (Khacho et al. 2016; Khacho et al. 2017; Beckervordersandforth et al. 2017; Zhang et al. 2016).

Considering that impaired mitochondrial function alters NSCs fate decisions impacting learning and memory, little is known as to how NSCs and their progeny respond and adapt to mitochondrial impairments typically seen in aging and neurodegeneration. Since Opa1 plays a critical role in the regulation of mitochondrial structure and function, and is implicated in a number of neurodegenerative diseases (Alavi and Fuhrmann 2013; Frezza et al. 2006; Patten et al. 2014), we generated an Opa1 inducible knockout in adult NSC as a model to study the effects of mitochondrial dysfunction on adult neurogenesis ((Kane et al. 2017; Ramonet et al. 2013). We

report in this study that loss of Opa1 and mitochondrial dysfunction leads to a decline in neurogenesis due to impaired stem cell activation and proliferation. Importantly, we identify ATF4 as a critical player in maintaining NSC survival during these conditions by enabling cellular adaption to stress. ATF4 facilitates glutathione production through Slc7a11 as a regulatory target to sustain stem cell survival under conditions of mitochondrial dysfunction typical of neurodegeneration.

RESULTS

Neurogenesis is impacted after Opa1 knockout in adult hippocampus.

To generate a model of mitochondrial/metabolic stress in adult neural stem cells and their progeny, we used a Tamoxifen (TAM)-inducible conditional knockout of Opa1 (Opa1cKO) in adult NSCs by breeding the Nestin-CreER^{T2}:Rosa26YFP reporter (Cicero et al. 2009; Srinivas et al. 2001) to mice carrying floxed alleles of Opa1 (Zhang et al. 2011). Control Transgenic (CT) animals were littermates carrying the Nestin-CreER^{T2}:Rosa26YFP reporter but do not contain the floxed Opa1 alleles. Five consecutive tamoxifen (TAM) treatments resulted in efficient recombination of the floxed Opa1 allele to generate an inducible Opa1 knockout in Nestin-expressing cells (Opa1cKO) **(Fig. 1A & Fig.S1A)**. Loss of Opa1 in adult SVZ FACS sorted cells resulted in a disrupted mitochondrial function **(Fig. 1G)** and decreased expression of key OXPHOS genes **(Fig.S1D)**, validating that mitochondria are disrupted within NSCs in this model. To elucidate the impact of mitochondrial dysfunction on adult hippocampal neurogenesis, we performed and histological analysis in the adult hippocampus of Opa1cKO and CT at 2-, 4- and 8-weeks post TAM treatment, and behavioral assessments at the 8-week time point **(Fig.1A)**. Contextual fear conditioning has long been utilized to assess fear memories (Maren, Phan, and Liberzon 2013; Saxe et al. 2006). Here, CT animals showed high activity pre-shock and exhibited a significant 'freezing' behaviour at 24 hrs and 7 days post shock, whereas Opa1cKO animals exhibited a significant reduction in "freezing" behaviour **(Fig.1B**), indicating an impairment in contextual memory. We then examined cellular changes related to neurogenesis in the SGZ at 2-, 4- and 8-weeks post TAM treatment. While no detectable differences were observed at 2 weeks post-TAM injection **(Fig.S1B)**, there was a drastic decrease in the generation of Dcx-expressing newborn neurons at 4-weeks (70% reduction) and 8-weeks (90% reduction) **(Fig.1C&D)**. Opa1cKO also resulted in a 61% and 97% decline in the number of transient amplifying progenitor cells (TAPs) detected by Tbr2^{+}YFP^{+} **(Fig.1E; S1C**). These results support our previous studies revealing that disruption in mitochondrial dynamics leads to impaired neurogenesis and deficits in learning and memory (Khacho et al, 2016). To determine if the underlying memory deficit originates from a diminishing pool of stem/progenitor cells, we quantified the total number of adult neural stem/progenitor cells, by co-staining with Sox2/YFP. While no decreases were detected at 2- and 4-weeks **(Fig.1F; S1B&C)**, there was a slight but significant 20% decline in total Sox2^{+} cells at 8-weeks post TAM **(Fig.1F)**. These data suggest that the decline in neurogenesis observed in this model may originate from defects within NSC pool.

Loss of OPA1 and mitochondrial disruption causes defects in NSC activation and proliferation

In order to understand the underlying cause for a decline in the number of NSCs, we first observed a general decrease in the percentage of proliferation in Opa1cKO NSCs (Ki67+Sox2+YFP+ staining) in total YFP^+ cells **(Fig.2A)**. Furthermore, although most adult NSC/progenitor cells survived and were maintained at 4-weeks, there was a significant decrease in proliferating NSC/progenitor cells ($Ki67^+Sox2^+/YFP^+$) at 4- (-60%) and 8-weeks (-95%) post-TAM (**Fig.2B)**, as well as proliferating TAP population ($Ki67^+Tbr2^+/YFP^+$) at 4- (-50%) and 8-weeks (-95%) post-TAM **(Fig.2C)**. These results reveal a significant proliferation defect in adult neural stem and progenitor cells in the Opa1cKO brains, that may account for the severe deficit in the generation of newborn neurons in the adult SGZ.

To determine whether the quiescent NSCs also exhibit a defect in activation and cell cycle re-entry, we performed an EdU retention assay (Furutachi et al. 2015). Animals were injected with one dose of EdU daily for 7 days prior to the TAM injection and loss of OPA1 in order to allow labeling of NSCs **(Fig.2D)**. Following TAM administration, SGZ cells were allowed to divide for four weeks before harvest. We reasoned that the EdU label would be diluted in actively dividing cells, such as activated NSCs and neural progenitors, meanwhile the EdU would be retained in quiescent/slowly dividing cells. In the Opa1cKO animals, more cells in the SGZ retained EdU labelling compared to CT animals **(Fig.2E&F)**. Interestingly, those EdU retaining cells in OPA1 cKO animals also did not expression Ki67 suggesting that they do not exist within the cell cycle and may represent the quiescent population of NSCs **(Fig.2G)**. To confirm that the EdU^+ retaining cells were NSCs, we used Hopx to co-label with EdU retaining quiescent cells in the dentate gyrus **(Fig.2J&K)**. We measured Hopx-expressing cells in YFP^+ cells (a marker for NSC in the SGZ (Berg et al. 2019). Like $Sox2^+$ cells at 4 weeks post-TAM **(Fig.1F)**, the total $Hopx^+$ cells are similar between CT and Opa1 cKO dentate gyrus **(Fig.2J)**, however there was a significant (7-fold increase) increase in EdU retention in $Hopx^+YFP^+$ cells in Opa1cKO relative to littermate CT animals **(Fig.2H&I)**. Thus, the increased number of EdU-retaining $Hopx^+$ cells in Opa1KO suggests an impairment in adult NSC activation. A concomitant increase in the percentage of quiescent NSCs measured by Sox2 and Hopx also identifies an impairment in NSC proceeding to activation **(Fig.2K,L)**. This is further confirmed by the decreased number of activated NSCs expressing Ascl1, a marker of activated NSCs (Raposo et al. 2015; Castro et al. 2011), with a 43% decrease in $Ascl1^+YFP^+$ cells in Opa1 cKO dentate gyrus at 4-weeks post-TAM **(Fig.2M)**. Taken together, our results reveal a significant impairment in NSC activation, demonstrated by an increase in the number of long-term EdU-retaining Hopx cells, a decrease NSC proliferation, and in the number of activated ASCL1-expressing stem/progenitor cells.

Mitochondrial dysregulation signals stress response by activating ATF4 pathway early in the neural stem cell pool.

To define the mechanisms underlying this NSC/progenitor cell defect resulting in impaired neurogenesis and memory deficits, we performed single-cell RNA-seq from cells isolated directly from the adult dentate gyrus. The neurogenic program produces diverse cell populations in the adult dentate gyrus. We utilized scRNAseq to elucidate how mitochondrial dysfunction impacts the different cell populations of the neuronal lineage. We FACS sorted YFP positive cells from microdissected SGZ of CT or Opa1cKO mouse brains at 4-weeks post TAM-induction **(Fig.3A)**. This time-point was chosen to allow a proportion of YFP^+ cells to finish their differentiation to newborn neurons. Furthermore, 4-weeks post-TAM is the onset of detectable defects whereby all the cell populations are still present and prior to major cell loss. The 10X Genomics Chromium platform was used to perform single cell RNA transcriptome analysis (Zheng et al. 2017). The library contains RNA transcriptomes from 4362 CT and 6296 Opa1 cKO cells after refining with cell quality control. Unsupervised clustering through nonlinear Uniform Manifold Approximation and Projection (UMAP) dimension reduction produced nine cell clusters **(Fig.S3A)**. The top five genes of each cluster are shown in the heatmap, and clusters were classified by known markers of brain cell types **(Fig.S3B)** (Becht et al. 2018). Four clusters of non-neuronal lineages were excluded from further study, including Cluster 3 - ependymal cells (Ccdc153), Cluster 4 - mural cells (Vtn), Cluster 7 - endothelial cells (Cldn5) and Cluster 8 - oligodendrocytes (Mbp) (Kalinina and Lagace 2022; Artegiani et al. 2017; He et al. 2016; Mizrak et al. 2019; Liu et al. 2022). The 2847 CT and 3466 Opa1 cKO cells from the neuronal lineage were regrouped and re-clustered and the UMAP distribution yielded three distinct populations namely cluster 0 that consists of Aldoc, Gfap, Sox2, Id3 that define resident glia-like neural stem cells (NSC pool); Cluster 1 that contains activated NSCs marked by Ascl1, and cluster 2 that includes a mixed population of neural progenitors (Mki67, Eomes), and differentiating neurons (Dcx, Sox4, Sox11 and Prox1) **(Fig.3B & S3C)**. Cell type-specific markers used to identify these clusters were based on the published cell markers (Artegiani et al. 2017) highlighted in the gene featured UMAP **(Fig.S3D)**. A subset of cluster markers is highlighted in violin plots and heat maps defining each cluster **(Fig.S3E&F)**. For example, Aldoc and ApoE are highly expressed in the quiescent NSCs (Urban, Blomfield, and Guillemot 2019), both of which are over-represented in Cluster 0 NSCs **(Fig. S3E&F)**. Ascl1 is an essential transcription factor for NSC activation, and its expression is induced specifically in Cluster 1 NSCs **(Fig. S3D&E)**(Andersen et al. 2014). Dcx, a marker of immature neurons, is over-represented in Cluster 2 **(Fig.S3D,E&F).** Unbiased transcriptional profiling suggests that there is a metabolic shift in Opa1 deficient cells due to the decline in mitochondrial OXPHOS genes such as mt-Nd1, mt-Nd4 and mt-Co1 **(Fig.3C&E)**. These populations also exhibit the activation of classic cellular stress response pathways, including the integrated stress response pathway (Atf4, Chac1, Slc7a11, Slc3a2, Ddit3 and Ddit4) in all the clusters of neuronal lineages **(Fig.3C&D)**. Differential expression analysis revealed a significant decrease in mitochondrial OXPHOS (mt-Co1 and mt-Nd1) genes in all three clusters as well as neuronal differentiation genes (Sox4 and Prox1) in Cluster 2, upon Opa1 cKO **(Fig.3C, D& E)**. In contrast, genes involved in the stress response were induced in Opa1 cKO cells, including Atf4 and Slc7a11, were elevated in all three clusters **(Fig.3C, D &E)**. Notably, the resident quiescent NSCs (cluster 0) showed a prominent

integrated stress response (ISR) lead by ATF4 and its downstream targets **(Fig.3C,D&E)**. While the number of NSCs was not different at 4-weeks post TAM *in vivo* **(Fig.1D)**, our sc-RNA-seq data clearly shows a perturbation in early NSCs manifested by induction of ISR, which may explain the impairment in NSC activation **(Fig.2C)**. This is in line with the observed early stress signalling in the SVZ FACS sorted cells 10 days post TAM **(Fig.1G&S1D)**. These results suggest the early onset of stress signalling in NSCs impair their function. We tested this hypothesis in neuronal differentiation process. Previously, an algorithm known as RNA Velocity, had been developed based on mRNA processing to predict the future fate of the cell (Bergen et al. 2021; La Manno et al. 2018). In Opa1 KO cells, 24% of mRNA is unspliced, as compared to 37% in CT controls, suggesting a lower new transcript synthesis **(Fig.3H)**. RNA velocity revealed a preserved neurogenesis progression from proliferating cells to neurons in CT cells. However, the loss of Opa1 led to aberrant differentiation, suggesting a tendency towards dedifferentiation in Opa1 cKO neuroblasts where arrows indicate a reverse trend to an undifferentiated state **(Fig.3F)**. Impaired differentiation is manifested by decreased differentiation markers in the cluster 2 of Opa1 cKO cells. For example, RNA velocity of proliferation markers (Mki67 & Pcna) and differentiation markers (Eomes, Dcx and Neurod1) showed a tendency of generating new transcripts in CT (more cells in green) but not in Opa1 KO (more cells in red) **(Fig.3G).** Our single cell analysis suggests that Opa1 loss results in an impairment in neurogenesis that begins in quiescent NSCs and reveals an induction of genes associated with stress response pathway. We therefore examined the impact of the ISR in adult NSC function under stress conditions.

Loss of Opa1 in NSCs induces the ISR as a result of mitochondrial dysfunction and oxidative stress

To validate the sc-RNA-seq findings revealing the induction of the ISR following impaired mitochondrial function, we first confirmed mitochondrial dysfunction upon Opa1 loss in our models. Compelling evidence reveals that disruption in mitochondrial dynamics proteins results in mitochondrial dysfunction (Khacho et al. 2017; Khacho et al. 2016; Beckervordersandforth et al. 2017; Iwata, Casimir, and Vanderhaeghen 2020; Baker et al. 2022; Patten et al. 2014). Given the scarcity of adult NSCs, it is difficult to perform functional analysis of mitochondria within this cell population. Thus to overcome this, we generated an embryonic model of Opa1 deficient NSCs by crossing *foxg1*/BF1-Cre (Hebert and McConnell 2000) with mice carrying floxed Opa1 alleles (Zhang et al. 2011). We collected cortical tissue at embryonic day 12.5 (E12.5) from littermate control transgenic (CT) and Opa1 conditional knockouts (KO). The embryonic model of OPA1 loss in NSCs recapitulated defects in neurogenesis observed as decreased protein and gene expression of key activation and neurogenic markers, including Ascl1, Notch (N^{ICD}) and Dcx **(Fig.S4A,B)**. Importantly, loss of OPA1 in embryonic NSCs also instigated the same integrated stress response as that observed in the adult OPA1 cKO model **(Fig.4A)**. Consistent with adult hippocampal Opa1cKO NSCs, NSCs derived from the embryonic cortex also exhibited activation of the ATF4 pathway, including increased ATF4 protein and activation of PERK, a known activator of the ISR **(Fig.4A)**. It was also noted that there was increased levels of the global

translational repressor EIF4EBP1 (Gomez et al. 2008) **(Fig. 4A)** suggesting that there is potential repression of global translation along with an induction of a stress response **(Fig.4A)**. Quantification of mitochondrial electron transport chain (ETC) proteins by Western blot revealed **(Fig. S4C&D)** a significant decrease in subunits representing complexes CI, CIII & CIV in Opa1 deficient cells. While ATP assays revealed no significant change in total ATP, there was a significant decrease in oligomycin-sensitive OXPHOS derived ATP in Opa1 KO tissue **(Fig. S4E)**. Furthermore, basal and ATP linked OCR are significantly reduced in Opa1 knockdown NSCs **(Fig. 4B)**. Using NAD^+ measurements as a readout of mitochondrial Complex I activity (Santidrian et al. 2013; Schwartz et al. 1974), revealed a significant decrease in total NAD^+ levels and NAD/NADH ratio in the Opa1 KD neurospheres **(Fig. S4F)**. As impaired OXPHOS can result in elevated ROS, mitochondrial ROS was measured using MitoSOX flowcytometry (Robinson, Janes, and Beckman 2008) revealing a significant increase in mitochondrial ROS levels **(Fig. 4C)**. Overall, these results confirms that Opa1 loss in NSCs results in impaired oxidative phosphorylation, decreased OCR, impaired mitochondrial ATP production, and elevated ROS levels.

To determine whether dysfunctional oxidative metabolism and redox stress is involved in ISR induction and impairment in NSC function, we asked if hypoxia (1% O_2), a strategy previously shown to be protective following mitochondrial dysfunction (Jain et al. 2016) could mitigate the ISR and rescue NSC function. To test this, CT and Opa1 cKO adult SVZ derived Nestin:YFP^+ cells were cultured under normoxic and hypoxic conditions and neurosphere formation was quantified. Under normoxic conditions, the Opa1 cKO derived stem cells formed fewer and smaller neurospheres, while significantly more neurospheres were produced from equal cell numbers under hypoxic conditions **(Fig 4D-F**. These results suggest that impairment in NSC function and progenitor proliferation could be at least partially rescued once oxidative stress is resolved. To evaluate the molecular changes in hypoxic conditions, we used E12.5 cortex-derived neurospheres tranduced with shctrl or shOpa1 lentivirus grown in normoxic and hypoxic conditions. This knockdown model of OPA1 again revealed a similar response involving the induction of ATF4 pathway as identified in adult NSCs **(Fig.4G&H)**. Importantly, incubation of shOPA1 transduced neurospheres in a hypoxic condition allowed ATF4 to resolve back to baseline levels **(Fig. 4G)** and decreased the expression of downstream stress response genes Slc7a11 and Chac1**(Fig. 4H)**. Furthermore, this was acompanied by a partial rescue in proliferation (Cyclin A), activation (Ascl1) relative to shOpa1 transduced neurospheres in normoxia **(Fig 4G)**. Taken together, our results reveal that oxidative stress induced by mitochondrial dysfunction triggers ATF4, which can be rescued when oxidative stress is resolved under conditions such as hypoxia. Of note, while performing analysis using the embryonic NSC model, it was also observed that OPA1 depletion increased levels of cleaved caspase 3 **(Fig.4A,G)**, a cell death marker, which was decreased upon incubation in hypoxia and alleviation of oxidative stress **(Fig.4G)**. NSC proliferation and activation defect measured by Cyclin A and Ascl1 also were rescued under hypoxic condition, suggesting a partial restore in NSC function **(Fig.4G)**. Given the striking

induction of the ATF4 pathway in NSCs following mitochondrial dysfunction, we next sought to investigated the role of ATF4 in preserving NSC survival and function under stress conditions.

ATF4 mediates a global stress response in NSCs to promote survival during mitochondrial stress.

To investigate the function of the ATF4 ISR pathway in NSCs we manipulated ATF4 expression levels in NSC cultures transduced with lentivirus of control or Opa1 shRNA. Under control conditions, EdU incorporation experiments revealed that ATF4 knockdown results in decreased proliferation while ATF4 overexpression increases the rate of proliferation **(Fig.5A&B).** In shOpa1-treated cells, where ATF4 is already at elevated levels, ATF4 knockdown further decreased cell proliferation **(Fig 5A&B)**. As expected, cell death measured by cleaved caspase 3 showed that Opa1 knockdown increases cell death **(Fig.5C,D)**. However, when ATF4 upregulation is prevented in shOPA1-transduced neurospheres, by means of an ATF4-mediated knockdown, cells exhibit a significant further increase in cell death **(Fig 5C&D)**. These results indicate the importance of ATF4 in maintaining the survival of NSC under mitochondrial stress conditions.

To identify ATF4 downstream targets that may be mediating these protective effects, we quantified potential ATF4 target genes by qPCR **(Fig 5E)**. Our results reveal a number of stress response genes that are responsive to ATF4 manipulation, including genes required for aminoacid transport (Slc7a11, SLc3a2, and Slc1a5) and tRNA charging (Aars, Cars and Gars) among other genes such as Chac1, Mthfd2 and Xpot. To determine if there is ATF4 binding on potential ATF4 target genes in NSCs, we performed ChIP using ATF4 or control IgG antibodies and detected significant enrichment of ATF4 at the transcriptional binding sites (TSS) of Chac1, Slc3a2, and Slc7a11, as described by (Han et al. 2013) **(Fig.5F,G)**. Histone H3 lysine 4 trimethylation (H3K4me3), which correlates with open chromatin (active transcription) was measured on the TSS of Chac1, Slc3a2 and Slc7a11 genes. While ChIP results reveal ATF4 enrichment at all potential target genes in all conditions relative to a negative locus in Opa1 knockdown conditions, there was a significantly higher enrichment of the H3K4me3 mark on Chac1, Sl3a2 and Slc7a11, consistent with increased transcription of Chac1, Slc3a2 and Slc7a11 **(Fig.5H)**.

Slc7a11 and xCT system provides the flux for survival through glutathione production under ATF4 induction.

As Slc7a11 is a promintent target for ATF4 and is highly induced under stress conditions, we asked whether ATF4-mediated induction of Slc7a11 plays a critical role in mediating cellular adaptation to stress through regulation of redox balance. xCT system is a heterodimeric transmembrane channel consists of Slc7a11 and Slc3a2 important for Cystine and glutamate exchange (Lim et al. 2019). We utilized Slc7a11 mutant mice (sut/sut) (Sato et al. 1999) and background control (Wildtype) littermates to determine if dysfunctional Slc7a11 xCT impacts adult hippocampal neurogenesis at 3 and 6 months of age. Histological assessment of NSCs and their progeny in the dentate gyrus of Slc7a11 mutant mice (sut/sut) reveal a significant decrease in proliferation

(phosphoHistone 3) at 6 months of age **(Fig.6A)**. Assessment of the NSC activation marker Ascl1 revealed a significant reduction of Ascl1 positive cells in sut mice at 6 months of age, consistent with a reduction in stem cell activation **(Fig.6B)**. Assessment of the number of the $Tbr2^+$ TAP cells **(Fig.6C)**, and Dcx^+ newborn neurons **(Fig.6D)** were also significantly reduced at both 3 and 6 month timepoints in sut mice. To ask if Slc7a11 plays an important role in NSC adaptation to stress under conditions of mitochondrial dysfunction, neurosphere assays were performed and sut mice produced significantly less neurospheres compared to controls **(Fig.S6A)**. To ask if Slc7a11 was important for proliferation and survival under stress, proliferation rate was measured by EdU incorporation and cell death was measure by quantifying the number of AC3-expressing cells. Our results show that sut mice derived NSCs proliferate less in control and Opa1 knockdown conditions **(Fig.6E)**. Importantly, the sut-derived NSCs were more sensitive to mitochondrial dysfunction-induced cell death when compared to shOpa1-treated wildtype cells **(Fig.6F**), suggesting an important role for Slc7a11 in maintaining NSC survival. These results signify the importance of Slc7a11 function in maintaining NSC function in basal and stressed conditions.

Consistent with ATF4 function in the regulation of glutathione production (Torrence et al. 2021), we further tested the impact of ATF4 pathway manipulation on the glutathione levels in the NSCs. Measurement of the glutathione ratio reveals an increase in GSH:GSSG levels in Opa1 knockdown with ATF4 overexpression conditions **(Fig.6G)** while total GSH levels remain similar under all conditions **(Fig.6H)**. These data suggest that ATF4 plays an important role in the generation of reduced glutathione levels through ATF4-target gene regulation, and that Slc7a11 is an important ATF4 target in the regulartion of NSC redox balance.To test the role for the increased GSH observed following Opa1 knockdown, the intracellular levels of GSH were manipulated by treatment with BSO, which causes the depletion of GSH, or addition of exogenous reduced GSH. Manipultion of GSH levels, by increasing or depleting the GSH pool, did not have a significant affect on NSC proliferation in shOpa1 knockdown cells compared to controls, as demonstrated by measuring the proportion of cells that incorporated EdU **(Fig.6I)**. However, depletion of the GSH pool, by treatment with BSO, in shOpa1 knockdown cells caused a significant increase in cell death **(Fig.6J)**. Together these findings demonstrate the critical role of ATF4 in mediating the protection of NSC under conditions of mitochondrial dysfunction by activating a global stress response and the generation of glutathione.

DISCUSSION

In this report, we reveal a novel mechanism by which neural stem and progenitor cells adapt to mitochondrial dysfunction, typically found in aging and neurodegeneration. We show that mitochondrial dysfunction leads to a decline in neurogenesis due to impaired stem cell activation and identify the ATF4 pathway as a critical mediator to enable cellular adaptation to stress. We show that ATF4 preserves NSC function under stress by mediating glutathione production through activation of Slc7a11 as a regulatory target, which is required to sustain NSC function and survival.

We, and others, have shown that proper maintenance of mitochondrial dynamics and metabolism is essential to maintain adult NSC function and neurogenesis, which we show impacts learning

and memory (Beckervordersandforth et al. 2017; Iwata, Casimir, and Vanderhaeghen 2020; Khacho et al. 2016). Our previous studies have shown that NSC differentiation is reliant on a metabolic switch from glycolysis to oxidative phosphorylation, whereby mitochondrial signalling is essential for neurogenesis (Khacho et al. 2016; Khacho et al. 2017; Khacho, Harris, and Slack 2019). A recent report suggests that new-born neurons acquire highly fragmented mitochondria and later undergo fusion to become mature mitochondria essential for neuronal maturation (Iwata, Casimir, and Vanderhaeghen 2020). This metabolic shift is important and sufficient to induce differentiation and neurogenesis. Here we show that, Opa1 deficiency-induced mitochondrial dysfunction impacts all stages of neurogenesis, from NSC at quiescent stages, throughout the progression of neurogenesis, differentiation and survival **(Fig.1, 3)**. Mitochondrial dysfunction impacts cellular metabolism which alters the molecular signatures associated with NSC activation, proliferation and neurogenesis (Inak et al. 2021). This suggests that the mitochondrial derived metabolites play an important role in executing the neurogenic program. The transcriptomic changes identified in Opa1 cKO highlight the importance of mitochondrial function in the regulation of NSC proliferation, activation, and differentiation. Through our embryonic knockdowns and sc-RNAseq, we show that key stages of neurogenesis are disrupted in Opa1 deficient cells. Besides the metabolic alterations, mitochondrial dysfunction leads to changes in gene expression (for example, Ascl1, Dcx, Sox4 and Sox11 are altered **Fig.3C&S4C**). Similar impairments in NSC function were observed in Alzeimer's disease, where hypo-maturation and de-differentiation have been reported (Mertens et al. 2021). Together, these studies support a de-differentiation phenotype in which mitochondrial dysfunction is central to this process. Here we mechanistically test this concept, using Opa1 deficient NSCs in the adult dentate gyrus. Our RNA velocity studies indicate a reversion in fate, where adult neuroblasts sustaining mitochondrial dysfunction begin to induce the expression of early progenitor genes rather than progressing through differentiation (eg., Eomes, Dcx, NeuroD1) **(Fig.3G)**. To ask if oxidative stress is the key mechanism underlying NSC impairments, we subjected Opa1 deficient cells to hypoxia to enable cells to adapt to OXPHOS-independent energy sources and thereby reduce oxidative stress. We show that hypoxic conditions can rescue NSC defects, including proliferation, expression of differentiation/activation genes (ASCL1), mitigation of ATF4 expression, and cell survival **(Fig.4D)**. These findings demonstrate that oxidative stress is a key mediator of the ISR in Opa1 deficient NSCs and suggests that the resultant dysfunctional NSCs and impairment in neurogenesis have the capacity to be rescued when mitochondrial oxidative stress is resolved through the appropriate treatments.

Our results reveal compelling evidence that the ISR plays a critical role in the adaptation of Opa1 in embryonic and adult Opa1 deficient NSCs. Single cell transcriptome analysis and embryonic Opa1 knockout experiments suggests that ATF4 triggers the ISR upon mitochondrial dysfunction. Although the number of NSCs in the adult dentate gyrus remained stable for 4 weeks post knockout, there was a clear transcriptomic change signifying the ISR, including the induction of ATF4 and its targets (ATF4, Slc7a11, Chac1 and Xpot; **Fig.3D**). ISR is a key adaptive mechanism to counteract cellular stresses including protein misfolding, nutrient deprivation and oxidative

stress restoring metabolic and protein homeostasis (Costa-Mattioli and Walter 2020). Our study finds that Opa1 deficiency-induced mitochondrial dysfunction triggers the ATF4 and ISR as described in the cell lines (Quiros et al. 2017; Fessler et al. 2020; Guo et al. 2020). Previously, the ISR was found to mitigate cardiomyopathy disease pathology induced by OXPHOS dysfunction in heart (Ahola et al. 2022), however, little is known regarding how the ISR impacts NSC function and survival in response to mitochondrial dysfunction. We show that the ATF4 pathway enables NSCs to adapt to stress and survive, and that this can be rescued by providing a hypoxic environment, which resulted in a suppression of ATF4 induction and its downstream targets. Under these conditions, Opa1 deficient NSCs could proliferate and survive, by rewiring their energetic pathways. Previous studies with cord blood hematopoietic stem cell (HSC) revealed that upregulation ATF4 was important for HSC survival under basal and nutrient deprivation conditions (van Galen et al. 2018). Unlike HSC and other immortalized cell lines, ATF4 is maintained at the low levels and degraded under basal conditions to strike a fine balance in metabolic function of NSCs. However, upon mitochondrial dysfunction, we demonstrate that ATF4 and ISR instigate a metabolic rewiring enabling NSCs to adapt to stress.

ATF4 induction induces the transcription of a series of downstream targets both in stimulated and stressed conditions (Torrence et al. 2021), and the cellular state dictates the dichotomous function of ATF4. For example, at basal levels without stress, ectopic ATF4 expression leads to cell growth and proliferation but the ATF4 under stress (by stimuli or overexpression) enhances survival **(Fig5B&D)**. Previous results suggest that ATF4 in control conditions increases cell proliferation through its targets that mimics a growth signal and induces an anabolic program (Torrence et al. 2021). In contrast, in the context of mitochondrial dysfunction, ATF4 activation triggers a stress response essential to sustain survival.

While ATF4 has multiple targets, it remains unknown which target is most critical in maintaining the survival of adult NSCs under mitochondrial dysfunction and metabolic stress. Slc7a11, a key target for ATF4 is highly induced in Opa1 deficient NSCs in vivo and in vitro. Our results suggest that depletion of GSH levels increases the vulnerability of Opa1 depleted NSCs. This is in line with previous report where blocking SLc7a11 by pharmacological agent Erastin was shown to deplete GSH levels and mediate the stress response in immortalized tumor cell lines resulting in ferroptosis (Yang et al. 2014). Also in muscle stem cells, Slc7a11 was shown to regulate GSH levels to mitigate oxidative damage and cell death (Baker et al. 2022). Our data show that under basal condition, Slc7a11 plays a crucial role in adult hippocampal neurogenesis, as loss of Slc7a11 (Sut mice) impairs hippocampal neurogenesis by reduced NSC proliferation and neurogenesis. We also show that Slc7a11 deficiency exacerbated cell death in NSCs in vitro following Opa1 knock-down, suggesting the importance of the Slc7a11 in NSC function under stress. Studies have shown that under oxidative stress conditions, ATF4 plays a critical role in the regulation of reduced Glutathione production under conditions of mitochondrial dysfunction.

In summary, we show that mitochondrial dysfunction typically found in neurodegenerative diseases (through Opa1 loss), impairs NSC function leading to impaired neurogenesis and deficits

in learning and memory. Opa1 loss alters the course of neural stem cell progression by impairing proliferation and neurogenesis confirming the essential role of mitochondrial function. Mitochondrial dysfunction triggers an adaptation of NSCs through ATF4 and ISR by enhancing cellular ROS defense mechanisms, in part, through Slc7a11.

REFERENCES

Ahola, S., P. Rivera Mejias, S. Hermans, S. Chandragiri, P. Giavalisco, H. Nolte, and T. Langer. 2022. 'OMA1-mediated integrated stress response protects against ferroptosis in mitochondrial cardiomyopathy', *Cell Metab*, 34: 1875-91 e7.

Alavi, M. V., and N. Fuhrmann. 2013. 'Dominant optic atrophy, OPA1, and mitochondrial quality control: understanding mitochondrial network dynamics', *Mol Neurodegener*, 8: 32.

Alexander, C., M. Votruba, U. E. Pesch, D. L. Thiselton, S. Mayer, A. Moore, M. Rodriguez, U. Kellner, B. Leo-Kottler, G. Auburger, S. S. Bhattacharya, and B. Wissinger. 2000. 'OPA1, encoding a dynamin-related GTPase, is mutated in autosomal dominant optic atrophy linked to chromosome 3q28', *Nat Genet*, 26: 211-5.

Andersen, J., N. Urban, A. Achimastou, A. Ito, M. Simic, K. Ullom, B. Martynoga, M. Lebel, C. Goritz, J. Frisen, M. Nakafuku, and F. Guillemot. 2014. 'A transcriptional mechanism integrating inputs from extracellular signals to activate hippocampal stem cells', *Neuron*, 83: 1085-97.

Artegiani, B., A. Lyubimova, M. Muraro, J. H. van Es, A. van Oudenaarden, and H. Clevers. 2017. 'A Single-Cell RNA Sequencing Study Reveals Cellular and Molecular Dynamics of the Hippocampal Neurogenic Niche', *Cell Rep*, 21: 3271-84.

Baker, N., S. Wade, M. Triolo, J. Girgis, D. Chwastek, S. Larrigan, P. Feige, R. Fujita, C. Crist, M. A. Rudnicki, Y. Burelle, and M. Khacho. 2022. 'The mitochondrial protein OPA1 regulates the quiescent state of adult muscle stem cells', *Cell Stem Cell*, 29: 1315-32 e9.

Becht, E., L. McInnes, J. Healy, C. A. Dutertre, I. W. H. Kwok, L. G. Ng, F. Ginhoux, and E. W. Newell. 2018. 'Dimensionality reduction for visualizing single-cell data using UMAP', *Nat Biotechnol*.

Beckervordersandforth, R., B. Ebert, I. Schaffner, J. Moss, C. Fiebig, J. Shin, D. L. Moore, L. Ghosh, M. F. Trinchero, C. Stockburger, K. Friedland, K. Steib, J. von Wittgenstein, S. Keiner, C. Redecker, S. M. Holter, W. Xiang, W. Wurst, R. Jagasia, A. F. Schinder, G. L. Ming, N. Toni, S. Jessberger, H. Song, and D. C. Lie. 2017. 'Role of Mitochondrial Metabolism in the Control of Early Lineage Progression and Aging Phenotypes in Adult Hippocampal Neurogenesis', *Neuron*, 93: 1518.

Berg, D. A., Y. Su, D. Jimenez-Cyrus, A. Patel, N. Huang, D. Morizet, S. Lee, R. Shah, F. R. Ringeling, R. Jain, J. A. Epstein, Q. F. Wu, S. Canzar, G. L. Ming, H. Song, and A. M. Bond. 2019. 'A Common Embryonic Origin of Stem Cells Drives Developmental and Adult Neurogenesis', *Cell*, 177: 654-68 e15.

Bergen, V., R. A. Soldatov, P. V. Kharchenko, and F. J. Theis. 2021. 'RNA velocity-current challenges and future perspectives', *Mol Syst Biol*, 17: e10282.

Cancino, G. I., A. P. Yiu, M. P. Fatt, C. B. Dugani, E. R. Flores, P. W. Frankland, S. A. Josselyn, F. D. Miller, and D. R. Kaplan. 2013. 'p63 Regulates adult neural precursor and newly born neuron survival to control hippocampal-dependent Behavior', *J Neurosci*, 33: 12569-85.

Castro, D. S., B. Martynoga, C. Parras, V. Ramesh, E. Pacary, C. Johnston, D. Drechsel, M. Lebel-Potter, L. G. Garcia, C. Hunt, D. Dolle, A. Bithell, L. Ettwiller, N. Buckley, and F. Guillemot. 2011. 'A novel function of the proneural factor Ascl1 in progenitor proliferation identified by genome-wide characterization of its targets', *Genes Dev*, 25: 930-45.

Cicero, S. A., D. Johnson, S. Reyntjens, S. Frase, S. Connell, L. M. Chow, S. J. Baker, B. P. Sorrentino, and M. A. Dyer. 2009. 'Cells previously identified as retinal stem cells are pigmented ciliary epithelial cells', *Proc Natl Acad Sci U S A*, 106: 6685-90.

Costa-Mattioli, M., and P. Walter. 2020. 'The integrated stress response: From mechanism to disease', *Science*, 368.

Delettre, C., G. Lenaers, J. M. Griffoin, N. Gigarel, C. Lorenzo, P. Belenguer, L. Pelloquin, J. Grosgeorge, C. Turc-Carel, E. Perret, C. Astarie-Dequeker, L. Lasquellec, B. Arnaud, B. Ducommun, J. Kaplan, and C. P. Hamel. 2000. 'Nuclear gene OPA1, encoding a mitochondrial dynamin-related protein, is mutated in dominant optic atrophy', *Nat Genet*, 26: 207-10.

Deng, W., J. B. Aimone, and F. H. Gage. 2010. 'New neurons and new memories: how does adult hippocampal neurogenesis affect learning and memory?', *Nat Rev Neurosci*, 11: 339-50.

Denoth-Lippuner, A., and S. Jessberger. 2021. 'Formation and integration of new neurons in the adult hippocampus', *Nat Rev Neurosci*, 22: 223-36.

Fessler, E., E. M. Eckl, S. Schmitt, I. A. Mancilla, M. F. Meyer-Bender, M. Hanf, J. Philippou-Massier, S. Krebs, H. Zischka, and L. T. Jae. 2020. 'A pathway coordinated by DELE1 relays mitochondrial stress to the cytosol', *Nature*, 579: 433-37.

Fong, B. C., I. Chakroun, M. A. Iqbal, S. Paul, J. Bastasic, D. O'Neil, E. Yakubovich, A. T. Bejjani, N. Ahmadi, A. Carter, A. Clark, G. Leone, D. S. Park, N. Ghanem, R. Vandenbosch, and R. S. Slack. 2022. 'The Rb/E2F axis is a key regulator of the molecular signatures instructing the quiescent and activated adult neural stem cell state', *Cell Rep*, 41: 111578.

Frezza, C., S. Cipolat, O. Martins de Brito, M. Micaroni, G. V. Beznoussenko, T. Rudka, D. Bartoli, R. S. Polishuck, N. N. Danial, B. De Strooper, and L. Scorrano. 2006. 'OPA1 controls apoptotic cristae remodeling independently from mitochondrial fusion', *Cell*, 126: 177-89.

Furutachi, S., H. Miya, T. Watanabe, H. Kawai, N. Yamasaki, Y. Harada, I. Imayoshi, M. Nelson, K. I. Nakayama, Y. Hirabayashi, and Y. Gotoh. 2015. 'Slowly dividing neural progenitors are an embryonic origin of adult neural stem cells', *Nat Neurosci*, 18: 657-65.

Gomez, E., M. L. Powell, A. Bevington, and T. P. Herbert. 2008. 'A decrease in cellular energy status stimulates PERK-dependent eIF2alpha phosphorylation and regulates protein synthesis in pancreatic beta-cells', *Biochem J*, 410: 485-93.

Guo, X., G. Aviles, Y. Liu, R. Tian, B. A. Unger, Y. T. Lin, A. P. Wiita, K. Xu, M. A. Correia, and M. Kampmann. 2020. 'Mitochondrial stress is relayed to the cytosol by an OMA1-DELE1-HRI pathway', *Nature*, 579: 427-32.

Han, J., S. H. Back, J. Hur, Y. H. Lin, R. Gildersleeve, J. Shan, C. L. Yuan, D. Krokowski, S. Wang, M. Hatzoglou, M. S. Kilberg, M. A. Sartor, and R. J. Kaufman. 2013. 'ER-stress-induced transcriptional regulation increases protein synthesis leading to cell death', *Nat Cell Biol*, 15: 481-90.

He, L., M. Vanlandewijck, E. Raschperger, M. Andaloussi Mae, B. Jung, T. Lebouvier, K. Ando, J. Hofmann, A. Keller, and C. Betsholtz. 2016. 'Analysis of the brain mural cell transcriptome', *Sci Rep*, 6: 35108.

Hebert, J. M., and S. K. McConnell. 2000. 'Targeting of cre to the Foxg1 (BF-1) locus mediates loxP recombination in the telencephalon and other developing head structures', *Dev Biol*, 222: 296-306.

Inak, G., A. Rybak-Wolf, P. Lisowski, T. M. Pentimalli, R. Juttner, P. Glazar, K. Uppal, E. Bottani, D. Brunetti, C. Secker, A. Zink, D. Meierhofer, M. T. Henke, M. Dey, U. Ciptasari, B. Mlody, T. Hahn, M. Berruezo-Llacuna, N. Karaiskos, M. Di Virgilio, J. A. Mayr, S. B. Wortmann, J. Priller, M. Gotthardt, D. P. Jones, E. Mayatepek, W. Stenzel, S. Diecke, R. Kuhn, E. E. Wanker, N. Rajewsky, M. Schuelke, and A. Prigione. 2021. 'Defective metabolic programming impairs early neuronal morphogenesis in neural cultures and an organoid model of Leigh syndrome', *Nat Commun*, 12: 1929.

Iqbal, M. A., B. C. Fong, and R. S. Slack. 2022. 'Direct FACS Isolation of Neural Stem/Progenitor Lineages from the Adult Brain', *Methods Mol Biol*, 2515: 117-27.

Iwata, R., P. Casimir, and P. Vanderhaeghen. 2020. 'Mitochondrial dynamics in postmitotic cells regulate neurogenesis', *Science*, 369: 858-62.

Jain, I. H., L. Zazzeron, R. Goli, K. Alexa, S. Schatzman-Bone, H. Dhillon, O. Goldberger, J. Peng, O. Shalem, N. E. Sanjana, F. Zhang, W. Goessling, W. M. Zapol, and V. K. Mootha. 2016. 'Hypoxia as a therapy for mitochondrial disease', *Science*, 352: 54-61.

Kalinina, A., and D. Lagace. 2022. 'Single-Cell and Single-Nucleus RNAseq Analysis of Adult Neurogenesis', *Cells*, 11.

Kane, M. S., J. Alban, V. Desquiret-Dumas, N. Gueguen, L. Ishak, M. Ferre, P. Amati-Bonneau, V. Procaccio, D. Bonneau, G. Lenaers, P. Reynier, and A. Chevrollier. 2017. 'Autophagy controls the pathogenicity of OPA1 mutations in dominant optic atrophy', *J Cell Mol Med*, 21: 2284-97.

Kee, N., C. M. Teixeira, A. H. Wang, and P. W. Frankland. 2007. 'Preferential incorporation of adult-generated granule cells into spatial memory networks in the dentate gyrus', *Nat Neurosci*, 10: 355-62.

Khacho, M., A. Clark, D. S. Svoboda, J. Azzi, J. G. MacLaurin, C. Meghaizel, H. Sesaki, D. C. Lagace, M. Germain, M. E. Harper, D. S. Park, and R. S. Slack. 2016. 'Mitochondrial Dynamics Impacts Stem Cell Identity and Fate Decisions by Regulating a Nuclear Transcriptional Program', *Cell Stem Cell*, 19: 232-47.

Khacho, M., A. Clark, D. S. Svoboda, J. G. MacLaurin, D. C. Lagace, D. S. Park, and R. S. Slack. 2017. 'Mitochondrial dysfunction underlies cognitive defects as a result of neural stem cell depletion and impaired neurogenesis', *Hum Mol Genet*, 26: 3327-41.

Khacho, M., R. Harris, and R. S. Slack. 2019. 'Mitochondria as central regulators of neural stem cell fate and cognitive function', *Nat Rev Neurosci*, 20: 34-48.

Khacho, M., and R. S. Slack. 2017. 'Mitochondrial activity in the regulation of stem cell self-renewal and differentiation', *Curr Opin Cell Biol*, 49: 1-8.

Kijima, K., C. Numakura, H. Izumino, K. Umetsu, A. Nezu, T. Shiiki, M. Ogawa, Y. Ishizaki, T. Kitamura, Y. Shozawa, and K. Hayasaka. 2005. 'Mitochondrial GTPase mitofusin 2 mutation in Charcot-Marie-Tooth neuropathy type 2A', *Hum Genet*, 116: 23-7.

La Manno, G., R. Soldatov, A. Zeisel, E. Braun, H. Hochgerner, V. Petukhov, K. Lidschreiber, M. E. Kastriti, P. Lonnerberg, A. Furlan, J. Fan, L. E. Borm, Z. Liu, D. van Bruggen, J. Guo, X. He, R. Barker, E. Sundstrom, G. Castelo-Branco, P. Cramer, I. Adameyko, S. Linnarsson, and P. V. Kharchenko. 2018. 'RNA velocity of single cells', *Nature*, 560: 494-98.

Lim, J. K. M., A. Delaidelli, S. W. Minaker, H. F. Zhang, M. Colovic, H. Yang, G. L. Negri, S. von Karstedt, W. W. Lockwood, P. Schaffer, G. Leprivier, and P. H. Sorensen. 2019. 'Cystine/glutamate antiporter xCT (SLC7A11) facilitates oncogenic RAS transformation by preserving intracellular redox balance', *Proc Natl Acad Sci U S A*, 116: 9433-42.

Liu, Y., B. Fong, R. Harris, M McNicoll, A Abdi, J Cuthbert, D. Cook, D. Figeys, J Wang, B Vanderhyden, and Slack. R. 2022. 'Alterations in neural stem cell quiescence and activation in the 3xTG-AD model of Alzheimer's Disease', *bioRxiv*.

Longo, F., S. Benedetti, A. A. Zambon, M. G. N. Sora, C. Di Resta, D. De Ritis, A. Quattrini, F. Maltecca, M. Ferrari, and S. C. Previtali. 2020. 'Impaired turnover of hyperfused mitochondria in severe axonal neuropathy due to a novel DRP1 mutation', *Hum Mol Genet*, 29: 177-88.

Luna, V. M., C. Anacker, N. S. Burghardt, H. Khandaker, V. Andreu, A. Millette, P. Leary, R. Ravenelle, J. C. Jimenez, A. Mastrodonato, C. A. Denny, A. A. Fenton, H. E. Scharfman, and R. Hen. 2019. 'Adult-born hippocampal neurons bidirectionally modulate entorhinal inputs into the dentate gyrus', *Science*, 364: 578-83.

Maren, S., K. L. Phan, and I. Liberzon. 2013. 'The contextual brain: implications for fear conditioning, extinction and psychopathology', *Nat Rev Neurosci*, 14: 417-28.

Mertens, J., J. R. Herdy, L. Traxler, S. T. Schafer, J. C. M. Schlachetzki, L. Bohnke, D. A. Reid, H. Lee, D. Zangwill, D. P. Fernandes, R. K. Agarwal, R. Lucciola, L. Zhou-Yang, L. Karbacher, F. Edenhofer, S. Stern, S. Horvath, A. C. M. Paquola, C. K. Glass, S. H. Yuan, M. Ku, A. Szucs, L. S. B. Goldstein, D. Galasko, and F. H. Gage. 2021. 'Age-dependent instability of mature neuronal fate in induced neurons from Alzheimer's patients', *Cell Stem Cell*, 28: 1533-48 e6.

Mick, E., D. V. Titov, O. S. Skinner, R. Sharma, A. A. Jourdain, and V. K. Mootha. 2020. 'Distinct mitochondrial defects trigger the integrated stress response depending on the metabolic state of the cell', *Elife*, 9.

Mizrak, D., H. M. Levitin, A. C. Delgado, V. Crotet, J. Yuan, Z. Chaker, V. Silva-Vargas, P. A. Sims, and F. Doetsch. 2019. 'Single-Cell Analysis of Regional Differences in Adult V-SVZ Neural Stem Cell Lineages', *Cell Rep*, 26: 394-406 e5.

Moreno-Jimenez, E. P., M. Flor-Garcia, J. Terreros-Roncal, A. Rabano, F. Cafini, N. Pallas-Bazarra, J. Avila, and M. Llorens-Martin. 2019. 'Adult hippocampal neurogenesis is abundant in neurologically healthy subjects and drops sharply in patients with Alzheimer's disease', *Nat Med*, 25: 554-60.

Patten, D. A., J. Wong, M. Khacho, V. Soubannier, R. J. Mailloux, K. Pilon-Larose, J. G. MacLaurin, D. S. Park, H. M. McBride, L. Trinkle-Mulcahy, M. E. Harper, M. Germain, and R. S. Slack. 2014. 'OPA1-dependent cristae modulation is essential for cellular adaptation to metabolic demand', *EMBO J*, 33: 2676-91.

Pham, J., S. M. Cabrera, C. Sanchis-Segura, and M. A. Wood. 2009. 'Automated scoring of fear-related behavior using EthoVision software', *J Neurosci Methods*, 178: 323-6.

Quiros, P. M., M. A. Prado, N. Zamboni, D. D'Amico, R. W. Williams, D. Finley, S. P. Gygi, and J. Auwerx. 2017. 'Multi-omics analysis identifies ATF4 as a key regulator of the mitochondrial stress response in mammals', *J Cell Biol*, 216: 2027-45.

Ramonet, D., C. Perier, A. Recasens, B. Dehay, J. Bove, V. Costa, L. Scorrano, and M. Vila. 2013. 'Optic atrophy 1 mediates mitochondria remodeling and dopaminergic neurodegeneration linked to complex I deficiency', *Cell Death Differ*, 20: 77-85.

Raposo, A. A., F. F. Vasconcelos, D. Drechsel, C. Marie, C. Johnston, D. Dolle, A. Bithell, S. Gillotin, D. L. van den Berg, L. Ettwiller, P. Flicek, G. E. Crawford, C. M. Parras, B. Berninger, N. J. Buckley, F. Guillemot, and D. S. Castro. 2015. 'Ascl1 Coordinately Regulates Gene Expression and the Chromatin Landscape during Neurogenesis', *Cell Rep*.

Robinson, K. M., M. S. Janes, and J. S. Beckman. 2008. 'The selective detection of mitochondrial superoxide by live cell imaging', *Nat Protoc*, 3: 941-7.

Santidrian, A. F., A. Matsuno-Yagi, M. Ritland, B. B. Seo, S. E. LeBoeuf, L. J. Gay, T. Yagi, and B. Felding-Habermann. 2013. 'Mitochondrial complex I activity and NAD+/NADH balance regulate breast cancer progression', *J Clin Invest*, 123: 1068-81.

Sato, H., M. Tamba, T. Ishii, and S. Bannai. 1999. 'Cloning and expression of a plasma membrane cystine/glutamate exchange transporter composed of two distinct proteins', *J Biol Chem*, 274: 11455-8.

Saxe, M. D., F. Battaglia, J. W. Wang, G. Malleret, D. J. David, J. E. Monckton, A. D. Garcia, M. V. Sofroniew, E. R. Kandel, L. Santarelli, R. Hen, and M. R. Drew. 2006. 'Ablation of hippocampal neurogenesis impairs contextual fear conditioning and synaptic plasticity in the dentate gyrus', *Proc Natl Acad Sci U S A*, 103: 17501-6.

Schindelin, J., I. Arganda-Carreras, E. Frise, V. Kaynig, M. Longair, T. Pietzsch, S. Preibisch, C. Rueden, S. Saalfeld, B. Schmid, J. Y. Tinevez, D. J. White, V. Hartenstein, K. Eliceiri, P. Tomancak, and A. Cardona. 2012. 'Fiji: an open-source platform for biological-image analysis', *Nat Methods*, 9: 676-82.

Schwartz, J. P., J. V. Passonneau, G. S. Johnson, and I. Pastan. 1974. 'The effect of growth conditions on NAD+ and NADH concentrations and the NAD+:NADH ratio in normal and transformed fibroblasts', *J Biol Chem*, 249: 4138-43.

Srinivas, S., T. Watanabe, C. S. Lin, C. M. William, Y. Tanabe, T. M. Jessell, and F. Costantini. 2001. 'Cre reporter strains produced by targeted insertion of EYFP and ECFP into the ROSA26 locus', *BMC Dev Biol*, 1: 4.

Terreros-Roncal, J., E. P. Moreno-Jimenez, M. Flor-Garcia, C. B. Rodriguez-Moreno, M. F. Trinchero, F. Cafini, A. Rabano, and M. Llorens-Martin. 2021. 'Impact of neurodegenerative diseases on human adult hippocampal neurogenesis', *Science*, 374: 1106-13.

Torrence, M. E., M. R. MacArthur, A. M. Hosios, A. J. Valvezan, J. M. Asara, J. R. Mitchell, and B. D. Manning. 2021. 'The mTORC1-mediated activation of ATF4 promotes protein and glutathione synthesis downstream of growth signals', *Elife*, 10.

Urban, N., I. M. Blomfield, and F. Guillemot. 2019. 'Quiescence of Adult Mammalian Neural Stem Cells: A Highly Regulated Rest', *Neuron*, 104: 834-48.

van Galen, P., N. Mbong, A. Kreso, E. M. Schoof, E. Wagenblast, S. W. K. Ng, G. Krivdova, L. Jin, H. Nakauchi, and J. E. Dick. 2018. 'Integrated Stress Response Activity Marks Stem Cells in Normal Hematopoiesis and Leukemia', *Cell Rep*, 25: 1109-17 e5.

Yang, W. S., R. SriRamaratnam, M. E. Welsch, K. Shimada, R. Skouta, V. S. Viswanathan, J. H. Cheah, P. A. Clemons, A. F. Shamji, C. B. Clish, L. M. Brown, A. W. Girotti, V. W. Cornish, S. L. Schreiber, and B. R. Stockwell. 2014. 'Regulation of ferroptotic cancer cell death by GPX4', *Cell*, 156: 317-31.

Zhang, H., D. Ryu, Y. Wu, K. Gariani, X. Wang, P. Luan, D. D'Amico, E. R. Ropelle, M. P. Lutolf, R. Aebersold, K. Schoonjans, K. J. Menzies, and J. Auwerx. 2016. 'NAD(+) repletion improves mitochondrial and stem cell function and enhances life span in mice', *Science*, 352: 1436-43.

Zhang, Z., N. Wakabayashi, J. Wakabayashi, Y. Tamura, W. J. Song, S. Sereda, P. Clerc, B. M. Polster, S. M. Aja, M. V. Pletnikov, T. W. Kensler, O. S. Shirihai, M. Iijima, M. A. Hussain, and H. Sesaki. 2011. 'The dynamin-related GTPase Opa1 is required for glucose-stimulated ATP production in pancreatic beta cells', *Mol Biol Cell*, 22: 2235-45.

Zheng, G. X., J. M. Terry, P. Belgrader, P. Ryvkin, Z. W. Bent, R. Wilson, S. B. Ziraldo, T. D. Wheeler, G. P. McDermott, J. Zhu, M. T. Gregory, J. Shuga, L. Montesclaros, J. G. Underwood, D. A. Masquelier, S. Y. Nishimura, M. Schnall-Levin, P. W. Wyatt, C. M. Hindson, R. Bharadwaj, A. Wong, K. D. Ness, L. W. Beppu, H. J. Deeg, C. McFarland, K. R. Loeb, W. J. Valente, N. G. Ericson, E. A. Stevens, J. P. Radich, T. S. Mikkelsen, B. J. Hindson, and J. H. Bielas. 2017. 'Massively parallel digital transcriptional profiling of single cells', *Nat Commun*, 8: 14049.

Zheng, X., L. Boyer, M. Jin, J. Mertens, Y. Kim, L. Ma, L. Ma, M. Hamm, F. H. Gage, and T. Hunter. 2016. 'Metabolic reprogramming during neuronal differentiation from aerobic glycolysis to neuronal oxidative phosphorylation', *Elife*, 5.

Zuchner, S., I. V. Mersiyanova, M. Muglia, N. Bissar-Tadmouri, J. Rochelle, E. L. Dadali, M. Zappia, E. Nelis, A. Patitucci, J. Senderek, Y. Parman, O. Evgrafov, P. D. Jonghe, Y. Takahashi, S. Tsuji, M. A. Pericak-Vance, A. Quattrone, E. Battaloglu, A. V. Polyakov, V. Timmerman, J. M. Schroder, and J. M. Vance. 2004. 'Mutations in the mitochondrial GTPase mitofusin 2 cause Charcot-Marie-Tooth neuropathy type 2A', *Nat Genet*, 36: 449-51.

FIGURE LEGENDS

Figure 1: Opa1 loss impacts neural stem cell commitment, activation, and neurogenesis in adult dentate gyrus: 1A) Experimental set up. **1B)** The graph indicates the percentage immobility in the same context at 24 hr and 1 week following exposure to shock in Opa1 CT and Opa1 cKO animals. Results indicated an association of the context of freezing in animals. (CT, n = 16; Opa1 cKO, n = 17 animals). Data are presented as mean ± SD (*p < 0.05, **p < 0.01, and ***p < 0.001, Student's t-test). **1C)** Representative images of coronal section dentate gyrus was immunostained for Dcx (red), YFP (green) and nuclear stain DAPI (blue) from control transgenic (CT) and Opa1 cKO animals from 4weeks post Tamoxifen administration. **1D-F)** Total number of cells per dentate is represented in bar graphs of Dcx (Newborn neurons), Tbr2 (Transiently Amplifying Progenitors, TAP) and Sox2 (uncommited stem cell pool) that are colocalized with YFP^+ cells at the listed time in the listed genotype. Quantification of total cells in SGZ these markers are plotted in the bar graph. (n = 3-6 animals); Data are presented as mean ± SD, (*p < 0.05, **p < 0.01, and ***p < 0.001, student's t-test). **1G)** RNAseq analysis of adult SVZ sort YFP+ cells. GO term analysis of top upregulated genes (shown in red) and downregulated genes (shown in green).

Figure1 supplementary: Opa1 loss stalls the stem cells from proliferation and activation in adult dentate gyrus: S1A) qPCR analysis of YFP sorted cells from adult SVZ of Opa1 and Slc7a11, normalized to β Actin. (n = 3 animals); Data are presented as mean ± SD, (*p < 0.05, **p < 0.01, and ***p < 0.001, student's t-test). **S1B)** Bar graphs of total number of cells per dentate in CT and Opa1 cKO 2weeks post Tamoxifen administration. **S1C)** Representative IHC images of Sox2, Ki67, Tbr2 and Dcx (red) colabelled with YFP (green). **S1D)** Heatmap of YFP sorted cells from adult SVZ of significant upregulated and downregulated genes (relative gene expression range from green -1 to red 1).

Figure 2: NSC proliferation and activation impedes after Opa1 knockout in adult hippocampus 2A) Bar graphs of total number of cells per dentate are represented in bar graphs of Ki67+ (proliferating cells). **2B)** Percentage of proliferating NSCs ($Ki67^+Sox2^+$ of total YFP^+ cell in adult dentate at the listed time in the listed genotype. **2C)** Percentage of proliferating TAP cells ($Ki67^+Tbr2^+$ of total YFP^+ cell in adult dentate. **2D)** Experimental set up. **2E)** Representative image of adult dentate with EdU label at the given time for the listed genotype. **2F)** Total EdU+ cells are quantified to show the number of EdU retaining cells at 4 weeks post TAM in the dentate gyrus. **2G)** Percentage of $EdU^-Ki67^+YFP^+$ of total YFP^+ cells at 4 weeks post TAM in adult dentate. **2H)** Representative image for $Hopx^+$ cells retaining EdU label at 4 weeks post TAM in CT and Opa1 cKO sections (Marked by the arrow). Scale bar = 100µm. **2I)** Percentage of $EdU^+Hopx^+YFP^+$ of total $Hopx^+YFP^+$ cells at 4 weeks post TAM in adult dentate. **2J)** Total number of $Hopx^+$ cells retaining EdU label at 4 weeks post TAM represented in bar graphs. **2K)** Percentage of $Hopx^+$ cells of total YPF^+ cells at 4 weeks post TAM represented in bar graphs. **2L)** Percentage of $Sox2^+$ cells of total YPF^+ cells at 4 weeks post TAM represented in bar graphs. **2M)** Total number of $Ascl1^+$ cells at 4 weeks post TAM per dentate is represented in bar graphs of Ascl1 (Activation marker) that are colocalized with YFP^+ cells. (n = 3-4 animals); Data are presented as mean ± SD, (*p < 0.05, **p < 0.01, and ***p < 0.001, student's t-test).

Figure 3: Single cell RNA-Seq analysis identifies Atf4 stress response pathway because of mitochondrial dysfunction: 3A) Experimental set up. **3B)** UMAP scatterplot shows the distribution of CT and Opa1 cKO derived cells clusters. **3C)** Heatmap of genes in representative cluster, reflecting genotype-specific differential gene expression. **3D)** Gene featured UMAP of individual genes that are differentially regulated in all these clusters highlighting Atf4 pathway. **3E)** The violin plots represent the gene expression of mitochondrial genes, stress response genes and differentiation genes in each cluster split by sample. **3F)** RNA velocity analysis shows the differentiation direction shown by the vectors separated by sample. **3G)** Panels are magnified views of transition between cluster 1 (activated NSCs) and cluster 2 (Differentiating NSCs). **3H)** The proportion of spliced and unspliced RNA in all the clusters split by sample.

Figure 3 supplementary: Validation of Single cell RNA-Seq and neurogenesis: 3A) Integrated UMAP projection of CT and Opa1 cKO cells using Seurat into nine cell clusters based on their unique gene expression profiles. 3B) Heatmap demonstrating genes representative of each cluster, reflecting cluster-specific gene expression. 3C) UMAP projections demonstrating curated clusters representative of neurogenesis. 3D) UMAP projections of cluster markers highlighting genes representative of each cluster, reflecting cluster-specific expression. 3E) The violin plots suggest the distinct pattern of cluster specific genes expression in each cluster. 3F) Heatmap of curated genes representative of different stages neurogenesis.

Figure 4: ATF4 pathway is activated by mitochondrial dysfunction and reductive metabolism under hypoxia resolves ATF4 activation. 4A) Western blot ISR pathway related proteins subunits in E12.5 embryonic cortex of CT and Opa1 KO post Opa1 deletion as mentioned in the plot. **4B)** Cellular oxygen consumption rate was measured using XF24 extracellular flux analyzer. Bar graphs represent the cellular respiration of basal, maximal, reserved and ATP-linked respiration between the listed conditions. n=3 animals. **4C)** Mean intensity of MitoSOX Red was calculated from live cells and plotted as bar graph. **4D)** Phase contrast images of neurospheres from Adult NSCs from CT and Opa1 cKO in listed Oxygen exposure conditions. **4E)** The number of primary neurospheres formed in Opa1 cKO neurospheres growing under hypoxic conditions. **4F)** The size of the neurospheres in Opa1 cKO in hypoxic condition is comparable to Opa1 cKO spheres grown in normoxic conditions. **4G)** Western blot analysis from total protein lysates of embryonic neurospheres (E12.5) grown treated with LV-shCtrl or shOpa1 were grown in normoxic and hypoxic conditions. **4H)** Shows qPCR results of stress response genes trends that is partially normalized under hypoxic condition. **(4F)** Western blot of total protein lysate from embryonic cortex of CT and Opa1 KO on E12.5 days. n=3-4 animals; Data are presented as mean ± SD (*p < 0.05, **p < 0.01, and ***p < 0.001, Student's t-test).

Figure 4 supplementary: Opa1 loss leads to severe mitochondrial defect and leading to stem cell defects. S4A&B). Western blot and quantification of neurogenesis markers Sox2, Tbr2, Dcx, Tuj1, Ascl1, N^{ICD} and Cyclin D2 **S4C&D)** Western blot and quantification of mitochondrial complex subunits in E12.5 embryonic cortex of CT and Opa1 KO post Opa1 deletion as mentioned

in the plot. Mean intensity was normalized to wildtype in the bar graph. n=3 animals; Data are presented as mean ± SD (*p < 0.05, **p < 0.01, and ***p < 0.001, Student's t-test). **S4E)** Quantification of total ATP using Cell titre-Glo assay from the embryonic cortex of BF1 Cre negative (Wildtype) and BF1 Cre positive Opa1 F/F mice on E12.5 days. n=3 animals; Data are presented as mean ± SD (*p < 0.05, **p < 0.01, and ***p < 0.001, Student's t-test). **S4F)** Total NAD+ and NAD+/NADH+ ratio from Control and Opa1 knockdown neurospheres. Values were normalized to the protein content of the cell lysate.

Figure 5: ATF4 function is required for cell proliferation and survival in normal and stressed state. 5A) Representative images of EdU and DAPI staining in above mentioned conditions. Cell proliferation is measured using EdU+ cells normalized to total DAPI. **5B)** Quantification of percent EdU+ over total DAPI+ cells represented in bar graph. **5C)** Representative images of cleaved Caspase 3 (cl-Cas-3) and DAPI staining in above mentioned conditions. Cell death is measured using cl-Cas3+ cells normalized to total DAPI. **5D)** Quantification of percent cleaved caspase 3+ over total DAPI+ cells represented in bar graph. **5E)** qPCR analysis in mentioned conditions is measured for listed genes that are ATF4 targets that are involved in aminoacid transport, tRNA aminoacylation, export, and one-carbon metabolism. n=3-6 animals; Data are presented as mean ± SD (*p < 0.05, **p < 0.01, and ***p < 0.001, One-way ANOVA). **5F)** Schematic of the Chac1, Slc3a2 and Slc7a11 genes indicating the ATF4 motifs. **5G)** ATF4 ChIP of chromatin from shCtrl and shOpa1 KD neurosphere. **5H)** H3K4me3 ChIP from shCtrl and shOpa1 KD neurosphere. n=3-6 animals; Data are presented as mean ± SEM (*p < 0.05, **p < 0.01, and ***p < 0.001, One-way ANOVA).

Figure 6: Slc7a11, a key target of ATF4 is required for xCT mediated glutathione production. 6D-G) Histological analysis of phospho Histone 3(Proliferation), Ascl1(Activation), Tbr2(TAP) and Dcx(Newborn neurons) in 3months and 6months old wildtype and sut/sut adult mice. n=4-5 animals; Data are presented as mean ± SD (*p < 0.05, **p < 0.01, and ***p < 0.001, Student's t-test). **6H)** In vitro monolayer culture of WT and Sut mice infected with scramble and shOpa1. Bar graph for percent EdU+ over total DAPI+ cells and **6I)** Cleaved caspase 3+ over total DAPI+ cells. **6J&K)** Glutathione measurement using HPLC of GSH:GSSG ratio and total GSH levels in embryonic neurospheres in mentioned conditions. n=3 animals; Data are presented as mean ± SD (*p < 0.05, **p < 0.01, and ***p < 0.001, One-way ANOVA).

Figures

Fig 1

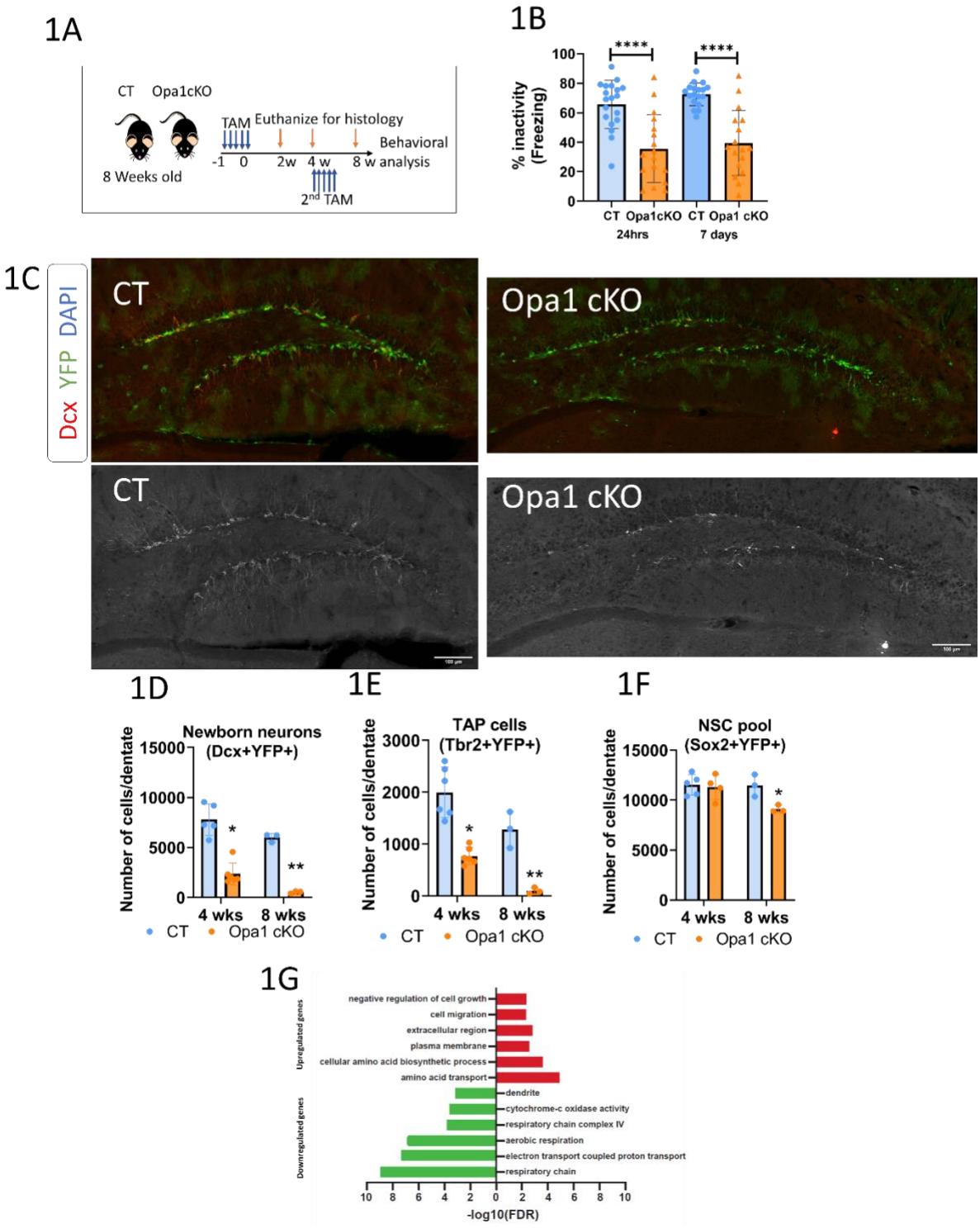

Supplementary figure 1

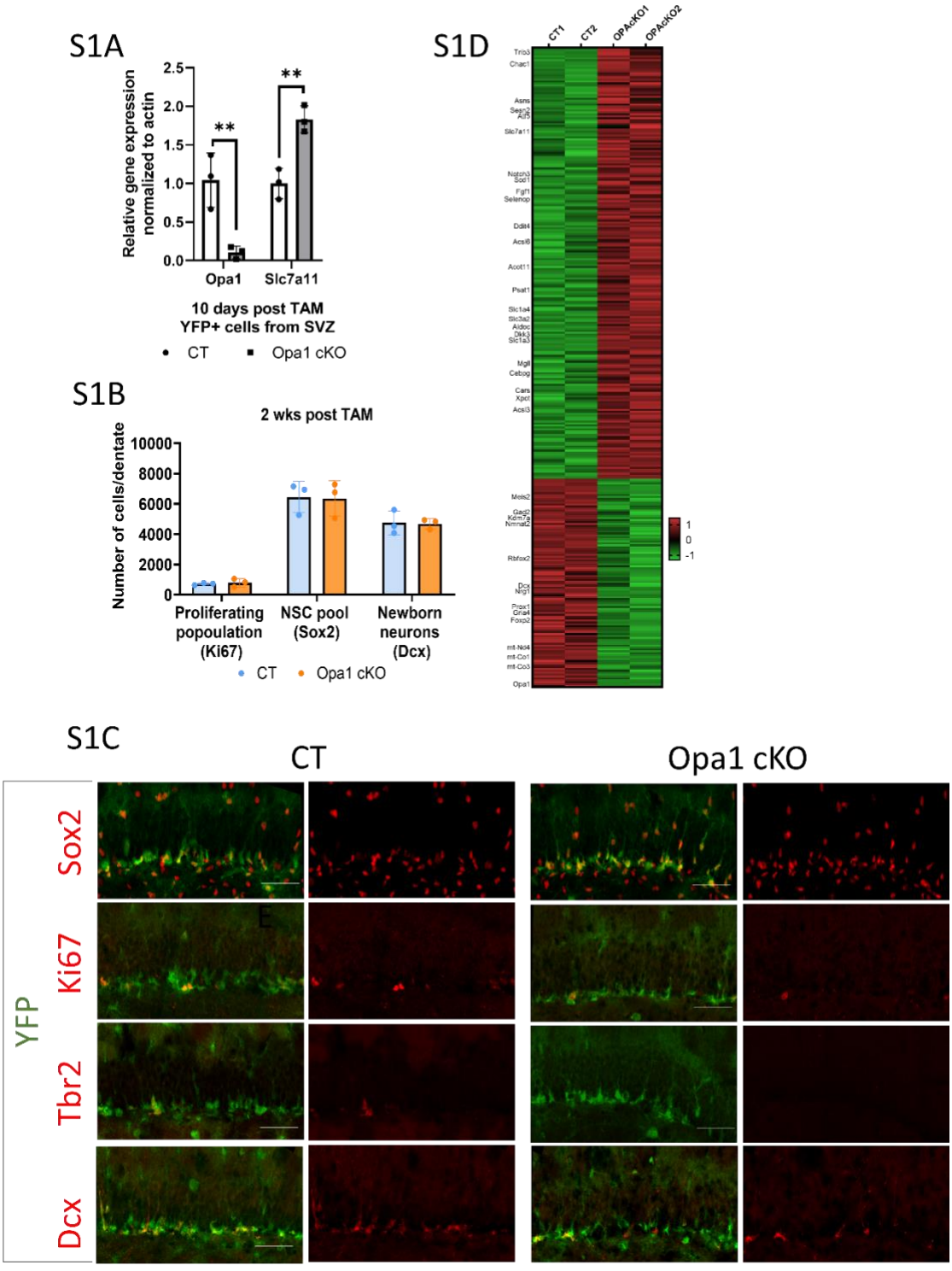

Fig 2

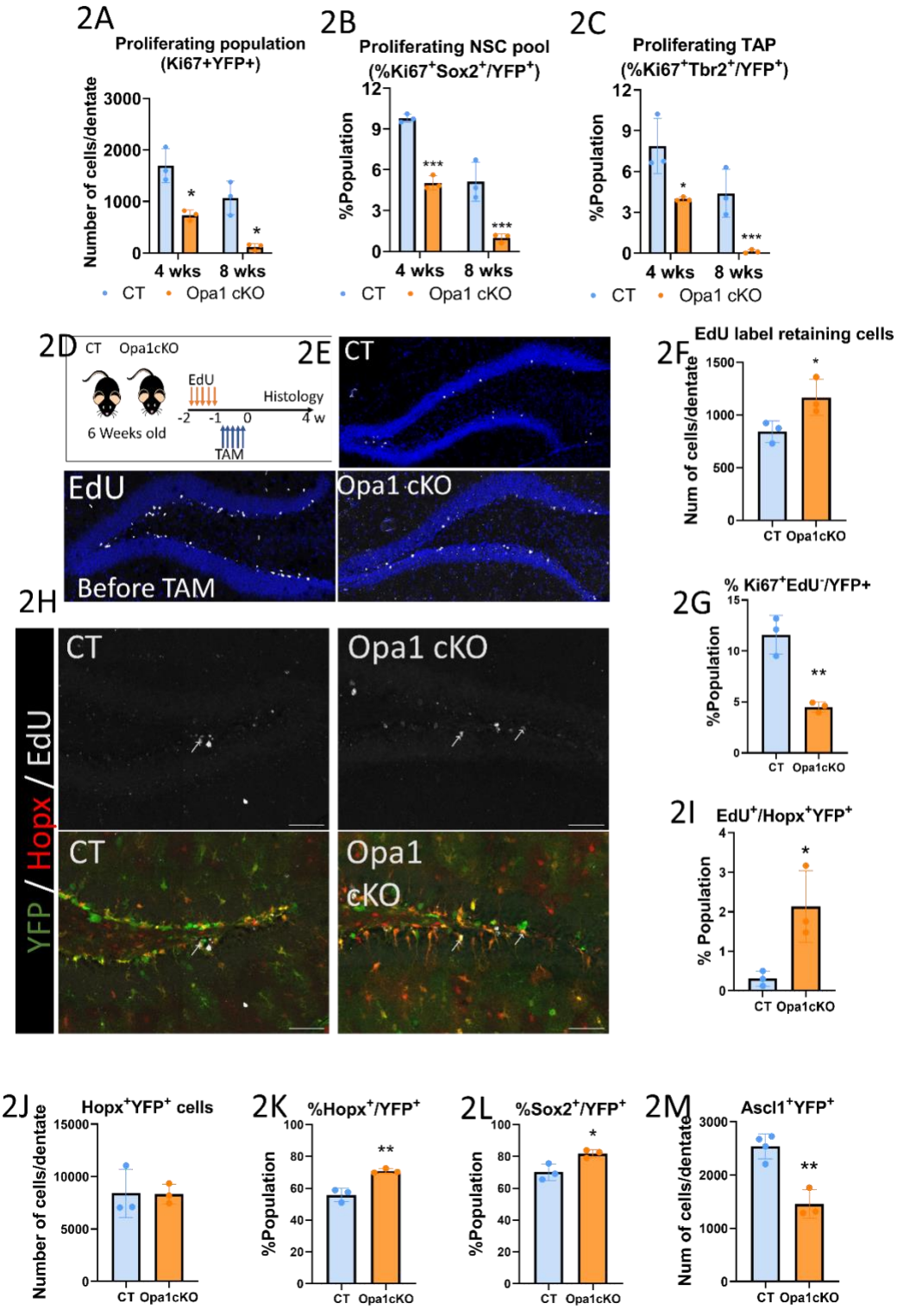
2A
Proliferating population (Ki67+YFP+)
Number of cells/dentate
3000
2000
1000
0
4 wks
8 wks
CT
Opa1 cKO
2B
Proliferating NSC pool (%Ki67+Sox2+/YFP+)
%Population
12
9
6
3
0
***
4 wks
8 wks
CT
Opa1 cKO
2C
Proliferating TAP (%Ki67+Tbr2+/YFP+)
%Population
12
9
6
3
0
*
***
4 wks
8 wks
CT
Opa1 cKO
2D
CT
Opa1cKO
6 Weeks old
EdU
TAM
Histology
-2
-1
0
4 w
2E
CT
EdU
Before TAM
Opa1 cKO
2F
EdU label retaining cells
Num of cells/dentate
1500
1000
500
0
*
CT
Opa1cKO
2H
YFP / Hopx / EdU
CT
Opa1 cKO
CT
Opa1 cKO
2G
% Ki67+EdU-/YFP+
%Population
15
10
5
0
**
CT
Opa1cKO
2I
EdU+/Hopx+YFP+
% Population
4
3
2
1
0
*
CT
Opa1cKO
2J
Hopx+YFP+ cells
Number of cells/dentate
15000
10000
5000
0
CT
Opa1cKO
2K
%Hopx+/YFP+
%Population
100
80
60
40
20
0
**
CT
Opa1cKO
2L
%Sox2+/YFP+
%Population
100
80
60
40
20
0
*
CT
Opa1cKO
2M
Ascl1+YFP+
Num of cells/dentate
3000
2000
1000
0
**
CT
Opa1cKO

Fig 3

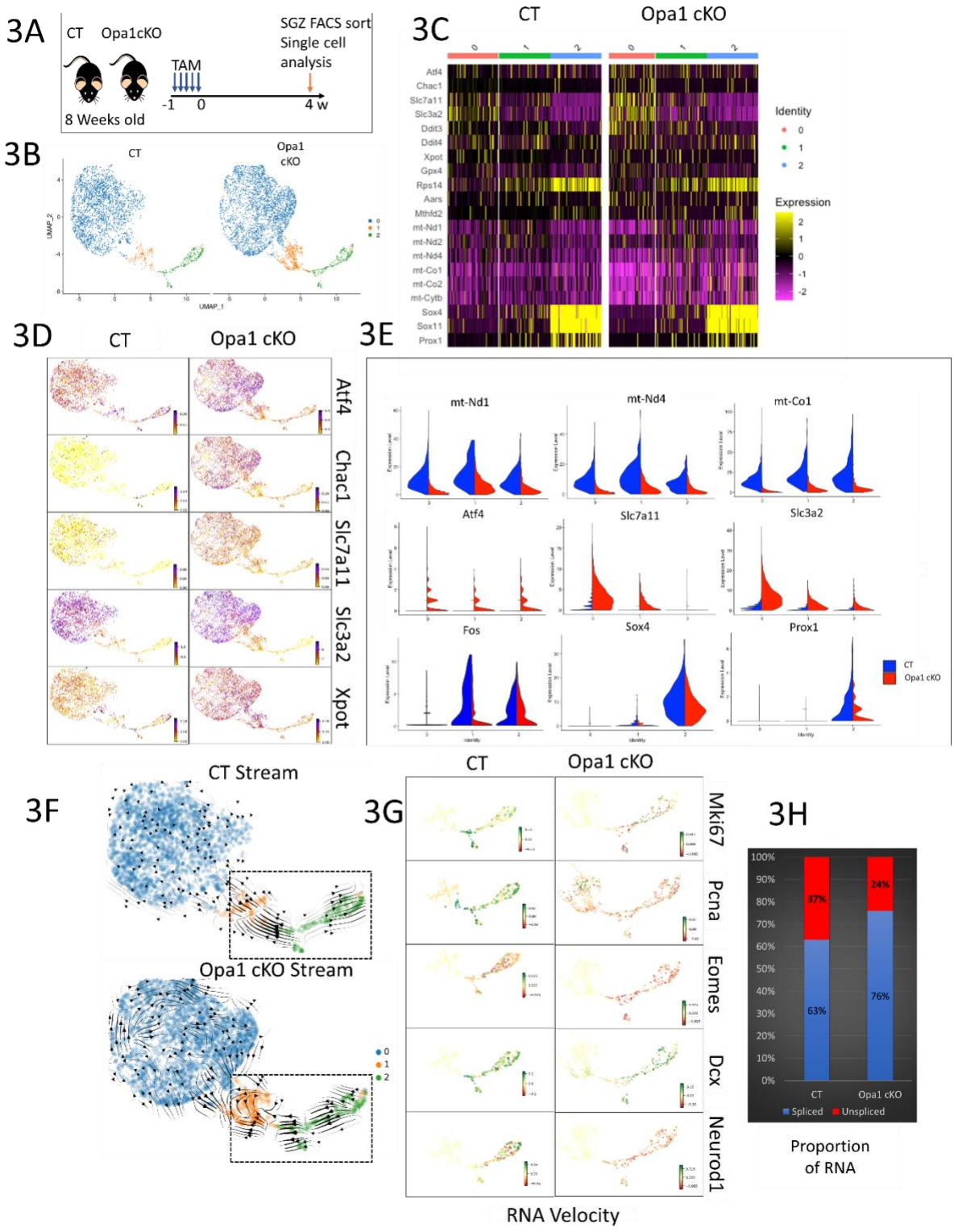
3A
CT
Opa1cKO
TAM
-1
0
4 w
SGZ FACS sort
Single cell analysis
8 Weeks old
3B
CT
Opa1 cKO
3C
CT
Opa1 cKO
Identity
Expression
Atf4
Chac1
Slc7a11
Slc3a2
Ddit3
Ddit4
Xpot
Gpx4
Rps14
Aars
Mthfd2
mt-Nd1
mt-Nd2
mt-Nd4
mt-Co1
mt-Co2
mt-Cytb
Sox4
Sox11
Prox1
3D
CT
Opa1 cKO
Atf4
Chac1
Slc7a11
Slc3a2
Xpot
3E
mt-Nd1
mt-Nd4
mt-Co1
Atf4
Slc7a11
Slc3a2
Fos
Sox4
Prox1
CT
Opa1 cKO
3F
CT Stream
Opa1 cKO Stream
3G
CT
Opa1 cKO
Mki67
Pcna
Eomes
Dcx
Neurod1
RNA Velocity
3H
100%
90%
80%
70%
60%
50%
40%
30%
20%
10%
0%
37%
63%
24%
76%
CT
Opa1 cKO
Spliced
Unspliced
Proportion of RNA

Supplementary figure 3

S3A

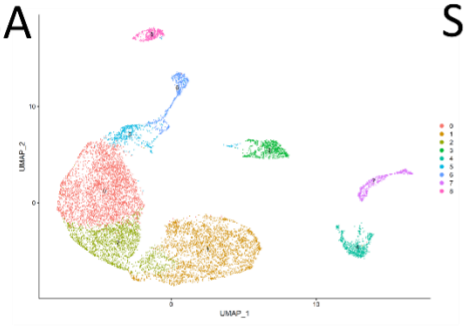

S3B

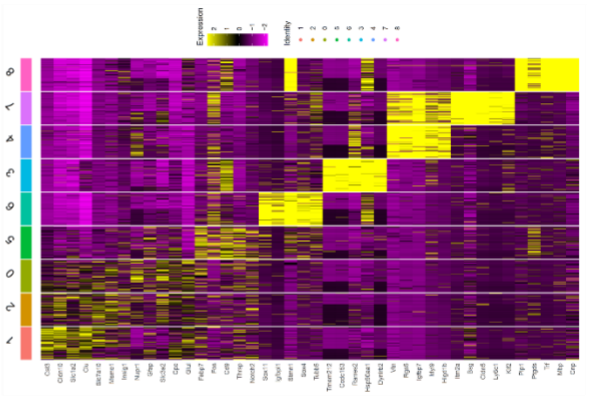

S3C

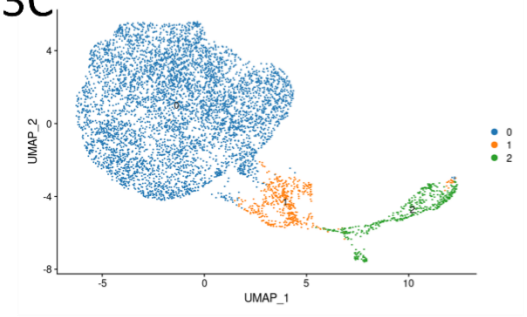

S3D

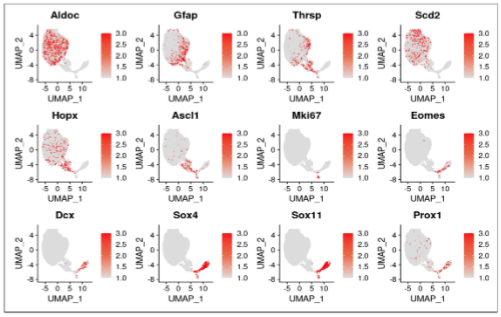

S3E

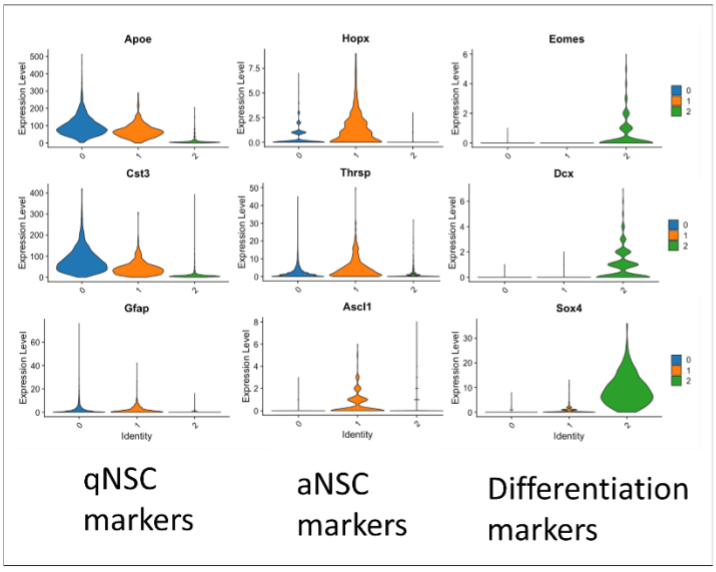

S3F

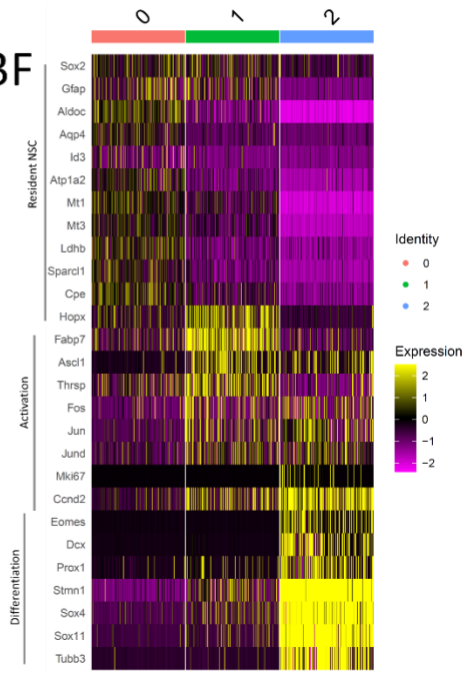

Fig 4

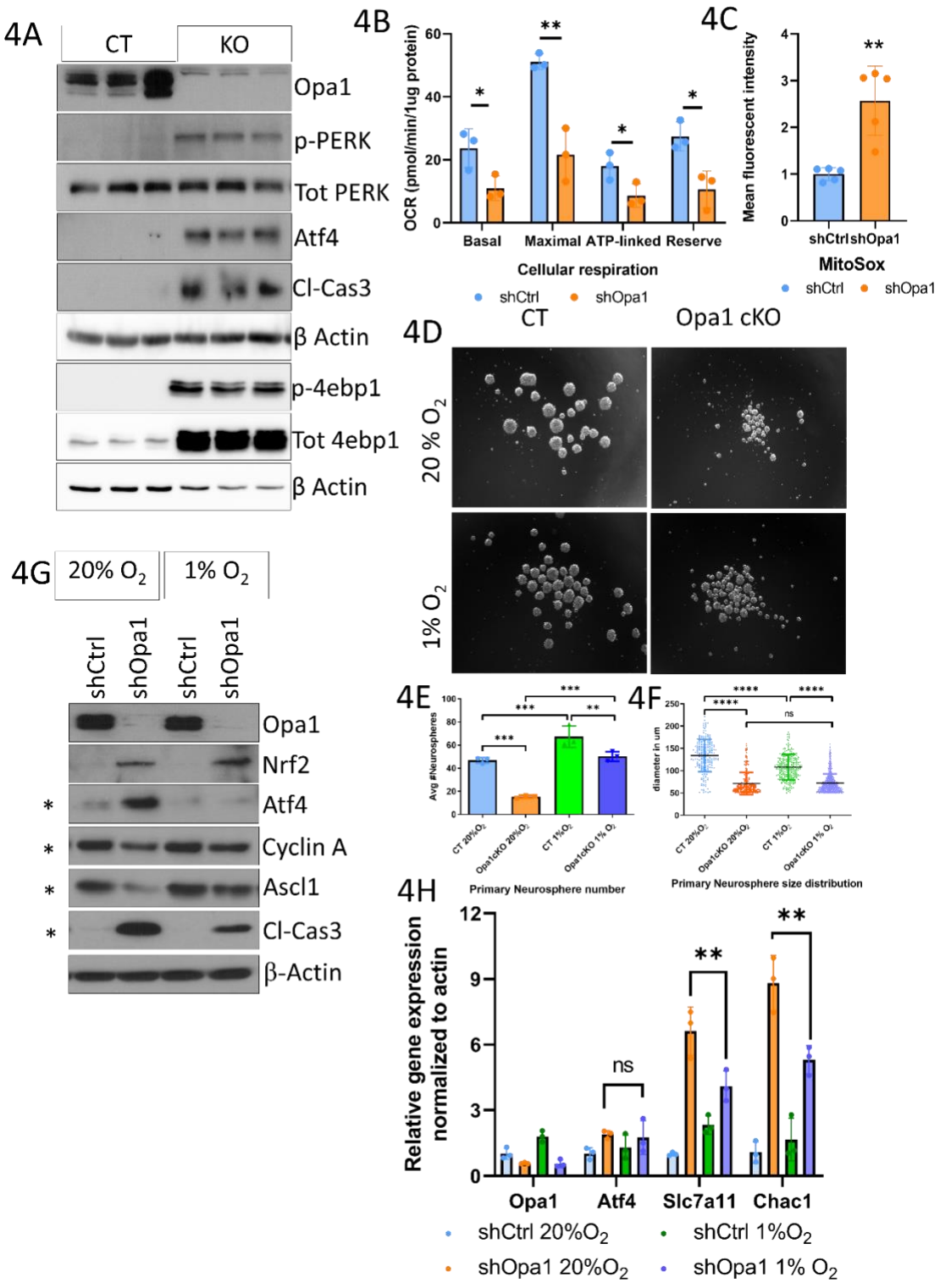
4A
CT
KO
Opa1
p-PERK
Tot PERK
Atf4
Cl-Cas3
β Actin
p-4ebp1
Tot 4ebp1
β Actin
4B
OCR (pmol/min/1ug protein)
Basal
Maximal
ATP-linked
Reserve
Cellular respiration
shCtrl
shOpa1
4C
Mean fluorescent intensity
shCtrl
shOpa1
MitoSox
4D
CT
Opa1 cKO
20 % O2
1% O2
4E
Avg #Neurospheres
Primary Neurosphere number
4F
diameter in um
Primary Neurosphere size distribution
4G
20% O2
1% O2
shCtrl
shOpa1
Opa1
Nrf2
Atf4
Cyclin A
Ascl1
Cl-Cas3
β-Actin
4H
Relative gene expression normalized to actin
Opa1
Atf4
Slc7a11
Chac1
shCtrl 20%O2
shCtrl 1%O2
shOpa1 20%O2
shOpa1 1% O2

Supplementary figure 4

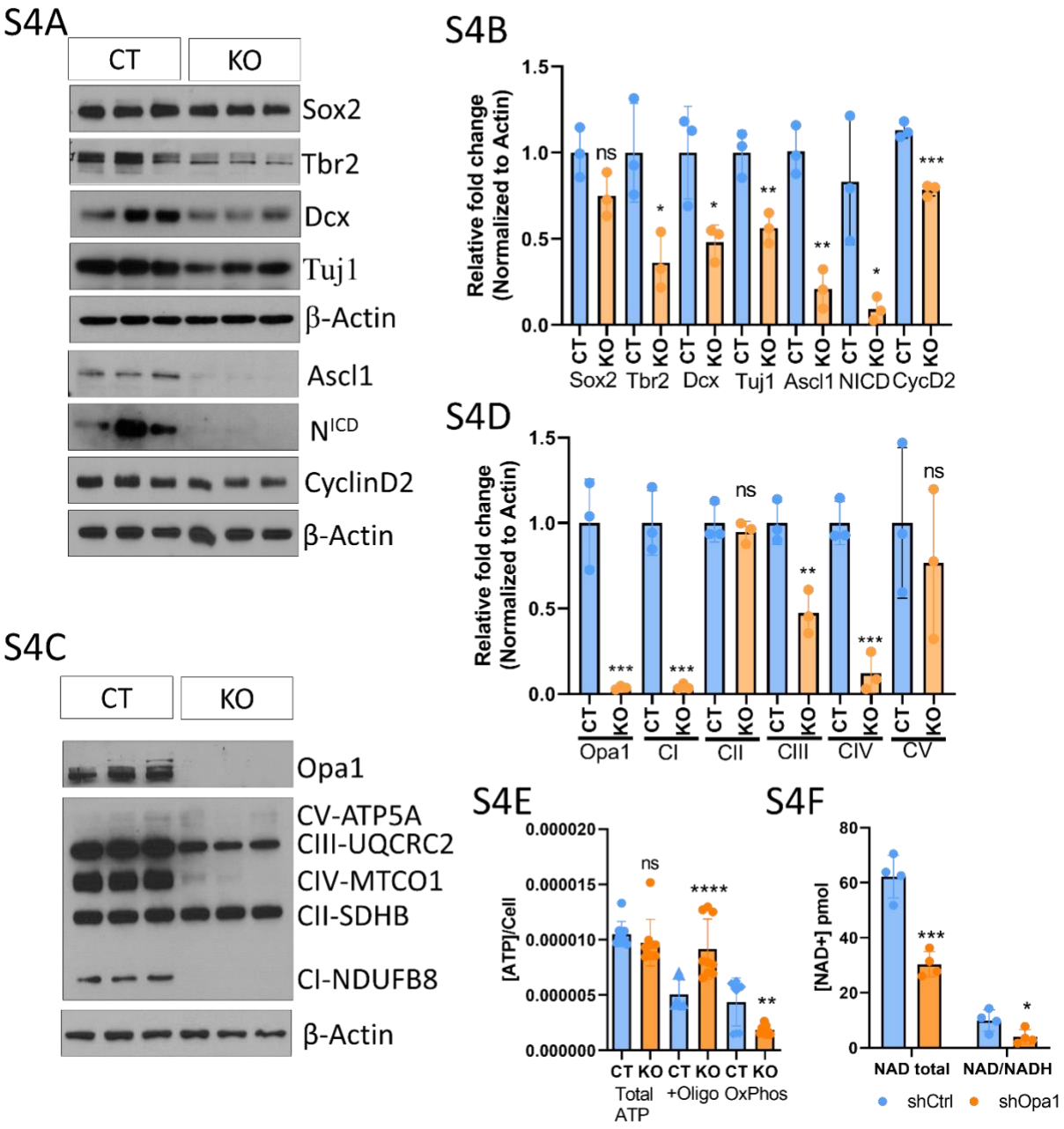

Fig 5

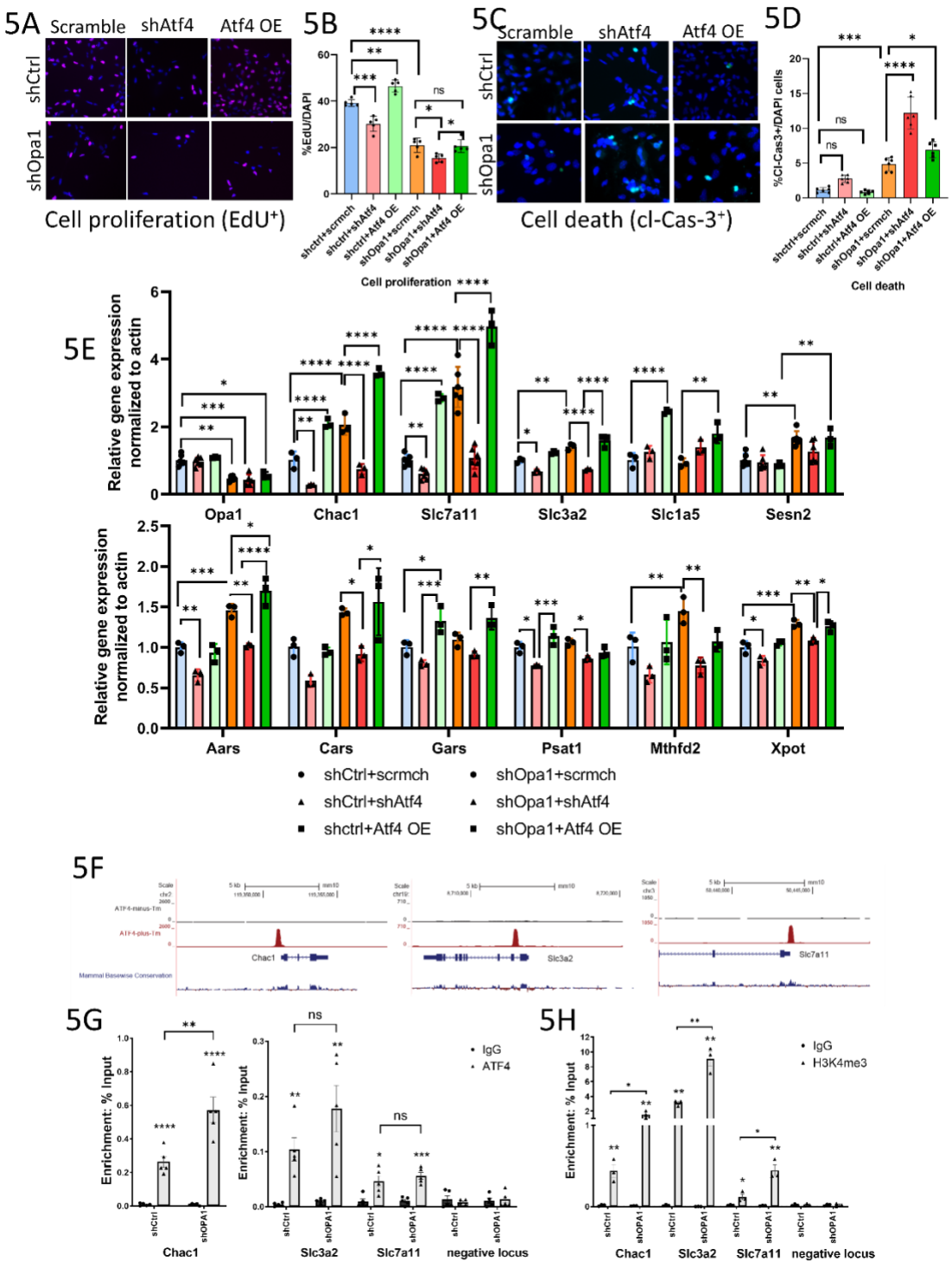
5A
Scramble
shAtf4
Atf4 OE
shCtrl
shOpa1
Cell proliferation (EdU+)
5B
%EdU/DAPI
shctrl+scrmch
shctrl+shAtf4
shctrl+Atf4 OE
shOpa1+scrmch
shOpa1+shAtf4
shOpa1+Atf4 OE
5C
Scramble
shAtf4
Atf4 OE
shCtrl
shOpa1
Cell death (cl-Cas-3+)
5D
%Cl-Cas3+/DAPI cells
Cell death
5E
Cell proliferation ****
Relative gene expression normalized to actin
Opa1
Chac1
Slc7a11
Slc3a2
Slc1a5
Sesn2
Aars
Cars
Gars
Psat1
Mthfd2
Xpot
shCtrl+scrmch
shCtrl+shAtf4
shctrl+Atf4 OE
shOpa1+scrmch
shOpa1+shAtf4
shOpa1+Atf4 OE
5F
ATF4-minus-Tm
ATF4-plus-Tm
Mammal Basewise Conservation
Chac1
Slc3a2
Slc7a11
5G
Enrichment: % Input
IgG
ATF4
Chac1
Slc3a2
Slc7a11
negative locus
5H
Enrichment: % Input
IgG
H3K4me3
Chac1
Slc3a2
Slc7a11
negative locus

Fig 6

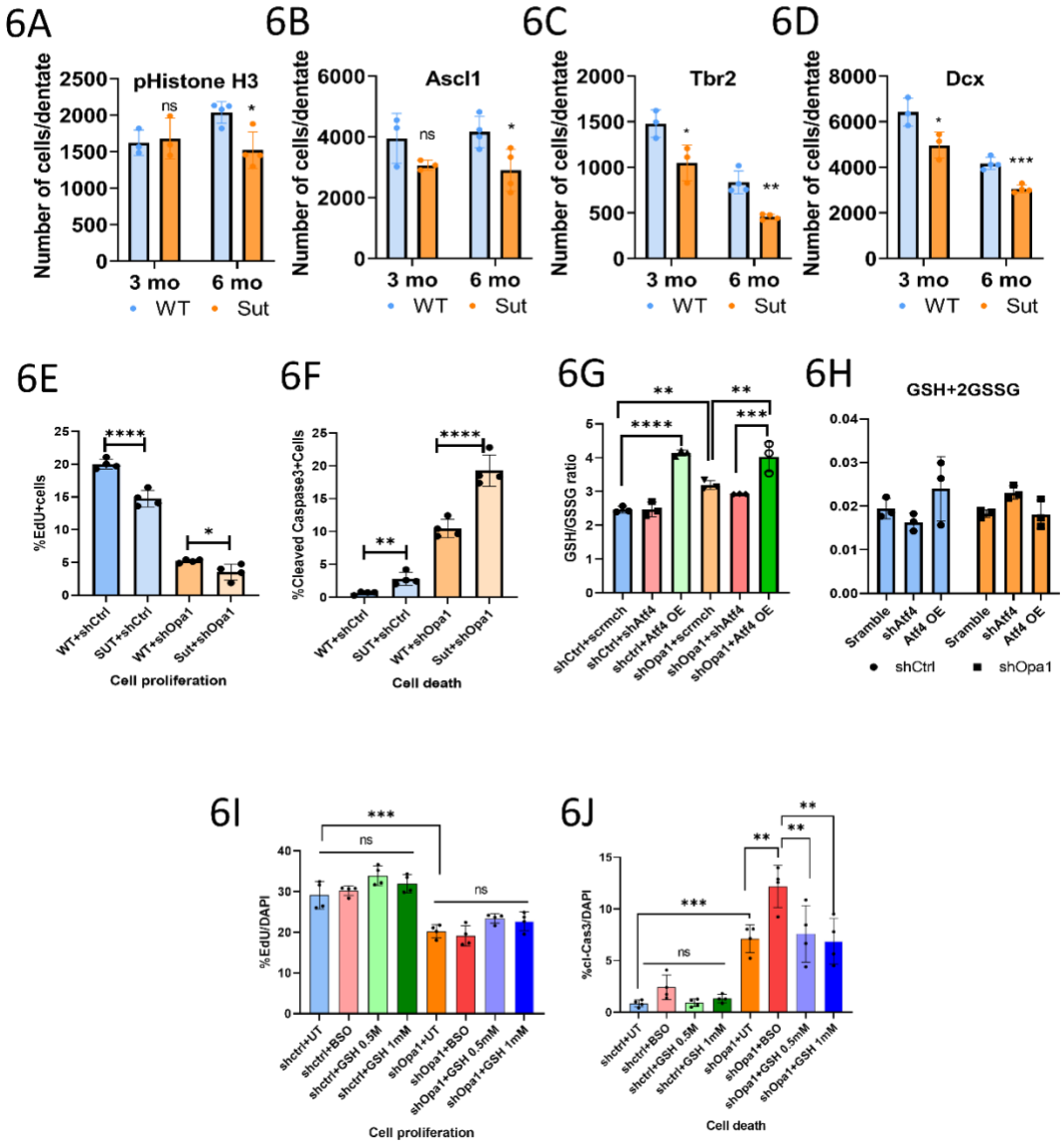
6A
pHistone H3
Number of cells/dentate
3 mo
6 mo
WT
Sut
6B
Ascl1
6C
Tbr2
6D
Dcx
6E
%EdU+cells
WT+shCtrl
SUT+shCtrl
WT+shOpa1
Sut+shOpa1
Cell proliferation
6F
%Cleaved Caspase3+Cells
Cell death
6G
GSH/GSSG ratio
shCtrl+scrmch
shCtrl+shAtf4
shCtrl+Atf4 OE
shOpa1+scrmch
shOpa1+shAtf4
shOpa1+Atf4 OE
6H
GSH+2GSSG
Sramble
shAtf4
Atf4 OE
shCtrl
shOpa1
6I
%EdU/DAPI
shctrl+UT
shctrl+BSO
shctrl+GSH 0.5M
shctrl+GSH 1mM
shOpa1+UT
shOpa1+BSO
shOpa1+GSH 0.5mM
shOpa1+GSH 1mM
Cell proliferation
6J
%cl-Cas3/DAPI
Cell death

Methods

Animals

All the animal protocols were approved by the Animal Care Ethics Committee of the University of Ottawa and adhered to the Guidelines of the Canadian Council on Animal Care. Animals were genotyped according to published protocols: primers are listed in Supplement.

We developed a Tamoxifen inducible reporter mouse Nestin-CreERT2 (Cicero et al. 2009); R26-stop-enhanced yellow fluorescent protein (YFP) (Srinivas et al. 2001) mice, a gift from S. Baker. Control transgenics (CT) were made by crossing Nestin-CreERT2 and R26-stop-enhanced yellow fluorescent protein (YFP) mice (Nestin-CreER^{T2}:Rosa26YFP) mice. To generate Opa1 inducible knockouts (Opa1 cKO) in Nestin expressing cells, Opa1flox/flox mice, a kind gift from Dr. Hiromi Sesaki were crossed with Nestin-CreERT2:Rosa26YFP to obtain Nestin-CreERT2:Rosa26YFPflox:Opa1flox line. All the mice were maintained on a C57/BL/6 background. All Nestin-CreER^{T2} animals used were heterozygotes for Cre expression. In all experiments, both females and males were used; all animals were 6-10 weeks old upon initial treatment.

BF1^{Cre}:Opa1 knockouts (Hebert and McConnell 2000) were generated by crossing BF1$^{Cre/+}$:Opa1$^{flox/+}$ with Opa1$^{flox/flox}$ mice. The BF1$^{+/+}$littermates were used as CT and BF1$^{Cre/+}$:Opa1$^{flox/flox}$ were used as Opa1 knockouts.

Tamoxifen injection

To generate the inducible Opa1 knockout in adult NestinCreER^{T2} animals, CT and Opa1cKO mice were administered tamoxifen (TAM) at 200 mg/kg/d for 5d (oral gavage; dissolved in 10% Ethanol/90% corn oil) (Fong et al. 2022). Animal weight at the beginning was used for calculating TAM dosage; weight after final injection was monitored and wellness checks were performed as per the University of Ottawa standards until euthanization.

Contextual Fear Conditioning Analysis:

Fear conditioning experiments were performed using the PhenoTyper box and Ethovision 10 XT video tracking system (Noldus Information Technology, North America) as previously described (Pham et al. 2009) with minor modifications. The method used for the fear conditioning test including the use of the foot shock sensitivity test to determine optimal shock was similar to (Khacho et al. 2016). The protocol used for contextual fear conditioning was similar to Cancino et al. 2014 (Cancino et al. 2013). Briefly, on Day 1 and 2 the mice were handled in the testing room for habituation, and on day 3 the mice were pre-exposed to the conditioning chamber for 10 minutes in the absence of a shock. On Day 4, approximately 24 hours after pre-exposure, the mice

were placed in the same conditioning context and 5 seconds later received an immediate foot shock (2sec, 0.7 mA) and after 1 minute were removed from the context. Twenty-four hours and 7 days after shock training, the mice were placed into the same conditioning context and freezing was assessed for a 6-minute period.

Histology

Systemic tissue perfusion and fixation was performed as previously described (McClellan et al., 2007). Briefly, animals were flushed with 0.9% saline and then perfused transcardially with 4% paraformaldehyde (PFA), immersed in 4% PFA overnight, and immersed in 20% sucrose for long-term storage. After removing the cerebellum to establish a flat coronal edge, fixed brains were frozen between -30 and -40 ºC in isopentane prior to cryo-sectioning. Brains were serially sectioned into 30 μm coronal sections, maintaining temperature between -20 and -25ºC, collecting the SVZ and hippocampal structure. Wells containing free-floating 1:9 serial sections were stored in PBS long-term at 4ºC.

Imunohistochemistry and Imaging, Cell Quantification, Statistical Analysis

Immunohistochemistry was performed as previously described (Vandenbosch et al., 2016). Antibodies are listed in Supplementary Table. Sections for quantifications of colocalized cells were imaged using Zeiss LSM800 confocal microscopes, employing a 40x objective. Z-stacks spanned 10 μm of post-processing section width, with 2.0 μm spacing between Z-positions. Sections quantifying single labelling were quantified on an Olympus BX-51 microscope. Images were analyzed using Fiji software (Schindelin et al. 2012).

All statistical comparisons in this study were performed using an unpaired two-tailed t test. Differences were considered significant with a p value of < 0.05 (*), **$p< 0.01$, ***$p < 0.001$, ****$p<0.0001$. Unless otherwise stated, all data is presented as the arithmetic mean, plus or minus the standard deviation of the mean (mean ± SD). For each experiment, biological replicates of >3-5 animals per genotype were used.

Single Cell Collection and Fluorescence-activated cell sorting (FACS)

Hippocampal YFP+ cells were isolated as described in (Iqbal, Fong, and Slack 2022). YFP-positive cells were collected from 3 mice of each genotype after viability screening with propidium iodide staining (ThermoFisher, Cat. # P3566) on a Beckman Coulter MoFlo platform in the Flow Cytometry and Cell Sorting Facility located in the Ottawa Hospital Sprott Center (Ottawa, Canada). Freshly collected YFP-positive cells were sent to StemCore Laboratories located in the Ottawa Hospital Sprott Center, for both CT and Opa1 cKO samples. The transcriptome of viable single cells was analyzed using the 10x Genomics Chromium Single Cell Assay platform, individually for each genotype. A single cell RNA library was created following the single cell 3' Reagent Kits v2 user guide (Cat: CG0052, 10x Genomics) on the Chromium Single Cell Instrument (10x Genomics) using Single Cell 3' Library & Gel Bead Kit v2 and Chip Kit (P/N

120236 and P/N 120237, 10x Genomics). The cDNA library was then purified with SPRIselect (Beckman Coulter). Agilent Fragment Analyzer was used to evaluate the size distribution and yield (Agilent). The sequencing was performed on Illumina NextSeq 500 instrument (Illumina) using the following parameters 28 bp Read1, 8 bp I7 Index, 0 bp I5 Index, and 98 bp Read2. Single-end reads were aligned to the reference genome, mm10, using the CellRanger pipeline (10X Genomics), after demultiplexing cell barcodes and UMI (unique molecular identifiers) barcodes. The output cell-gene matrix contains UMI counts by genes and by cell barcodes. Gene expression profiles were then mapped using Seurat v3 (or latest) in R studio (Stuart et al., 2019).

Single Cell Selection and Clustering

Cells were filtered with following criteria for further analysis: 1) Cells with more than 600 genes recorded; 2) with less than 7500 genes recorded; 3) with mitochondria content less than 20% of total RNA counts; and 4) with detectable YFP expression. RNA reads were normalized with the function of sctransform "SCT". Based on normalized RNA reads, cells were clustered using the following parameters: 1) dims =1:8; and 2) resolution = 0.2. Ten cell clusters were identified based on normalized expression profiles of each cell. Based on the original RNA reads, cluster-specific markers were calculated with the function of FindAllMarkers. Differential expression between CT and Opa1 cKO for each cluster was analyzed with the function of FindMarkers. Heatmaps of cluster-specific genes were mapped on normalized data. FeaturePlot (Umap) and VlnPlot (violin plot) of specific genes were mapped on original RNA reads.

Cell clusters with characteristics of the neurogenic lineage were sub-grouped to show differential expression of selected genes. Activated NSC, TAP and Neurons were sub-grouped and reclustered using the following parameters: 1) dims =1:12; and 2) resolution = 0.1. Gene expression and RNA velocity data were generated in Seurat based on normalized data and analyzed in Python-based Spyder program using the "deterministic" mode (La Manno et al., 2018; Stuart et al., 2019).

FACS and RNA isolation

Isolation of YFP+ cell population from SVZ or SGZ were performed as previously described (Iqbal, Fong, Slack 2022), employing tissue micro-dissected from mice 30 days post-tamoxifen injection. The YFP+ cell population was FACS-isolated using a cutoff of 488-FL-Log-Height ≥ 102. For RNA-Seq input, cell pellets containing minimum 200,000 YFP+ cells were frozen, and RNA isolated using the Arcturus® PicoPure® RNA Isolation Kit (ThermoFisher). Isolated RNA was used for qPCR validation of knockout or differential gene expression.

Flow cytometry analysis.

Cells were incubated with MitoSOX Red (Molecular Probe) for 15 min followed by one wash with PBS before fluorescence measurements as previously described (Khacho et al. 2016). A FACS Caliber (BD) and Flowjo software were used for analysis.

qRT-PCR

Samples for RNA quantification were prepared using the Rotor-Gene SYBR® Green PCR Kit (Qiagen) and quantified on a Qiagen Rotor-Gene Q Real-Time PCR Machine. RNA concentrations for each primer set were normalized using standard curves prepared from wild-type adult NSCs as standard. Primers used are listed in Supplementary Table 3, and RNA quantifications are expressed relative to β-Actin (normalized to 1).

Plasmids and Lentiviral Vector production

Lentivirus vectors shRNA scramble control (shCtrl sequence;5'-CAACAAGATGAAGAGCACCAA-3'), and mouse specific shRNA to OPA1 (shOPA1 sequence; 5'-GCCTGACTTTATATGGGAAAT-3') were prepared using previously established protocols (Khacho 2016). For ATF4 manipulation, pLVX-scramble-mCherry lentiviral expression vector construct was commercially obtained (Clontech 631987) and used as control. shATF4 (5'-CCAGAGCATTCCTTTAGTTTA-3') to generate pLV-U6-[shAtf4]-mCherry were ordered from Vectorbuilder. ATF4 overexpression from Origene (MR205957) was cloned into the expression vector to generate a PLVX-E2F1a-Atf4-Myc-DDK-V5-IRES-mCherry. Lentiviruses were produced in 293T HEK cells using PEI transfection. The lentivirus was purified by ultracentrifugation, following established protocols (TANG et al., 2015), and was resuspended in PBS into small aliquots. Viruses with reporter were live titred using 293T cells. shCtrl and shOpa1 viruses were titred using p24 antigen using QuickTiter™ Lentivirus Titer Kit (VPK-107) For use in vitro, cells from embryonic cortex were transduced with lentiviral particles at a multiplicity of infection (MOI) of 15, before neurosphere differentiation after 5-7 days.

In Vitro neurosphere and monolayer Culture

Embryonic cortices were collected at Embryonic day 12-13 as previously described (Khacho et al. 2016). After removing meninges, the cortices were passed through 1ml pipette tip. The cell suspension was then filtered through 70um mesh filter. The obtained single cell suspension was treated with appropriate lentivirus for 2 hrs at 37C prior to seeding. DMEM/F12 (Gibco 11330-032) is supplemented with B27 without Vitamin A (Gibco 12587010), EGF (Sigma E-1257), bFGF (Sigma F-0291), heparin (Sigma H-3149) and Penicillin/Streptomycin (Gibco 1570-063) to encourage neurosphere formation. Neurospheres were collected after 5 days in culture. For hypoxia experiments, cells were placed in Biospherix X3 Xvivo System and incubated in 1% O2 levels; 5% CO2 and 80% Humidity.

ATP Assay

Cells from developing cortex from CT and Opa1 cKO were incubated in black wall optical bottom 96 well plate with or without 10μM Oligomycin. ATP concentrations were measured with the

CellTiter-Glo Luminescent Assay (Promega) using a BioTek Synergy H1 microplate reader according to manufacturer's protocol. Data were collected from multiple replicate wells for each experiment. The ATP concentrations were normalized to cell counts determined by trypan blue dye exclusion.

NAD measurement

NAD and NADH levels were measured using the NAD/NADH Quantitation Colorimetric Kit (BioVision). Neurospheres of different conditions were lysed using the lysis buffer provided by the supplier. Colorimetric reading was detected using Biotek Synergy H1 microplate reader.

Cellular Oxygen Consumption

The Seahorse XF24 Extracellular Flux Analyzer (Seahorse Biosciences) was used to measure oxygen consumption in cells. Cells derived from neurosphere cultures were seeded onto Cell Tak-coated (22.4 μg/ml) 24-well Seahorse plates at a density of 200,000 cells/well in 100 μl stem cell media (SCM) media supplemented with additional 0.5 mM sodium pyruvate. Plates were immediately spun at 200 × g for 1 min and allowed to stop without brakes and then placed at 37°C for 25 min. 500 μl SCM was slowly added to each well, followed by an additional incubation of 20 min at 37°C prior to loading into the XF Analyzer. Following measurements of resting respiration, cells were treated sequentially with oligomycin (1 μg/μl) to measure the nonphosphorylating OCR, FCCP (2 μM) to get the maximal OCR, and Antimycin A (1 μM) to measure the extramitochondrial OCR. Each measurement was taken over a 2-min interval followed by 2 min of mixing and 2 min of incubation. Three measurements were taken for the resting OCR: after oligomycin treatment, after FCCP, and after Antimycin A treatment.

Western Blot

Cell pellets of cultured neurospheres were washed with PBS and lysed with 4% SDS in PBS, samples were sheared by passing through a 26- gauge needle to denature DNA. Lysates were spun at high speed to remove particles. Primary antibodies were incubated for overnight at 4ºC. A secondary antibody conjugated to horseradish peroxidase (Jackson ImmunoResearch) was used and detected by Clarity™ Western ECL Substrate (BioRad). Chemiluminescence signal were captured in either radiograph films or Bio-Rad Chemidoc imaging system. Western blot bands were quantified using FIJI (Schneider et al., 2012).

In vitro cell staining:

Dissociated single cells with appropriate conditions were grown in 8 well multichamber slides (Thermo Fisher Scientific 154941PK). After the endpoint, the cells were washed with cold PBS and then fixed with 4% PFA for 20 minutes. Cells were then washed 3x10mins with PBS. The fixed cells were blocked with 5% BSA in PBS. Cells with primary antibodies were incubated for

overnight at 4ºC. A secondary fluorophore antibody with DAPI were incubated and imaged at Observer D1 fluorescent microscope.

ChIP

ChIP assays followed by quantitative real-time PCR (qPCR) were performed as previously described (Julian et al., 2016; Liu et al., 2010). 10 µg of 30 min cross-linked chromatin and 0.8 µg of antibodies were used in ChIP assays. Antibodies are listed in Supplementary Table 1, and qPCR primers are listed in Supplementary Table 4.

ChIP-seq analysis

ChIP-seq data on ATF4 binding sites in MEFs was performed by Randal J. Kaufman lab at Sanford Burnham Medical Research Institute (Han et al. 2013) under the Gene Expression Omnibus accession number GSE35681.

GSH and GSSG measurement by high-performance liquid chromatography

GSH and GSSG levels were determined by Agilent 1100 series HPLC system. Briefly the neurospheres were cultured in 100mm Petri dishes with the indicated conditions. Upon endpoint, they were collected and washed with ice-cold PBS. Cells were lysed on ice for 20 min in 1:1 homogenization buffer made of 125 mM sucrose, 1.5 mM EDTA, 5 mM Tris, 0.5% TFA, and 0.5% MPA in 50% mobile phase (10% HPLC grade methanol, 0.09% TFA – 0.2µm filtered). Homogenates were spun at 14.000 g for 20 min at 4 °C. Supernatant of each sample was collected and processed in duplicate using an Agilent HPLC system equipped with a Pursuit C18 column (150 ×4.6 mm, 5µm; Agilent Technologies) operating at a flow rate of 1ml/min and detected at 215nm. Standards of GSH and GSSG were made in the same 1:1 homogenization buffer at the indicated concentrations. All values were normalized to the protein amount in each sample.

Acknowledgements

We thank members of the Behaviour and physiology core, Cell biology and image acquisition core, Flow Cytometry and virometry core, Louise Pelletier Histology Core and Stemcore laboratories at the University of Ottawa. This work was supported by grants from the CIHR foundation grant to RSS and Mito2i fellowship to MAI.

Author contributions

Conceptualization and methods, M.A.I, B.C.F., I.C., S.P., ME.H., M.Khacho., and R.S.S.; investigation, M.A.I., V.J., B.C.F., M.B., I.C., Y.L., S.P., J.C., M.Kannan.,; resources, ME.H., and R.S.S.; writing, M.A.I., S.P., Y.L., I.C., and R.S.S.; review, all authors.

Chapter 4
General discussion

Thesis summary and major findings:

Multiple intrinsic factors converge to tightly coordinate and regulate every step of adult neurogenesis. The choice between quiescence or activation is a critical step in tissue homeostasis and regeneration. In this dissertation, two key mechanisms of NSC regulation were studied; the role of Rb-pocket protein pathway in the regulation of NSC quiescence in chapter 2; and how mitochondrial dynamics regulates stem cell function, survival, and stress response in chapter 3. Together, these studies provide a better understanding of NSC regulation giving insights into aging, neurodegenerative disease pathology and aspects of therapeutic strategies. The results from these studies support several key conclusions:

Rb family proteins and its expanding role in stem cell quiescence

Findings from our laboratory as well as others suggest a functional compensation amongst the Rb family proteins in regulating proliferation of NSCs (Jaafar et al. 2016; Vandenbosch et al. 2016). The loss of a single protein of the Rb family yields a subtle phenotype in NSC expansion but does not impact its quiescence. p107 regulates NSC self-renewal and neuronal commitment through Notch signaling. Loss of p107 results in expansion of NSCs and reduced neuronal differentiation mediated by elevated Hes1 (Vanderluit et al. 2004; Vanderluit et al. 2007). Previous to this finding, the role of Rb in NSC cycle regulation and survival through cell cycle exit in newborn neurons during development and in the adult hippocampus was established. Loss of Rb in the developing cortex resulted in unregulated cell proliferation and expansion (Ferguson et al. 2005; Ferguson et al. 2002), which prevents new neurons from exiting the cell cycle resulting in

cell death instead of proceeding towards maturation in the adult hippocampus (Vandenbosch et al. 2016).

The finding that the collective deletion of Rb family (Rb-TKO) results in loss of quiescence leading to NSC exhaustion in the adult V-SVZ and SGZ stem cell niche is described in Chapter 2. Histological examination indicate that the Rb family of proteins such as pRb, p107 and p130 have overlapping function and collective loss leads to massive stem cell expansion followed by exhaustion. Ectopic proliferation of uncommited neuroblasts suggest a conserved regulatory role for the Rb family in the cell cycle. The role of the Rb family in long-term maintenance of NSCs through quiescence has been established in other models where the loss of the Rb family results in ectopic proliferation (Jiang et al. 2010; Sage et al. 2000; Viatour et al. 2008). Alternatively, inactivation through Rb mutation promotes reprogramming of differentiated cells to a pluripotent state indicating a cell cycle-independent function (Kareta et al. 2015). Recently, pRb deletion was shown to impact olfactory neurogenesis affecting neuronal maturation in an age-specific manner, suggesting that Rb plays an important role in survival of adult-born neuroblasts in mid- and old-age mice (Omais et al. 2022). Collectively, findings by others and the results obtained from studies in chapter 2 indicate the involvement of the Rb family in quiescence and activation of NSCs.

Since E2Fs has been well established as the target of Rb family, the function of activator E2Fs was observed using E2F1/3 double-knockout mice. Histological analysis of thse mice showed decrease in NSC proliferation, activation, and differentiation. These results reinforce the role of Rb/E2F axis, particularly, the requirement for activator E2F1/3 in regulating NSC activation and neurogenesis. An earlier loss-of-E2F1 study showed that activator E2F1 regulates adult V-SVZ and SGZ NSC proliferation and cell death, suggesting the importance of E2F1 in NSC activation and cell death regulation for generation of adult-born granule cells (Cooper-Kuhn

et al. 2002). Previously, our laboratory showed the opposing effect of E2F3a and 3b isoforms in regulating Sox2 gene expression in the context of embryonic cortical development (Julian et al. 2013). Together, these findings and studies described in Chapter 2 demonstrate that the activator E2F1/3 regulates NSC activation and transcriptional regulation of neurogenesis progression.

Contrasting findings in the regulation of RB and E2F in NSC regulation

Transcriptome signature of pocket proteins knockout suggests a NSC activation-like phenotype, which includes upregulation of cell cycle genes, Shh, Wnt signaling, Jak2 pathways, and downregulation of NSC quiescence signature genes including *Aqp4*, *Id3*, *Pdgfrb*, *Aldoc*, *Fgfr3* and *Dbi*. Conversely, E2F1/3 knockout upregulated *Aqp4*, *Id3*, *Pdgfrb*, *Aldoc*, *Fgfr3* and *Dbi* and decrease in activation signature such as *Ezh2* and *PCNA*. Taken together, transcriptional analysis demonstrated the critical regulation of Rb family and activator E2F targets two opposing stands on NSC regulation. Thus, this study highlights a previously unknown mechanism of quiescence and activation regulated by polarizing interactions of Rb and E2Fs.

Both, pocket proteins knockout and E2Fs knockout, downregulated differentiation genes such as Sox4 and Sox11, which indicated that either aberrant activation or enhanced quiescence impairs neuronal differentiation. As demonstrated earlier and given the role of Rb/E2F axis in the regulation of quiescence, involvement of others mediators was explored. Among these, REST, a transcriptional repressor mediates a dichotomous role in NSC quiescence and progenitor proliferation (Mukherjee et al. 2016), and correspondingly loss of either Rb family or E2F1/3, dysregulated several REST targets. Previous studies using transcriptomic analysis showed downregulation of several proneural targets with REST binding sites (Bergsland et al. 2006; Lepagnol-Bestel et al. 2009), such as Dcx, Sox4 and Sox11 that are downregulated in Rb-TKO and E2F1/3-DKO. Given the evidence, REST-mediated repression of proneural genes was

observed in Rb-TKO (triple knockout) and E2F1/3-DKO (double knockout), indicating the involvement of REST in both the models.

REST as a common target of RB/E2F axis

The enrichment of REST signatures in Rb-TKO and E2F1/3-DKO indicate the recruitment of REST in both pathways. Given that Rb-TKO and E2F1/3-DKO generate contrasting transcriptome profile in regulation of quiescence and activation, the common involvement of REST and its targets may appear contrary. Loss of Rb family or E2F1/3 increases REST and the downregulation of proneural transition genes *Dcx*, *Sox4* and *Sox11* that have RE1-binding site (Bergsland et al. 2006; Lepagnol-Bestel et al. 2009). The typical signature of induced quiescence and impaired activation of NSC in E2F1/3-DKO can be explained by the involvement of REST-mediated repression of proneural transition-like quiescence signature seen in previous studies (Gao et al. 2011; Mukherjee et al. 2016). Repressive role of activator E2Fs are uncommon. In an earlier study, activator E2Fs have been shown to act in context-specific roles as repressors during cell differentiation in the small intestine (Chong et al. 2009). Similarly, a further increase in REST target gene repression in E2F1/3-DKO when compared to Rb-TKO was observed in the current study. Combining transcriptome analysis of ChIP data together, direct binding of p107, p130, E2F3 and E2F4 at the regulatory sites of REST gene in adult NSCs was demonstrated in the current study giving rise to the speculation that activator E2Fs recruit pocket proteins such as p107 and 130 to repress REST function in adult NSCs.

Loss of quiescence and aberrant NSC expansion in the Rb-TKO mediated increased cell death marked by AC3, which may be attributed to aberrant fate decision. The expansion of Sox2+ and Dcx+ population in the SGZ at 4 weeks, which was depleted at 8 weeks post-TAM timepoint is evidence of cell death. Increased REST levels in the Rb-TKO with persistant higher expression

throughout differentiation seen in the *in vitro* studies may indicate the regulation of neuronal differentiation by Rb family through the RE1 silencing function of REST. In accordance, upregulation of REST higher mRNA in human medulloblastoma increased stemness and decreased differentiation providing advantage in tumorigenicity (Conti et al. 2012; Su et al. 2006). Rescuing NSC function by suppression of REST function following the loss of Rb family was explored by blocking REST in NSCs *in vivo* 14 days post-virus injection and tested *in vitro* for 3 days of differentiation.

Rb/E2F axis regulate ASCL1 directly and through REST

The expansion of NSC activation and induction of Ascl1+ NSCs in the SGZ was described in Chapter 3. The question was if there were direct interaction of pocket proteins and E2Fs at the regulatory site of ASCL1. Indeed, a direct interaction of p107/p130 and E2F3/E2F4 at ASCL1 gene regulatory site was revealed by ChIP data indicating a repression of ASCL1 through this interaction. From *in vitro* studies, suppression of REST through dominent-negative (dn)REST resulted in robust increase in ASCL1 and Sox 11 levels, which is consistent with pervious studies on REST transcriptional regulation of SoxB family of proteins (Bergsland et al. 2006). These findings explain the increase in *in vitro* levels of ASCL1 in Rb-TKO with dnREST lentivirus transduction. These results corroborate with earlier studies showing high levels of REST are needed to maintain quiescence of qNSCs, and reduction in REST level accompanies NSC activation, which is complemented by higher ASCL1 levels (Gao et al. 2011). Collectively, a novel direct transcriptional regulation of REST and ASCL1 was identified in the current study.

Furthermore, the repression of REST-mediated regulation in Rb-TKO increased survival of ASCL1+ cells in the adult SGZ. Inhibition of REST using dnREST partially rescued the depletion of adult NSCs in Rb-TKO 14 days after the dnREST injection, compared to mcherry lentivirus

injected control animals. Collectively, a mechanism whereby the Rb/E2F axis directly and indirectly regulates NSC fate decisions through REST was identified in this study.

Requirement for Opa1 in cognitive function

Recently, the central role of mitochondrial dynamics in maintaining optimal mitochondrial function has emerged as an important regulator of stem cell function (Baker et al. 2022; Iwata, Casimir, and Vanderhaeghen 2020; Khacho et al. 2016). Our laboratory and others have shown that loss of Opa1 results in imbalanced mitochondrial dynamics disrupting mitochondrial function (Anand et al. 2014; Baker et al. 2022; Kane et al. 2017; Khacho et al. 2016; Patten et al. 2021; Patten et al. 2014). From results described in Chapter 3, several important conclusions can be made. Namely, mitochondrial dynamics is important to maintain adult NSC state and disruption induced by Opa1 deficiency impairs learning and memory. Our laboratory has previously demonstrated that loss of mitochondrial function impacts long-term NSC maintenance and neuronal differentiation implying that mitochondrial function and dynamics play a crucial role in adult NSC function (Khacho et al. 2016; Khacho et al. 2017).

Adult newborn neurons provide cognitive flexibility that is quantifiable through memory recalling tasks (Anacker and Hen 2017). Though the role of newborn neurons in the DG is not fully understood, they are thought to be important for hippocampal plasticity by acting as novel encoding units that provide feedback inhibition, thereby decreasing interference in overlapping context (Anacker and Hen 2017; Johnston et al. 2016; McAvoy, Besnard, and Sahay 2015; Tuncdemir, Lacefield, and Hen 2019). Opa1- deficient mice exhibit a freezing behavior indicating a deficit in memory recall that is further corroborated by decline in Dcx+ neuroblasts suggesting a possible disruption of information encoded through adult-generated granule cells in the hippocampus (Kee et al. 2007). Cognitive learning processes include context encoding and context

conditioning (Maren, Phan, and Liberzon 2013) and contextual learning deficits are attributed to aging-associated decline in neurogenesis. Given such importance, promoting neurogenesis through overexpression of cell cycle regulators (Cdk4/CyclinD1) rescues aging related defects in memory consolidation (Berdugo-Vega et al. 2020). Previous findings of age-related decline of Dcx+ neuroblasts and ensuing memory deficits support observations made in the Opa1 cKO mice in the current study, which showed impaired contextual learning with loss of Opa1. Maintaining adult neurogenesis throughout life is important to preserve hippocampus-associated memory consolidation and aging, indicating a central role for Opa1 in rodent cognitive functions, warranting the need to further characterize Opa1 in NSC function.

Loss of Opa1 has early impacts in NSC function

The finding that Opa1 deficiency-mediated mitochondrial dysfunction impacts early stages of NSC progression that persists throughout neurogenesis was demonstrated in Chapter 3. The histological assessment of impaired NSC proliferation indicates the requirement for Opa1 in proliferation and activation of stem cells, and thereby their function. The reduction in NSC proliferation, diminished progenitor pool and neuroblasts due to loss of Opa1 suggest an impairment in stem cell progression, resulting in NSCs that remain dormant at the expense of activation. The expression profile of the activation marker, Ascl1, in combination with EdU retention in HopX+ cells imply an induced quiescence, collectively indicating an impairment in NSC function that has early impacts due to mitochondrial dysfunction.

This quiescent phenotype of Opa1-deficient NSCs is supported by bulk RNAseq data generated from adult V-SVZ 10 days post-TAM injection. The decrease in key mitochondrial complex genes such as *mt-Nd1/4/5/6*, *mt-Co1/2/3*, *mt-Cytb*, and *mt-Atp6*T in Opa1-deficient NSCs indicate mitochondrial dysfunction, compounded by decreased expression of neurogenesis genes

Dcx, *Nrg1*, and *Prox1*, as well as early expression of quiescence-related signature genes such as *Notch 3*, *Hey1*, *Scd1* and *Mgll*, seen 10 days after Opa1 knockout (Harada et al. 2021; Rieskamp, Denninger, and Dause 2018; Hamilton et al. 2022). Overall, these results indicate that Opa1-deficient NSCs enter dormancy and quiescence and are unable to get activated.

Moreover, sc-RNAseq captured NSCs in transition to different stages of adult hippocampal neurogenesis, confirming a defect in neurogenesis in all clusters of Opa1 cKO but more prominent in impaired differentiation. The observation of increase in *ID4* in resident NSC cluster, a quiescent related gene may indicate an observed reduction of ASCL1+ cells in DG of Opa1cKO mice (Blomfield et al. 2019), These results demonstrated that these findings in combination with bulk RNAseq and histological observations validate the role of Opa1 in NSC quiescence. The gene regulation changes identified in Opa1 cKO signify the importance of mitochondrial dynamics in broad transcriptional regulation of NSC proliferation, activation, and differentiation, which highlights mitochondrial function as a key modulator of neurogenesis among other regulators of adult neurogenesis. While an ever-increasing reliance on mitochondrial metabolism during neurogenesis has been well characterized (Beckervordersandforth et al. 2017; Khacho et al. 2016; Shin et al. 2015), the present findings emphasize the requirement for Opa1 in stem cell activation during early neurogenesiss. Without Opa1, stem cell activation is impaired impacting any further stem cell functions.

Results from other stem cell models do not corroborate the quiescence in NSCs observed following loss of Opa1. For instance, Baker et al described that Opa1 maintains quiescence in muscle stem cells (muSC). Loss of Opa1 results in an increase in activation and commitment by msSC depletion (Baker et al. 2022). The authors elaborate that four days after Opa1 knockout, Pax7+ muSC showed increase in proliferation, increase in activation (MyoD+ cells) and cell

commitment (MyoG+). However, Baker et al. (2022) induced cardiotoxin (Ctx)-mediated injury that triggered regeneration in muSC, which primed stem cells to expand and repopulate injury sites. As well, ischemic brain injury could lead to stem cell activation at the expense of quiescence (Llorens-Bobadilla et al. 2015). Thus, the bias in muSC towards activation following loss of Opa1 may be due to direct stimulation by injury, or alteration of cell fate decisions due to immune invasion and inflammation, or inherent differences between NSC and muSC in the proximity to blood that could influence fate decisions through excessive growth factors availability. Interestingly, uninjured and chronic Opa1 knockout animals did not show any loss in the Pax7+ muSC pool after 3 months whereas their injured muscle fibers showed a dramatic loss of muSC and a significant decrease in cell proliferation *in vitro*. These findings are in agreement with the defects observed in DG-NSC in the current study where a steady state decline in the NSC pool after two months of following Opa1 knockout resulted in proliferation defects.

Oxidative stress as a primary effect of Opa1 loss-induced mitochondrial dysfunction.

The investigation into mitochondrial dynamics disruption leading to dysfunction phenotype in NSCs conflates several distinct cellular and molecular outcomes. Results from NSCs of embryonic and adult origin indicate that mitochondrial defects precede observable stem cell defect both *in vitro* and *in vivo*. Mitochondrial dysfunction phenotype was observed in the adult V-SVZ 10 days post-TAM but SGZ did not reveal any cell loss at similar timepoints indicating that mitochondrial dysfunction accumulates and results in later appearance of cellular phenotype. The observed mitochondrial defect impacts cellular respiration, Complex I function, ATP generation and promotes mitochondrial ROS. Particularly, defects in ROS scavenging along with impaired oxidative metabolism inhibit stem cell expansion and differentiation. Complex I and III are the two major sites of electron leak, which contributes to ROS generation in mitochondria

(Murphy 2009; Wong et al. 2017). Mitochondrial mutagenesis through inactivation of mitochondrial replicative DNA polymerase gamma (Polg) results in accumulation of mutations in mitochondrial ETC core proteins. NSCs in this mutator mice show dysfunction *in vivo* and *in vitro*. ROS scavengers such as NAC rescues self-renewal capacity (Ahlqvist et al. 2012), which implies that mitochondrial dysfunction-induced oxidative stress underlies the stem cell dysfunction phenotype, which can be rescued by ROS scavenging. Mitochondrial ROS levels alter fate decisions in several stem cell pools; reviewed here (Tan and Suda 2018) and physiological variations in ROS level alters cellular state. It has been shown that HSCs with low levels of basal ROS have the highest level of self-renewal capacity. ROS levels are moderately elevated during proliferation, commitment, and proliferation (Jang and Sharkis 2007; Tan and Suda 2018). Variations in ROS levels exert ROS defense through the FoxO family of transcription factors (Ito and Suda 2014). Loss of FoxO 1/2/3-mediated ROS elevation increased cell proliferation and brain size at the expense of self-renewal in adult NSCs (Paik et al. 2009; Renault et al. 2009). Thus, previous findings showing that ROS concentration-mediated transcriptional regulation of NSC fate is linked to ROS defense and from findings of the current study demonstrate that excessive ROS accumulation in stem cells can affect quiescence and induce cell death (Tan and Suda 2018). Though mild elevation in cellular ROS levels increases NSC proliferation (Le Belle et al. 2011), the long-term effect on self-renewal capacity and chronic oxidative stress effect remains elusive. The balance between ROS generation and antioxidant defense decides the level of oxidative stress. In the adult DG, ROS concentrations range from low to high in NSCs which is shown to be higher than NSCs in V-SVZ (Adusumilli et al. 2021). The NSC fraction with high ROS levels has a distinct molecular profile, which corresponds to HopX+ qNSC described by Berg et al (Adusumilli et al. 2021; Berg et al. 2019). However, an increase in ROS levels beyond physiological levels

could have detrimental effect on NSC self-renewal. Thus, evidence from the current study shows manifestation of mitochondrial dysfunction that is augmented by excessive mitochondrial ROS and defects in cellular energetics. Impairments in key blocks of these complexes in all tested models indicate elevation in ROS and oxidative stress, the latter being considered a key factor in disease manifestations of several neurological conditions.

Benefits of ROS mitigation through low oxygen exposure in stem cell function

An hypoxic environment insulates living systems from oxidative stress by modulating the dependency of OXPHOS and reducing the accumulation of ROS in NSCs (Mohyeldin, Garzon-Muvdi, and Quinones-Hinojosa 2010). ROS scavenging mitigates oxidative stress in NSCs and rescues proliferation defect (Khacho et al. 2016). Hypoxia also modulates oxidative stress through redox-sensitive pathways. This idea has been explored as a therapeutic strategy for Leigh syndrome, a neurological condition of mitochondrial disease (Jain et al. 2016). Since NSC impairment is considered a root cause of neurodegenerative diseases, improving NSC function through exposure to hypoxia was explored. Indeed, NSC proliferation, survival and activation were rescued under hypoxia in the current study, suggesting that oxidative stress leads to stem cell dysfunction. Hypoxia rescued key stem cell activation proteins, ASCL1 and cell cycle genes and cell death, which were perhaps mediated by the direct effect of reduced oxygen levels to decrease in ROS levels and reduce oxidative stress. Alternatively, hypoxia-induced signaling (predominantly through hypoxia-inducible factor; HIF1α) may also be a reason since hypoxia-stabilized HIF1α was shown to enhance metabolic reprogramming of glycolysis through transcriptional upregulation (Guimaraes-Camboa et al. 2015). HIF1α-mediated metabolic change offers an advantage to certain cancer cells that are grown under nutrient-limiting conditions (Eales, Hollinshead, and Tennant 2016). Moreover, hypoxia independent of HIF1α affects NSC survival

by blocking caspase-dependent cell death pathway, suggesting an inherent role for hypoxia in defining stem cell fate preservation (Clarke and van der Kooy 2009).

This study also uncovered a mechanism by which NSC and its lineages cope with excessive mitochondrial fragmentation and dysfunction induced by loss of Opa1. The function of ISR in NSCs identified in the current study is unique and adaptive to the underlying mitochondrial defects, which indicates that the upregulation of the stress signature in mitochondrial dysfunction can be partially resolved under hypoxic conditions. Stress resolved under hypoxia is indicated by reduction in the expression of *ATF4* and its target genes. Some models show direct regulation by HIF1α on *ATF4* repression (Guimaraes-Camboa et al. 2015), warranting the need to further characterize the role of ATF4 in metabolic sensing and rewiring in NSCs.

ISR activation due to loss of Opa1-induced mitochondrial dysfunction

Induction of ATF4 affects a series of downstream targets in both basal and stressed conditions. Interestingly, however, the cellular state dictates the dichotomous function of ATF4. At basal levels without any stress, upregulation of cellular ATF4 leads to cell growth and proliferation but under stress, ATF4 improves survival. Thus, ATF4 in control condition increases cell proliferation through its targets that mimics a growth signal and leads to an anabolic program (Torrence et al. 2021). However, the lack of key metabolic factors in mitochondrial dysfunction causes activated ATF4 to mediate a stress response that sustains life.

ATF4 function is represented by one of its downstream targets, Slc7a11, which under basal condition, plays a crucial role in adult hippocampal neurogenesis. This can be speculated by the benefits of amino acid acquisition from the adult tissue niche. Mutational loss of Slc7a11 function leads to brain atrophy and reduced astrocyte proliferation and survival (Shih et al. 2006). Under

stress conditions, such as oxidative stress, ATF4-induced Slc7a11 is essential for transport of cysteine, which is necessary for glutathione production. The findings of the current study show that glutathione production is significantly enhanced by ATF4 through Slc7a11 to mediate stress responses.

The major conclusion of the current study is that loss of Opa1 alters the course of NSC progression by impairing proliferation and neurogenesis, confirming the essential role of mitochondrial function. Loss of Opa1 allows stem cells to adapt stress and survival through ATF4 and ISR by improving ROS defense.

The limitations and future directions of this study

There are several limitations in this study that could be addressed in future studies. NSC is an umbrella term for heterogeneous stem cells that originate from different niches with unique features that are currently under investigation. The parallel mechanisms of pocket proteins (pRb, p107, p130), activator E2Fs (E2F1 & E2F3), and Opa1 that have an effect on adult neurogenesis is a dynamic process of real time cross talk among several pathways that remains a challenge to decipher. Despite minimal handling of bulk RNAseq *in vitro* to characterize heterogenous NSCs from their niche, they may not fully depict the *in vivo* phenotype. For instance, key regulators such as Ascl1 that play functional and essential roles in NSCs exhibit oscillating gene expression, and the gene expression studied only reflects its status at cell harvest.

Due to scalability issues, bulk RNAseq was performed using NSCs in the V-SVZ niche to understand the function of pocket proteins and E2Fs, whereas histological characterization was predominantly performed on the SGZ. Though ample information distinguishes these two niches with their innate functions, sc-RNAseq may have been a better comparison since it provides a

glimpse into the heterogeneity of different clusters, which bulk RNAseq does not provide. The resolution of data is limited by the shallow number of readable transcripts originating from individual cells. Currently, the read depth is limited and only a fraction of whole cell transcripts results in high confidence prediction that is restricted to highly abundant genes.

Hypoxia-related benefits were prominent in limited experiments in this study and would therefore be gained from future investigations on transcriptomic and metabolomic analysis. Omics data offer advantages to understand the role of unfolded protein underlying the rescue experiments that were executed. Since ATF4 has numerous targets and coactivators (Han et al. 2013), bulk RNAseq may offer a better alternative to better understand ATF4 regulation. Since understanding the role of ATF4 in global translation, tRNA aminoacylation, and the mTORC pathway may require additional conditions, RNAseq may be a better tool to examine the involvement of ATF4 in executing stress response during mitochondrial dysfunction. Neurogenesis is a shared process across all the mammals and much advancements were made in murine models yet the controversial involvement in humans put a limitation in the application in human diseases. Lastly, due to the nature of preclinical models used in these studies, the molecular pathways and genes examined must be cautiously extrapolated to human diseases.

Conclusion

Regulation of adult neurogenesis is a complex process. In this dissertation, several experimental models were used to demonstrate mechanisms underlying quiescence and activation that regulate adult neurogenesis. The Rb/E2F pathway was demonstrated to regulate quiescence and activation through REST and its target, ASCL1. Secondly, loss of Opa1 altered the course of NSC progression by impairing proliferation and neurogenesis confirming the essential role of mitochondrial function. Mitochondrial dynamics regulates NSC function and loss of Opa1 resulted

in mitochondrial dysfunction leading to impaired neurogenesis and deficits in learning and memory. Mitochondrial dysfunction triggered NSCs to adapt through ATF4 and ISR by enhancing cellular ROS defense mechanisms, in part, through Slc7a11.

References

Adusumilli, V. S., T. L. Walker, R. W. Overall, G. M. Klatt, S. A. Zeidan, S. Zocher, D. G. Kirova, K. Ntitsias, T. J. Fischer, A. M. Sykes, S. Reinhardt, A. Dahl, J. Mansfeld, A. E. Runker, and G. Kempermann. 2021. 'ROS Dynamics Delineate Functional States of Hippocampal Neural Stem Cells and Link to Their Activity-Dependent Exit from Quiescence', *Cell Stem Cell*, 28: 300-14 e6.

Agathocleous, M., N. K. Love, O. Randlett, J. J. Harris, J. Liu, A. J. Murray, and W. A. Harris. 2012. 'Metabolic differentiation in the embryonic retina', *Nat Cell Biol*, 14: 859-64.

Ahlqvist, K. J., R. H. Hamalainen, S. Yatsuga, M. Uutela, M. Terzioglu, A. Gotz, S. Forsstrom, P. Salven, A. Angers-Loustau, O. H. Kopra, H. Tyynismaa, N. G. Larsson, K. Wartiovaara, T. Prolla, A. Trifunovic, and A. Suomalainen. 2012. 'Somatic progenitor cell vulnerability to mitochondrial DNA mutagenesis underlies progeroid phenotypes in Polg mutator mice', *Cell Metab*, 15: 100-9.

Ahola, S., P. Rivera Mejias, S. Hermans, S. Chandragiri, P. Giavalisco, H. Nolte, and T. Langer. 2022. 'OMA1-mediated integrated stress response protects against ferroptosis in mitochondrial cardiomyopathy', *Cell Metab*, 34: 1875-91 e7.

Aime, P., X. Sun, N. Zareen, A. Rao, Z. Berman, L. Volpicelli-Daley, P. Bernd, J. F. Crary, O. A. Levy, and L. A. Greene. 2015. 'Trib3 Is Elevated in Parkinson's Disease and Mediates Death in Parkinson's Disease Models', *J Neurosci*, 35: 10731-49.

Akers, K. G., A. Martinez-Canabal, L. Restivo, A. P. Yiu, A. De Cristofaro, H. L. Hsiang, A. L. Wheeler, A. Guskjolen, Y. Niibori, H. Shoji, K. Ohira, B. A. Richards, T. Miyakawa, S. A. Josselyn, and P. W. Frankland. 2014. 'Hippocampal neurogenesis regulates forgetting during adulthood and infancy', *Science*, 344: 598-602.

Alavi, M. V., and N. Fuhrmann. 2013. 'Dominant optic atrophy, OPA1, and mitochondrial quality control: understanding mitochondrial network dynamics', *Mol Neurodegener*, 8: 32.

Alexander, C., M. Votruba, U. E. Pesch, D. L. Thiselton, S. Mayer, A. Moore, M. Rodriguez, U. Kellner, B. Leo-Kottler, G. Auburger, S. S. Bhattacharya, and B. Wissinger. 2000. 'OPA1, encoding a dynamin-related GTPase, is mutated in autosomal dominant optic atrophy linked to chromosome 3q28', *Nat Genet*, 26: 211-5.

Alvarez-Buylla, A., and S. Temple. 1998. 'Stem cells in the developing and adult nervous system', *J Neurobiol*, 36: 105-10.

Anacker, C., and R. Hen. 2017. 'Adult hippocampal neurogenesis and cognitive flexibility - linking memory and mood', *Nat Rev Neurosci*, 18: 335-46.

Anand, R., T. Wai, M. J. Baker, N. Kladt, A. C. Schauss, E. Rugarli, and T. Langer. 2014. 'The i-AAA protease YME1L and OMA1 cleave OPA1 to balance mitochondrial fusion and fission', *J Cell Biol*, 204: 919-29.

Andersen, J., N. Urban, A. Achimastou, A. Ito, M. Simic, K. Ullom, B. Martynoga, M. Lebel, C. Goritz, J. Frisen, M. Nakafuku, and F. Guillemot. 2014. 'A transcriptional mechanism integrating inputs from extracellular signals to activate hippocampal stem cells', *Neuron*, 83: 1085-97.

Andrusiak, M. G., K. A. McClellan, D. Dugal-Tessier, L. M. Julian, S. P. Rodrigues, D. S. Park, T. E. Kennedy, and R. S. Slack. 2011. 'Rb/E2F regulates expression of neogenin during neuronal migration', *Mol Cell Biol*, 31: 238-47.

Arnold, S. J., G. J. Huang, A. F. Cheung, T. Era, S. Nishikawa, E. K. Bikoff, Z. Molnar, E. J. Robertson, and M. Groszer. 2008. 'The T-box transcription factor Eomes/Tbr2 regulates neurogenesis in the cortical subventricular zone', *Genes Dev*, 22: 2479-84.

Artegiani, B., A. Lyubimova, M. Muraro, J. H. van Es, A. van Oudenaarden, and H. Clevers. 2017. 'A Single-Cell RNA Sequencing Study Reveals Cellular and Molecular Dynamics of the Hippocampal Neurogenic Niche', *Cell Rep*, 21: 3271-84.

Arvidsson, A., T. Collin, D. Kirik, Z. Kokaia, and O. Lindvall. 2002. 'Neuronal replacement from endogenous precursors in the adult brain after stroke', *Nat Med*, 8: 963-70.

Atkin, J. D., M. A. Farg, A. K. Walker, C. McLean, D. Tomas, and M. K. Horne. 2008. 'Endoplasmic reticulum stress and induction of the unfolded protein response in human sporadic amyotrophic lateral sclerosis', *Neurobiol Dis*, 30: 400-07.

Babu, H., J. H. Claasen, S. Kannan, A. E. Runker, T. Palmer, and G. Kempermann. 2011. 'A protocol for isolation and enriched monolayer cultivation of neural precursor cells from mouse dentate gyrus', *Front Neurosci*, 5: 89.

Baker, N., S. Wade, M. Triolo, J. Girgis, D. Chwastek, S. Larrigan, P. Feige, R. Fujita, C. Crist, M. A. Rudnicki, Y. Burelle, and M. Khacho. 2022. 'The mitochondrial protein OPA1 regulates the quiescent state of adult muscle stem cells', *Cell Stem Cell*, 29: 1315-32 e9.

Bartesaghi, S., V. Graziano, S. Galavotti, N. V. Henriquez, J. Betts, J. Saxena, V. Minieri, D. A, A. Karlsson, L. M. Martins, M. Capasso, P. Nicotera, S. Brandner, V. De Laurenzi, and P. Salomoni. 2015. 'Inhibition of oxidative metabolism leads to p53 genetic inactivation and transformation in neural stem cells', *Proc Natl Acad Sci U S A*, 112: 1059-64.

Basak, O., T. G. Krieger, M. J. Muraro, K. Wiebrands, D. E. Stange, J. Frias-Aldeguer, N. C. Rivron, M. van de Wetering, J. H. van Es, A. van Oudenaarden, B. D. Simons, and H. Clevers. 2018. 'Troy+ brain stem cells cycle through quiescence and regulate their number by sensing niche occupancy', *Proc Natl Acad Sci U S A*, 115: E610-E19.

Batista-Brito, R., J. Close, R. Machold, and G. Fishell. 2008. 'The distinct temporal origins of olfactory bulb interneuron subtypes', *J Neurosci*, 28: 3966-75.

Baur, K., Y. Abdullah, C. Mandl, G. Holzl-Wenig, Y. Shi, U. Edelkraut, P. Khatri, A. M. Hagenston, M. Irmler, J. Beckers, and F. Ciccolini. 2022. 'A novel stem cell type at the basal side of the subventricular zone maintains adult neurogenesis', *EMBO Rep*, 23: e54078.

Becht, E., L. McInnes, J. Healy, C. A. Dutertre, I. W. H. Kwok, L. G. Ng, F. Ginhoux, and E. W. Newell. 2018. 'Dimensionality reduction for visualizing single-cell data using UMAP', *Nat Biotechnol*.

Beckervordersandforth, R., B. Ebert, I. Schaffner, J. Moss, C. Fiebig, J. Shin, D. L. Moore, L. Ghosh, M. F. Trinchero, C. Stockburger, K. Friedland, K. Steib, J. von Wittgenstein, S. Keiner, C. Redecker, S. M. Holter, W. Xiang, W. Wurst, R. Jagasia, A. F. Schinder, G. L. Ming, N. Toni, S. Jessberger, H. Song, and D. C. Lie. 2017. 'Role of Mitochondrial Metabolism in the Control of Early Lineage Progression and Aging Phenotypes in Adult Hippocampal Neurogenesis', *Neuron*, 93: 1518.

Beckervordersandforth, R., P. Tripathi, J. Ninkovic, E. Bayam, A. Lepier, B. Stempfhuber, F. Kirchhoff, J. Hirrlinger, A. Haslinger, D. C. Lie, J. Beckers, B. Yoder, M. Irmler, and M. Gotz. 2010. 'In vivo fate mapping and expression analysis reveals molecular hallmarks of prospectively isolated adult neural stem cells', *Cell Stem Cell*, 7: 744-58.

Belvindrah, R., D. Graus-Porta, S. Goebbels, K. A. Nave, and U. Muller. 2007. 'Beta1 integrins in radial glia but not in migrating neurons are essential for the formation of cell layers in the cerebral cortex', *J Neurosci*, 27: 13854-65.

Berdugo-Vega, G., G. Arias-Gil, A. Lopez-Fernandez, B. Artegiani, J. M. Wasielewska, C. C. Lee, M. T. Lippert, G. Kempermann, K. Takagaki, and F. Calegari. 2020. 'Increasing neurogenesis refines hippocampal activity rejuvenating navigational learning strategies and contextual memory throughout life', *Nat Commun*, 11: 135.

Berg, D. A., Y. Su, D. Jimenez-Cyrus, A. Patel, N. Huang, D. Morizet, S. Lee, R. Shah, F. R. Ringeling, R. Jain, J. A. Epstein, Q. F. Wu, S. Canzar, G. L. Ming, H. Song, and A. M. Bond. 2019. 'A Common Embryonic Origin of Stem Cells Drives Developmental and Adult Neurogenesis', *Cell*, 177: 654-68 e15.

Bergen, V., R. A. Soldatov, P. V. Kharchenko, and F. J. Theis. 2021. 'RNA velocity-current challenges and future perspectives', *Mol Syst Biol*, 17: e10282.

Bergsland, M., M. Werme, M. Malewicz, T. Perlmann, and J. Muhr. 2006. 'The establishment of neuronal properties is controlled by Sox4 and Sox11', *Genes Dev*, 20: 3475-86.

Blomfield, I. M., B. Rocamonde, M. D. M. Masdeu, E. Mulugeta, S. Vaga, D. L. van den Berg, E. Huillard, F. Guillemot, and N. Urban. 2019. 'Id4 promotes the elimination of the pro-activation factor Ascl1 to maintain quiescence of adult hippocampal stem cells', *Elife*, 8.

Bond, A. M., G. L. Ming, and H. Song. 2015. 'Adult Mammalian Neural Stem Cells and Neurogenesis: Five Decades Later', *Cell Stem Cell*, 17: 385-95.

Borrett, M. J., B. T. Innes, D. Jeong, N. Tahmasian, M. A. Storer, G. D. Bader, D. R. Kaplan, and F. D. Miller. 2020. 'Single-Cell Profiling Shows Murine Forebrain Neural Stem Cells Reacquire a Developmental State when Activated for Adult Neurogenesis', *Cell Rep*, 32: 108022.

Bottes, S., B. N. Jaeger, G. A. Pilz, D. J. Jorg, J. D. Cole, M. Kruse, L. Harris, V. I. Korobeynyk, I. Mallona, F. Helmchen, F. Guillemot, B. D. Simons, and S. Jessberger. 2021. 'Long-term self-renewing stem cells in the adult mouse hippocampus identified by intravital imaging', *Nat Neurosci*, 24: 225-33.

Brandt, M. D., S. Jessberger, B. Steiner, G. Kronenberg, K. Reuter, A. Bick-Sander, W. von der Behrens, and G. Kempermann. 2003. 'Transient calretinin expression defines early postmitotic step of neuronal differentiation in adult hippocampal neurogenesis of mice', *Mol Cell Neurosci*, 24: 603-13.

Cancino, G. I., A. P. Yiu, M. P. Fatt, C. B. Dugani, E. R. Flores, P. W. Frankland, S. A. Josselyn, F. D. Miller, and D. R. Kaplan. 2013. 'p63 Regulates adult neural precursor and newly born neuron survival to control hippocampal-dependent Behavior', *J Neurosci*, 33: 12569-85.

Carelli, V., O. Musumeci, L. Caporali, C. Zanna, C. La Morgia, V. Del Dotto, A. M. Porcelli, M. Rugolo, M. L. Valentino, L. Iommarini, A. Maresca, P. Barboni, M. Carbonelli, C. Trombetta, E. M. Valente, S. Patergnani, C. Giorgi, P. Pinton, G. Rizzo, C. Tonon, R. Lodi, P. Avoni, R. Liguori, A. Baruzzi, A. Toscano, and M. Zeviani. 2015. 'Syndromic parkinsonism and dementia associated with OPA1 missense mutations', *Ann Neurol*, 78: 21-38.

Castro, D. S., B. Martynoga, C. Parras, V. Ramesh, E. Pacary, C. Johnston, D. Drechsel, M. Lebel-Potter, L. G. Garcia, C. Hunt, D. Dolle, A. Bithell, L. Ettwiller, N. Buckley, and F. Guillemot. 2011. 'A novel function of the proneural factor Ascl1 in progenitor proliferation identified by genome-wide characterization of its targets', *Genes Dev*, 25: 930-45.

Cebrian-Silla, A., M. A. Nascimento, S. A. Redmond, B. Mansky, D. Wu, K. Obernier, R. Romero Rodriguez, S. Gonzalez-Granero, J. M. Garcia-Verdugo, D. A. Lim, and A. Alvarez-Buylla. 2021. 'Single-cell analysis of the ventricular-subventricular zone reveals signatures of dorsal and ventral adult neurogenesis', *Elife*, 10.

Chakrabarty, R. P., and N. S. Chandel. 2021. 'Mitochondria as Signaling Organelles Control Mammalian Stem Cell Fate', *Cell Stem Cell*, 28: 394-408.

Chan, D. C. 2006a. 'Mitochondria: dynamic organelles in disease, aging, and development', *Cell*, 125: 1241-52.

———. 2006b. 'Mitochondrial fusion and fission in mammals', *Annu Rev Cell Dev Biol*, 22: 79-99.

———. 2020. 'Mitochondrial Dynamics and Its Involvement in Disease', *Annu Rev Pathol*, 15: 235-59.

Chandel, N. S., H. Jasper, T. T. Ho, and E. Passegue. 2016. 'Metabolic regulation of stem cell function in tissue homeostasis and organismal ageing', *Nat Cell Biol*, 18: 823-32.

Chang, R. C., A. K. Wong, H. K. Ng, and J. Hugon. 2002. 'Phosphorylation of eukaryotic initiation factor-2alpha (eIF2alpha) is associated with neuronal degeneration in Alzheimer's disease', *Neuroreport*, 13: 2429-32.

Chellappan, S. P., S. Hiebert, M. Mudryj, J. M. Horowitz, and J. R. Nevins. 1991. 'The E2F transcription factor is a cellular target for the RB protein', *Cell*, 65: 1053-61.

Chen, H., S. A. Detmer, A. J. Ewald, E. E. Griffin, S. E. Fraser, and D. C. Chan. 2003. 'Mitofusins Mfn1 and Mfn2 coordinately regulate mitochondrial fusion and are essential for embryonic development', *J Cell Biol*, 160: 189-200.

Cheng, A., R. Wan, J. L. Yang, N. Kamimura, T. G. Son, X. Ouyang, Y. Luo, E. Okun, and M. P. Mattson. 2012. 'Involvement of PGC-1alpha in the formation and maintenance of neuronal dendritic spines', *Nat Commun*, 3: 1250.

Cheung, T. H., and T. A. Rando. 2013. 'Molecular regulation of stem cell quiescence', *Nat Rev Mol Cell Biol*, 14: 329-40.

Chong, J. L., P. L. Wenzel, M. T. Saenz-Robles, V. Nair, A. Ferrey, J. P. Hagan, Y. M. Gomez, N. Sharma, H. Z. Chen, M. Ouseph, S. H. Wang, P. Trikha, B. Culp, L. Mezache, D. J. Winton, O. J. Sansom, D. Chen, R. Bremner, P. G. Cantalupo, M. L. Robinson, J. M. Pipas, and G. Leone. 2009. 'E2f1-3 switch from activators in progenitor cells to repressors in differentiating cells', *Nature*, 462: 930-4.

Chou, A., K. Krukowski, T. Jopson, P. J. Zhu, M. Costa-Mattioli, P. Walter, and S. Rosi. 2017. 'Inhibition of the integrated stress response reverses cognitive deficits after traumatic brain injury', *Proc Natl Acad Sci U S A*, 114: E6420-E26.

Cicero, S. A., D. Johnson, S. Reyntjens, S. Frase, S. Connell, L. M. Chow, S. J. Baker, B. P. Sorrentino, and M. A. Dyer. 2009. 'Cells previously identified as retinal stem cells are pigmented ciliary epithelial cells', *Proc Natl Acad Sci U S A*, 106: 6685-90.

Cipolat, S., O. Martins de Brito, B. Dal Zilio, and L. Scorrano. 2004. 'OPA1 requires mitofusin 1 to promote mitochondrial fusion', *Proc Natl Acad Sci U S A*, 101: 15927-32.

Clarke, L., and D. van der Kooy. 2009. 'Low oxygen enhances primitive and definitive neural stem cell colony formation by inhibiting distinct cell death pathways', *Stem Cells*, 27: 1879-86.

Clelland, C. D., M. Choi, C. Romberg, G. D. Clemenson, Jr., A. Fragniere, P. Tyers, S. Jessberger, L. M. Saksida, R. A. Barker, F. H. Gage, and T. J. Bussey. 2009. 'A functional role for adult hippocampal neurogenesis in spatial pattern separation', *Science*, 325: 210-3.

Codega, P., V. Silva-Vargas, A. Paul, A. R. Maldonado-Soto, A. M. Deleo, E. Pastrana, and F. Doetsch. 2014. 'Prospective identification and purification of quiescent adult neural stem cells from their in vivo niche', *Neuron*, 82: 545-59.

Conti, L., L. Crisafulli, V. Caldera, M. Tortoreto, E. Brilli, P. Conforti, F. Zunino, L. Magrassi, D. Schiffer, and E. Cattaneo. 2012. 'REST controls self-renewal and tumorigenic competence of human glioblastoma cells', *PLoS One*, 7: e38486.

Cooper-Kuhn, C. M., M. Vroemen, J. Brown, H. Ye, M. A. Thompson, J. Winkler, and H. G. Kuhn. 2002. 'Impaired adult neurogenesis in mice lacking the transcription factor E2F1', *Mol Cell Neurosci*, 21: 312-23.

Costa-Mattioli, M., D. Gobert, H. Harding, B. Herdy, M. Azzi, M. Bruno, M. Bidinosti, C. Ben Mamou, E. Marcinkiewicz, M. Yoshida, H. Imataka, A. C. Cuello, N. Seidah, W. Sossin, J. C. Lacaille, D. Ron, K. Nader, and N. Sonenberg. 2005. 'Translational control of hippocampal synaptic plasticity and memory by the eIF2alpha kinase GCN2', *Nature*, 436: 1166-73.

Costa-Mattioli, M., and P. Walter. 2020. 'The integrated stress response: From mechanism to disease', *Science*, 368.

Couillard-Despres, S., B. Winner, C. Karl, G. Lindemann, P. Schmid, R. Aigner, J. Laemke, U. Bogdahn, J. Winkler, J. Bischofberger, and L. Aigner. 2006. 'Targeted transgene expression in neuronal precursors: watching young neurons in the old brain', *Eur J Neurosci*, 24: 1535-45.

Crouch, E. E., and F. Doetsch. 2018. 'FACS isolation of endothelial cells and pericytes from mouse brain microregions', *Nat Protoc*, 13: 738-51.

Delettre, C., G. Lenaers, J. M. Griffoin, N. Gigarel, C. Lorenzo, P. Belenguer, L. Pelloquin, J. Grosgeorge, C. Turc-Carel, E. Perret, C. Astarie-Dequeker, L. Lasquellec, B. Arnaud, B. Ducommun, J. Kaplan, and C. P. Hamel. 2000. 'Nuclear gene OPA1, encoding a mitochondrial dynamin-related protein, is mutated in dominant optic atrophy', *Nat Genet*, 26: 207-10.

Demmings, M. D., E. C. Tennyson, G. N. Petroff, H. E. Tarnowski-Garner, and S. P. Cregan. 2021. 'Activating transcription factor-4 promotes neuronal death induced by Parkinson's disease neurotoxins and alpha-synuclein aggregates', *Cell Death Differ*, 28: 1627-43.

Deng, W., J. B. Aimone, and F. H. Gage. 2010. 'New neurons and new memories: how does adult hippocampal neurogenesis affect learning and memory?', *Nat Rev Neurosci*, 11: 339-50.

Denny, C. A., N. S. Burghardt, D. M. Schachter, R. Hen, and M. R. Drew. 2012. '4- to 6-week-old adult-born hippocampal neurons influence novelty-evoked exploration and contextual fear conditioning', *Hippocampus*, 22: 1188-201.

Denoth-Lippuner, A., and S. Jessberger. 2021. 'Formation and integration of new neurons in the adult hippocampus', *Nat Rev Neurosci*, 22: 223-36.

Dhaliwal, J., and D. C. Lagace. 2011. 'Visualization and genetic manipulation of adult neurogenesis using transgenic mice', *Eur J Neurosci*, 33: 1025-36.

Eales, K. L., K. E. Hollinshead, and D. A. Tennant. 2016. 'Hypoxia and metabolic adaptation of cancer cells', *Oncogenesis*, 5: e190.

Ferguson, K. L., K. A. McClellan, J. L. Vanderluit, W. C. McIntosh, C. Schuurmans, F. Polleux, and R. S. Slack. 2005. 'A cell-autonomous requirement for the cell cycle regulatory protein, Rb, in neuronal migration', *EMBO J*, 24: 4381-91.

Ferguson, K. L., J. L. Vanderluit, J. M. Hebert, W. C. McIntosh, E. Tibbo, J. G. MacLaurin, D. S. Park, V. A. Wallace, M. Vooijs, S. K. McConnell, and R. S. Slack. 2002. 'Telencephalon-specific Rb knockouts reveal enhanced neurogenesis, survival and abnormal cortical development', *EMBO J*, 21: 3337-46.

Fessler, E., E. M. Eckl, S. Schmitt, I. A. Mancilla, M. F. Meyer-Bender, M. Hanf, J. Philippou-Massier, S. Krebs, H. Zischka, and L. T. Jae. 2020. 'A pathway coordinated by DELE1 relays mitochondrial stress to the cytosol', *Nature*, 579: 433-37.

Fong, B. C., I. Chakroun, M. A. Iqbal, S. Paul, J. Bastasic, D. O'Neil, E. Yakubovich, A. T. Bejjani, N. Ahmadi, A. Carter, A. Clark, G. Leone, D. S. Park, N. Ghanem, R. Vandenbosch, and R. S. Slack. 2022. 'The Rb/E2F axis is a key regulator of the molecular signatures instructing the quiescent and activated adult neural stem cell state', *Cell Rep*, 41: 111578.

Frank, C. L., X. Ge, Z. Xie, Y. Zhou, and L. H. Tsai. 2010. 'Control of activating transcription factor 4 (ATF4) persistence by multisite phosphorylation impacts cell cycle progression and neurogenesis', *J Biol Chem*, 285: 33324-37.

Frezza, C., S. Cipolat, O. Martins de Brito, M. Micaroni, G. V. Beznoussenko, T. Rudka, D. Bartoli, R. S. Polishuck, N. N. Danial, B. De Strooper, and L. Scorrano. 2006. 'OPA1 controls apoptotic cristae remodeling independently from mitochondrial fusion', *Cell*, 126: 177-89.

Friedman, J. R., L. L. Lackner, M. West, J. R. DiBenedetto, J. Nunnari, and G. K. Voeltz. 2011. 'ER tubules mark sites of mitochondrial division', *Science*, 334: 358-62.

Furutachi, S., H. Miya, T. Watanabe, H. Kawai, N. Yamasaki, Y. Harada, I. Imayoshi, M. Nelson, K. I. Nakayama, Y. Hirabayashi, and Y. Gotoh. 2015. 'Slowly dividing neural progenitors are an embryonic origin of adult neural stem cells', *Nat Neurosci*, 18: 657-65.

Gao, Z., K. Ure, P. Ding, M. Nashaat, L. Yuan, J. Ma, R. E. Hammer, and J. Hsieh. 2011. 'The master negative regulator REST/NRSF controls adult neurogenesis by restraining the neurogenic program in quiescent stem cells', *J Neurosci*, 31: 9772-86.

Garcia-Verdugo, J. M., F. Doetsch, H. Wichterle, D. A. Lim, and A. Alvarez-Buylla. 1998. 'Architecture and cell types of the adult subventricular zone: in search of the stem cells', *J Neurobiol*, 36: 234-48.

Gomez, E., M. L. Powell, A. Bevington, and T. P. Herbert. 2008. 'A decrease in cellular energy status stimulates PERK-dependent eIF2alpha phosphorylation and regulates protein synthesis in pancreatic beta-cells', *Biochem J*, 410: 485-93.

Goncalves, J. T., S. T. Schafer, and F. H. Gage. 2016. 'Adult Neurogenesis in the Hippocampus: From Stem Cells to Behavior', *Cell*, 167: 897-914.

Gonzalez-Bohorquez, D., I. M. Gallego Lopez, B. N. Jaeger, S. Pfammatter, M. Bowers, C. F. Semenkovich, and S. Jessberger. 2022. 'FASN-dependent de novo lipogenesis is required for brain development', *Proc Natl Acad Sci U S A*, 119.

Gotz, M. 2018. 'Revising concepts about adult stem cells', *Science*, 359: 639-40.

Gu, Y., M. Arruda-Carvalho, J. Wang, S. R. Janoschka, S. A. Josselyn, P. W. Frankland, and S. Ge. 2012. 'Optical controlling reveals time-dependent roles for adult-born dentate granule cells', *Nat Neurosci*, 15: 1700-6.

Guez-Barber, D., S. Fanous, B. K. Harvey, Y. Zhang, E. Lehrmann, K. G. Becker, M. R. Picciotto, and B. T. Hope. 2012. 'FACS purification of immunolabeled cell types from adult rat brain', *J Neurosci Methods*, 203: 10-8.

Guimaraes-Camboa, N., J. Stowe, I. Aneas, N. Sakabe, P. Cattaneo, L. Henderson, M. S. Kilberg, R. S. Johnson, J. Chen, A. D. McCulloch, M. A. Nobrega, S. M. Evans, and A. C. Zambon. 2015. 'HIF1alpha Represses Cell Stress Pathways to Allow Proliferation of Hypoxic Fetal Cardiomyocytes', *Dev Cell*, 33: 507-21.

Guneykaya, D., A. Ivanov, D. P. Hernandez, V. Haage, B. Wojtas, N. Meyer, M. Maricos, P. Jordan, A. Buonfiglioli, B. Gielniewski, N. Ochocka, C. Comert, C. Friedrich, L. S. Artiles, B. Kaminska, P. Mertins, D. Beule, H. Kettenmann, and S. A. Wolf. 2018. 'Transcriptional and Translational Differences of Microglia from Male and Female Brains', *Cell Rep*, 24: 2773-83 e6.

Guo, X., G. Aviles, Y. Liu, R. Tian, B. A. Unger, Y. T. Lin, A. P. Wiita, K. Xu, M. A. Correia, and M. Kampmann. 2020. 'Mitochondrial stress is relayed to the cytosol by an OMA1-DELE1-HRI pathway', *Nature*, 579: 427-32.

Hamalainen, R. H., K. J. Ahlqvist, P. Ellonen, M. Lepisto, A. Logan, T. Otonkoski, M. P. Murphy, and A. Suomalainen. 2015. 'mtDNA Mutagenesis Disrupts Pluripotent Stem Cell Function by Altering Redox Signaling', *Cell Rep*, 11: 1614-24.

Hamilton, L. K., M. Dufresne, S. E. Joppe, S. Petryszyn, A. Aumont, F. Calon, F. Barnabe-Heider, A. Furtos, M. Parent, P. Chaurand, and K. J. Fernandes. 2015. 'Aberrant Lipid Metabolism in the Forebrain Niche Suppresses Adult Neural Stem Cell Proliferation in an Animal Model of Alzheimer's Disease', *Cell Stem Cell*, 17: 397-411.

Hamilton, L. K., G. Moquin-Beaudry, C. L. Mangahas, F. Pratesi, M. Aubin, A. Aumont, S. E. Joppe, A. Legiot, A. Vachon, M. Plourde, C. Mounier, M. Tetreault, and K. J. L. Fernandes. 2022. 'Stearoyl-CoA Desaturase inhibition reverses immune, synaptic and cognitive impairments in an Alzheimer's disease mouse model', *Nat Commun*, 13: 2061.

Han, J., S. H. Back, J. Hur, Y. H. Lin, R. Gildersleeve, J. Shan, C. L. Yuan, D. Krokowski, S. Wang, M. Hatzoglou, M. S. Kilberg, M. A. Sartor, and R. J. Kaufman. 2013. 'ER-stress-induced transcriptional regulation increases protein synthesis leading to cell death', *Nat Cell Biol*, 15: 481-90.

Harada, Y., M. Yamada, I. Imayoshi, R. Kageyama, Y. Suzuki, T. Kuniya, S. Furutachi, D. Kawaguchi, and Y. Gotoh. 2021. 'Cell cycle arrest determines adult neural stem cell ontogeny by an embryonic Notch-nonoscillatory Hey1 module', *Nat Commun*, 12: 6562.

Harris, L., P. Rigo, T. Stiehl, Z. B. Gaber, S. H. L. Austin, M. D. M. Masdeu, A. Edwards, N. Urban, A. Marciniak-Czochra, and F. Guillemot. 2021a. 'Coordinated changes in cellular behavior ensure the lifelong maintenance of the hippocampal stem cell population', *Cell Stem Cell*, 28: 863-76 e6.

———. 2021b. 'Coordinated changes in cellular behavior ensure the lifelong maintenance of the hippocampal stem cell population', *Cell Stem Cell*.

He, C. H., P. Gong, B. Hu, D. Stewart, M. E. Choi, A. M. Choi, and J. Alam. 2001. 'Identification of activating transcription factor 4 (ATF4) as an Nrf2-interacting protein. Implication for heme oxygenase-1 gene regulation', *J Biol Chem*, 276: 20858-65.

He, L., M. Vanlandewijck, E. Raschperger, M. Andaloussi Mae, B. Jung, T. Lebouvier, K. Ando, J. Hofmann, A. Keller, and C. Betsholtz. 2016. 'Analysis of the brain mural cell transcriptome', *Sci Rep*, 6: 35108.

Hebert, J. M., and S. K. McConnell. 2000. 'Targeting of cre to the Foxg1 (BF-1) locus mediates loxP recombination in the telencephalon and other developing head structures', *Dev Biol*, 222: 296-306.

Hochgerner, H., A. Zeisel, P. Lonnerberg, and S. Linnarsson. 2018. 'Conserved properties of dentate gyrus neurogenesis across postnatal development revealed by single-cell RNA sequencing', *Nat Neurosci*, 21: 290-99.

Hodge, R. D., B. R. Nelson, R. J. Kahoud, R. Yang, K. E. Mussar, S. L. Reiner, and R. F. Hevner. 2012. 'Tbr2 is essential for hippocampal lineage progression from neural stem cells to intermediate progenitors and neurons', *J Neurosci*, 32: 6275-87.

Homem, C. C. F., V. Steinmann, T. R. Burkard, A. Jais, H. Esterbauer, and J. A. Knoblich. 2014. 'Ecdysone and mediator change energy metabolism to terminate proliferation in Drosophila neural stem cells', *Cell*, 158: 874-88.

Homem, C. C., M. Repic, and J. A. Knoblich. 2015. 'Proliferation control in neural stem and progenitor cells', *Nat Rev Neurosci*, 16: 647-59.

Hoozemans, J. J., E. S. van Haastert, P. Eikelenboom, R. A. de Vos, J. M. Rozemuller, and W. Scheper. 2007. 'Activation of the unfolded protein response in Parkinson's disease', *Biochem Biophys Res Commun*, 354: 707-11.

Iannielli, A., S. Bido, L. Folladori, A. Segnali, C. Cancellieri, A. Maresca, L. Massimino, A. Rubio, G. Morabito, L. Caporali, F. Tagliavini, O. Musumeci, G. Gregato, E. Bezard, V. Carelli, V. Tiranti, and V. Broccoli. 2018. 'Pharmacological Inhibition of Necroptosis Protects from Dopaminergic Neuronal Cell Death in Parkinson's Disease Models', *Cell Rep*, 22: 2066-79.

Inak, G., A. Rybak-Wolf, P. Lisowski, T. M. Pentimalli, R. Juttner, P. Glazar, K. Uppal, E. Bottani, D. Brunetti, C. Secker, A. Zink, D. Meierhofer, M. T. Henke, M. Dey, U. Ciptasari, B. Mlody, T. Hahn, M. Berruezo-Llacuna, N. Karaiskos, M. Di Virgilio, J. A. Mayr, S. B. Wortmann, J. Priller, M. Gotthardt, D. P. Jones, E. Mayatepek, W. Stenzel, S. Diecke, R. Kuhn, E. E. Wanker, N. Rajewsky, M. Schuelke, and A. Prigione. 2021. 'Defective metabolic programming impairs early neuronal morphogenesis in neural cultures and an organoid model of Leigh syndrome', *Nat Commun*, 12: 1929.

Iqbal, M. A., B. C. Fong, and R. S. Slack. 2022. 'Direct FACS Isolation of Neural Stem/Progenitor Lineages from the Adult Brain', *Methods Mol Biol*, 2515: 117-27.

Ito, K., and T. Suda. 2014. 'Metabolic requirements for the maintenance of self-renewing stem cells', *Nat Rev Mol Cell Biol*, 15: 243-56.

Iwano, T., A. Masuda, H. Kiyonari, H. Enomoto, and F. Matsuzaki. 2012. 'Prox1 postmitotically defines dentate gyrus cells by specifying granule cell identity over CA3 pyramidal cell fate in the hippocampus', *Development*, 139: 3051-62.

Iwata, R., P. Casimir, and P. Vanderhaeghen. 2020. 'Mitochondrial dynamics in postmitotic cells regulate neurogenesis', *Science*, 369: 858-62.

Jaafar, C., S. Omais, S. Al Lafi, N. El Jamal, M. Noubani, L. Skaf, and N. Ghanem. 2016. 'Role of Rb during Neurogenesis and Axonal Guidance in the Developing Olfactory System', *Front Mol Neurosci*, 9: 81.

Jain, I. H., L. Zazzeron, R. Goli, K. Alexa, S. Schatzman-Bone, H. Dhillon, O. Goldberger, J. Peng, O. Shalem, N. E. Sanjana, F. Zhang, W. Goessling, W. M. Zapol, and V. K. Mootha. 2016. 'Hypoxia as a therapy for mitochondrial disease', *Science*, 352: 54-61.

James, D. I., P. A. Parone, Y. Mattenberger, and J. C. Martinou. 2003. 'hFis1, a novel component of the mammalian mitochondrial fission machinery', *J Biol Chem*, 278: 36373-9.

Jang, Y. Y., and S. J. Sharkis. 2007. 'A low level of reactive oxygen species selects for primitive hematopoietic stem cells that may reside in the low-oxygenic niche', *Blood*, 110: 3056-63.

Jiang, Z., T. Deng, R. Jones, H. Li, J. I. Herschkowitz, J. C. Liu, V. J. Weigman, M. S. Tsao, T. F. Lane, C. M. Perou, and E. Zacksenhaus. 2010. 'Rb deletion in mouse mammary progenitors induces luminal-B or basal-like/EMT tumor subtypes depending on p53 status', *J Clin Invest*, 120: 3296-309.

John Lin, C. C., K. Yu, A. Hatcher, T. W. Huang, H. K. Lee, J. Carlson, M. C. Weston, F. Chen, Y. Zhang, W. Zhu, C. A. Mohila, N. Ahmed, A. J. Patel, B. R. Arenkiel, J. L. Noebels, C. J. Creighton, and B. Deneen. 2017. 'Identification of diverse astrocyte populations and their malignant analogs', *Nat Neurosci*, 20: 396-405.

Johnston, S. T., M. Shtrahman, S. Parylak, J. T. Goncalves, and F. H. Gage. 2016. 'Paradox of pattern separation and adult neurogenesis: A dual role for new neurons balancing memory resolution and robustness', *Neurobiol Learn Mem*, 129: 60-8.

Julian, L. M., R. Vandenbosch, C. A. Pakenham, M. G. Andrusiak, A. P. Nguyen, K. A. McClellan, D. S. Svoboda, D. C. Lagace, D. S. Park, G. Leone, A. Blais, and R. S. Slack. 2013. 'Opposing regulation of Sox2 by cell-cycle effectors E2f3a and E2f3b in neural stem cells', *Cell Stem Cell*, 12: 440-52.

Kalamakis, G., D. Brune, S. Ravichandran, J. Bolz, W. Fan, F. Ziebell, T. Stiehl, F. Catala-Martinez, J. Kupke, S. Zhao, E. Llorens-Bobadilla, K. Bauer, S. Limpert, B. Berger, U. Christen, P. Schmezer, J. P. Mallm, B. Berninger, S. Anders, A. Del Sol, A. Marciniak-Czochra, and A. Martin-Villalba. 2019. 'Quiescence Modulates Stem Cell Maintenance and Regenerative Capacity in the Aging Brain', *Cell*, 176: 1407-19 e14.

Kalinina, A., and D. Lagace. 2022. 'Single-Cell and Single-Nucleus RNAseq Analysis of Adult Neurogenesis', *Cells*, 11.

Kane, M. S., J. Alban, V. Desquiret-Dumas, N. Gueguen, L. Ishak, M. Ferre, P. Amati-Bonneau, V. Procaccio, D. Bonneau, G. Lenaers, P. Reynier, and A. Chevrollier. 2017. 'Autophagy controls the pathogenicity of OPA1 mutations in dominant optic atrophy', *J Cell Mol Med*, 21: 2284-97.

Kareta, M. S., L. L. Gorges, S. Hafeez, B. A. Benayoun, S. Marro, A. F. Zmoos, M. J. Cecchini, D. Spacek, L. F. Batista, M. O'Brien, Y. H. Ng, C. E. Ang, D. Vaka, S. E. Artandi, F. A. Dick, A. Brunet, J. Sage, and M. Wernig. 2015. 'Inhibition of pluripotency networks by the Rb tumor suppressor restricts reprogramming and tumorigenesis', *Cell Stem Cell*, 16: 39-50.

Kee, N., C. M. Teixeira, A. H. Wang, and P. W. Frankland. 2007. 'Preferential incorporation of adult-generated granule cells into spatial memory networks in the dentate gyrus', *Nat Neurosci*, 10: 355-62.

Kempermann, G., H. Song, and F. H. Gage. 2015. 'Neurogenesis in the Adult Hippocampus', *Cold Spring Harb Perspect Biol*, 7: a018812.

Khacho, M., A. Clark, D. S. Svoboda, J. Azzi, J. G. MacLaurin, C. Meghaizel, H. Sesaki, D. C. Lagace, M. Germain, M. E. Harper, D. S. Park, and R. S. Slack. 2016. 'Mitochondrial Dynamics Impacts Stem Cell Identity and Fate Decisions by Regulating a Nuclear Transcriptional Program', *Cell Stem Cell*, 19: 232-47.

Khacho, M., A. Clark, D. S. Svoboda, J. G. MacLaurin, D. C. Lagace, D. S. Park, and R. S. Slack. 2017. 'Mitochondrial dysfunction underlies cognitive defects as a result of neural stem cell depletion and impaired neurogenesis', *Hum Mol Genet*, 26: 3327-41.

Khacho, M., R. Harris, and R. S. Slack. 2019. 'Mitochondria as central regulators of neural stem cell fate and cognitive function', *Nat Rev Neurosci*, 20: 34-48.

Khacho, M., and R. S. Slack. 2017a. 'Mitochondrial activity in the regulation of stem cell self-renewal and differentiation', *Curr Opin Cell Biol*, 49: 1-8.

———. 2017b. 'Mitochondrial and Reactive Oxygen Species Signaling Coordinate Stem Cell Fate Decisions and Life Long Maintenance', *Antioxid Redox Signal*.

Kijima, K., C. Numakura, H. Izumino, K. Umetsu, A. Nezu, T. Shiiki, M. Ogawa, Y. Ishizaki, T. Kitamura, Y. Shozawa, and K. Hayasaka. 2005. 'Mitochondrial GTPase mitofusin 2 mutation in Charcot-Marie-Tooth neuropathy type 2A', *Hum Genet*, 116: 23-7.

Kleele, T., T. Rey, J. Winter, S. Zaganelli, D. Mahecic, H. Perreten Lambert, F. P. Ruberto, M. Nemir, T. Wai, T. Pedrazzini, and S. Manley. 2021. 'Distinct fission signatures predict mitochondrial degradation or biogenesis', *Nature*, 593: 435-39.

Knobloch, M., S. M. Braun, L. Zurkirchen, C. von Schoultz, N. Zamboni, M. J. Arauzo-Bravo, W. J. Kovacs, O. Karalay, U. Suter, R. A. Machado, M. Roccio, M. P. Lutolf, C. F. Semenkovich, and S. Jessberger. 2013. 'Metabolic control of adult neural stem cell activity by Fasn-dependent lipogenesis', *Nature*, 493: 226-30.

Knobloch, M., G. A. Pilz, B. Ghesquiere, W. J. Kovacs, T. Wegleiter, D. L. Moore, M. Hruzova, N. Zamboni, P. Carmeliet, and S. Jessberger. 2017. 'A Fatty Acid Oxidation-Dependent Metabolic Shift Regulates Adult Neural Stem Cell Activity', *Cell Rep*, 20: 2144-55.

Koizumi, H., H. Higginbotham, T. Poon, T. Tanaka, B. C. Brinkman, and J. G. Gleeson. 2006. 'Doublecortin maintains bipolar shape and nuclear translocation during migration in the adult forebrain', *Nat Neurosci*, 9: 779-86.

Kuhn, H. G., A. J. Eisch, K. Spalding, and D. A. Peterson. 2016. 'Detection and Phenotypic Characterization of Adult Neurogenesis', *Cold Spring Harb Perspect Biol*, 8: a025981.

La Manno, G., R. Soldatov, A. Zeisel, E. Braun, H. Hochgerner, V. Petukhov, K. Lidschreiber, M. E. Kastriti, P. Lonnerberg, A. Furlan, J. Fan, L. E. Borm, Z. Liu, D. van Bruggen, J. Guo, X. He, R. Barker, E. Sundstrom, G. Castelo-Branco, P. Cramer, I. Adameyko, S. Linnarsson, and P. V. Kharchenko. 2018. 'RNA velocity of single cells', *Nature*, 560: 494-98.

Lange, C., M. Turrero Garcia, I. Decimo, F. Bifari, G. Eelen, A. Quaegebeur, R. Boon, H. Zhao, B. Boeckx, J. Chang, C. Wu, F. Le Noble, D. Lambrechts, M. Dewerchin, C. J. Kuo, W. B. Huttner, and P. Carmeliet. 2016. 'Relief of hypoxia by angiogenesis promotes neural stem cell differentiation by targeting glycolysis', *EMBO J*, 35: 924-41.

Lavado, A., and G. Oliver. 2007. 'Prox1 expression patterns in the developing and adult murine brain', *Dev Dyn*, 236: 518-24.

Le Belle, J. E., N. M. Orozco, A. A. Paucar, J. P. Saxe, J. Mottahedeh, A. D. Pyle, H. Wu, and H. I. Kornblum. 2011. 'Proliferative neural stem cells have high endogenous ROS levels that regulate self-renewal and neurogenesis in a PI3K/Akt-dependant manner', *Cell Stem Cell*, 8: 59-71.

Leeman, D. S., K. Hebestreit, T. Ruetz, A. E. Webb, A. McKay, E. A. Pollina, B. W. Dulken, X. Zhao, R. W. Yeo, T. T. Ho, S. Mahmoudi, K. Devarajan, E. Passegue, T. A. Rando, J. Frydman, and A. Brunet. 2018. 'Lysosome activation clears aggregates and enhances quiescent neural stem cell activation during aging', *Science*, 359: 1277-83.

Lepagnol-Bestel, A. M., A. Zvara, G. Maussion, F. Quignon, B. Ngimbous, N. Ramoz, S. Imbeaud, Y. Loe-Mie, K. Benihoud, N. Agier, P. A. Salin, A. Cardona, S. Khung-Savatovsky, P. Kallunki, J. M. Delabar, L. G. Puskas, H. Delacroix, L. Aggerbeck, A. L. Delezoide, O. Delattre, P. Gorwood, J. M. Moalic, and M. Simonneau. 2009. 'DYRK1A interacts with the REST/NRSF-SWI/SNF chromatin remodelling complex to deregulate gene clusters involved in the neuronal phenotypic traits of Down syndrome', *Hum Mol Genet*, 18: 1405-14.

Lim, J. K. M., A. Delaidelli, S. W. Minaker, H. F. Zhang, M. Colovic, H. Yang, G. L. Negri, S. von Karstedt, W. W. Lockwood, P. Schaffer, G. Leprivier, and P. H. Sorensen. 2019. 'Cystine/glutamate antiporter xCT (SLC7A11) facilitates oncogenic RAS transformation by preserving intracellular redox balance', *Proc Natl Acad Sci U S A*, 116: 9433-42.

Liu, Y., B. Fong, R. Harris, M McNicoll, A Abdi, J Cuthbert, D. Cook, D. Figeys, J Wang, B Vanderhyden, and Slack. R. 2022. 'Alterations in neural stem cell quiescence and activation in the 3xTG-AD model of Alzheimer's Disease', *bioRxiv*.

Lledo, P. M., and M. Valley. 2016. 'Adult Olfactory Bulb Neurogenesis', *Cold Spring Harb Perspect Biol*, 8.

Llorens-Bobadilla, E., S. Zhao, A. Baser, G. Saiz-Castro, K. Zwadlo, and A. Martin-Villalba. 2015. 'Single-Cell Transcriptomics Reveals a Population of Dormant Neural Stem Cells that Become Activated upon Brain Injury', *Cell Stem Cell*, 17: 329-40.

Longo, F., S. Benedetti, A. A. Zambon, M. G. N. Sora, C. Di Resta, D. De Ritis, A. Quattrini, F. Maltecca, M. Ferrari, and S. C. Previtali. 2020. 'Impaired turnover of hyperfused mitochondria in severe axonal neuropathy due to a novel DRP1 mutation', *Hum Mol Genet*, 29: 177-88.

Lugert, S., O. Basak, P. Knuckles, U. Haussler, K. Fabel, M. Gotz, C. A. Haas, G. Kempermann, V. Taylor, and C. Giachino. 2010. 'Quiescent and active hippocampal neural stem cells with distinct morphologies respond selectively to physiological and pathological stimuli and aging', *Cell Stem Cell*, 6: 445-56.

Luna, V. M., C. Anacker, N. S. Burghardt, H. Khandaker, V. Andreu, A. Millette, P. Leary, R. Ravenelle, J. C. Jimenez, A. Mastrodonato, C. A. Denny, A. A. Fenton, H. E. Scharfman, and R. Hen. 2019. 'Adult-born hippocampal neurons bidirectionally modulate entorhinal inputs into the dentate gyrus', *Science*, 364: 578-83.

Lundberg, A. S., and R. A. Weinberg. 1998. 'Functional inactivation of the retinoblastoma protein requires sequential modification by at least two distinct cyclin-cdk complexes', *Mol Cell Biol*, 18: 753-61.

Madhavan, L., V. Ourednik, and J. Ourednik. 2006. 'Increased "vigilance" of antioxidant mechanisms in neural stem cells potentiates their capability to resist oxidative stress', *Stem Cells*, 24: 2110-9.

Mann, I. K., R. Chatterjee, J. Zhao, X. He, M. T. Weirauch, T. R. Hughes, and C. Vinson. 2013. 'CG methylated microarrays identify a novel methylated sequence bound by the CEBPB|ATF4 heterodimer that is active in vivo', *Genome Res*, 23: 988-97.

Maren, S., K. L. Phan, and I. Liberzon. 2013. 'The contextual brain: implications for fear conditioning, extinction and psychopathology', *Nat Rev Neurosci*, 14: 417-28.

Martin, D., and A. Grapin-Botton. 2017. 'The Importance of REST for Development and Function of Beta Cells', *Front Cell Dev Biol*, 5: 12.

McAvoy, K., A. Besnard, and A. Sahay. 2015. 'Adult hippocampal neurogenesis and pattern separation in DG: a role for feedback inhibition in modulating sparseness to govern population-based coding', *Front Syst Neurosci*, 9: 120.

Menn, B., J. M. Garcia-Verdugo, C. Yaschine, O. Gonzalez-Perez, D. Rowitch, and A. Alvarez-Buylla. 2006. 'Origin of oligodendrocytes in the subventricular zone of the adult brain', *J Neurosci*, 26: 7907-18.

Merkle, F. T., A. D. Tramontin, J. M. Garcia-Verdugo, and A. Alvarez-Buylla. 2004. 'Radial glia give rise to adult neural stem cells in the subventricular zone', *Proc Natl Acad Sci U S A*, 101: 17528-32.

Mertens, J., J. R. Herdy, L. Traxler, S. T. Schafer, J. C. M. Schlachetzki, L. Bohnke, D. A. Reid, H. Lee, D. Zangwill, D. P. Fernandes, R. K. Agarwal, R. Lucciola, L. Zhou-Yang, L. Karbacher, F. Edenhofer, S. Stern, S. Horvath, A. C. M. Paquola, C. K. Glass, S. H. Yuan, M. Ku, A. Szucs, L. S. B. Goldstein, D. Galasko, and F. H. Gage. 2021. 'Age-dependent instability of mature neuronal fate in induced neurons from Alzheimer's patients', *Cell Stem Cell*, 28: 1533-48 e6.

Ming, G. L., and H. Song. 2011. 'Adult neurogenesis in the mammalian brain: significant answers and significant questions', *Neuron*, 70: 687-702.

Mizrak, D., H. M. Levitin, A. C. Delgado, V. Crotet, J. Yuan, Z. Chaker, V. Silva-Vargas, P. A. Sims, and F. Doetsch. 2019. 'Single-Cell Analysis of Regional Differences in Adult V-SVZ Neural Stem Cell Lineages', *Cell Rep*, 26: 394-406 e5.

Mohyeldin, A., T. Garzon-Muvdi, and A. Quinones-Hinojosa. 2010. 'Oxygen in stem cell biology: a critical component of the stem cell niche', *Cell Stem Cell*, 7: 150-61.

Moreno-Jimenez, E. P., M. Flor-Garcia, J. Terreros-Roncal, A. Rabano, F. Cafini, N. Pallas-Bazarra, J. Avila, and M. Llorens-Martin. 2019. 'Adult hippocampal neurogenesis is abundant in neurologically healthy subjects and drops sharply in patients with Alzheimer's disease', *Nat Med*, 25: 554-60.

Morizur, L., A. Chicheportiche, L. R. Gauthier, M. Daynac, F. D. Boussin, and M. A. Mouthon. 2018. 'Distinct Molecular Signatures of Quiescent and Activated Adult Neural Stem Cells Reveal Specific Interactions with Their Microenvironment', *Stem Cell Reports*, 11: 565-77.

Morshead, C. M., C. G. Craig, and D. van der Kooy. 1998. 'In vivo clonal analyses reveal the properties of endogenous neural stem cell proliferation in the adult mammalian forebrain', *Development*, 125: 2251-61.

Mukherjee, S., R. Brulet, L. Zhang, and J. Hsieh. 2016. 'REST regulation of gene networks in adult neural stem cells', *Nat Commun*, 7: 13360.

Murphy, M. P. 2009. 'How mitochondria produce reactive oxygen species', *Biochem J*, 417: 1-13.

Omais, S., R. N. Hilal, N. N. Halaby, C. Jaafar, and N. Ghanem. 2022. 'Aging entails distinct requirements for Rb at maintaining adult neurogenesis', *Aging Brain*, 2: 100041.

Otsuki, L., and A. H. Brand. 2019. 'Dorsal-Ventral Differences in Neural Stem Cell Quiescence Are Induced by p57(KIP2)/Dacapo', *Dev Cell*, 49: 293-300 e3.

Paik, J. H., Z. Ding, R. Narurkar, S. Ramkissoon, F. Muller, W. S. Kamoun, S. S. Chae, H. Zheng, H. Ying, J. Mahoney, D. Hiller, S. Jiang, A. Protopopov, W. H. Wong, L. Chin, K. L. Ligon, and R. A. DePinho. 2009. 'FoxOs cooperatively regulate diverse pathways governing neural stem cell homeostasis', *Cell Stem Cell*, 5: 540-53.

Pakos-Zebrucka, K., I. Koryga, K. Mnich, M. Ljujic, A. Samali, and A. M. Gorman. 2016. 'The integrated stress response', *EMBO Rep*, 17: 1374-95.

Pastrana, E., L. C. Cheng, and F. Doetsch. 2009. 'Simultaneous prospective purification of adult subventricular zone neural stem cells and their progeny', *Proc Natl Acad Sci U S A*, 106: 6387-92.

Pastrana, E., V. Silva-Vargas, and F. Doetsch. 2011. 'Eyes wide open: a critical review of sphere-formation as an assay for stem cells', *Cell Stem Cell*, 8: 486-98.

Patten, D. A., S. McGuirk, U. Anilkumar, G. Antoun, K. Gandhi, G. Parmar, M. A. Iqbal, J. Wong, R. B. Richardson, J. St-Pierre, R. S. Slack, and M. E. Harper. 2021. 'Altered mitochondrial fusion drives defensive glutathione synthesis in cells able to switch to glycolytic ATP production', *Biochim Biophys Acta Mol Cell Res*, 1868: 118854.

Patten, D. A., J. Wong, M. Khacho, V. Soubannier, R. J. Mailloux, K. Pilon-Larose, J. G. MacLaurin, D. S. Park, H. M. McBride, L. Trinkle-Mulcahy, M. E. Harper, M. Germain, and R. S. Slack. 2014. 'OPA1-dependent cristae modulation is essential for cellular adaptation to metabolic demand', *EMBO J*, 33: 2676-91.

Petrelli, F., V. Scandella, S. Montessuit, N. Zamboni, J. C. Martinou, and M. Knobloch. 2023. 'Mitochondrial pyruvate metabolism regulates the activation of quiescent adult neural stem cells', *Sci Adv*, 9: eadd5220.

Pham, J., S. M. Cabrera, C. Sanchis-Segura, and M. A. Wood. 2009. 'Automated scoring of fear-related behavior using EthoVision software', *J Neurosci Methods*, 178: 323-6.

Pilz, G. A., S. Bottes, M. Betizeau, D. J. Jorg, S. Carta, B. D. Simons, F. Helmchen, and S. Jessberger. 2018. 'Live imaging of neurogenesis in the adult mouse hippocampus', *Science*, 359: 658-62.

Pilz, G. A., A. Shitamukai, I. Reillo, E. Pacary, J. Schwausch, R. Stahl, J. Ninkovic, H. J. Snippert, H. Clevers, L. Godinho, F. Guillemot, V. Borrell, F. Matsuzaki, and M. Gotz. 2013. 'Amplification of progenitors in the mammalian telencephalon includes a new radial glial cell type', *Nat Commun*, 4: 2125.

Poulin, J. F., J. Zou, J. Drouin-Ouellet, K. Y. Kim, F. Cicchetti, and R. B. Awatramani. 2014. 'Defining midbrain dopaminergic neuron diversity by single-cell gene expression profiling', *Cell Rep*, 9: 930-43.

Quiros, P. M., M. A. Prado, N. Zamboni, D. D'Amico, R. W. Williams, D. Finley, S. P. Gygi, and J. Auwerx. 2017. 'Multi-omics analysis identifies ATF4 as a key regulator of the mitochondrial stress response in mammals', *J Cell Biol*, 216: 2027-45.

Ramonet, D., C. Perier, A. Recasens, B. Dehay, J. Bove, V. Costa, L. Scorrano, and M. Vila. 2013. 'Optic atrophy 1 mediates mitochondria remodeling and dopaminergic neurodegeneration linked to complex I deficiency', *Cell Death Differ*, 20: 77-85.

Ramosaj, M., S. Madsen, V. Maillard, V. Scandella, D. Sudria-Lopez, N. Yuizumi, L. Telley, and M. Knobloch. 2021. 'Lipid droplet availability affects neural stem/progenitor cell metabolism and proliferation', *Nat Commun*, 12: 7362.

Raposo, A. A., F. F. Vasconcelos, D. Drechsel, C. Marie, C. Johnston, D. Dolle, A. Bithell, S. Gillotin, D. L. van den Berg, L. Ettwiller, P. Flicek, G. E. Crawford, C. M. Parras, B. Berninger, N. J. Buckley, F. Guillemot, and D. S. Castro. 2015. 'Ascl1 Coordinately Regulates Gene Expression and the Chromatin Landscape during Neurogenesis', *Cell Rep*.

Renault, V. M., V. A. Rafalski, A. A. Morgan, D. A. Salih, J. O. Brett, A. E. Webb, S. A. Villeda, P. U. Thekkat, C. Guillerey, N. C. Denko, T. D. Palmer, A. J. Butte, and A. Brunet. 2009. 'FoxO3 regulates neural stem cell homeostasis', *Cell Stem Cell*, 5: 527-39.

Richards, B. A., and P. W. Frankland. 2017. 'The Persistence and Transience of Memory', *Neuron*, 94: 1071-84.

Rieskamp, J. D., J. K. Denninger, and T. J. Dause. 2018. 'Identifying the Unique Role of Notch3 in Adult Neural Stem Cell Maintenance', *J Neurosci*, 38: 3157-59.

Robinson, K. M., M. S. Janes, and J. S. Beckman. 2008. 'The selective detection of mitochondrial superoxide by live cell imaging', *Nat Protoc*, 3: 941-7.

Roidl, D., N. Hellbach, P. P. Bovio, A. Villarreal, S. Heidrich, S. Nestel, B. A. Gruning, U. Boenisch, and T. Vogel. 2016. 'DOT1L Activity Promotes Proliferation and Protects Cortical Neural Stem Cells from Activation of ATF4-DDIT3-Mediated ER Stress In Vitro', *Stem Cells*, 34: 233-45.

Ryan, T. J., and P. W. Frankland. 2022. 'Forgetting as a form of adaptive engram cell plasticity', *Nat Rev Neurosci*, 23: 173-86.

Sage, J., G. J. Mulligan, L. D. Attardi, A. Miller, S. Chen, B. Williams, E. Theodorou, and T. Jacks. 2000. 'Targeted disruption of the three Rb-related genes leads to loss of G(1) control and immortalization', *Genes Dev*, 14: 3037-50.

Sahay, A., K. N. Scobie, A. S. Hill, C. M. O'Carroll, M. A. Kheirbek, N. S. Burghardt, A. A. Fenton, A. Dranovsky, and R. Hen. 2011. 'Increasing adult hippocampal neurogenesis is sufficient to improve pattern separation', *Nature*, 472: 466-70.

Santidrian, A. F., A. Matsuno-Yagi, M. Ritland, B. B. Seo, S. E. LeBoeuf, L. J. Gay, T. Yagi, and B. Felding-Habermann. 2013. 'Mitochondrial complex I activity and NAD+/NADH balance regulate breast cancer progression', *J Clin Invest*, 123: 1068-81.

Sato, H., M. Tamba, T. Ishii, and S. Bannai. 1999. 'Cloning and expression of a plasma membrane cystine/glutamate exchange transporter composed of two distinct proteins', *J Biol Chem*, 274: 11455-8.

Saxe, M. D., F. Battaglia, J. W. Wang, G. Malleret, D. J. David, J. E. Monckton, A. D. Garcia, M. V. Sofroniew, E. R. Kandel, L. Santarelli, R. Hen, and M. R. Drew. 2006. 'Ablation of hippocampal neurogenesis impairs contextual fear conditioning and synaptic plasticity in the dentate gyrus', *Proc Natl Acad Sci U S A*, 103: 17501-6.

Scharfman, H. E., and R. Hen. 2007. 'Neuroscience. Is more neurogenesis always better?', *Science*, 315: 336-8.

Schindelin, J., I. Arganda-Carreras, E. Frise, V. Kaynig, M. Longair, T. Pietzsch, S. Preibisch, C. Rueden, S. Saalfeld, B. Schmid, J. Y. Tinevez, D. J. White, V. Hartenstein, K. Eliceiri, P. Tomancak, and A. Cardona. 2012. 'Fiji: an open-source platform for biological-image analysis', *Nat Methods*, 9: 676-82.

Schwartz, J. P., J. V. Passonneau, G. S. Johnson, and I. Pastan. 1974. 'The effect of growth conditions on NAD+ and NADH concentrations and the NAD+:NADH ratio in normal and transformed fibroblasts', *J Biol Chem*, 249: 4138-43.

Sena, L. A., and N. S. Chandel. 2012. 'Physiological roles of mitochondrial reactive oxygen species', *Mol Cell*, 48: 158-67.

Sharma, V., R. Sood, A. Khlaifia, M. J. Eslamizade, T. Y. Hung, D. Lou, A. Asgarihafshejani, M. Lalzar, S. J. Kiniry, M. P. Stokes, N. Cohen, A. J. Nelson, K. Abell, A. P. Possemato, S. Gal-Ben-Ari, V. T. Truong, P. Wang, A. Yiannakas, F. Saffarzadeh, A. C. Cuello, K. Nader, R. J. Kaufman, M. Costa-Mattioli, P. V. Baranov, A. Quintana, E. Sanz, A. Khoutorsky, J. C. Lacaille, K. Rosenblum, and N. Sonenberg. 2020. 'eIF2alpha controls memory consolidation via excitatory and somatostatin neurons', *Nature*, 586: 412-16.

Shih, A. Y., H. Erb, X. Sun, S. Toda, P. W. Kalivas, and T. H. Murphy. 2006. 'Cystine/glutamate exchange modulates glutathione supply for neuroprotection from oxidative stress and cell proliferation', *J Neurosci*, 26: 10514-23.

Shin, J., D. A. Berg, Y. Zhu, J. Y. Shin, J. Song, M. A. Bonaguidi, G. Enikolopov, D. W. Nauen, K. M. Christian, G. L. Ming, and H. Song. 2015. 'Single-Cell RNA-Seq with Waterfall Reveals Molecular Cascades underlying Adult Neurogenesis', *Cell Stem Cell*, 17: 360-72.

Shors, T. J., G. Miesegaes, A. Beylin, M. Zhao, T. Rydel, and E. Gould. 2001. 'Neurogenesis in the adult is involved in the formation of trace memories', *Nature*, 410: 372-6.

Shyh-Chang, N., G. Q. Daley, and L. C. Cantley. 2013. 'Stem cell metabolism in tissue development and aging', *Development*, 140: 2535-47.

Sierra, A., S. Martin-Suarez, R. Valcarcel-Martin, J. Pascual-Brazo, S. A. Aelvoet, O. Abiega, J. J. Deudero, A. L. Brewster, I. Bernales, A. E. Anderson, V. Baekelandt, M. Maletic-Savatic, and J. M. Encinas. 2015. 'Neuronal hyperactivity accelerates depletion of neural stem cells and impairs hippocampal neurogenesis', *Cell Stem Cell*, 16: 488-503.

Snyder, J. S., N. S. Hong, R. J. McDonald, and J. M. Wojtowicz. 2005. 'A role for adult neurogenesis in spatial long-term memory', *Neuroscience*, 130: 843-52.

Srinivas, S., T. Watanabe, C. S. Lin, C. M. William, Y. Tanabe, T. M. Jessell, and F. Costantini. 2001. 'Cre reporter strains produced by targeted insertion of EYFP and ECFP into the ROSA26 locus', *BMC Dev Biol*, 1: 4.

Stein, L. R., and S. Imai. 2014. 'Specific ablation of Nampt in adult neural stem cells recapitulates their functional defects during aging', *EMBO J*, 33: 1321-40.

Su, X., V. Gopalakrishnan, D. Stearns, K. Aldape, F. F. Lang, G. Fuller, E. Snyder, C. G. Eberhart, and S. Majumder. 2006. 'Abnormal expression of REST/NRSF and Myc in neural stem/progenitor cells causes cerebellar tumors by blocking neuronal differentiation', *Mol Cell Biol*, 26: 1666-78.

Sueda, R., I. Imayoshi, Y. Harima, and R. Kageyama. 2019. 'High Hes1 expression and resultant Ascl1 suppression regulate quiescent vs. active neural stem cells in the adult mouse brain', *Genes Dev*, 33: 511-23.

Suh, H., A. Consiglio, J. Ray, T. Sawai, K. A. D'Amour, and F. H. Gage. 2007. 'In vivo fate analysis reveals the multipotent and self-renewal capacities of Sox2+ neural stem cells in the adult hippocampus', *Cell Stem Cell*, 1: 515-28.

Sun, X., and J. C. St John. 2016. 'The role of the mtDNA set point in differentiation, development and tumorigenesis', *Biochem J*, 473: 2955-71.

Sun, Y., X. Lin, B. Liu, Y. Zhang, W. Li, S. Zhang, F. He, H. Tian, X. Zhu, X. Liu, J. Wu, J. Cai, and M. Li. 2021. 'Loss of ATF4 leads to functional aging-like attrition of adult hematopoietic stem cells', *Sci Adv*, 7: eabj6877.

Swartzlander, D. B., N. E. Propson, E. R. Roy, T. Saito, T. Saido, B. Wang, and H. Zheng. 2018. 'Concurrent cell type-specific isolation and profiling of mouse brains in inflammation and Alzheimer's disease', *JCI Insight*, 3.

Takahashi, Y., J. B. Rayman, and B. D. Dynlacht. 2000. 'Analysis of promoter binding by the E2F and pRB families in vivo: distinct E2F proteins mediate activation and repression', *Genes Dev*, 14: 804-16.

Tan, D. Q., and T. Suda. 2018. 'Reactive Oxygen Species and Mitochondrial Homeostasis as Regulators of Stem Cell Fate and Function', *Antioxid Redox Signal*, 29: 149-68.

Taverna, E., M. Gotz, and W. B. Huttner. 2014. 'The cell biology of neurogenesis: toward an understanding of the development and evolution of the neocortex', *Annu Rev Cell Dev Biol*, 30: 465-502.

Teo, A. K., S. J. Arnold, M. W. Trotter, S. Brown, L. T. Ang, Z. Chng, E. J. Robertson, N. R. Dunn, and L. Vallier. 2011. 'Pluripotency factors regulate definitive endoderm specification through eomesodermin', *Genes Dev*, 25: 238-50.

Terreros-Roncal, J., E. P. Moreno-Jimenez, M. Flor-Garcia, C. B. Rodriguez-Moreno, M. F. Trinchero, F. Cafini, A. Rabano, and M. Llorens-Martin. 2021. 'Impact of neurodegenerative diseases on human adult hippocampal neurogenesis', *Science*, 374: 1106-13.

Tiklova, K., A. K. Bjorklund, L. Lahti, A. Fiorenzano, S. Nolbrant, L. Gillberg, N. Volakakis, C. Yokota, M. M. Hilscher, T. Hauling, F. Holmstrom, E. Joodmardi, M. Nilsson, M. Parmar, and T. Perlmann. 2019. 'Single-cell RNA sequencing reveals midbrain dopamine neuron diversity emerging during mouse brain development', *Nat Commun*, 10: 581.

Toda, T., S. L. Parylak, S. B. Linker, and F. H. Gage. 2019. 'The role of adult hippocampal neurogenesis in brain health and disease', *Mol Psychiatry*, 24: 67-87.

Torrence, M. E., M. R. MacArthur, A. M. Hosios, A. J. Valvezan, J. M. Asara, J. R. Mitchell, and B. D. Manning. 2021. 'The mTORC1-mediated activation of ATF4 promotes protein and glutathione synthesis downstream of growth signals', *Elife*, 10.

Treves, A., A. Tashiro, M. P. Witter, and E. I. Moser. 2008. 'What is the mammalian dentate gyrus good for?', *Neuroscience*, 154: 1155-72.

Tuncdemir, S. N., C. O. Lacefield, and R. Hen. 2019. 'Contributions of adult neurogenesis to dentate gyrus network activity and computations', *Behav Brain Res*, 374: 112112.

Urban, N., I. M. Blomfield, and F. Guillemot. 2019. 'Quiescence of Adult Mammalian Neural Stem Cells: A Highly Regulated Rest', *Neuron*, 104: 834-48.

Urban, N., and T. H. Cheung. 2021. 'Stem cell quiescence: the challenging path to activation', *Development*, 148.

Urban, N., D. L. van den Berg, A. Forget, J. Andersen, J. A. Demmers, C. Hunt, O. Ayrault, and F. Guillemot. 2016. 'Return to quiescence of mouse neural stem cells by degradation of a proactivation protein', *Science*, 353: 292-5.

van Galen, P., N. Mbong, A. Kreso, E. M. Schoof, E. Wagenblast, S. W. K. Ng, G. Krivdova, L. Jin, H. Nakauchi, and J. E. Dick. 2018. 'Integrated Stress Response Activity Marks Stem Cells in Normal Hematopoiesis and Leukemia', *Cell Rep*, 25: 1109-17 e5.

van Praag, H., G. Kempermann, and F. H. Gage. 1999. 'Running increases cell proliferation and neurogenesis in the adult mouse dentate gyrus', *Nat Neurosci*, 2: 266-70.

van Praag, H., T. Shubert, C. Zhao, and F. H. Gage. 2005. 'Exercise enhances learning and hippocampal neurogenesis in aged mice', *J Neurosci*, 25: 8680-5.

Vandenbosch, R., A. Clark, B. C. Fong, S. Omais, C. Jaafar, D. Dugal-Tessier, J. Dhaliwal, D. C. Lagace, D. S. Park, N. Ghanem, and R. S. Slack. 2016. 'RB regulates the production and the survival of newborn neurons in the embryonic and adult dentate gyrus', *Hippocampus*, 26: 1379-92.

Vanderluit, J. L., K. L. Ferguson, V. Nikoletopoulou, M. Parker, V. Ruzhynsky, T. Alexson, S. M. McNamara, D. S. Park, M. Rudnicki, and R. S. Slack. 2004. 'p107 regulates neural precursor cells in the mammalian brain', *J Cell Biol*, 166: 853-63.

Vanderluit, J. L., C. A. Wylie, K. A. McClellan, N. Ghanem, A. Fortin, S. Callaghan, J. G. MacLaurin, D. S. Park, and R. S. Slack. 2007. 'The Retinoblastoma family member p107 regulates the rate of progenitor commitment to a neuronal fate', *J Cell Biol*, 178: 129-39.

Varanita, T., M. E. Soriano, V. Romanello, T. Zaglia, R. Quintana-Cabrera, M. Semenzato, R. Menabo, V. Costa, G. Civiletto, P. Pesce, C. Viscomi, M. Zeviani, F. Di Lisa, M. Mongillo, M. Sandri, and L. Scorrano. 2015. 'The OPA1-dependent mitochondrial cristae remodeling pathway controls atrophic, apoptotic, and ischemic tissue damage', *Cell Metab*, 21: 834-44.

Viatour, P., T. C. Somervaille, S. Venkatasubrahmanyam, S. Kogan, M. E. McLaughlin, I. L. Weissman, A. J. Butte, E. Passegue, and J. Sage. 2008. 'Hematopoietic stem cell quiescence is maintained by compound contributions of the retinoblastoma gene family', *Cell Stem Cell*, 3: 416-28.

Villeda, S. A., J. Luo, K. I. Mosher, B. Zou, M. Britschgi, G. Bieri, T. M. Stan, N. Fainberg, Z. Ding, A. Eggel, K. M. Lucin, E. Czirr, J. S. Park, S. Couillard-Despres, L. Aigner, G. Li, E. R. Peskind, J. A. Kaye, J. F. Quinn, D. R. Galasko, X. S. Xie, T. A. Rando, and T. Wyss-Coray. 2011. 'The ageing systemic milieu negatively regulates neurogenesis and cognitive function', *Nature*, 477: 90-4.

Vorhees, C. V., and M. T. Williams. 2006. 'Morris water maze: procedures for assessing spatial and related forms of learning and memory', *Nat Protoc*, 1: 848-58.

Walker, T. L., and G. Kempermann. 2014. 'One mouse, two cultures: isolation and culture of adult neural stem cells from the two neurogenic zones of individual mice', *J Vis Exp*: e51225.

Wallace, D. C., W. Fan, and V. Procaccio. 2010. 'Mitochondrial energetics and therapeutics', *Annu Rev Pathol*, 5: 297-348.

Wang, W., Y. Esbensen, D. Kunke, R. Suganthan, L. Rachek, M. Bjoras, and L. Eide. 2011. 'Mitochondrial DNA damage level determines neural stem cell differentiation fate', *J Neurosci*, 31: 9746-51.

Wang, W., P. Osenbroch, R. Skinnes, Y. Esbensen, M. Bjoras, and L. Eide. 2010. 'Mitochondrial DNA integrity is essential for mitochondrial maturation during differentiation of neural stem cells', *Stem Cells*, 28: 2195-204.

Wei, P., K. K. Dove, C. Bensard, J. C. Schell, and J. Rutter. 2018. 'The Force Is Strong with This One: Metabolism (Over)powers Stem Cell Fate', *Trends Cell Biol*.

Wong, H. S., P. A. Dighe, V. Mezera, P. A. Monternier, and M. D. Brand. 2017. 'Production of superoxide and hydrogen peroxide from specific mitochondrial sites under different bioenergetic conditions', *J Biol Chem*, 292: 16804-09.

Wrann, C. D., J. P. White, J. Salogiannnis, D. Laznik-Bogoslavski, J. Wu, D. Ma, J. D. Lin, M. E. Greenberg, and B. M. Spiegelman. 2013. 'Exercise induces hippocampal BDNF through a PGC-1alpha/FNDC5 pathway', *Cell Metab*, 18: 649-59.

Wu, Z., P. Puigserver, U. Andersson, C. Zhang, G. Adelmant, V. Mootha, A. Troy, S. Cinti, B. Lowell, R. C. Scarpulla, and B. M. Spiegelman. 1999. 'Mechanisms controlling mitochondrial biogenesis and respiration through the thermogenic coactivator PGC-1', *Cell*, 98: 115-24.

Yang, W. S., R. SriRamaratnam, M. E. Welsch, K. Shimada, R. Skouta, V. S. Viswanathan, J. H. Cheah, P. A. Clemons, A. F. Shamji, C. B. Clish, L. M. Brown, A. W. Girotti, V. W. Cornish, S. L. Schreiber, and B. R. Stockwell. 2014. 'Regulation of ferroptotic cancer cell death by GPX4', *Cell*, 156: 317-31.

Zhang, H., D. Ryu, Y. Wu, K. Gariani, X. Wang, P. Luan, D. D'Amico, E. R. Ropelle, M. P. Lutolf, R. Aebersold, K. Schoonjans, K. J. Menzies, and J. Auwerx. 2016. 'NAD(+) repletion improves mitochondrial and stem cell function and enhances life span in mice', *Science*, 352: 1436-43.

Zhang, Z., N. Wakabayashi, J. Wakabayashi, Y. Tamura, W. J. Song, S. Sereda, P. Clerc, B. M. Polster, S. M. Aja, M. V. Pletnikov, T. W. Kensler, O. S. Shirihai, M. Iijima, M. A. Hussain, and H. Sesaki. 2011. 'The dynamin-related GTPase Opa1 is required for glucose-stimulated ATP production in pancreatic beta cells', *Mol Biol Cell*, 22: 2235-45.

Zhao, X., E. S. Fisher, Y. Wang, K. Zuloaga, L. Manley, and S. Temple. 2022. '4D imaging analysis of the aging mouse neural stem cell niche reveals a dramatic loss of progenitor cell dynamism regulated by the RHO-ROCK pathway', *Stem Cell Reports*, 17: 245-58.

Zheng, G. X., J. M. Terry, P. Belgrader, P. Ryvkin, Z. W. Bent, R. Wilson, S. B. Ziraldo, T. D. Wheeler, G. P. McDermott, J. Zhu, M. T. Gregory, J. Shuga, L. Montesclaros, J. G. Underwood, D. A. Masquelier, S. Y. Nishimura, M. Schnall-Levin, P. W. Wyatt, C. M. Hindson, R. Bharadwaj, A. Wong, K. D. Ness, L. W. Beppu, H. J. Deeg, C. McFarland, K. R. Loeb, W. J. Valente, N. G. Ericson, E. A. Stevens, J. P. Radich, T. S. Mikkelsen, B. J. Hindson, and J. H. Bielas. 2017. 'Massively parallel digital transcriptional profiling of single cells', *Nat Commun*, 8: 14049.

Zheng, X., L. Boyer, M. Jin, J. Mertens, Y. Kim, L. Ma, L. Ma, M. Hamm, F. H. Gage, and T. Hunter. 2016. 'Metabolic reprogramming during neuronal differentiation from aerobic glycolysis to neuronal oxidative phosphorylation', *Elife*, 5.

Zuchner, S., I. V. Mersiyanova, M. Muglia, N. Bissar-Tadmouri, J. Rochelle, E. L. Dadali, M. Zappia, E. Nelis, A. Patitucci, J. Senderek, Y. Parman, O. Evgrafov, P. D. Jonghe, Y. Takahashi, S. Tsuji, M. A. Pericak-Vance, A. Quattrone, E. Battaloglu, A. V. Polyakov, V. Timmerman, J. M. Schroder, and J. M. Vance. 2004. 'Mutations in the mitochondrial GTPase mitofusin 2 cause Charcot-Marie-Tooth neuropathy type 2A', *Nat Genet*, 36: 449-51.

APPENDIX I:

Direct FACS Isolation of Neural Stem/Progenitor Lineages from the Adult Brain

Mohamed Ariff Iqbal, Bensun C. Fong, and Ruth S. Slack

Book chapter

Neuronal Cell Death: Methods and Protocols,

Methods in Molecular Biology, vol. 2515,

https://doi.org/10.1007/978-1-0716-2409-8_8

Direct FACS isolation of neural stem/progenitor lineages from the adult brain

Mohamed Ariff Iqbal, Bensun Fong, Ruth S Slack*

University of Ottawa Brain and Mind Research Institute, Dept of Cellular and Molecular Medicine, Faculty of Medicine, University of Ottawa

*Correspondence to: rslack@uottawa.ca

Abstract

Adult neural stem and progenitor cells reside in the neurogenic niche of the adult brain and have tremendous potential in regenerative medicine. Compelling evidence suggests that adult neurogenesis plays an important role in hippocampal memory formation, plasticity, and mood regulation. Understanding the mechanisms that regulate the function of neural stem/progenitor cells within the brain is a critical step for the development of regenerative strategies to maintain or enhance neurological function. A major challenge in studying these cells is the limited cell number of adult neural stem cells, and the significant changes in their properties induced by *in vitro* culture and expansion. To best understand the regulation of these cells, they must be studied within their niche context. In this chapter, we provide a simplified protocol for the harvest and isolation of neural stem cell lineages directly from the murine brain, to provide input material for single-cell RNA-seq. This approach will elucidate the true transcriptional signatures and activated pathways in neural stem cell lineages, within the context of their niche environment.

Running title: FACS isolation of neural stem cells

Keywords: Neural stem and progenitor cells, FACS, Transcriptomics, Single-cell RNA seq

1. Introduction

The mammalian brain is a complex tissue comprised of diverse cell types. Modern studies have revealed compelling evidence that adult neurogenesis plays an important role in learning and memory (Snyder et al. 2005). During this process, neural stem (NSC) and progenitor cells (collectively called NSPCs) continually divide and diversify into adult born neurons; their continual integration into the existing neural circuitry is important and has been shown to promote brain plasticity. These cells dynamically respond to the environment to modify the level of integration allowing maturation of the circuits, thus creating a dynamic system (Pilz et al. 2018; Harris et al. 2021b). This process is involved in new learning and memory formation (Alvarez-Buylla and Temple 1998). Recently, the adult human brain was shown to exhibit hippocampal circuit plasticity through adult hippocampal neurogenesis. This finding has implications for pathological conditions such as Alzheimer's Disease (AD) where adult neurogenesis is impaired (Moreno-Jimenez et al. 2019). Understanding these elaborate networks begins with fundamental analysis of the individual function of NSPCs and their journey.

In adult mice, NSCs and their progeny persist in restricted neurogenic niches, the most well-established being the ventricular-subventricular zone (SVZ) and the subgranular zone (SGZ) of the hippocampal dentate gyrus (DG). The stem cell niche maintains and specifies distinct cell types derived from quiescent stem cells, proceeding through the processes of activation, self-renewal, differentiation, and neuronal commitment. These processes are tightly regulated in NSPCs, receiving input from intrinsic signals as well as signals derived from the surrounding niche (Shin et al. 2015). There is further compelling evidence that the adult stem cell population is severely affected by aging, brain injury and during the pathology of neurodegenerative disease (Llorens-Bobadilla et al. 2015; Moreno-Jimenez et al. 2019; Harris et al. 2021a).

A major challenge in studying adult NSPC cell biology, however, is the limited number of these cells, and that, *in vitro* expansion of these cells disrupts their properties and signaling mechanisms

due to the loss of critical interactions within their niche in the brain. Thus, to best understand the molecular mechanisms that control adult NSPC function and cellular response in the context of health and disease, NSPCs and their progeny should be isolated directly from the adult brain for biochemical and molecular analysis. Along with *in vivo* assessment, fluorescent activated cell sorting (FACS) has been used to isolate and enrich different cell types to study their function as an improvement over isolation during *in vitro* culture (Pastrana, Cheng, and Doetsch 2009).

In this chapter, we present a modified protocol for the streamlined isolation of adult NSPCs that can be used for numerous applications. We discuss utilization of transgenic mice with reporter genes combining immunofluorescence-based enrichment of NSCs and their derivatives. Upon enrichment, these cells can be used as input for downstream functional analysis such as bulk or single cell RNA sequencing. This experimental setup and sorting strategy allows us to perform a rapid harvest of healthy brain derived NSPCs (neural stem and progenitor cells) with minimal intervention.

2. Materials

2.1. Equipment and reagents

Dissecting stereo microscope (Leica MZ6)

Scissors

Dumont #5 - Fine Forceps (Fine Science Cat. # 11254-20)

Adult Mouse Brain Slicer Matrix (Zivic Cat. # BSMAS005-1)

Razor Blades (single edge)

Scalpel handle #3

Scalpel blade #15 (Bard-Parker)

250 mL Stericup Filter Unit

2.2. Preparation of Solutions:

2.2.1. Artificial Cerebro-Spinal Fluid: 26 mM NaHCO3, 124 mM NaCl, 5 mM KCl, 2 mM CaCl2*2H2O, 1.3 mM MgCl2*6H2O, Pen/Strep (TC) 1X, dissolved in Sterile Water, adjust pH to 7.4 and then sterile filtered.

2.2.2 Digestion medium: 20 U/ml Papain Suspension (Worthington Cat. PAP3126), 1.2 mM EDTA (Invitrogen Cat. # 15675-038), resuspended in DMEM/F12 (without phenol red) Invitrogen Life Tech. Cat. # 21041-025. Prepared in fresh and in sterile environment. Prior to brain dissection, incubate in 37˚C to resuspend Papain.

2.2.3 Resuspension buffer**:** 0.5 mg/mL DNASE 1 (Roche Cat. # 11284932001), 10% fetal bovine serum, resuspended in DMEM/F12 (without phenol red).

2.2.4. Cre-inducible reporter mice: Nestin CreER^{T2}:Rosa26^{YFP}(Jackson lab).

2.2.5. anti-CD15 (SSEA-1) antibody conjugated to a fluorescent probe (BD Cat. # 560120).

2.2.6. pentobarbital sodium solution

3. Methods

3.1. Animal models

Our goal is to enrich NSPCs from the tissue derived cell suspension. There are several animal models available to discern the desired cell fraction from the pool. Utilization of transgenic animals facilitates design of Cre-inducible reporters to stably express reporter fluorescent proteins under certain cell marker promoters (Kuhn et al. 2016), some are listed below (***see*** Note #1). Upon expression of desired gene, the clones and their derivatives can be traced, isolated, and stained using cellular markers. (A list of relevant cell type markers are listed in this review (Dhaliwal and Lagace 2011) (and ***see*** Note #2). Using such reporters, the cells of interest are constitutively labelled prior to FACS. Similarly, viral vectors with reporter proteins can be utilized to label cells in specific regions prior to being processed for FACS. The details of each step as follows.

3.2. set up

1. Prepare the solutions as described. ACSF can be prepared one day in advance, the remainder the morning of dissection.
2. Place the sterile filtered ACSF in a -80 ˚C freezer for 30 minutes prior to dissections. Every 10 minutes, agitate the ACSF to form a “slush” consistency. (Once dissection has started, slushy ACSF can be maintained, short-term, in a 4 ˚C fridge).
3. Place the matrix on ice to chill.
4. Immediately prior to dissections, fill a small petri dish or wells of a 6-well plate (useful for multiple conditions) with chilled ACSF, and place in ice bucket.
5. Procedures are done in aseptic environment; surface clean all dissection tools with 70% ethanol.
6. Set up the dissection microscope with light source from bottom.

3.3. Brain dissection

1. Euthanize 8–12-week-old mice with euthanyl (pentobarbital sodium) via intraperitoneal injection (120mg/Kg). Once the animal no longer responds to force test of limbs, perform cervical dislocation with forceps and decapitation using scissors.
2. Using scissors, cut into the skull at the base of the spinal cord as well as between the eye sockets. From these points, use the scissors to lightly score the midline of the brain without harming the brain underneath.
3. Using your forceps, gently pry skull from the scored midline to expose the intact brain. Then, clip/remove the meninges covering the brain (running along the midline from the olfactory bulb), before scooping the brain from the skull, starting from the olfactory bulb. From the ventral side, clip the cranial nerves to detach the brain.
4. Collect the dissected brain into the petri dish / 6-well plate containing chilled ACSF.

3.4. Brain slicing

1. On the dissection scope, place two 100mm petri dishes side by side. On the left, place the chilled matrix adjacent to the wall of the dish. On the right, place petri dish for dissection directly under the microscope.
2. Fill Eppendorf tubes with 500 µl ACSF per condition.
3. Pour ACSF over matrix and into dissection dish.

4. Move first brain to matrix, and place 1st razor blade into matrix (at approx. -1mm from Bregma for SVZ, +1mm from Bregma for DG), balancing other edge of the blade on the wall of the petri dish. Moving rostrally, place blades into alternating matrix slots (1mm spacing) until olfactory bulbs are reached.
5. Move the matrix away from the wall of the petri dish and slice all razor blades at once to generate 1mm coronal sections suitable for SVZ/DG dissection. Transfer to dissection plate containing slushy ACSF, using scalpel to separate tissue from the razor blades. (**See** figure 1).

3.5. Microdissection of SVZ and SGZ

1. Coronal slices allow micro-dissection of the SVZ and DG using the forceps and scalpel. Use these tools to gently pull apart the tissue along the medial-lateral axis to expose the lateral ventricles and isolate the SVZ (***See*** Note #3 for more information).
2. To collect the SGZ, trace the hippocampal formation. Using the sharp forceps, or optionally a fine-gauge needle, trim the excess off the hippocampus to separate the desired suprapyramidal and infrapyramidal blades of the DG, from the CA1 and CA3 (***See*** Note #4&5 for more information).
3. To collect substantia nigra, collect the coronal sections of the mouse mid-brain where the hippocampus is further lateral (***See*** figure 2).
4. Collect the dissected tissues in the prepared Eppendorf tubes containing chilled ACSF.
5. Repeat for all brains and conditions (***See*** Note #6 for more information).

3.6. Enzymatic digestion of each condition

6. Use a scalpel to break up dissected tissue, cutting against the tube in vertical motions. Precautions should be taken to avoid sample to sample contamination.
7. Carefully pipette out excess ACSF remaining inside the 1.5ml tube. Do not aspirate to avoid sample loss.
8. Add 500 µl Digestion Media per 1.5ml tube with dissected tissue. This is optimized for the SVZ of 2-3 mice and can be scaled up as needed.
9. Incubate for 10 minutes in a 37˚C shaker incubator at gentle rotation at 130 rpm.
10. After 10 minutes, add equal volume (in this case 500 µl) of Resuspension Media. Transfer to a new 15mL falcon tube, and slowly triturate 5-10 times with a P1000 micropipette.
11. Incubate at room temperature for 5 minutes to let large chunks settle out. Transfer majority of supernatant to a new 15 mL tube and then repeat with another 1 ml of Resuspension Media. If no further chunks are seen after the initial settle, transfer immediately and proceed to next step.
12. During the incubation, prepare a 100% Percoll-PBS buffer solution, from 9 parts Percoll to 1-part 10X PBS. Make sure to inverse Percoll bottle prior to use. Subsequently, also mix Percoll-PBS solution by inversion.
13. After trituration, add an additional ~1.9 mL of Resuspension Media to bring final volume to 3.9 mL. Add 1.1 ml of Percoll-PBS, to a final concentration of 22% vol/vol Percoll. Cap, and mix by inversion 5x to evenly distribute Percoll in the solution (***See*** Note #7 for more information).
14. Centrifuge the cell suspension at 4˚C for 12.5 mins at 500 x g.

15. Proceed along Options Immunostain- or reporter-based isolation.

3.7. FACS of NSPCs (Immunostain-based)

1. In this example, we will employ an antibody against the cell surface marker, CD-15 (SSEA), following the manufacturer's specifications for the antibody of choice.
2. During the centrifugation, prepare Incubation Media: 15 mL of DMEM:F12 without Phenol Red, containing 1% Bovine Serum Albumin (BSA). As well, prepare a separate 15 mL Falcon tube containing 1 mL of DMEM:F12 without Phenol Red, for the unstained control.
3. Once centrifugation is done, aspirate supernatant and resuspend cells in 200 µl of Incubation Media.
4. At this stage, add a small amount (5 µl) of cell suspension to the prepared Falcon tube containing 1mL of DMEM:F12 without Phenol Red. Resuspend (Unstained control for FACS gating).
5. Add 50 µl of anti-CD15 (SSEA-1) antibody conjugated to a fluorescent probe (BD Cat. # 560120), performed in the dark. Propidium iodide can be used to eliminate undesired dead cells.
6. Place cells inside an ice bucket and incubate in 4˚C fridge for 15 minutes.
7. Resuspend cells in 5 mL of Incubation Media, then centrifuge cells at 4 ˚C for 4 mins at 900 x g, to wash out remaining antibody.
8. Follow steps below, additionally providing the unstained control to set up FACS gating to isolate CD15-positive population.

3.8. FACS of NSPCs (Reporter-based)

1. Once centrifugation is done (***procedure*** 3.6-15), aspirate supernatant and resuspend cells in 700 µL of DMEM:F12 without Phenol Red.
2. Cell suspension can now be sorted using FACS. For single-cell RNASeq, Propidium Iodide is used as a cell viability stain (***See*** Note #8 for further details).
3. If collecting for RNA isolation, decontaminate the flow cytometer with RNaseZAPP prior to FACS. Then, collect into tubes containing DMEM:F12 with Phenol Red (this will distinguish tubes in the event of a label mix-up).
4. Freshly isolated cells can be used for downstream assays without further delay (***See*** Note #9&10 for more information).
5. If desired to store the cells for RNA extraction, the isolated cells can be collected at 4 ˚C for 5 mins at 900 x g, remove the media and store at -80 ˚C (***See*** Note #11 for more information).

4. Notes

1. List of transgenic reporter mice for targeted NSPC population: NSPCs, Nestin-CreERT2 (Pastrana, Cheng, and Doetsch 2009), GFAP:GFP (Beckervordersandforth et al. 2010), Glast-CreERT2(Llorens-Bobadilla et al. 2015); Activated NSCs, Ascl1-CreERT2 (Codega et al. 2014; Bottes et al. 2021; Pilz et al. 2018); Cell cycle label retaining cells, H2B:GFP (Kalamakis et al. 2019); Quiescent NSCs, Gli1-CreERT2 (Codega et al. 2014; Bottes et al. 2021); Neuroblasts, Dcx-eGFP (Couillard-Despres et al. 2006); Astrocytes, GFAP-CreERT2, Glast-CreERT2 Aldh1l1–eGFP (John Lin et al. 2017); Dopaminergic neurons, Pitx3eGFP, Slc6a3::Cre (Tiklova et al. 2019; Poulin et al. 2014)

2. List of immune-labelling markers for targeted NSPC population: Slow dividing NSCs, CD15, LIF, Lex (Morizur et al. 2018); Activated NSCs, $GFAP^+CD133^+EGFR^+$ (Codega et al. 2014); Quiescent NSCs, $GFAP^+CD133^+EGFR^-$ (Codega et al. 2014); Neuroblasts, CD24+ (Pastrana, Cheng, and Doetsch 2009); Astrocytes, $GFAP^+$ (Pastrana, Cheng, and Doetsch 2009); Proliferation, EdU and BrdU (Kuhn et al. 2016); PAN Neurons, NeuN (Guez-Barber et al. 2012); Dopaminergic neurons, $NeuN^+TH^+$ (Poulin et al. 2014); Microglia, CD45, CD11b (Swartzlander et al. 2018; Guneykaya et al. 2018); Endothelial cells, CD13, CD71 (Crouch and Doetsch 2018; Guez-Barber et al. 2012).
3. The dissection method is designed for ease of landmark recognition and assumes more intuitive knowledge of structure based on multiple coronal sections than similar anatomical methods described elsewhere (Walker and Kempermann 2014).
4. The NSPC isolation/purification method is largely based on the method employed by *Codega et al* and *Pastrana et al* (Codega et al. 2014; Pastrana, Silva-Vargas, and Doetsch 2011), with modifications to improve efficiency and to alternately employ DMEM:F12 and fetal bovine serum (FBS).
5. Because of the delicate nature of the process, all the procedures are performed on ice or at 4 ˚C unless otherwise specified (e.g., Papain digestion).
6. Microdissections are done at narrowed boundaries to limit collecting unintended regions.
7. The 22% Percoll gradient is used to remove interconnected myelin from the cell body that might interfere with downstream processing. The advantages of the 22% Percoll gradient have been described elsewhere (Babu et al. 2011). Minimizing percoll presence after the isolation improves viability.
8. Maintaining enhanced cell viability throughout is essential to increase cell recovery. Using propidium iodide labelling to eliminate dead cells and performing a hemocytometer count (with Trypan blue) of live cells post-sort will provide precise quantification of cells for downstream analysis.
9. Minimizing the number of spins to concentrate cells will enhance cell viability and decrease *in-vitro* stress. If there is concern over the FACS input despite the optimized protocol, we recommend maintaining singlet fraction using a 40 μM P1000-mounted tip filter. Avoiding clumping improves FACS efficiency.
10. Isolating intact cells with minimal dead cells provide low ambient RNA in the cell suspension, which is crucial for single cell RNA sequencing.
11. In summary, the cells obtained will enable analysis of cells directly from the brain in their niche context and will yield valuable information on the NSPC transcriptome and signaling pathways through bulk or single cell RNA-seq analysis.

References

1. Snyder JS, Hong NS, McDonald RJ, Wojtowicz JM (2005) A role for adult neurogenesis in spatial long-term memory. Neuroscience 130 (4):843-852. doi:10.1016/j.neuroscience.2004.10.009

2. Pilz GA, Bottes S, Betizeau M, Jorg DJ, Carta S, Simons BD, Helmchen F, Jessberger S (2018) Live imaging of neurogenesis in the adult mouse hippocampus. Science 359 (6376):658-662. doi:10.1126/science.aao5056

3. Harris L, Rigo P, Stiehl T, Gaber ZB, Austin SHL, Masdeu MDM, Edwards A, Urban N, Marciniak-Czochra A, Guillemot F (2021) Coordinated changes in cellular behavior ensure the

lifelong maintenance of the hippocampal stem cell population. Cell Stem Cell. doi:10.1016/j.stem.2021.01.003
4. Alvarez-Buylla A, Temple S (1998) Stem cells in the developing and adult nervous system. J Neurobiol 36 (2):105-110
5. Moreno-Jimenez EP, Flor-Garcia M, Terreros-Roncal J, Rabano A, Cafini F, Pallas-Bazarra N, Avila J, Llorens-Martin M (2019) Adult hippocampal neurogenesis is abundant in neurologically healthy subjects and drops sharply in patients with Alzheimer's disease. Nat Med 25 (4):554-560. doi:10.1038/s41591-019-0375-9
6. Shin J, Berg DA, Zhu Y, Shin JY, Song J, Bonaguidi MA, Enikolopov G, Nauen DW, Christian KM, Ming GL, Song H (2015) Single-Cell RNA-Seq with Waterfall Reveals Molecular Cascades underlying Adult Neurogenesis. Cell Stem Cell 17 (3):360-372. doi:10.1016/j.stem.2015.07.013
7. Llorens-Bobadilla E, Zhao S, Baser A, Saiz-Castro G, Zwadlo K, Martin-Villalba A (2015) Single-Cell Transcriptomics Reveals a Population of Dormant Neural Stem Cells that Become Activated upon Brain Injury. Cell Stem Cell 17 (3):329-340. doi:10.1016/j.stem.2015.07.002
8. Harris L, Rigo P, Stiehl T, Gaber ZB, Austin SHL, Masdeu MDM, Edwards A, Urban N, Marciniak-Czochra A, Guillemot F (2021) Coordinated changes in cellular behavior ensure the lifelong maintenance of the hippocampal stem cell population. Cell Stem Cell 28 (5):863-876 e866. doi:10.1016/j.stem.2021.01.003
9. Pastrana E, Cheng LC, Doetsch F (2009) Simultaneous prospective purification of adult subventricular zone neural stem cells and their progeny. Proc Natl Acad Sci U S A 106 (15):6387-6392. doi:10.1073/pnas.0810407106
10. Kuhn HG, Eisch AJ, Spalding K, Peterson DA (2016) Detection and Phenotypic Characterization of Adult Neurogenesis. Cold Spring Harb Perspect Biol 8 (3):a025981. doi:10.1101/cshperspect.a025981
11. Dhaliwal J, Lagace DC (2011) Visualization and genetic manipulation of adult neurogenesis using transgenic mice. Eur J Neurosci 33 (6):1025-1036. doi:10.1111/j.1460-9568.2011.07600.x
12. Beckervordersandforth R, Tripathi P, Ninkovic J, Bayam E, Lepier A, Stempfhuber B, Kirchhoff F, Hirrlinger J, Haslinger A, Lie DC, Beckers J, Yoder B, Irmler M, Gotz M (2010) In vivo fate mapping and expression analysis reveals molecular hallmarks of prospectively isolated adult neural stem cells. Cell Stem Cell 7 (6):744-758. doi:10.1016/j.stem.2010.11.017
13. Codega P, Silva-Vargas V, Paul A, Maldonado-Soto AR, Deleo AM, Pastrana E, Doetsch F (2014) Prospective identification and purification of quiescent adult neural stem cells from their in vivo niche. Neuron 82 (3):545-559. doi:10.1016/j.neuron.2014.02.039
14. Bottes S, Jaeger BN, Pilz GA, Jorg DJ, Cole JD, Kruse M, Harris L, Korobeynyk VI, Mallona I, Helmchen F, Guillemot F, Simons BD, Jessberger S (2021) Long-term self-renewing stem cells in the adult mouse hippocampus identified by intravital imaging. Nat Neurosci 24 (2):225-233. doi:10.1038/s41593-020-00759-4
15. Kalamakis G, Brune D, Ravichandran S, Bolz J, Fan W, Ziebell F, Stiehl T, Catala-Martinez F, Kupke J, Zhao S, Llorens-Bobadilla E, Bauer K, Limpert S, Berger B, Christen U, Schmezer P, Mallm JP, Berninger B, Anders S, Del Sol A, Marciniak-Czochra A, Martin-Villalba A (2019) Quiescence Modulates Stem Cell Maintenance and Regenerative Capacity in the Aging Brain. Cell 176 (6):1407-1419 e1414. doi:10.1016/j.cell.2019.01.040
16. Couillard-Despres S, Winner B, Karl C, Lindemann G, Schmid P, Aigner R, Laemke J, Bogdahn U, Winkler J, Bischofberger J, Aigner L (2006) Targeted transgene expression in

neuronal precursors: watching young neurons in the old brain. Eur J Neurosci 24 (6):1535-1545. doi:10.1111/j.1460-9568.2006.05039.x
17. John Lin CC, Yu K, Hatcher A, Huang TW, Lee HK, Carlson J, Weston MC, Chen F, Zhang Y, Zhu W, Mohila CA, Ahmed N, Patel AJ, Arenkiel BR, Noebels JL, Creighton CJ, Deneen B (2017) Identification of diverse astrocyte populations and their malignant analogs. Nat Neurosci 20 (3):396-405. doi:10.1038/nn.4493
18. Tiklova K, Bjorklund AK, Lahti L, Fiorenzano A, Nolbrant S, Gillberg L, Volakakis N, Yokota C, Hilscher MM, Hauling T, Holmstrom F, Joodmardi E, Nilsson M, Parmar M, Perlmann T (2019) Single-cell RNA sequencing reveals midbrain dopamine neuron diversity emerging during mouse brain development. Nat Commun 10 (1):581. doi:10.1038/s41467-019-08453-1
19. Poulin JF, Zou J, Drouin-Ouellet J, Kim KY, Cicchetti F, Awatramani RB (2014) Defining midbrain dopaminergic neuron diversity by single-cell gene expression profiling. Cell Rep 9 (3):930-943. doi:10.1016/j.celrep.2014.10.008
20. Morizur L, Chicheportiche A, Gauthier LR, Daynac M, Boussin FD, Mouthon MA (2018) Distinct Molecular Signatures of Quiescent and Activated Adult Neural Stem Cells Reveal Specific Interactions with Their Microenvironment. Stem Cell Reports 11 (2):565-577. doi:10.1016/j.stemcr.2018.06.005
21. Guez-Barber D, Fanous S, Harvey BK, Zhang Y, Lehrmann E, Becker KG, Picciotto MR, Hope BT (2012) FACS purification of immunolabeled cell types from adult rat brain. J Neurosci Methods 203 (1):10-18. doi:10.1016/j.jneumeth.2011.08.045
22. Swartzlander DB, Propson NE, Roy ER, Saito T, Saido T, Wang B, Zheng H (2018) Concurrent cell type-specific isolation and profiling of mouse brains in inflammation and Alzheimer's disease. JCI Insight 3 (13). doi:10.1172/jci.insight.121109
23. Guneykaya D, Ivanov A, Hernandez DP, Haage V, Wojtas B, Meyer N, Maricos M, Jordan P, Buonfiglioli A, Gielniewski B, Ochocka N, Comert C, Friedrich C, Artiles LS, Kaminska B, Mertins P, Beule D, Kettenmann H, Wolf SA (2018) Transcriptional and Translational Differences of Microglia from Male and Female Brains. Cell Rep 24 (10):2773-2783 e2776. doi:10.1016/j.celrep.2018.08.001
24. Crouch EE, Doetsch F (2018) FACS isolation of endothelial cells and pericytes from mouse brain microregions. Nat Protoc 13 (4):738-751. doi:10.1038/nprot.2017.158
25. Walker TL, Kempermann G (2014) One mouse, two cultures: isolation and culture of adult neural stem cells from the two neurogenic zones of individual mice. J Vis Exp (84):e51225. doi:10.3791/51225
26. Pastrana E, Silva-Vargas V, Doetsch F (2011) Eyes wide open: a critical review of sphere-formation as an assay for stem cells. Cell Stem Cell 8 (5):486-498. doi:10.1016/j.stem.2011.04.007
27. Babu H, Claasen JH, Kannan S, Runker AE, Palmer T, Kempermann G (2011) A protocol for isolation and enriched monolayer cultivation of neural precursor cells from mouse dentate gyrus. Front Neurosci 5:89. doi:10.3389/fnins.2011.00089

Figure Legends

Figure 1: Brain slicing: The photos show the brain placement on the matrix **(1A)**. A serial arrangement of blades shows the slicing method **(1B)** and the slices under the dissection microscope **(1C)**.

Figure 2: Brain microdissection: Schematic illustration of murine brain dorsal and sagittal view shows the distinct brain regions. The dotted line marks the slice thickness using brain matrix. Directions **L**: Lateral; **R**: Rostral; **M**: Medial; **C**: Caudal **(2A&B)**. The coronal sections show the neural stem cell niches as listed. The dotted rectangle marks the ideal boundaries for microdissection of various brain regions of interest **(2C, D&E)**. Abbreviations: **CC**: Corpus Callosum; **V**: Ventricle; **LV**: Lateral ventricle; **SVZ**: Subventricular zone, **SGZ**: Subgranular zone, **VTA**: Ventral Tegmental area, **SNc**: Substantia nigra pars compacta.

Acknowledgements:

This work was supported by a CIHR grant to RSS. We thank Smitha Paul for review of this manuscript. MAI was supported by a scholarship from Mito2i Canada.

Figure 1: Brain slicing method

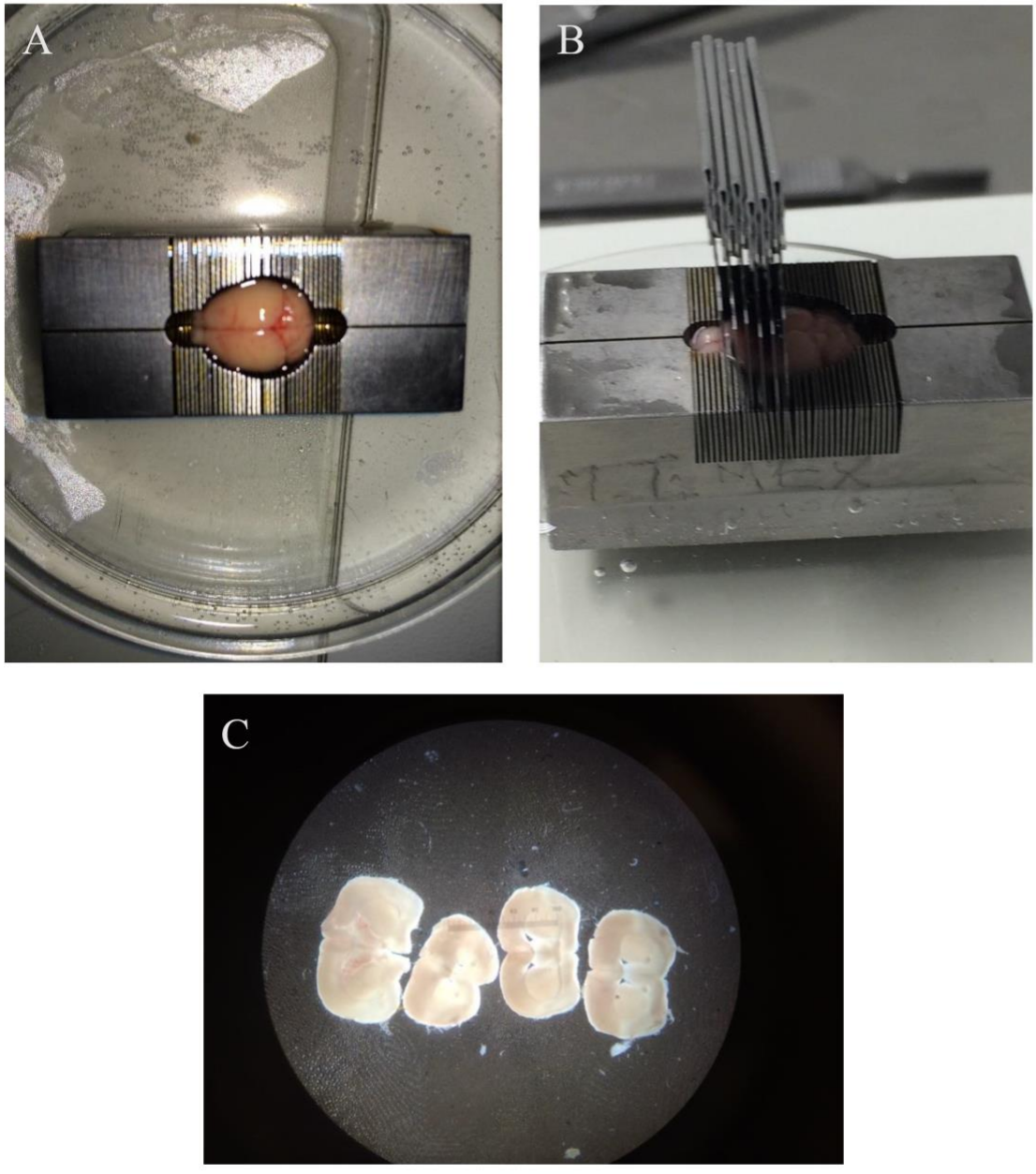

Figure 2: Brain microdissection of various regions

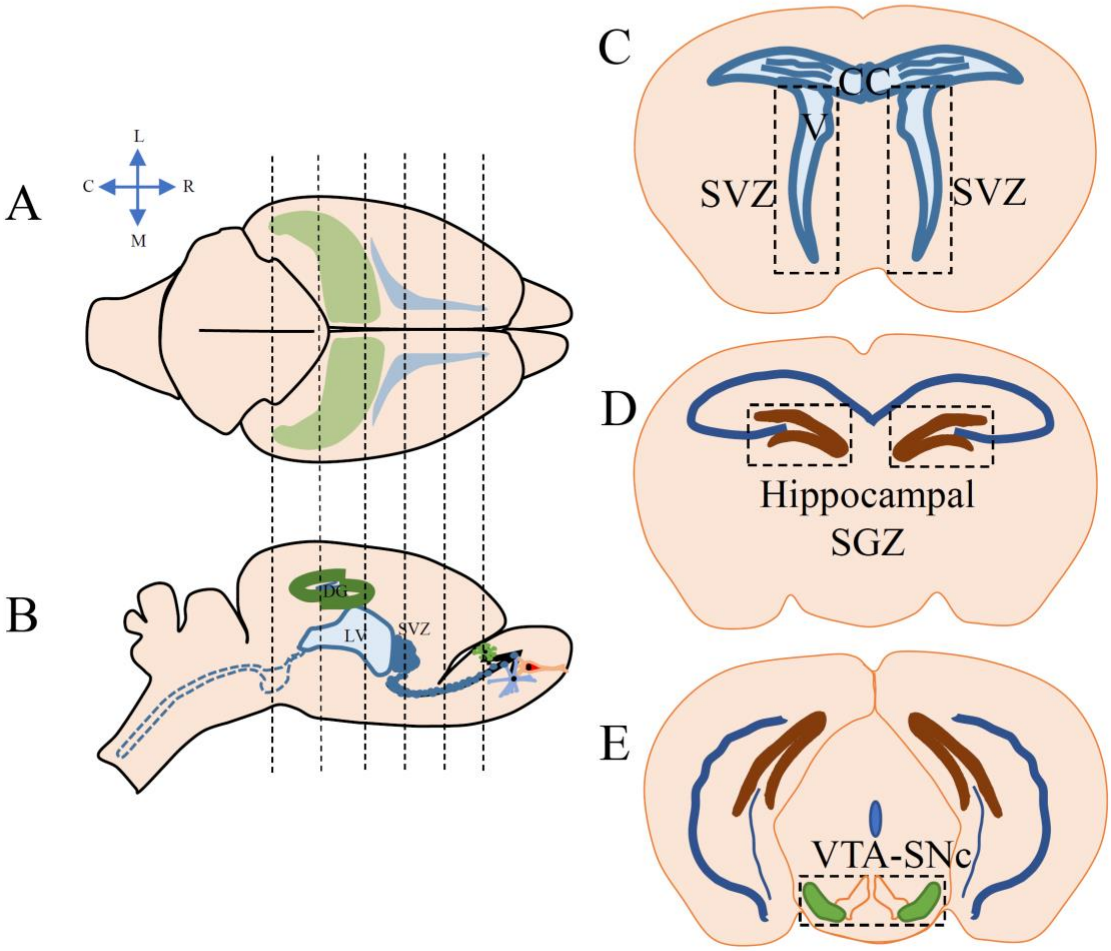

APPENDIX II: Permission for reprint

Permission to reprint Introduction Figure 1 & 2

ELSEVIER LICENSE
TERMS AND CONDITIONS
Jun 04, 2023

This Agreement between University of Ottawa -- Mohamed Ariff Iqbal ("You") and Elsevier ("Elsevier") consists of your license details and the terms and conditions provided by Elsevier and Copyright Clearance Center.

License Number	5562261176557
License date	Jun 04, 2023
Licensed Content Publisher	Elsevier
Licensed Content Publication	Neuron
Licensed Content Title	Quiescence of Adult Mammalian Neural Stem Cells: A Highly Regulated Rest
Licensed Content Author	Noelia Urbán,Isabelle Maria Blomfield,François Guillemot
Licensed Content Date	Dec 4, 2019
Licensed Content Volume	104
Licensed Content Issue	5
Licensed Content Pages	15
Start Page	834
End Page	848
Type of Use	reuse in a thesis/dissertation
Portion	figures/tables/illustrations
Number of figures/tables/illustrations	2
Format	both print and electronic
Are you the author of this Elsevier article?	No
Will you be translating?	No

Title	Mitochondrial dynamics in the regulation of adult neurogenesis
Institution name	University of Ottawa
Expected presentation date	Jul 2023
Order reference number	MAI-INT-0001
Portions	Figure 1 and Figure 3
	University of Ottawa 451 Smyth Rd
Requestor Location	
	Ottawa, ON K1H 8M5 Canada Attn: University of Ottawa
Publisher Tax ID	GB 494 6272 12
Total	0.00 USD

Terms and Conditions

INTRODUCTION

1. The publisher for this copyrighted material is Elsevier. By clicking "accept" in connection with completing this licensing transaction, you agree that the following terms and conditions apply to this transaction (along with the Billing and Payment terms and conditions established by Copyright Clearance Center, Inc. ("CCC"), at the time that you opened your Rightslink account and that are available at any time at http://myaccount.copyright.com).

GENERAL TERMS

2. Elsevier hereby grants you permission to reproduce the aforementioned material subject to the terms and conditions indicated.

3. Acknowledgement: If any part of the material to be used (for example, figures) has appeared in our publication with credit or acknowledgement to another source, permission must also be sought from that source. If such permission is not obtained then that material may not be included in your publication/copies. Suitable acknowledgement to the source must be made, either as a footnote or in a reference list at the end of your publication, as follows:

"Reprinted from Publication title, Vol /edition number, Author(s), Title of article / title of chapter, Pages No., Copyright (Year), with permission from Elsevier [OR APPLICABLE SOCIETY COPYRIGHT OWNER]." Also Lancet special credit -

"Reprinted from The Lancet, Vol. number, Author(s), Title of article, Pages No., Copyright (Year), with permission from Elsevier."

4. Reproduction of this material is confined to the purpose and/or media for which permission is hereby given.

5. Altering/Modifying Material: Not Permitted. However figures and illustrations may be altered/adapted minimally to serve your work. Any other abbreviations, additions, deletions and/or any other alterations shall be made only with prior written authorization of Elsevier Ltd. (Please contact Elsevier's permissions helpdesk here). No modifications can be made to any Lancet figures/tables and they must be reproduced in full.

6. If the permission fee for the requested use of our material is waived in this instance, please be advised that your future requests for Elsevier materials may attract a fee.

7. Reservation of Rights: Publisher reserves all rights not specifically granted in the combination of (i) the license details provided by you and accepted in the course of this licensing transaction, (ii) these terms and conditions and (iii) CCC's Billing and Payment terms and conditions.

8. License Contingent Upon Payment: While you may exercise the rights licensed immediately upon issuance of the license at the end of the licensing process for the transaction, provided that you have disclosed complete and accurate details of your proposed use, no license is finally effective unless and until full payment is received from you (either by publisher or by CCC) as provided in CCC's Billing and Payment terms and conditions. If full payment is not received on a timely basis, then any license preliminarily granted shall be deemed automatically revoked and shall be void as if never granted. Further, in the event that you breach any of these terms and conditions or any of CCC's Billing and Payment terms and conditions, the license is automatically revoked and shall be void as if never granted. Use of materials as described in a revoked license, as well as any use of the materials beyond the scope of an unrevoked license, may constitute copyright infringement and publisher reserves the right to take any and all action to protect its copyright in the materials.

9. Warranties: Publisher makes no representations or warranties with respect to the licensed material.

10. Indemnity: You hereby indemnify and agree to hold harmless publisher and CCC, and their respective officers, directors, employees and agents, from and

against any and all claims arising out of your use of the licensed material other than as specifically authorized pursuant to this license.

11. No Transfer of License: This license is personal to you and may not be sublicensed, assigned, or transferred by you to any other person without publisher's written permission.

12. No Amendment Except in Writing: This license may not be amended except in a writing signed by both parties (or, in the case of publisher, by CCC on publisher's behalf).

13. Objection to Contrary Terms: Publisher hereby objects to any terms contained in any purchase order, acknowledgment, check endorsement or other writing prepared by you, which terms are inconsistent with these terms and conditions or CCC's Billing and Payment terms and conditions. These terms and conditions, together with CCC's Billing and Payment terms and conditions (which are incorporated herein), comprise the entire agreement between you and publisher (and CCC) concerning this licensing transaction. In the event of any conflict between your obligations established by these terms and conditions and those established by CCC's Billing and Payment terms and conditions, these terms and conditions shall control.

14. Revocation: Elsevier or Copyright Clearance Center may deny the permissions described in this License at their sole discretion, for any reason or no reason, with a full refund payable to you. Notice of such denial will be made using the contact information provided by you. Failure to receive such notice will not alter or invalidate the denial. In no event will Elsevier or Copyright Clearance Center be responsible or liable for any costs, expenses or damage incurred by you as a result of a denial of your permission request, other than a refund of the amount(s) paid by you to Elsevier and/or Copyright Clearance Center for denied permissions.

LIMITED LICENSE

The following terms and conditions apply only to specific license types:

15. **Translation**: This permission is granted for non-exclusive world **English** rights only unless your license was granted for translation rights. If you licensed translation rights you may only translate this content into the languages you requested. A professional translator must perform all translations and reproduce the content word for word preserving the integrity of the article.

16. **Posting licensed content on any Website**: The following terms and conditions apply as follows: Licensing material from an Elsevier journal: All content posted to the web site must maintain the copyright information line on the bottom of each image; A hyper-text must be included to the Homepage of the journal from which you are licensing at http://www.sciencedirect.com/science/journal/xxxxx or the Elsevier homepage for books at http://www.elsevier.com; Central Storage: This license does not include permission for a scanned version of the material to be stored in a central repository such as that provided by Heron/XanEdu.

Licensing material from an Elsevier book: A hyper-text link must be included to the Elsevier homepage at http://www.elsevier.com . All content posted to the web site must maintain the copyright information line on the bottom of each image.

Posting licensed content on Electronic reserve: In addition to the above the following clauses are applicable: The web site must be password-protected and made available only to bona fide students registered on a relevant course. This permission is granted for 1 year only. You may obtain a new license for future website posting.

17. **For journal authors:** the following clauses are applicable in addition to the above:

Preprints:

A preprint is an author's own write-up of research results and analysis, it has not been peer-reviewed, nor has it had any other value added to it by a publisher (such as formatting, copyright, technical enhancement etc.).

Authors can share their preprints anywhere at any time. Preprints should not be added to or enhanced in any way in order to appear more like, or to substitute for, the final versions of articles however authors can update their preprints on arXiv or RePEc with their Accepted Author Manuscript (see below).

If accepted for publication, we encourage authors to link from the preprint to their formal publication via its DOI. Millions of researchers have access to the formal publications on ScienceDirect, and so links will help users to find, access, cite and use the best available version. Please note that Cell Press, The Lancet and some society-owned have different preprint policies. Information on these policies is available on the journal homepage.

Accepted Author Manuscripts: An accepted author manuscript is the manuscript of an article that has been accepted for publication and which typically includes author-incorporated changes suggested during submission, peer review and editor-author communications.

Authors can share their accepted author manuscript:

- immediately
    - via their non-commercial person homepage or blog
    - by updating a preprint in arXiv or RePEc with the accepted manuscript
    - via their research institute or institutional repository for internal institutional uses or as part of an invitation-only research collaboration work-group
    - directly by providing copies to their students or to research collaborators for their personal use
    - for private scholarly sharing as part of an invitation-only work group on commercial sites with which Elsevier has an agreement
- After the embargo period
    - via non-commercial hosting platforms such as their institutional repository
    - via commercial sites with which Elsevier has an agreement

In all cases accepted manuscripts should:

- link to the formal publication via its DOI
- bear a CC-BY-NC-ND license - this is easy to do
- if aggregated with other manuscripts, for example in a repository or other site, be shared in alignment with our hosting policy not be added to or enhanced in any way to appear more like, or to substitute for, the published journal article.

Published journal article (JPA): A published journal article (PJA) is the definitive final record of published research that appears or will appear in the journal and embodies all value-adding publishing activities including peer review co-ordination, copy-editing, formatting, (if relevant) pagination and online enrichment.

Policies for sharing publishing journal articles differ for subscription and gold open access articles:

Subscription Articles: If you are an author, please share a link to your article rather than the full-text. Millions of researchers have access to the formal publications on ScienceDirect, and so links will help your users to find, access, cite, and use the best available version.

Theses and dissertations which contain embedded PJAs as part of the formal submission can be posted publicly by the awarding institution with DOI links back to the formal publications on ScienceDirect.

If you are affiliated with a library that subscribes to ScienceDirect you have additional private sharing rights for others' research accessed under that agreement. This includes use for classroom teaching and internal training at the institution (including use in course packs and courseware programs), and inclusion of the article for grant funding purposes.

Gold Open Access Articles: May be shared according to the author-selected end-user license and should contain a CrossMark logo, the end user license, and a DOI link to the formal publication on ScienceDirect.

Please refer to Elsevier's posting policy for further information.

18. **For book authors** the following clauses are applicable in addition to the above: Authors are permitted to place a brief summary of their work online only. You are not allowed to download and post the published electronic version of your chapter, nor may you scan the printed edition to create an electronic version. **Posting to a repository:** Authors are permitted to post a summary of their chapter only in their institution's repository.

19. **Thesis/Dissertation**: If your license is for use in a thesis/dissertation your thesis may be submitted to your institution in either print or electronic form. Should your thesis be published commercially, please reapply for permission. These requirements include permission for the Library and Archives of Canada to supply single copies, on demand, of the complete thesis and include permission for Proquest/UMI to supply single copies, on demand, of the complete thesis. Should your thesis be published commercially, please reapply for permission. Theses and dissertations which contain embedded PJAs as part of the formal submission can be posted publicly by the awarding institution with DOI links back to the formal publications on ScienceDirect.

must be made available on the same conditions. The full details of the license are available at http://creativecommons.org/licenses/by-nc-sa/4.0.

CC BY NC ND: The CC BY-NC-ND license allows users to copy and distribute the Article, provided this is not done for commercial purposes and further does not permit distribution of the Article if it is changed or edited in any way, and provided the user gives appropriate credit (with a link to the formal publication through the relevant DOI), provides a link to the license, and that the licensor is not represented as endorsing the use made of the work. The full details of the license are available at http://creativecommons.org/licenses/by-nc-nd/4.0. Any commercial reuse of Open Access articles published with a CC BY NC SA or CC BY NC ND license requires permission from Elsevier and will be subject to a fee.

Commercial reuse includes:

- Associating advertising with the full text of the Article
- Charging fees for document delivery or access
- Article aggregation
- Systematic distribution via e-mail lists or share buttons

Posting or linking by commercial companies for use by customers of those companies.

20. **Other Conditions**:

v1.10
Questions? customercare@copyright.com.

Permission to reprint Introduction Figure 3 & 4

Order Date

23-May-2023

Order License ID

1357915-1

ISSN

1553-4014

Type of Use

Republish in a thesis/dissertation

Publisher

ANNUAL REVIEWS

Portion

Image/photo/illustration

LICENSED CONTENT

Publication Title

Annual review of pathology

Date

01/01/2006

Language

English

Country

United States of America

Rightsholder

Annual Reviews, Inc.

Publication Type

e-Journal

URL

http://arjournals.annualreviews.org/loi/pathmechdis

REQUEST DETAILS

Portion Type

Image/photo/illustration

Number of Images / Photos / Illustrations

2

Format (select all that apply)

Print

Who Will Republish the Content?

Academic institution

Duration of Use

Life of current edition

Lifetime Unit Quantity

Up to 499

Rights Requested

Main product

Distribution

Worldwide

Translation

Original language of publication

Copies for the Disabled?

No

Minor Editing Privileges?

No

Incidental Promotional Use?

No

Currency

USD

NEW WORK DETAILS

Title

Mitochondrial dynamics in the regulation of adult neurogenesis

Instructor Name

Mohamed Ariff Iqbal

Institution Name

University of Ottawa

Expected Presentation Date

2023-06-30

ADDITIONAL DETAILS

Order Reference Number

MAI-INT-0004

The Requesting Person/Organization to Appear on the License

Mohamed Ariff Iqbal

REQUESTED CONTENT DETAILS

Title, Description or Numeric Reference of the Portion(s)

Figure 1 & 2

Editor of Portion(s)

N/A

Volume / Edition

N/A

Page or Page Range of Portion

4&8

Title of the Article/Chapter the Portion Is From

Mitochondrial Dynamics and Its Involvement in Disease

Author of Portion(s)

David C. Chan

Issue, if Republishing an Article From a Serial

N/A

Publication Date of Portion

2006-01-01

Marketplace Permissions General Terms and Conditions

The following terms and conditions ("General Terms"), together with any applicable Publisher Terms and Conditions, govern User's use of Works pursuant to the Licenses granted by Copyright Clearance Center, Inc. ("CCC") on behalf of the applicable Rightsholders of such Works through CCC's applicable Marketplace transactional licensing services (each, a "Service").

- 1)**Definitions.**For purposes of these General Terms, the following definitions apply:

  "License" is the licensed use the User obtains via the Marketplace platform in a particular licensing transaction, as set forth in the Order Confirmation.

  "Order Confirmation" is the confirmation CCC provides to the User at the conclusion of each Marketplace transaction. "Order Confirmation Terms" are additional terms set forth on specific Order Confirmations not set forth in the General Terms that can include terms applicable to a particular CCC transactional licensing service and/or any Rightsholder-specific terms.

  "Rightsholder(s)" are the holders of copyright rights in the Works for which a User obtains licenses via the Marketplace platform, which are displayed on specific Order Confirmations.

  "Terms" means the terms and conditions set forth in these General Terms and any additional Order Confirmation Terms collectively.

  "User" or "you" is the person or entity making the use granted under the relevant License. Where the person accepting the Terms on behalf of a User is a freelancer or other third party who the User authorized to accept the General Terms on the User's behalf, such person shall be deemed jointly a User for purposes of such Terms.

  "Work(s)" are the copyright protected works described in relevant Order Confirmations.

- 2)**Description of Service.**CCC's Marketplace enables Users to obtain Licenses to use one or more Works in accordance with all relevant Terms. CCC grants Licenses as an agent on behalf of the copyright rightsholder identified in the relevant Order Confirmation.
- 3)**Applicability of Terms.**The Terms govern User's use of Works in connection with the relevant License. In the event of any conflict between General Terms and Order Confirmation Terms, the latter shall govern. User acknowledges that Rightsholders have complete discretion whether to grant any permission, and whether to place any limitations on any grant, and that CCC has no right to supersede or to modify any such discretionary act by a Rightsholder.
- 4)**Representations; Acceptance.**By using the Service, User represents and warrants that User has been duly authorized by the User to accept, and hereby does accept, all Terms.
- 5)**Scope of License; Limitations and Obligations.**All Works and all rights therein, including copyright rights, remain the sole and exclusive property of the Rightsholder. The License provides only those rights expressly set forth in the terms and conveys no other rights in any Works
- 6)**General Payment Terms.**User may pay at time of checkout by credit card or choose to be invoiced. If the User chooses to be invoiced, the User shall: (i) remit payments in the manner identified on specific invoices, (ii) unless otherwise specifically stated in an Order Confirmation or separate written agreement, Users shall remit payments upon receipt of the relevant invoice from CCC, either by delivery or notification of availability of the invoice via the Marketplace platform, and (iii) if the User does not pay the invoice within 30 days of receipt, the User may incur a service charge of 1.5% per month or the maximum rate allowed by applicable law, whichever is less. While User may exercise the rights in the License immediately upon receiving the Order Confirmation, the License is automatically revoked and is null and void, as if it had never been issued, if CCC does not receive complete payment on a timely basis.
- 7)**General Limits on Use.**Unless otherwise provided in the Order Confirmation, any grant of rights to User (i) involves only the rights set forth in the Terms and does not include subsequent or additional uses, (ii) is non-exclusive and non-transferable, and (iii) is subject to any and all limitations and restrictions (such as, but not limited to, limitations on duration of use or circulation) included in the Terms. Upon completion of the licensed use as set forth in the Order Confirmation, User shall either secure a new permission for further use of the Work(s) or immediately cease any new use of the Work(s) and shall render inaccessible (such as by deleting or by removing or severing links or other locators) any further copies of the Work. User may only make alterations to the Work if and as expressly set forth in the Order Confirmation. No Work may be used in any way that is unlawful, including without limitation if such use would violate applicable sanctions laws or regulations, would be defamatory, violate the rights of third parties (including such third parties' rights of copyright, privacy, publicity, or other tangible or intangible property), or is otherwise illegal, sexually explicit, or obscene. In addition, User may not conjoin a Work with any other material that may result in damage to the reputation of the Rightsholder. Any unlawful use will render any licenses hereunder null and void. User agrees to inform CCC if it becomes aware of any infringement of any rights in a Work and to cooperate with any reasonable request of CCC or the Rightsholder in connection therewith.
- 8)**Third Party Materials.**In the event that the material for which a License is sought includes third party materials (such as photographs, illustrations, graphs, inserts and similar materials) that are identified in such material as having been used by permission (or a similar indicator), User is responsible for identifying, and seeking separate licenses (under this Service, if

available, or otherwise) for any of such third party materials; without a separate license, User may not use such third party materials via the License.

- 9)**Copyright Notice.**Use of proper copyright notice for a Work is required as a condition of any License granted under the Service. Unless otherwise provided in the Order Confirmation, a proper copyright notice will read substantially as follows: "Used with permission of [Rightsholder's name], from [Work's title, author, volume, edition number and year of copyright]; permission conveyed through Copyright Clearance Center, Inc." Such notice must be provided in a reasonably legible font size and must be placed either on a cover page or in another location that any person, upon gaining access to the material which is the subject of a permission, shall see, or in the case of republication Licenses, immediately adjacent to the Work as used (for example, as part of a by-line or footnote) or in the place where substantially all other credits or notices for the new work containing the republished Work are located. Failure to include the required notice results in loss to the Rightsholder and CCC, and the User shall be liable to pay liquidated damages for each such failure equal to twice the use fee specified in the Order Confirmation, in addition to the use fee itself and any other fees and charges specified.
- 10)**Indemnity.**User hereby indemnifies and agrees to defend the Rightsholder and CCC, and their respective employees and directors, against all claims, liability, damages, costs, and expenses, including legal fees and expenses, arising out of any use of a Work beyond the scope of the rights granted herein and in the Order Confirmation, or any use of a Work which has been altered in any unauthorized way by User, including claims of defamation or infringement of rights of copyright, publicity, privacy, or other tangible or intangible property.
- 11)**Limitation of Liability.**UNDER NO CIRCUMSTANCES WILL CCC OR THE RIGHTSHOLDER BE LIABLE FOR ANY DIRECT, INDIRECT, CONSEQUENTIAL, OR INCIDENTAL DAMAGES (INCLUDING WITHOUT LIMITATION DAMAGES FOR LOSS OF BUSINESS PROFITS OR INFORMATION, OR FOR BUSINESS INTERRUPTION) ARISING OUT OF THE USE OR INABILITY TO USE A WORK, EVEN IF ONE OR BOTH OF THEM HAS BEEN ADVISED OF THE POSSIBILITY OF SUCH DAMAGES. In any event, the total liability of the Rightsholder and CCC (including their respective employees and directors) shall not exceed the total amount actually paid by User for the relevant License. User assumes full liability for the actions and omissions of its principals, employees, agents, affiliates, successors, and assigns.
- 12)**Limited Warranties.**THE WORK(S) AND RIGHT(S) ARE PROVIDED "AS IS." CCC HAS THE RIGHT TO GRANT TO USER THE RIGHTS GRANTED IN THE ORDER CONFIRMATION DOCUMENT. CCC AND THE RIGHTSHOLDER DISCLAIM ALL OTHER WARRANTIES RELATING TO THE WORK(S) AND RIGHT(S), EITHER EXPRESS OR IMPLIED, INCLUDING WITHOUT LIMITATION IMPLIED WARRANTIES OF MERCHANTABILITY OR FITNESS FOR A PARTICULAR PURPOSE. ADDITIONAL RIGHTS MAY BE REQUIRED TO USE ILLUSTRATIONS, GRAPHS, PHOTOGRAPHS, ABSTRACTS, INSERTS, OR OTHER PORTIONS OF THE WORK (AS OPPOSED TO THE ENTIRE WORK) IN A MANNER CONTEMPLATED BY USER; USER UNDERSTANDS AND AGREES THAT NEITHER CCC NOR THE RIGHTSHOLDER MAY HAVE SUCH ADDITIONAL RIGHTS TO GRANT.
- 13)**Effect of Breach.**Any failure by User to pay any amount when due, or any use by User of a Work beyond the scope of the License set forth in the Order Confirmation and/or the Terms, shall be a material breach of such License. Any breach not cured within 10 days of written notice thereof shall result in immediate termination of such License without further notice. Any unauthorized (but licensable) use of a Work that is terminated immediately upon notice thereof may be liquidated by payment of the Rightsholder's ordinary license price therefor; any unauthorized (and unlicensable) use that is not terminated immediately for any reason

(including, for example, because materials containing the Work cannot reasonably be recalled) will be subject to all remedies available at law or in equity, but in no event to a payment of less than three times the Rightsholder's ordinary license price for the most closely analogous licensable use plus Rightsholder's and/or CCC's costs and expenses incurred in collecting such payment.

- 14)**Additional Terms for Specific Products and Services.**If a User is making one of the uses described in this Section 14, the additional terms and conditions apply:
    - a)***Print Uses of Academic Course Content and Materials (photocopies for academic coursepacks or classroom handouts).***For photocopies for academic coursepacks or classroom handouts the following additional terms apply:
        - i) The copies and anthologies created under this License may be made and assembled by faculty members individually or at their request by on-campus bookstores or copy centers, or by off-campus copy shops and other similar entities.
        - ii) No License granted shall in any way: (i) include any right by User to create a substantively non-identical copy of the Work or to edit or in any other way modify the Work (except by means of deleting material immediately preceding or following the entire portion of the Work copied) (ii) permit "publishing ventures" where any particular anthology would be systematically marketed at multiple institutions.
        - iii) Subject to any Publisher Terms (and notwithstanding any apparent contradiction in the Order Confirmation arising from data provided by User), any use authorized under the academic pay-per-use service is limited as follows:
            - A) any License granted shall apply to only one class (bearing a unique identifier as assigned by the institution, and thereby including all sections or other subparts of the class) at one institution;
            - B) use is limited to not more than 25% of the text of a book or of the items in a published collection of essays, poems or articles;
            - C) use is limited to no more than the greater of (a) 25% of the text of an issue of a journal or other periodical or (b) two articles from such an issue;
            - D) no User may sell or distribute any particular anthology, whether photocopied or electronic, at more than one institution of learning;
            - E) in the case of a photocopy permission, no materials may be entered into electronic memory by User except in order to produce an identical copy of a Work before or during the academic term (or analogous period) as to which any particular permission is granted. In the event that User shall choose to retain materials that are the subject of a photocopy permission in electronic memory for purposes of producing identical copies more than one day after such retention (but

still within the scope of any permission granted), User must notify CCC of such fact in the applicable permission request and such retention shall constitute one copy actually sold for purposes of calculating permission fees due; and

- F) any permission granted shall expire at the end of the class. No permission granted shall in any way include any right by User to create a substantively non-identical copy of the Work or to edit or in any other way modify the Work (except by means of deleting material immediately preceding or following the entire portion of the Work copied).

- iv) Books and Records; Right to Audit. As to each permission granted under the academic pay-per-use Service, User shall maintain for at least four full calendar years books and records sufficient for CCC to determine the numbers of copies made by User under such permission. CCC and any representatives it may designate shall have the right to audit such books and records at any time during User's ordinary business hours, upon two days' prior notice. If any such audit shall determine that User shall have underpaid for, or underreported, any photocopies sold or by three percent (3%) or more, then User shall bear all the costs of any such audit; otherwise, CCC shall bear the costs of any such audit. Any amount determined by such audit to have been underpaid by User shall immediately be paid to CCC by User, together with interest thereon at the rate of 10% per annum from the date such amount was originally due. The provisions of this paragraph shall survive the termination of this License for any reason.

- b)***Digital Pay-Per-Uses of Academic Course Content and Materials (e-coursepacks, electronic reserves, learning management systems, academic institution intranets).***For uses in e-coursepacks, posts in electronic reserves, posts in learning management systems, or posts on academic institution intranets, the following additional terms apply:
  - i) The pay-per-uses subject to this Section 14(b) include:

    - A)**Posting e-reserves, course management systems, e-coursepacks for text-based content,**which grants authorizations to import requested material in electronic format, and allows electronic access to this material to members of a designated college or university class, under the direction of an instructor designated by the college or university, accessible only under appropriate electronic controls (e.g., password);
    - B)**Posting e-reserves, course management systems, e-coursepacks for material consisting of photographs or other still images not embedded in text,**which grants not only the authorizations described in Section 14(b)(i)(A) above, but also the following authorization: to include the requested material in course materials for use consistent with Section 14(b)(i)(A) above, including any necessary resizing, reformatting or modification of the resolution

of such requested material (provided that such modification does not alter the underlying editorial content or meaning of the requested material, and provided that the resulting modified content is used solely within the scope of, and in a manner consistent with, the particular authorization described in the Order Confirmation and the Terms), but not including any other form of manipulation, alteration or editing of the requested material;

- C)**Posting e-reserves, course management systems, e-coursepacks or other academic distribution for audiovisual content,**which grants not only the authorizations described in Section 14(b)(i)(A) above, but also the following authorizations: (i) to include the requested material in course materials for use consistent with Section 14(b)(i)(A) above; (ii) to display and perform the requested material to such members of such class in the physical classroom or remotely by means of streaming media or other video formats; and (iii) to "clip" or reformat the requested material for purposes of time or content management or ease of delivery, provided that such “clipping” or reformatting does not alter the underlying editorial content or meaning of the requested material and that the resulting material is used solely within the scope of, and in a manner consistent with, the particular authorization described in the Order Confirmation and the Terms. Unless expressly set forth in the relevant Order Conformation, the License does not authorize any other form of manipulation, alteration or editing of the requested material.

- ii) Unless expressly set forth in the relevant Order Confirmation, no License granted shall in any way: (i) include any right by User to create a substantively non-identical copy of the Work or to edit or in any other way modify the Work (except by means of deleting material immediately preceding or following the entire portion of the Work copied or, in the case of Works subject to Sections 14(b)(1)(B) or (C) above, as described in such Sections) (ii) permit "publishing ventures" where any particular course materials would be systematically marketed at multiple institutions.

- iii) Subject to any further limitations determined in the Rightsholder Terms (and notwithstanding any apparent contradiction in the Order Confirmation arising from data provided by User), any use authorized under the electronic course content pay-per-use service is limited as follows:

    - A) any License granted shall apply to only one class (bearing a unique identifier as assigned by the institution, and thereby including all sections or other subparts of the class) at one institution;

    - B) use is limited to not more than 25% of the text of a book or of the items in a published collection of essays, poems or articles;

    - C) use is limited to not more than the greater of (a) 25% of the text of an issue of a journal or other periodical or (b) two articles from such an issue;

- D) no User may sell or distribute any particular materials, whether photocopied or electronic, at more than one institution of learning;
- E) electronic access to material which is the subject of an electronic-use permission must be limited by means of electronic password, student identification or other control permitting access solely to students and instructors in the class;
- F) User must ensure (through use of an electronic cover page or other appropriate means) that any person, upon gaining electronic access to the material, which is the subject of a permission, shall see:
    - a proper copyright notice, identifying the Rightsholder in whose name CCC has granted permission,
    - a statement to the effect that such copy was made pursuant to permission,
    - a statement identifying the class to which the material applies and notifying the reader that the material has been made available electronically solely for use in the class, and
    - a statement to the effect that the material may not be further distributed to any person outside the class, whether by copying or by transmission and whether electronically or in paper form, and User must also ensure that such cover page or other means will print out in the event that the person accessing the material chooses to print out the material or any part thereof.
- G) any permission granted shall expire at the end of the class and, absent some other form of authorization, User is thereupon required to delete the applicable material from any electronic storage or to block electronic access to the applicable material.

- iv) Uses of separate portions of a Work, even if they are to be included in the same course material or the same university or college class, require separate permissions under the electronic course content pay-per-use Service. Unless otherwise provided in the Order Confirmation, any grant of rights to User is limited to use completed no later than the end of the academic term (or analogous period) as to which any particular permission is granted.
- v) Books and Records; Right to Audit. As to each permission granted under the electronic course content Service, User shall maintain for at least four full calendar years books and records sufficient for CCC to determine the numbers of copies made by User under such permission. CCC and any representatives it may designate shall have the right to audit such books and records at any time during User's ordinary business hours, upon two days' prior notice. If any

such audit shall determine that User shall have underpaid for, or underreported, any electronic copies used by three percent (3%) or more, then User shall bear all the costs of any such audit; otherwise, CCC shall bear the costs of any such audit. Any amount determined by such audit to have been underpaid by User shall immediately be paid to CCC by User, together with interest thereon at the rate of 10% per annum from the date such amount was originally due. The provisions of this paragraph shall survive the termination of this license for any reason.

- c)***Pay-Per-Use Permissions for Certain Reproductions (Academic photocopies for library reserves and interlibrary loan reporting) (Non-academic internal/external business uses and commercial document delivery).***The License expressly excludes the uses listed in Section (c)(i)-(v) below (which must be subject to separate license from the applicable Rightsholder) for: academic photocopies for library reserves and interlibrary loan reporting; and non-academic internal/external business uses and commercial document delivery.
  - i) electronic storage of any reproduction (whether in plain-text, PDF, or any other format) other than on a transitory basis;
  - ii) the input of Works or reproductions thereof into any computerized database;
  - iii) reproduction of an entire Work (cover-to-cover copying) except where the Work is a single article;
  - iv) reproduction for resale to anyone other than a specific customer of User;
  - v) republication in any different form. Please obtain authorizations for these uses through other CCC services or directly from the rightsholder.

  Any license granted is further limited as set forth in any restrictions included in the Order Confirmation and/or in these Terms.

- d)***Electronic Reproductions in Online Environments (Non-Academic-email, intranet, internet and extranet).***For "electronic reproductions", which generally includes e-mail use (including instant messaging or other electronic transmission to a defined group of recipients) or posting on an intranet, extranet or Intranet site (including any display or performance incidental thereto), the following additional terms apply:
  - i) Unless otherwise set forth in the Order Confirmation, the License is limited to use completed within 30 days for any use on the Internet, 60 days for any use on an intranet or extranet and one year for any other use, all as measured from the "republication date" as identified in the Order Confirmation, if any, and otherwise from the date of the Order Confirmation.
  - ii) User may not make or permit any alterations to the Work, unless expressly set forth in the Order Confirmation (after request by User and approval by Rightsholder); provided, however, that a Work consisting of photographs or other still images not embedded in text may, if necessary, be resized,

reformatted or have its resolution modified without additional express permission, and a Work consisting of audiovisual content may, if necessary, be "clipped" or reformatted for purposes of time or content management or ease of delivery (provided that any such resizing, reformatting, resolution modification or “clipping” does not alter the underlying editorial content or meaning of the Work used, and that the resulting material is used solely within the scope of, and in a manner consistent with, the particular License described in the Order Confirmation and the Terms.

- 15)**Miscellaneous.**
    - a) User acknowledges that CCC may, from time to time, make changes or additions to the Service or to the Terms, and that Rightsholder may make changes or additions to the Rightsholder Terms. Such updated Terms will replace the prior terms and conditions in the order workflow and shall be effective as to any subsequent Licenses but shall not apply to Licenses already granted and paid for under a prior set of terms.
    - b) Use of User-related information collected through the Service is governed by CCC's privacy policy, available online at www.copyright.com/about/privacy-policy/.
    - c) The License is personal to User. Therefore, User may not assign or transfer to any other person (whether a natural person or an organization of any kind) the License or any rights granted thereunder; provided, however, that, where applicable, User may assign such License in its entirety on written notice to CCC in the event of a transfer of all or substantially all of User's rights in any new material which includes the Work(s) licensed under this Service.
    - d) No amendment or waiver of any Terms is binding unless set forth in writing and signed by the appropriate parties, including, where applicable, the Rightsholder. The Rightsholder and CCC hereby object to any terms contained in any writing prepared by or on behalf of the User or its principals, employees, agents or affiliates and purporting to govern or otherwise relate to the License described in the Order Confirmation, which terms are in any way inconsistent with any Terms set forth in the Order Confirmation, and/or in CCC's standard operating procedures, whether such writing is prepared prior to, simultaneously with or subsequent to the Order Confirmation, and whether such writing appears on a copy of the Order Confirmation or in a separate instrument.
    - e) The License described in the Order Confirmation shall be governed by and construed under the law of the State of New York, USA, without regard to the principles thereof of conflicts of law. Any case, controversy, suit, action, or proceeding arising out of, in connection with, or related to such License shall be brought, at CCC's sole discretion, in any federal or state court located in the County of New York, State of New York, USA, or in any federal or state court whose geographical jurisdiction covers the location of the Rightsholder set forth in the Order Confirmation. The parties expressly submit to the personal jurisdiction and venue of each such federal or state court.

Last updated October 2022

Permission to reprint Introduction Figure 5

JOHN WILEY AND SONS LICENSE
TERMS AND CONDITIONS
Jun 05, 2023

This Agreement between University of Ottawa -- Mohamed Ariff Iqbal ("You") and John Wiley and Sons ("John Wiley and Sons") consists of your license details and the terms and conditions provided by John Wiley and Sons and Copyright Clearance Center.

License Number	5553300818593
License date	May 20, 2023
Licensed Content Publisher	John Wiley and Sons
Licensed Content Publication	EMBO Reports
Licensed Content Title	The integrated stress response
Licensed Content Author	Adrienne M Gorman, Afshin Samali, Mila Ljujic, et al
Licensed Content Date	Sep 14, 2016
Licensed Content Volume	17
Licensed Content Issue	10
Licensed Content Pages	22
Type of use	Dissertation/Thesis
Requestor type	University/Academic
Format	Print and electronic
Portion	Figure/table
Number of figures/tables	1
Will you be translating?	No
Title	Mitochondrial dynamics in the regulation of adult neurogenesis
Institution name	University of Ottawa
Expected presentation date	Jul 2023
Order reference number	MAI-INT-0003

Portions	Figure 1 University of Ottawa 451 Smyth Rd
Requestor Location	Ottawa, ON K1H 8M5 Canada Attn: University of Ottawa
Publisher Tax ID	EU826007151
Total	0.00 USD
Terms and Conditions	

TERMS AND CONDITIONS

This copyrighted material is owned by or exclusively licensed to John Wiley & Sons, Inc. or one of its group companies (each a"Wiley Company") or handled on behalf of a society with which a Wiley Company has exclusive publishing rights in relation to a particular work (collectively "WILEY"). By clicking "accept" in connection with completing this licensing transaction, you agree that the following terms and conditions apply to this transaction (along with the billing and payment terms and conditions established by the Copyright Clearance Center Inc., ("CCC's Billing and Payment terms and conditions"), at the time that you opened your RightsLink account (these are available at any time at http://myaccount.copyright.com).

Terms and Conditions

- The materials you have requested permission to reproduce or reuse (the "Wiley Materials") are protected by copyright.
- You are hereby granted a personal, non-exclusive, non-sub licensable (on a stand-alone basis), non-transferable, worldwide, limited license to reproduce the Wiley Materials for the purpose specified in the licensing process. This license, **and any CONTENT (PDF or image file) purchased as part of your order,** is for a one-time use only and limited to any maximum distribution number specified in the license. The first instance of republication or reuse granted by this license must be completed within two years of the date of the grant of this license (although copies prepared before the end date may be distributed thereafter). The Wiley Materials shall not be used in any other manner or for any other purpose,

beyond what is granted in the license. Permission is granted subject to an appropriate acknowledgement given to the author, title of the material/book/journal and the publisher. You shall also duplicate the copyright notice that appears in the Wiley publication in your use of the Wiley Material. Permission is also granted on the understanding that nowhere in the text is a previously published source acknowledged for all or part of this Wiley Material. Any third party content is expressly excluded from this permission.

- With respect to the Wiley Materials, all rights are reserved. Except as expressly granted by the terms of the license, no part of the Wiley Materials may be copied, modified, adapted (except for minor reformatting required by the new Publication), translated, reproduced, transferred or distributed, in any form or by any means, and no derivative works may be made based on the Wiley Materials without the prior permission of the respective copyright owner.**For STM Signatory Publishers clearing permission under the terms of the STM Permissions Guidelines only, the terms of the license are extended to include subsequent editions and for editions in other languages, provided such editions are for the work as a whole in situ and does not involve the separate exploitation of the permitted figures or extracts,** You may not alter, remove or suppress in any manner any copyright, trademark or other notices displayed by the Wiley Materials. You may not license, rent, sell, loan, lease, pledge, offer as security, transfer or assign the Wiley Materials on a stand-alone basis, or any of the rights granted to you hereunder to any other person.

- The Wiley Materials and all of the intellectual property rights therein shall at all times remain the exclusive property of John Wiley & Sons Inc, the Wiley Companies, or their respective licensors, and your interest therein is only that of having possession of and the right to reproduce the Wiley Materials pursuant to Section 2 herein during the continuance of this Agreement. You agree that you own no right, title or interest in or to the Wiley Materials or any of the intellectual property rights therein. You shall have no rights hereunder other than the license as provided for above in Section 2. No right, license or interest to any trademark, trade name, service mark or other branding ("Marks") of WILEY or its licensors is

granted hereunder, and you agree that you shall not assert any such right, license or interest with respect thereto

- NEITHER WILEY NOR ITS LICENSORS MAKES ANY WARRANTY OR REPRESENTATION OF ANY KIND TO YOU OR ANY THIRD PARTY, EXPRESS, IMPLIED OR STATUTORY, WITH RESPECT TO THE MATERIALS OR THE ACCURACY OF ANY INFORMATION CONTAINED IN THE MATERIALS, INCLUDING, WITHOUT LIMITATION, ANY IMPLIED WARRANTY OF MERCHANTABILITY, ACCURACY, SATISFACTORY QUALITY, FITNESS FOR A PARTICULAR PURPOSE, USABILITY, INTEGRATION OR NON-INFRINGEMENT AND ALL SUCH WARRANTIES ARE HEREBY EXCLUDED BY WILEY AND ITS LICENSORS AND WAIVED BY YOU.

- WILEY shall have the right to terminate this Agreement immediately upon breach of this Agreement by you.

- You shall indemnify, defend and hold harmless WILEY, its Licensors and their respective directors, officers, agents and employees, from and against any actual or threatened claims, demands, causes of action or proceedings arising from any breach of this Agreement by you.

- IN NO EVENT SHALL WILEY OR ITS LICENSORS BE LIABLE TO YOU OR ANY OTHER PARTY OR ANY OTHER PERSON OR ENTITY FOR ANY SPECIAL, CONSEQUENTIAL, INCIDENTAL, INDIRECT, EXEMPLARY OR PUNITIVE DAMAGES, HOWEVER CAUSED, ARISING OUT OF OR IN CONNECTION WITH THE DOWNLOADING, PROVISIONING, VIEWING OR USE OF THE MATERIALS REGARDLESS OF THE FORM OF ACTION, WHETHER FOR BREACH OF CONTRACT, BREACH OF WARRANTY, TORT, NEGLIGENCE, INFRINGEMENT OR OTHERWISE (INCLUDING, WITHOUT LIMITATION, DAMAGES BASED ON LOSS OF PROFITS, DATA, FILES, USE, BUSINESS OPPORTUNITY OR CLAIMS OF THIRD PARTIES), AND WHETHER OR NOT THE PARTY HAS BEEN ADVISED OF THE POSSIBILITY OF SUCH DAMAGES. THIS LIMITATION SHALL APPLY NOTWITHSTANDING ANY FAILURE OF ESSENTIAL PURPOSE OF ANY LIMITED REMEDY PROVIDED HEREIN.

- Should any provision of this Agreement be held by a court of competent jurisdiction to be illegal, invalid, or unenforceable, that provision shall be deemed amended to achieve as nearly as possible the same economic effect as the original provision, and the legality, validity and enforceability

of the remaining provisions of this Agreement shall not be affected or impaired thereby.

- The failure of either party to enforce any term or condition of this Agreement shall not constitute a waiver of either party's right to enforce each and every term and condition of this Agreement. No breach under this agreement shall be deemed waived or excused by either party unless such waiver or consent is in writing signed by the party granting such waiver or consent. The waiver by or consent of a party to a breach of any provision of this Agreement shall not operate or be construed as a waiver of or consent to any other or subsequent breach by such other party.

- This Agreement may not be assigned (including by operation of law or otherwise) by you without WILEY's prior written consent.

- Any fee required for this permission shall be non-refundable after thirty (30) days from receipt by the CCC.

- These terms and conditions together with CCC's Billing and Payment terms and conditions (which are incorporated herein) form the entire agreement between you and WILEY concerning this licensing transaction and (in the absence of fraud) supersedes all prior agreements and representations of the parties, oral or written. This Agreement may not be amended except in writing signed by both parties. This Agreement shall be binding upon and inure to the benefit of the parties' successors, legal representatives, and authorized assigns.

- In the event of any conflict between your obligations established by these terms and conditions and those established by CCC's Billing and Payment terms and conditions, these terms and conditions shall prevail.

- WILEY expressly reserves all rights not specifically granted in the combination of (i) the license details provided by you and accepted in the course of this licensing transaction, (ii) these terms and conditions and (iii) CCC's Billing and Payment terms and conditions.

- This Agreement will be void if the Type of Use, Format, Circulation, or Requestor Type was misrepresented during the licensing process.

- This Agreement shall be governed by and construed in accordance with the laws of the State of New York, USA, without regards to such state's conflict of law rules. Any legal action, suit or proceeding arising out of or relating to these Terms and Conditions or the breach thereof shall be instituted in a court of competent jurisdiction in New York County in the State of New York in the United States of America and each party hereby consents and submits to the personal jurisdiction of such court, waives any objection to venue in such court and consents to service of process by registered or certified mail, return receipt requested, at the last known address of such party.

WILEY OPEN ACCESS TERMS AND CONDITIONS

Wiley Publishes Open Access Articles in fully Open Access Journals and in Subscription journals offering Online Open. Although most of the fully Open Access journals publish open access articles under the terms of the Creative Commons Attribution (CC BY) License only, the subscription journals and a few of the Open Access Journals offer a choice of Creative Commons Licenses. The license type is clearly identified on the article.

The Creative Commons Attribution License

The Creative Commons Attribution License (CC-BY) allows users to copy, distribute and transmit an article, adapt the article and make commercial use of the article. The CC-BY license permits commercial and non-

Creative Commons Attribution Non-Commercial License

The Creative Commons Attribution Non-Commercial (CC-BY-NC)License permits use, distribution and reproduction in any medium, provided the original work is properly cited and is not used for commercial purposes.(see below)

Creative Commons Attribution-Non-Commercial-NoDerivs License

The Creative Commons Attribution Non-Commercial-NoDerivs License (CC-BY-NC-ND) permits use, distribution and reproduction in any medium, provided the original work is properly cited, is not used for commercial purposes and no modifications or adaptations are made. (see below)

Use by commercial "for-profit" organizations

Permission to reprint: Fong et al 2022

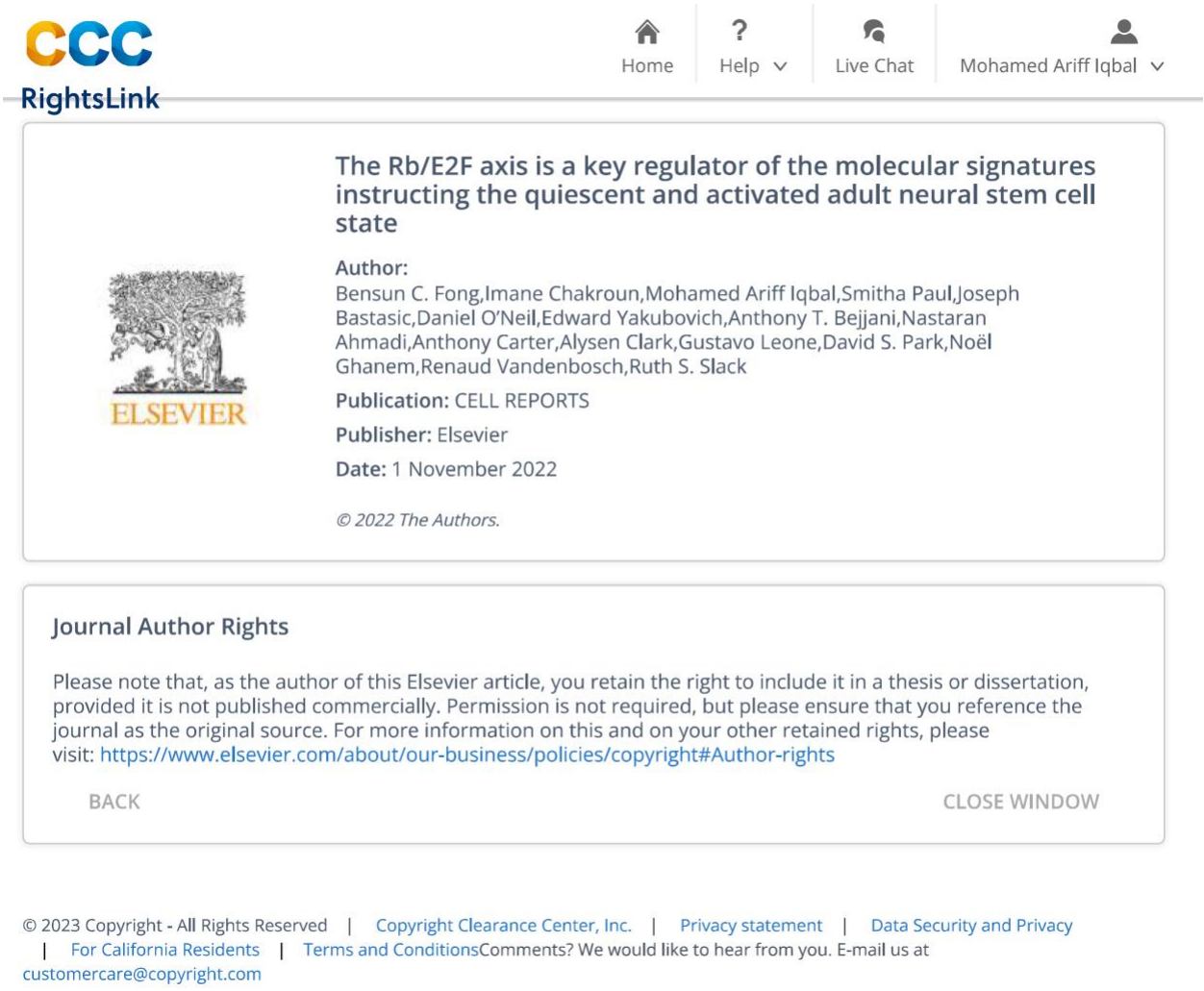

RightsLink

Home | Help | Live Chat | Mohamed Ariff Iqbal

The Rb/E2F axis is a key regulator of the molecular signatures instructing the quiescent and activated adult neural stem cell state

Author:
Bensun C. Fong,Imane Chakroun,Mohamed Ariff Iqbal,Smitha Paul,Joseph Bastasic,Daniel O'Neil,Edward Yakubovich,Anthony T. Bejjani,Nastaran Ahmadi,Anthony Carter,Alysen Clark,Gustavo Leone,David S. Park,Noël Ghanem,Renaud Vandenbosch,Ruth S. Slack

Publication: CELL REPORTS

Publisher: Elsevier

Date: 1 November 2022

© 2022 The Authors.

Journal Author Rights

Please note that, as the author of this Elsevier article, you retain the right to include it in a thesis or dissertation, provided it is not published commercially. Permission is not required, but please ensure that you reference the journal as the original source. For more information on this and on your other retained rights, please visit: https://www.elsevier.com/about/our-business/policies/copyright#Author-rights

BACK CLOSE WINDOW

Permission to reprint: Iqbal et al 2021

SPRINGER NATURE LICENSE
TERMS AND CONDITIONS
Jun 06, 2023

This Agreement between University of Ottawa -- Mohamed Ariff Iqbal ("You") and Springer Nature ("Springer Nature") consists of your license details and the terms and conditions provided by Springer Nature and Copyright Clearance Center.

License Number	5563421107899
License date	Jun 06, 2023
Licensed Content Publisher	Springer Nature
Licensed Content Publication	Springer eBook
Licensed Content Title	Direct FACS Isolation of Neural Stem/Progenitor Lineages from the Adult Brain
Licensed Content Author	Mohamed Ariff Iqbal, Bensun C. Fong, Ruth S. Slack
Licensed Content Date	Jan 1, 2022
Type of Use	Thesis/Dissertation
Requestor type	academic/university or research institute
Format	print and electronic
Portion	full article/chapter
Will you be translating?	no
Circulation/distribution	100 - 199
Author of this Springer Nature content	yes
Title	Mitochondrial dynamics in the regulation of adult neurogenesis
Institution name	University of Ottawa

Expected presentation date	Jul 2023
Order reference number	MAI-INT-0005
Requestor Location	University of Ottawa 451 Smyth Rd Ottawa, ON K1H 8M5 Canada Attn: University of Ottawa
Billing Type	Invoice
Billing Address	University of Ottawa 451 Smyth Rd Ottawa, ON K1H 8M5 Canada Attn: University of Ottawa
Total	0.00 USD

Terms and Conditions

Springer Nature Customer Service Centre GmbH Terms and Conditions

The following terms and conditions ("Terms and Conditions") together with the terms specified in your [RightsLink] constitute the License ("License") between you as Licensee and Springer Nature Customer Service Centre GmbH as Licensor. By clicking 'accept' and completing the transaction for your use of the material ("Licensed Material"), you confirm your acceptance of and obligation to be bound by these Terms and Conditions.

1. **Grant and Scope of License**

    1. The Licensor grants you a personal, non-exclusive, non-transferable, non-sublicensable, revocable, world-wide License to reproduce, distribute, communicate to the public, make available, broadcast, electronically transmit or create derivative works using the Licensed Material for the purpose(s) specified in your RightsLink Licence Details only. Licenses are granted for the specific use requested in the

order and for no other use, subject to these Terms and Conditions. You acknowledge and agree that the rights granted to you under this License do not include the right to modify, edit, translate, include in collective works, or create derivative works of the Licensed Material in whole or in part unless expressly stated in your RightsLink Licence Details. You may use the Licensed Material only as permitted under this Agreement and will not reproduce, distribute, display, perform, or otherwise use or exploit any Licensed Material in any way, in whole or in part, except as expressly permitted by this License.

2. You may only use the Licensed Content in the manner and to the extent permitted by these Terms and Conditions, by your RightsLink Licence Details and by any applicable laws.

3. A separate license may be required for any additional use of the Licensed Material, e.g. where a license has been purchased for print use only, separate permission must be obtained for electronic re-use. Similarly, a License is only valid in the language selected and does not apply for editions in other languages unless additional translation rights have been granted separately in the License.

4. Any content within the Licensed Material that is owned by third parties is expressly excluded from the License.

5. Rights for additional reuses such as custom editions, computer/mobile applications, film or TV reuses and/or any other derivative rights requests require additional permission and may be subject to an additional fee. Please apply to journalpermissions@springernature.com or bookpermissions@springernature.com for these rights.

2. **Reservation of Rights**

Licensor reserves all rights not expressly granted to you under this License. You acknowledge and agree that nothing in this License limits or restricts Licensor's rights in or use of the Licensed Material in any way. Neither this License, nor any act, omission, or statement by Licensor or you, conveys any ownership right to you in any Licensed Material, or to any element or portion thereof. As between Licensor and you, Licensor owns and retains all right, title, and interest in and to the Licensed Material subject to the license granted in Section 1.1. Your permission to use the Licensed Material is expressly

conditioned on you not impairing Licensor's or the applicable copyright owner's rights in the Licensed Material in any way.

3. **Restrictions on use**

    1. Minor editing privileges are allowed for adaptations for stylistic purposes or formatting purposes provided such alterations do not alter the original meaning or intention of the Licensed Material and the new figure(s) are still accurate and representative of the Licensed Material. Any other changes including but not limited to, cropping, adapting, and/or omitting material that affect the meaning, intention or moral rights of the author(s) are strictly prohibited.

    2. You must not use any Licensed Material as part of any design or trademark.

    3. Licensed Material may be used in Open Access Publications (OAP), but any such reuse must include a clear acknowledgment of this permission visible at the same time as the figures/tables/illustration or abstract and which must indicate that the Licensed Material is not part of the governing OA license but has been reproduced with permission. This may be indicated according to any standard referencing system but must include at a minimum 'Book/Journal title, Author, Journal Name (if applicable), Volume (if applicable), Publisher, Year, reproduced with permission from SNCSC'.

4. **STM Permission Guidelines**

    1. An alternative scope of license may apply to signatories of the STM Permissions Guidelines ("STM PG") as amended from time to time and made available at https://www.stm-assoc.org/intellectual-property/permissions/permissions-guidelines/.

    2. For content reuse requests that qualify for permission under the STM PG, and which may be updated from time to time, the STM PG supersede the terms and conditions contained in this License.

3. If a License has been granted under the STM PG, but the STM PG no longer apply at the time of publication, further permission must be sought from the Rightsholder.
   Contact journalpermissions@springernature.com or bookpermissions@springernature.com for these rights.

5. **Duration of License**

1. Unless otherwise indicated on your License, a License is valid from the date of purchase ("License Date") until the end of the relevant period in the below table:

Reuse in a medical communications project	Reuse up to distribution or time period indicated in License
Reuse in a dissertation/thesis	Lifetime of thesis
Reuse in a journal/magazine	Lifetime of journal/magazine
Reuse in a book/textbook	Lifetime of edition
Reuse on a website	1 year unless otherwise specified in the License
Reuse in a presentation/slide kit/poster	Lifetime of presentation/slide kit/poster. Note: publication whether electronic or in print of presentation/slide kit/poster may require further permission.
Reuse in conference proceedings	Lifetime of conference proceedings
Reuse in an annual report	Lifetime of annual report
Reuse in training/CME materials	Reuse up to distribution or time period indicated in License
Reuse in newsmedia	Lifetime of newsmedia
Reuse in coursepack/classroom materials	Reuse up to distribution and/or time period indicated in license

6.

7. **Acknowledgement**

    1. The Licensor's permission must be acknowledged next to the Licensed Material in print. In electronic form, this acknowledgement must be visible at the same time as the figures/tables/illustrations or abstract and must be hyperlinked to the journal/book's homepage.

    2. Acknowledgement may be provided according to any standard referencing system and at a minimum should include "Author, Article/Book Title, Journal name/Book imprint, volume, page number, year, Springer Nature".

8. **Reuse in a dissertation or thesis**

    1. Where 'reuse in a dissertation/thesis' has been selected, the following terms apply: Print rights of the Version of Record are provided for; electronic rights for use only on institutional repository as defined by the Sherpa guideline (www.sherpa.ac.uk/romeo/) and only up to what is required by the awarding institution.

    2. For theses published under an ISBN or ISSN, separate permission is required. Please contact journalpermissions@springernature.com or bookpermissions@springernature.com for these rights.

    3. Authors must properly cite the published manuscript in their thesis according to current citation standards and include the following acknowledgement: '*Reproduced with permission from Springer Nature*'.

9. **License Fee**

You must pay the fee set forth in the License Agreement (the "License Fees"). All amounts payable by you under this License are exclusive of any sales, use, withholding, value added or similar taxes, government fees or levies or other assessments. Collection and/or remittance of such taxes to the relevant tax authority shall be the responsibility of the party who has the legal obligation to do so.

10. **Warranty**

1. The Licensor warrants that it has, to the best of its knowledge, the rights to license reuse of the Licensed Material. **You are solely responsible for ensuring that the material you wish to license is original to the Licensor and does not carry the copyright of another entity or third party (as credited in the published version).** If the credit line on any part of the Licensed Material indicates that it was reprinted or adapted with permission from another source, then you should seek additional permission from that source to reuse the material.

2. EXCEPT FOR THE EXPRESS WARRANTY STATED HEREIN AND TO THE EXTENT PERMITTED BY APPLICABLE LAW, LICENSOR PROVIDES THE LICENSED MATERIAL "AS IS" AND MAKES NO OTHER REPRESENTATION OR WARRANTY. LICENSOR EXPRESSLY DISCLAIMS ANY LIABILITY FOR ANY CLAIM ARISING FROM OR OUT OF THE CONTENT, INCLUDING BUT NOT LIMITED TO ANY ERRORS, INACCURACIES, OMISSIONS, OR DEFECTS CONTAINED THEREIN, AND ANY IMPLIED OR EXPRESS WARRANTY AS TO MERCHANTABILITY OR FITNESS FOR A PARTICULAR PURPOSE. IN NO EVENT SHALL LICENSOR BE LIABLE TO YOU OR ANY OTHER PARTY OR ANY OTHER PERSON OR FOR ANY SPECIAL, CONSEQUENTIAL, INCIDENTAL, INDIRECT, PUNITIVE, OR EXEMPLARY DAMAGES, HOWEVER CAUSED, ARISING OUT OF OR IN CONNECTION WITH THE DOWNLOADING, VIEWING OR USE OF THE LICENSED MATERIAL REGARDLESS OF THE FORM OF ACTION,

WHETHER FOR BREACH OF CONTRACT, BREACH OF WARRANTY, TORT, NEGLIGENCE, INFRINGEMENT OR OTHERWISE (INCLUDING, WITHOUT LIMITATION, DAMAGES BASED ON LOSS OF PROFITS, DATA, FILES, USE, BUSINESS OPPORTUNITY OR CLAIMS OF THIRD PARTIES), AND WHETHER OR NOT THE PARTY HAS BEEN ADVISED OF THE POSSIBILITY OF SUCH DAMAGES. THIS LIMITATION APPLIES NOTWITHSTANDING ANY FAILURE OF ESSENTIAL PURPOSE OF ANY LIMITED REMEDY PROVIDED HEREIN.

11. **Termination and Cancellation**

1. The License and all rights granted hereunder will continue until the end of the applicable period shown in Clause 5.1 above. Thereafter, this license will be terminated and all rights granted hereunder will cease.

2. Licensor reserves the right to terminate the License in the event that payment is not received in full or if you breach the terms of this License.

12. **General**

1. The License and the rights and obligations of the parties hereto shall be construed, interpreted and determined in accordance with the laws of the Federal Republic of Germany without reference to the stipulations of the CISG (United Nations Convention on Contracts for the International Sale of Goods) or to Germany´s choice-of-law principle.

2. The parties acknowledge and agree that any controversies and disputes arising out of this License shall be decided exclusively by the courts of

or having jurisdiction for Heidelberg, Germany, as far as legally permissible.

3. This License is solely for Licensor's and Licensee's benefit. It is not for the benefit of any other person or entity.

END OF THESIS